

AN INVESTIGATION OF THE SOLVENT
EXTRACTION KINETICS OF GERMANIUM BY
7-ALKYLATED-8-HYDROXYQUINOLINE EXTRACTANTS

(VOLUME 1)

By

Stephen James Foster

Submitted in partial fulfillment of the
requirements for the degree of Doctor of Philosophy,
in the Department of Chemistry and Applied Chemistry,
University of Natal, 1990.

Durban

1990

PREFACE

This thesis presents work carried out by the author and has not been submitted in part, or in whole, to any other University. Where use has been made of the work of others it has been duly acknowledged in the text.

The work described in this thesis was performed in the Department of Chemistry and Applied Chemistry, University of Natal, King George V Avenue, Durban, 4001, from June 1988 to December 1990 under the supervision of Professor L.F.Salter.

ACKNOWLEDGEMENTS

I am indebted to the Council for Mineral Technology (MINTEK), Randburg, South Africa, for financial assistance provided for the course of this work and for the loan of the AKUFVE apparatus.

I am grateful to my supervisor, Professor L.F.Salter, for his guidance, helpful suggestions and enthusiasm in the development of this research program and for his interest in the development of my cultural acumen. I would also like to thank my colleagues for many interesting conversations and for creating an enjoyable social atmosphere.

The gratis supply of Lix 26 by Trochem S.A. (Pty) Ltd, a division of Henkel, Germany and of Kelex 100, TN 02181 and TN 01787 and technical data relating to these reagents by Schering AG, Germany, are gratefully acknowledged.

I am grateful to Miss Merle Smuts of the University of Natal, Pietermaritzburg, for GC/MS determinations.

ABSTRACT

Equilibrium and kinetic data for the solvent extraction of germanium by three impure commercial 7-alkylated-8-hydroxyquinoline extractants which vary in structure at the 7-alkyl group, are evaluated in order to elucidate an holistic kinetic extraction model which accounts for the various reactions and partition effects occurring during the metal-ion chelation process.

It is proposed that for the extraction process, which is first order in germanium concentration, by the ligand reagents Lix 26, TN 01787 and TN 02181, the rate-determining step, on stereochemical grounds, is the attachment of either a neutral ligand or a protonated ligand species to the biligand intermediate GeL_2^{2+} (L:ligand) at the interface.

In high speed shaking/mixing assemblies the extraction process was observed to occur in two discrete reaction regimes : a fast initial rate for which the orders with respect to ligand reagent are 1,06, 2,10 and 1,77 for TN 02181, Lix 26 and TN 01787 respectively, and a slower subsequent rate for which the apparent reaction orders with respect to ligand concentration are 1,12, 2,70 and 3,08 for TN 02181, Lix 26 and TN 01787 respectively. For the slower reaction regime, orders between 1 and 3 are explicable if the steady state approximation is invoked for the intermediate germanium species GeL^{3+} and GeL_2^{2+} formed at the interface. In the fast

reaction regime, it is proposed that the accelerated extraction rates are a function of (i) the speciation of germanium and (ii) participation in the rate-determining step by the protonated ligand moiety $H_2L^+HSO_4^-$ which is rapidly formed after phase contact.

At low ligand concentration, the following order of ligand efficacy has been observed :



whereas at high concentration ligand efficacies are similar because the interface is saturated with ligand.

Orders with respect to $[H^+]$ for the reagents vary from -1 to -3 during the course of reaction, indicating complex mixed-order behaviour.

The effects upon extraction of ionic strength, temperature, the addition of organic modifiers and diluent nature are investigated as well as the kinetics of germanium stripping by aqueous hydroxide.

The physical effects of interfacial tension, viscosity and relative dielectric constant are also reported and suggestions are made as to their effect upon the extraction characteristics. Computer modelling of the extractants has been used as an aid in describing size, structure and stereochemical considerations of the ligands and the chelate products.

LIST OF CONTENTS

VOLUME 1

	PAGE
1. INTRODUCTION	1
1.1 The Uses, Mineral Origins and Traditional Procedure for the Recovery of Germanium from Multi-element Acidic Leach Liquors	8
1.2 Separation Procedures for the Recovery of Germanium in Aqueous Solution	14
1.3 General Description of an Elementary Kinetic Model for Metal Extraction by Chelating Ligands	22
2. EXPERIMENTAL	37
2.1 Materials	38
2.1.1 Chemicals for Solvent Extraction and Stripping Experiments	38
2.1.2 Chemicals for Preparing Buffered pH Solutions	38
2.1.3 Chemicals for Phenylfluorone UV Determination of Germanium	39
2.1.4 Chemicals For Germanium Titration With Mannitol	39
2.1.5 Chemical Modifiers Used in Extraction Experiments	39
2.1.6 Chemicals for Thin Layer Chromatography	39
2.1.7 Chemicals for Column Chromatography	40
2.1.8 Chemicals for Acid-wash Purification of Ligand Preparations	40
2.1.9 Chemicals for Zinc Extraction Trials	40
2.1.10 Addresses of Chemical Suppliers	40

2.2 Reagent Purity, Technique For Purification, Isolation and Identification of the Active Ligand Components and Impurities	42
2.2.1 Description of the Ligand Preparations	42
2.2.2 Thin Layer and Column Chromatographic Separation of Reagent Components	50
2.2.2.1 Thin Layer Chromatography	51
2.2.2.2 Purification of Sample Components Via Low Pressure Column Chromatography	61
2.2.2.3 GC/MS Analysis of the Components of Lix 26, TN 02181 and TN 01787	64
2.2.2.4 Other Techniques for the Purification of 7-Alkylated-8-hydroxyquinoline Extractants	76
2.3 Techniques for the Quantification of Germanium in Aqueous Solution	80
2.3.1 The Quantification of Germanium by Mannitol Titration	83
2.3.2 The Colorimetric Quantification of Germanium by Phenylfluorone	84
2.3.2.1 Experimental Procedure	84
2.3.2.2 Accuracy and Precision of the Phenylfluorone Technique and Associated Microanalysis	88
2.3.2.3 The Stability of the Germanium- Phenylfluorone Complex	90
2.3.2.4 The Kinetics of the Phenylfluorone Complexation Reaction	94
2.3.3 Quantification of Germanium in Aqueous Solution by Atomic Absorption Spectroscopy	103
2.4 Experimental Techniques for the Study of the Extraction Kinetics of Germanium in Quasi Steady-State and Vigorously-Stirred Systems	106
2.4.1 Experiments for the Study of Mass Transfer Across a Quiescent Interface	106

2.4.2	Procedures for the Investigation of Solvent Extraction Kinetics of Vigorously-Stirred Systems	111
2.4.2.1	The AKUFVE Solvent Extraction System	112
2.4.2.2	The Investigation of Liquid-Liquid Solvent Extraction Kinetics With a Simple Mechanical Shaker	121
2.4.2.2.1	Preparation of Ligand and Germanium Solutions	123
2.4.2.2.2	Adjustment of Aqueous Phase pH	124
2.4.2.2.3	The Effect of Free 8-hydroxyquinoline on Germanium Extraction	125
2.4.2.2.4	The Effect of Ionic Strength on Germanium Extraction Kinetics	127
2.4.2.2.5	The Effect of the Aqueous/Organic Phase Ratio	128
2.4.2.2.6	Choice of Diluent	129
2.4.2.2.7	The Effect of Chemical Modifiers	131
2.4.2.2.8	Studies With 'Purified' Reagents	132
2.4.2.2.9	Investigation of the Kinetics of Stripping Germanium-Loaded Ligand	133
2.4.2.2.10	Investigation of the Selectivity of the Ligand Reagents for Germanium	135
2.4.2.2.11	Determination of the Uptake of Acid into Ligand Organic Phases by Lix 26, TN 02181 and TN 01787	137
2.5	Techniques for the Investigation of Physical Parameters Important in the Study of Solvent Extraction	138
2.5.1	The Measurement of Interfacial Tension	139
2.5.2	Dielectric Constant Measurements	140
2.5.3	Measurement of Solution Viscosity	142
2.5.4	Investigation of Extractant Aggregation by Infra-red Spectroscopy	143
2.6	The Alchemy Modelling Program	144

3 RESULTS AND DISCUSSION	149
3.1 The Kinetics of Germanium Extraction Across a Quiescent Interface: The Lewis Cell	150
3.1.1 Kinetic Analysis: The Relationship Between the Mass-Transfer Coefficient and Volume/Area	150
3.1.2 The Effect of Impeller Speed Upon the Rate of Extraction	155
3.1.3 The Effect of Ligand Concentration on the Extraction Kinetics of Germanium in the Lewis Cell	163
3.1.4 The Relevance of Lewis Cell Extraction Data to Turbulent Systems	174
3.2 Factors Affecting the Kinetics of Germanium Extraction in High Speed Mixing Assemblies	175
3.2.1 The Effect of Ligand Concentration on Extraction Kinetics	176
3.2.1.1 Kinetic Treatment	176
3.2.1.2 Determination of the Order of Reaction With Respect to [Lix 26]	177
3.2.1.3 The Apparent Reaction Orders With Respect to Ligand for TN 01787 and TN 02181	190
3.2.1.4 A Comparison of the Rate of Germanium Extraction by Lix 26, TN 01787 and TN 02181	194
3.2.1.5 The Equilibrium Percentage Extraction of Germanium by Lix 26, TN 02181 and TN 01787	196
3.2.1.6 The Magnitude of the Observed Reverse Rate Constants for Germanium Extraction by Lix 26, TN 02181 and TN 01787	204
3.2.1.7 The Lack of Correlation Between the Data Obtained from the Lewis Cell and the Shaking Apparatus	206

3.3 The Influence of 8-Hydroxyquinoline on the Extraction of Germanium by 7-Alkylated Derivatives	213
3.3.1 The Distribution Coefficient of 8-Hydroxyquinoline Between Toluene and 1,5 M H ₂ SO ₄	216
3.3.2 The Effect of Free Oxine on the Rate of Germanium Extraction by Lix 26/toluene Solutions	216
3.4 The Influence of the Aqueous Phase pH on Germanium Extraction. Speciation Studies	219
3.4.1 Influence of Aqueous Phase pH on Germanium Extraction by Lix 26	219
3.4.2 The Influence of Aqueous Phase pH on Germanium Extraction by TN 02181	228
3.4.3 The Influence of Aqueous Phase pH on the Rate of Germanium Extraction by TN 01787	234
3.4.4 Comparison of the Equilibrium Percentage Extraction of Germanium by the Various Extractants	240
3.4.5 Germanium Speciation and the Nature of the Reactions Competing for Active Ligand Sites	243
3.4.6 The Nature of Extracted Germanium Species.	255

VOLUME 2

3.5 The Effect of the Aqueous Phase Ionic Strength on Germanium Extraction Kinetics by 7-Alkylated -8-hydroxyquinoline Extractants	281
3.6 The Importance of the Choice of Diluent on Germanium Extraction Kinetics	294
3.7 The Enhancement of Extraction Kinetics and Improvement in Percentage Extraction Resulting from the Inclusion of Chemical Modifiers	298

3.7.1 Kinetic and Equilibrium Data Relating to Lix 26 and Chemical Modifiers	301
3.7.2 The Effect of Modifiers on Germanium Extraction by TN 02181 and TN 01787	312
3.7.3 The Effect of Increasing Modifier Concentration on the Equilibrium Percentage Extraction of Germanium by Lix 26	320
3.8 The Extraction Kinetics of 'Acid-Purified' Lix 26	323
3.9 The Use of the AKUFVE Apparatus for Following the Extraction Kinetics of Germanium	325
3.9.1 A Comparison of the Rate Data Obtained With the AKUFVE and Mechanical Shaker	326
3.9.2 The Determination of Thermodynamic Parameters via AKUFVE Data	331
3.10 The Kinetics of Germanium Stripping by Aqueous Hydroxide Solutions	345
3.10.1 The Effect of Hydroxide Concentration on the Rate and Equilibrium Percentage of Stripping	348
3.10.2 Determination of an Optimum Aqueous:Organic Phase Ratio for Germanium Stripping of Lix 26 by Sodium Hydroxide	360
3.10.3 Comparison of the Germanium Stripping Rates by NaOH from Loaded Lix 26 Organic Solution With and Without an Added Modifier	362
3.11 Physical Parameters Important for the Development of a Solvent Extraction Model	366
3.11.1 Infra-red Spectrophotometric Investigation of Ligand Aggregation	367
3.11.2 The Use of Interfacial Tension Data in the Interpretation of Surface Population of 7-Alkylated-8-hydroxyquinoline Extractants and in the Determination of the Area Occupied per Molecule at the Interface	371

3.11.2.1	The Gibbs Adsorption Equation	372
3.11.2.2	Interfacial Tension Data Pertaining to Ligand Solutions in Contact With Aqueous Phases 1,5 M in H ₂ SO ₄	373
3.11.2.3	Interfacial Excess of Alkylated 8-Hydroxy- quinoline Extractants at the Aqueous/ Toluene Interface as a Function of Aqueous pH	379
3.11.2.4	The Estimation of the Apparent Interfacial Acid Dissociation Constant K_a^{int}	388
3.11.2.5	Application of the Langmuir Isotherm to Interfacial Pressure Data for Lix 26/ toluene Systems	395
3.11.3	The Change in Solution Viscosity With Increasing Ligand Concentration	403
3.11.4	Correlations Between Dielectric Constant of Organic Media and Extractant Performance	408
3.12	The Selectivity for Germanium by 7-Alkylated-8- hydroxyquinoline Extractants from Aqueous Feed Solutions Containing Zn ²⁺	413
3.13	The Visualization of Metal-Chelate Structures, Stereochemical Effects and the Determination of Minimum Energy Conformations by Alchemy	423
3.13.1	Minimum Energy Conformations, Structural Differences and Geometrical Areas of TN 01787, TN 02181, Lix 26 and Some Ligand Reagent Impurities	424
3.13.2	Size and Structure Relationships of the Tri- Ligand Chelates of Germanium	433
3.14	The Chelation of Germanium-Hydroxy Species by 7-Alkylated-8-hydroxyquinoline Derivatives at Low pH	446

3.15 A Proposed Holistic Kinetic Model for Germanium Extraction by Commercial 7-Alkylated-8-hydroxy- quinoline Reagents	449
4 SUMMARY OF CONCLUSIONS	464
5 SUGGESTIONS FOR FUTURE WORK	478
REFERENCES	485
APPENDIX A	

LIST OF FIGURES

	PAGE
Figure (1). Flow diagram of the solvent extraction process.	4
Figure (2). Post 1976 Kelex 100, 7-(4-ethyl-1-methyl-octyl)-8-hydroxyquinoline.	16
Figure (3). Structure of the charge-neutral complex CuR_2 (R : Kelex 100 anionic species).	19
Figure (4). Structures of (a) TN 02181 and (b) TN 01787.	21
Figure (5). Classical scheme for the solvent extraction of a metal-ion, M^{n+} , by an organic-soluble ligand, HL.	23
Figure (6). The Alchemy-minimized tri-ligand Lix 26 -germanium chelate.	34
Figure (7). Structures of (a) TN 02181 ; 7-alkyl = $\text{C}_{12}\text{H}_{23}$ (β -dodecenyl) and (b) TN 01787 ; 7-alkyl = $\text{C}_{11}\text{H}_{21}$ (α -undecenyl).	42
Figure (8). Preparative route for the synthesis of 7-alkylated-8-hydroxyquinoline extractants.	46
Figure (9). Resolution of the components via TLC of (A) TN 01787, (B) TN 02181 and (C) Lix 26.	51
Figure (10a). Infrared spectrum of 8-hydroxyquinoline in carbon tetrachloride.	54
Figure (10b). Infrared spectrum of the active component of Lix 26 in carbon tetrachloride, separated from its constituent impurities by preparative TLC.	55
Figure (11). (a) UV/Vis spectrum of 8-hydroxyquinoline in CCl_4 in concentrations of (i) $6,90 \times 10^{-3}$ M, (ii) $3,45 \times 10^{-3}$ M and (iii) $1,72 \times 10^{-3}$ M, uv maxima at 264,7 and 321,7 nm. (b) UV/Vis spectrum of the	58

active component of Lix 26 in CCl_4 ,
(approx 0,1 g in 100 ml)
separated via preparative TLC from other
constituent impurities.

- Figure (12). ^1nmr spectra of (a) 8-hydroxyquinoline 59
and (b) the active Lix 26 ligand.
- Figure (13). Column chromatography apparatus. 63
- Figure (14). GC spectrum and mass spectrum for 8- 65
hydroxyquinoline.
- Figure (15). GC spectrum and mass spectrum for Lix 26 67
in CCl_4 .
- Figure (16). GC spectrum and mass spectrum for TN 01787 70
in CCl_4 .
- Figure (17). Proposed structure for one of the 73
furoquinoline impurities in TN 01787.
- Figure (18). GC spectrum and mass spectra for the 74
components eluting at (a) 8,81 min and
(b) 9,10 min for TN 02181.
- Figure (19). Absorbance of the aqueous phase at two 79
wavelengths (315 and 360 nm) after contact
with a Lix 26/toluene solution as a
function of the number of strip cycles.
- Figure (20). Structure of phenylfluorone, 2,6,7-tri 82
hydroxy-9-phenyl-3-H-xanthan-3-one.
- Figure (21). Calibration curve for the germanium- 86
phenylfluorone complex at 510 nm.
- Figure (22). The UV/VIS spectra of the germanium- 87
phenylfluorone complex, GePh_2 , and
phenylfluorone.
- Figure (23). The visible absorption stability of the 92
germanium-phenylfluorone complex at
510 nm if prepared in solution in the
absence of a polyol (method of Pedrosa
and Paul).
- Figure (24). Absorbance at 510 nm as a function of time 93
for the formation of the germanium-
phenylfluorone complex.

Figure (25).	Pictorial representation of the stereochemically-hindered reaction between phenylfluorone and the GePh^{3+} intermediate.	95
Figure (26).	First order kinetic plot of $\ln(A_{510}^{\infty} - A_{510}^t)$ as a function of time for the formation of GePh_2^{2+} .	97
Figure (27).	Structures of (a) Salicylfluorone : 9-(o-hydroxyphenyl)-2,3,7-trihydroxy-6-fluorone and (b) 1-hydroxyxanthone.	99
Figure (28).	The yields of Ge^{4+} , GePh^{3+} and GePh_2^{2+} predicted by CAKE as a function of time.	101
Figure (29).	The yield of GePh_2 predicted by CAKE as a function of time assuming that $A_{510}^t \propto (A_{510}\text{GePh}^{3+} + A_{510}\text{GePh}_2^{2+})$.	102
Figure (30).	Original design of the Lewis cell.	107
Figure (31).	a) Essential design features of the adapted Lewis arrangement used for fixed-interface kinetic studies, b) Detail of the dual phase impeller, c) Teflon insert with approximately half the original interfacial area.	109
Figure (32).	Diagram of the AKUFVE liquid flow system.	114
Figure (33).	The principle of operation of the H-centrifuge.	114
Figure (34).	The AKUFVE system with H-33tr centrifuge.	115
Figure (35).	a). AKUFVE centrifuge speed under load as a function of air pressure, b). AKUFVE mixer setting versus actual circumferential speed.	120
Figure (36).	Extraction kinetics of germanium in the Lewis Cell assembly.	156
Figure (37).	First order kinetic plot (Equation 50) for germanium extraction in the Lewis Cell.	157
Figure (38).	Observed rate constant versus impeller speed for the Lewis Cell.	160

- Figure (39). Log k_{obs} versus log[HL] for Lix 26, TN 02181 and TN 01787 in the Lewis Cell. 166
- Figure (40). Percentage extraction versus time in the Lewis Cell for Lix 26, TN 01787 and TN 02181 at concentrations of 50 and 100 g/l in toluene. 168
- Figure (41). Log k_{obs} versus log [HL] for active-constituent corrected concentrations of extractants. 173
- Figure (42a). Kinetics of germanium extraction in the vigorous shaker for 50 g/l Lix 26 in toluene and ~ 0,62 g/l Ge in 1,5 M H_2SO_4 . 179
- Figure (42b). Percentage germanium extraction as a function of time for vigorous shaking. 180
- Figure (43a). Plot of Log(Observed rate constant) as a function of log[Lix 26] obtained in the vigorous shaker for concentrations of germanium of 0,65 g/l and 0,20 g/l. 183
- Figure (43b). Comparison of the percentage extraction obtained at equilibrium (i.e. when no further extraction is observed) as a function of Lix 26 concentration for two initial germanium concentrations viz 0,20 and 0,65 g/l. 187
- Figure (44). Log(Initial rate) versus log[Lix 26] for germanium extraction by various concentrations of Lix 26 in a mechanical shaker. 189
- Figure (45). Log(Observed rate constant) versus log[HL] for germanium extraction by TN 02181 and TN 01787 in the slow kinetic regime. Vigorous shaking. 191
- Figure (46). Log(Initial rate) versus log[HL] for germanium extraction by TN 02181 and TN 01787 in the shaking apparatus. 193

- Figure (47). Log(Observed rate constant) versus log[HL] 195
(corrected for percentage active constituent) for TN 01787, TN 02181 and Lix 26.
- Figure (48). Percentage germanium extraction versus time 197
for TN 02181 solutions of varying concentration obtained with a mechanical shaking apparatus.
- Figure (49). Percentage germanium extraction versus time 198
for Lix 26 solutions of varying concentration obtained with a mechanical shaker.
- Figure (50). Percentage germanium extraction versus time 199
for TN 01787 solutions of varying concentration. Vigorous shaking.
- Figure (51). A comparison of the percentage germanium 200
extraction as a function of time by TN 02181, TN 01787 and Lix 26 in a mechanical shaker at two ligand concentrations.
- Figure (52). Log D versus log[HL] for Lix 26, TN 02181 203
and TN 01787 at low ligand concentration (< 50 g/l reagent).
- Figure (53). Interfacial tension, γ , as a function 208
of [HL] for Lix 26, TN 02181 and TN 01787.
- Figure (54). Comparison of the rates of extraction using 209
the Lewis Cell or vigorous shaking by Lix 26.
- Figure (55). The effect of 8-hydroxyquinoline on the 218
kinetics and equilibrium percentage extraction of germanium.
- Figure (56). Percentage extraction as a function of 220
pH for Lix 26.
- Figure (57). Initial rate of germanium extraction by 223
Lix 26 as a function of aqueous phase pH in the mechanical shaker.
- Figure (58). Log(Initial rate) of germanium extraction 224
by Lix 26 as a function of pH under vigorous stirring conditions.

Figure (59).	Log(Observed rate constant) for germanium extraction as a function of pH for Lix 26 under conditions of vigorous shaking.	225
Figure (60).	Percentage extraction as a function of pH for TN 02181.	230
Figure (61).	Log(Initial rate) of germanium extraction by TN 02181 as a function of aqueous phase pH in the mechanical shaker.	232
Figure (62).	Log(Observed rate constant) for germanium extraction as a function of pH for TN 02181 under conditions of vigorous shaking.	233
Figure (63).	Percentage extraction as a function of pH for TN 01787.	235
Figure (64).	Log(Initial rate) of germanium extraction by TN 01787 as a function of aqueous phase pH.	238
Figure (65).	Log(Observed rate constant) for germanium extraction by TN 01787 as a function of pH under conditions of vigorous shaking.	239
Figure (66).	Comparison of the percentage extraction of germanium as a function of pH for TN 01787, TN 02181 and Lix 26 in the mechanical shaker.	242
Figure (67).	Distribution of germanium species as a function of pH for $[\text{GeO}_2] \leq 1 \times 10^{-2}$ M.	245
Figure (68).	Distribution isotherms of sulphuric acid between an aqueous solution and kerosene containing various concentrations of Kelex 100, (after Marchon, Cote and Bauer).	248
Figure (69).	Concentration of sulphuric acid in the organic phase $[\text{H}_2\text{SO}_4]_{\text{org}}$ after 24 hours shaking of solutions of Lix 26, TN 01787 and TN 02181 in toluene with aqueous phases of 1,5 M H_2SO_4 .	252

- Figure (70). The Alchemy-minimized structure of the 260
triligand chelate of germanium with Lix 26,
 $\text{GeL}_3^+\text{HSO}_4^-$.
- Figure (71). The Alchemy-minimized structure of the 261
biligand hydroxylated chelate molecule
between Lix 26 and germanium, $\text{GeL}_2(\text{OH})_2$.
- Figure (72). Comparison of the percentage of germanium 265
extracted as a function of time for
acid pre-equilibrated and non-equilibrated
Lix 26.
- Figure (73). Initial rate of germanium extraction by 268
Lix 26 (50 g/l in toluene) as a function
of the percentage Ge^{4+} in aqueous solution
calculated from Figure (67) for the pH
region $< 0,24$.
- Figure (74). The rate of acid uptake plotted as $[\text{H}_2\text{SO}_4]$ 276
in the organic phase as a function of time
by a 100 g/l (0,270 M) solution of TN 02181
in AR toluene.
- Figure (75). Percentage extraction of germanium in the 279
fast initial regime as a function of $[\text{H}_2\text{SO}_4]$
in the organic phase.
- Figure (76). Percentage extraction of germanium by 284
Lix 26 from 0,5 M H_2SO_4 aqueous
solutions containing Na_2SO_4 , as a
function of the ionic strength.
- Figure (77). Log(Initial rate) of germanium extraction 285
by Lix 26 as a function of aqueous ionic
strength.
- Figure (78). Log(Observed rate constant) for germanium 285
extraction by Lix 26 as a function of ionic
strength.
- Figure (79). Percentage extraction of germanium as a 295
function of time by Lix 26 dissolved in
various diluents.
- Figure (80). Semi-logarithmic plots of Equation (46) 297
as a function of time for germanium

- extraction by Lix 26 in various diluents.
- Figure (81). Percentage extraction obtained by varying the nature of the modifier added to Lix 26 in toluene. 303
- Figure (82). Comparison of the extraction kinetics of germanium by Lix 26 solutions containing various modifiers. 304
- Figure (83). Forward rate constant for germanium extraction (Equation (46)) as a function of the relative dielectric constant of 10% v/v modifier solutions of Lix 26 (45 g/l) in toluene. 306
- Figure (84). Hydrogen bonding interaction between n-octanol and Lix 26. 309
- Figure (85). Hydrogen bonding interaction between a molecule of benzyl alcohol and Lix 26. 310
- Figure (86). Hydrogen bonding interaction between a molecule of n-butanol and Lix 26. 311
- Figure (87). Percentage extraction obtained by varying the nature of the modifier added to TN 01787 in toluene. 314
- Figure (88). Percentage extraction obtained by varying the nature of the modifier added to TN 02181 in toluene. 315
- Figure (89). Forward rate constants for germanium extraction (calculated via Equation (46)) as a function of the relative dielectric constant of 10% v/v modifier solutions of TN 02181 (upper curve) and TN 01787 (lower curve) in toluene. 317
- Figure (90). Hydrogen bonding interaction between n-butanol and TN 02181 (structure A). 319
- Figure (91). Percentage extraction of germanium by Lix 26 as a function of added n-octanol modifier concentration. 322
- Figure (92). Comparison of the extraction kinetics of acid-purified Lix 26 with the impure 324

- as-received commercial material.
- Figure (93). Comparison of the extraction kinetics of Lix 26 in the AKUFVE apparatus with those observed with a mechanical shaker. 327
- Figure (94). A comparison of the germanium extraction kinetics observed using the AKUFVE and mechanical shaker. 328
- Figure (95). The effect of temperature on percentage extraction of germanium by Lix 26. All plots obtained with the AKUFVE assembly. 335
- Figure (96). Arrhenius plots of $\ln(k_{obs})$ vs $1/T$ for the extraction of germanium from 1,5 M H_2SO_4 solutions by 50 g/l Lix 26 solutions in toluene using the AKUFVE apparatus. 336
- Figure (97). Log of the distribution coefficient as a function of temperature for a 50 g/l solution of Lix 26 in toluene. 339
- Figure (98). Observed initial rate for the complexation of germanium by Lix 26 as a function of temperature in the AKUFVE apparatus. 340
- Figure (99). Observed reverse rate constants k_b , calculated via plots of Equation (47), for the germanium extraction process: 342
- $$Ge_{aq} \xrightleftharpoons[k_b]{k_f} Ge_{org}$$
- as a function of time for various temperatures in the AKUFVE apparatus.
- Figure (100). Observed change in the reverse rate constant as defined for Figure (99), as a function of temperature in the AKUFVE apparatus. 344
- Figure (101). The species distribution of germanium in the pH range 4-14. 347

- Figure (102). Percentage germanium stripped from germanium-loaded Lix 26 by various concentrations of NaOH in the aqueous phase (pH = 13,7-14,7). 350
- Figure (103). Semi-logarithmic kinetic plots for germanium-loaded toluene/Lix 26 stripping by various NaOH solutions. 355
- Figure (104). Log(Observed rate) for the stripping of germanium from loaded Lix 26 as a function of log[OH] in the aqueous phase. 357
- Figure (105). Percentage germanium stripped from a loaded Lix 26/toluene organic phase by 1,0 M NaOH as a function of contact time and a:o phase ratios from 5:1 to 1:4. 361
- Figure (106). The effect of an organic modifier (n-octanol) on the stripping kinetics of germanium from loaded Lix 26. 363
- Figure (107). Semi-logarithmic plot for the first-order stripping of germanium from Lix 26/toluene and Lix 26/toluene/n-octanol systems by 2,5 M NaOH. 365
- Figure (108). Absorbance of the intramolecular H-bonding peak (3400 cm^{-1}) as a function of Lix 26 concentration in CCl_4 . 370
- Figure (109). Interfacial tension (γ_c) as a function of [HL] for Lix 26, TN 02181 and TN 01787. 374
- Figure (110). Interfacial tension between organic phases containing Lix 26 and aqueous phases at various pH's versus the concentration of active-constituent corrected Lix 26 concentration in AR toluene. 381
- Figure (111). Interfacial tension between organic phases containing Lix 26 and aqueous phases at various pH's, versus log[Lix 26] (corrected for active-constituent purity). 382
- Figure (112). Interfacial excess (Γ) calculated from the gradients of the γ_c versus log[Lix 26] 385

- plots of Figure (110) as a function of the aqueous phase pH.
- Figure (113). Alchemy-minimized structures of protonated and deprotonated Lix 26, showing approximate interfacial area of the molecule. 387
- Figure (114). The interfacial pressure, Π , between solutions of Lix 26 in toluene and aqueous phases of various pH, as a function of [Lix 26], corrected for active constituent purity. 390
- Figure (115). Plot of $\log m$, where m is the gradient of the straight line plots of $\Pi = m[\text{HL}]$ obtained at very low Lix 26 concentration, versus the pH of the aqueous phase for which interfacial tension measurements were made. 394
- Figure (116). Langmuir-type isotherm (Equation (148)) obtained from interfacial tension data for Lix 26 solutions of various concentration and an aqueous phase 1,5 M in H_2SO_4 . 397
- Figure (117). Langmuir-type isotherm obtained from interfacial tension data for Lix 26 solutions of various concentration and an aqueous phase of pH 1,75. 398
- Figure (118). Langmuir-type isotherm obtained from interfacial tension data for Lix 26 solutions of various concentration and an aqueous phase of pH 10,00. 399
- Figure (119). Change in organic solution viscosity of Lix 26, TN 02181 and TN 01787 as a function of the quantity of ligand reagent added to the toluene diluent. 405
- Figure (120). The change in the relative dielectric constant of solutions of Lix 26 in BDH Distillate as a function of the volume percent of n-octanol added. 410

- Figure (121).** The change in the relative dielectric constant of Lix 26 in AR toluene as a function of the Lix 26 concentration added. 412
- Figure (122).** The percentage extraction of Zn^{2+} by Lix 26 in methyl-isobutyl-ketone as a function of aqueous phase pH, after Rao and Ramesh. 416
- Figure (123).** The distribution of zinc species in aqueous solution as a function of aqueous phase pH. 418
- Figure (124).** The percentage of germanium extracted from aqueous solution by 50 g/l solutions of Lix 26 in toluene as a function of time for various aqueous phase composition. 420
- Figure (125).** Spacefill Alchemy-minimized structures of (a) 8-hydroxyquinoline, (b) Lix 26, (c) TN 01787, (d) TN 02181A, (e) TN 02181B, (f) TN 02181C, (g) TN 02181D, (h) Kelex 100, (i) Impurity 4, (j) Impurity 5 and (k) Impurity 8. 425
- Figure (126).** Some of the possible structures of TN 02181. 429
- Figure (127).** Size, structure pictorial representation of the rate-determining step in the chelation of germanium by Lix 26. 435
- Figure (128).** Alchemy-minimized structure representation of germanium chelated to three 8-hydroxyquinoline moieties (meridionally coordinated) showing the deviation from the normal sp^3d^2 bond angle of 90° . 436
- Figure (129).** Alchemy-minimized structure of germanium bound to three molecules of Lix 26. 438
- Figure (130).** Alchemy-minimized structure of germanium bound to three molecules of TN 02181A. 439

- Figure (131).** The difference in the conformation of the 441
Alchemy-minimized tri-ligand chelates of
germanium with Lix 26 coordinated in the
facial and meridional arrangements.
- Figure (132).** A visual representation of the difference 445
in the most stable conformations of the
tri-ligand chelates of germanium with
TN 01787, Kelex 100, Lix 26 and TN 02181.
- Figure (133).** Proposed reaction scheme for the 448
chelation of germanium-hydroxy species
by 7-alkylated-8-hydroxyquinoline
extractants.
- Figure (134).** An holistic kinetic model for the 451
complexation of germanium by 7-alkylated-
8-hydroxyquinoline extractants.
- Figure (135).** Percentage germanium extraction by a 462
solution of 75 g/l Lix 26 in toluene as
a function of the ratio of the aqueous
phase(a) to the organic phase(o).

LIST OF TABLES

	PAGE
Table (1). World production of germanium in 1977.	10
Table (2). Germanium content of some of the ore deposits at Tsumeb in Namibia.	11
Table (3). Composition of a sample of fume from the Tsumeb zinc smelter. Source of coal: Morupule coal field, Botswana.	12
Table (4). Some of the chelating (a-g) and acidic (h,i) extractants with application in germanium recovery by solvent extraction.	17
Table (5). Percentage composition and identity of the components of TN 01787,	44
Table (6). The structure of the impurities and their approximate percentage in commercially available Kelex 100.	47
Table (7). R_f values of the components of the ligand preparations separated by TLC.	52
Table (8). Characteristic Infra-red stretching frequencies of 8-hydroxyquinoline.	56
Table (9). Chemical shifts and possible assignments of the ^1nmr spectrum of Lix 26.	60
Table (10). m/z values and fragmentation pattern for 8-hydroxyquinoline.	66
Table (11). Retention times, molecular weights and possible identities of the major constituents of TN 01787.	71
Table (12). Results for the acidimetric mannitol titration of germanium.	84
Table (13). Results for the phenylfluorone determination of germanium.	89

Table (14).	Values of $\log K_{eq}$ for various metal ion complexes (ML) of 1-hydroxyxanthone.	99
Table (15).	Percentage error obtained for the direct determination of germanium by Atomic Absorption Spectroscopy.	104
Table (16).	Comparison of the relative error in germanium quantification via the phenyl-fluorone and ETA-AAS technique.	105
Table (17).	Technical data for the H-centrifuge of the AKUFVE apparatus, type H-33tr.	116
Table (18).	Materials of the components of the AKUFVE apparatus.	118
Table (19).	Components for the preparation of buffered germanium solutions.	125
Table (20).	Solution preparation for investigating the effect of ionic strength on extraction kinetics.	128
Table (21).	Aqueous:Organic phase ratios investigated to determine optimal conditions.	129
Table (22).	Ratio of volume of strip solution to germanium-loaded organic phase for the determination of an optimum ratio.	134
Table (23).	Details of experiments performed to investigate the selectivity of 7-alkylated-8-hydroxyquinoline extractants for germanium over zinc.	135
Table (24).	Rates of mass transfer across the quiescent interface of the Lewis Cell.	159
Table (25).	Values of k_{obs} calculated from plots utilising Equation (50).	163
Table (26).	Half-life data taken from Figure (36).	165
Table (27).	Germanium extraction kinetic data.	177
Table (28).	Data obtained for the extraction of germanium by Lix 26 in a mechanical shaker.	182

Table (29).	Values of $k_b(\text{obs})$ and the ratio $k_f(\text{obs})/k_b(\text{obs})$ for the germanium extraction process.	205
Table (30).	Initial extraction rates and observed forward rate constants for the slower first order reaction regime for the extraction of $\sim 0,65$ g/l Ge at varying aqueous phase pH by a 50 g/l Lix 26/toluene solution.	222
Table (31).	Initial rates and observed forward rate constants for the 'equilibrium' reaction regime for germanium extraction by TN 02181 at varying aqueous phase pH.	229
Table (32).	Values of Initial Rates and $k_f(\text{obs})$ for the slow kinetic regime for germanium extraction by TN 01787.	234
Table (33).	Comparison of extraction efficiencies of Lix 26, TN 02181 and TN 01787.	236
Table (34).	'Equilibrium' percentage germanium extraction by Lix 26, TN 01787 and TN 02181 at various aqueous phase pH's.	240
Table (35).	Values of K_i for germanium-hydroxy complexes at 25°C .	243
Table (36).	Concentrations of H_2SO_4 extracted by Lix 26 into the organic phase after 24 hours shaking with an aqueous phase initially containing 1,485 M H_2SO_4 .	249
Table (37).	Concentration of $[\text{H}_2\text{SO}_4]_{\text{org}}$ at equilibrium after 24 hours shaking of solutions of TN 01787 of varying concentration with 1,497 M H_2SO_4 .	250
Table (38).	The uptake of sulphuric acid into the organic phase by TN 02181 in toluene via Equation (81) after vigorous shaking for 24 hours with a 1,497 M solution of H_2SO_4 .	251

Table (39).	Comparison of the distribution of germanium species in the aqueous phase before and after contact of a 1,485 M H ₂ SO ₄ solution with a 50 g/l Lix 26/ toluene organic solution.	254
Table (40).	Percentage germanium extracted during the initial 'fast' extraction regime and initial rates versus sulphuric acid concentration.	267
Table (41).	Percentage germanium extracted during the initial fast step versus [Lix 26].	269
Table (42).	The effect of aqueous phase ionic strength on germanium extraction kinetics by Lix 26.	283
Table (43).	Values of formation constants for the species Ge(OH) _i ⁽⁴⁻ⁱ⁾⁺ (i = 0,1,2,3) at different ionic strengths (after Nazarenko).	286
Table (44).	Values of log γ_{\pm} predicted by the Davies Equation for ionic strengths in the range 0,715 - 8,215 M.	292
Table (45).	Relative dielectric constants for various diluents.	294
Table (46).	Physical constants of chemical modifiers and toluene.	300
Table (47).	Effect of alcohol modifiers on the extraction kinetics of germanium by Lix 26 (45 g/l in toluene with 10% v/v modifier).	305
Table (48).	Values of observed forward rate constants for germanium extraction by TN 01787 and TN 02181 in toluene, containing 10% v/v alcohol modifiers and dielectric constants of the solutions.	313
Table (49).	Comparison of observed forward rate constants for germanium extraction in the slower 'equilibrium' regime by Lix 26 in the AKUFVE apparatus and mechanical shaker.	329

Table (50).	Values of $k_f(\text{obs})$ for the 'slow' equilibrium region for the mechanical shaker and AKUFVE apparatus at pH 1,00 and 1,94.	329
Table (51).	Activation energies for various metal-ligand chelate complexation solvent extraction reactions and reaction assemblies.	333
Table (52).	Observed values of forward rate constants for germanium extraction by Lix 26 as a function of temperature.	334
Table (53).	Values of observed reverse reaction rate at various temperatures for the extraction of germanium by Lix 26 in the AKUFVE apparatus.	341
Table (54).	Percentage germanium stripped by NaOH solutions of various concentrations as a function of time.	349
Table (55).	Values of observed stripping rate constants for germanium stripping from metal loaded Lix 26 at various hydroxide concentrations.	356
Table (56).	Percentage transmittance and absorbance of the 3400 cm^{-1} peak of varying concentration of Lix 26 in CCl_4 .	369
Table (57).	Interfacial parameters calculated from interfacial tension measurements for Lix 26, TN 02181 and TN 01787 in AR toluene. Aqueous phase : 1,5 M H_2SO_4 .	375
Table (58).	Extractant areas predicted by the Gibbs Adsorption Isotherm treatment of interfacial tension data and molecular modelling by Alchemy.	376
Table (59).	Interfacial excess, Γ , and apparent interfacial area of Lix 26 in toluene as a function of aqueous pH.	383

Table (60).	Values of the constants p and q in Equation (148) calculated from Langmuir type plots of interfacial pressure data for Lix 26 in toluene.	400
Table (61).	Viscosities of Lix 26, TN 02181 and TN 01787 and toluene at 25°C.	404
Table (62).	Values of formation constants for Equations (164) to (166), all at 25°C.	422
Table (63).	Energy terms for the minimum energy conformations of extractant molecules and some impurities.	431
Table (64).	Energy terms determined by Alchemy for germanium complexed with two and three Lix 26 ligands.	437
Table (65).	Minimum energies determined by Alchemy for facial and meridionally coordinated Lix 26 and TN 02181A in the GeL_3^+ complex.	442
Table (66).	Minimum total energies and values of the parameters minimized by Alchemy.	444

LIST OF ABBREVIATIONS

The following abbreviations and symbols are used in this work.

8-HQ	8-hydroxyquinoline
a : o	The ratio of the volume of the aqueous phase to the volume of the organic phase
HR / HL	Neutral ligand species
H_2L^+	Protonated ligand
HOx	Neutral molecule of 8-hydroxyquinoline
L^-	Deprotonated form of the ligand HL
Ox^-	The deprotonated form of 8-hydroxyquinoline
γ	Interfacial tension ($N\ m^{-1}$)
π	Interfacial pressure ($N\ m^{-1}$)
Γ	Interfacial excess ($mol\ m^{-2}$)
ϵ_c^r	Relative dielectric constant
η	Viscosity ($N\ s\ m^{-2}$)

CONVENTIONS FOLLOWED

In order to describe the processes occurring in the different phases during solvent extraction, it is necessary to adopt a convention which unambiguously describes in which phase a species resides. Unless otherwise specified, the sites of species will be denoted by right subscripts as shown in the following examples:

HL_{org} : Organic phase species

HL_{int} : Interfacial species

M : Aqueous phase species

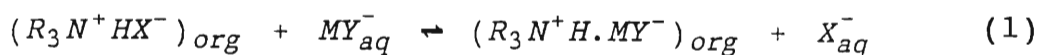
Aqueous phase species are therefore usually not subscripted, however occasionally where clarity is needed, aqueous phase species are right subscripted with 'aq'.

In some instances, as in the case of the definition of constants, the phase to which the parameter refers appears as a superscript. This is to conform to other conventions, e.g. the apparent interfacial dissociation constant will be defined as K_a^{int} which denotes the value of the acid dissociation constant at the interface.

Uncertainties in the fit of linear behaviour to experimental data will be specified as the correlation coefficient (r) which expresses the strength of the linear relationship between the two variables concerned.

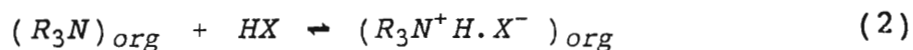
CHAPTER 1
INTRODUCTION

Solvent extraction is a separation technique in which a solute, which is often a metal ion, is transferred from one liquid phase to another immiscible or partially miscible liquid which is in contact with the first phase. In hydrometallurgy, the aqueous phase contains the metal(s) which are to be concentrated into the organic phase. Currently, liquid-liquid extraction is a highly sophisticated industrial chemical process with wide applications in analytical chemistry, radiochemistry, in the oil and heavy organic industries, in the pharmaceutical industry and in the extraction of metal ions in trace and macro levels from liquors originating from acid-leached ore samples, however it was the nuclear industry⁽¹⁻¹⁶⁾ which pioneered the industrial use of a solvent extraction technique for the separation and purification of metals, particularly uranium. Most of the methods for the purification of uranium involve the use of a tertiary amine, R_3N . The usefulness of these reagents depends essentially on their ability to form an ion-pair with an anionic species of the metal in the aqueous phase viz.

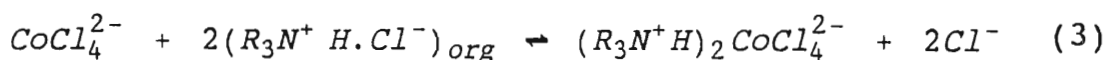


where M is the metal ion, Y is the counter ion of M and HX is an inorganic acid. The species formed via this exchange is electrically neutral and therefore compatible with non-aqueous solvents. In order to achieve the exchange given by Equation

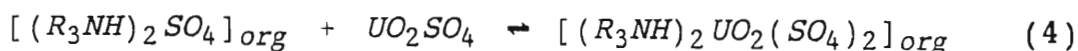
(1), the amine is first converted to the appropriate amine salt to provide an anion to exchange with the metal ion i.e.



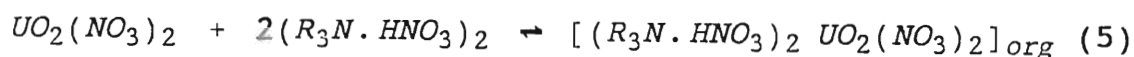
On contacting the organic phase species formed in Equation (2) with the metal anion species, the phase exchange occurs. For example, for the case of the extraction of $CoCl_4^{2-}$, the following equation may be written,



For the case of the extraction of uranium from sulphate media by tertiary amine extractants, another extraction mechanism has been shown to operate, viz. the extraction of a neutral uranium sulphate species⁽¹⁷⁾ as follows:



and similarly for extraction from nitrate media⁽¹⁸⁾:



Since early pioneering studies such as these, the solvent extraction industry has been developed for a wide range of

metals⁽¹⁹⁻²³⁾ including iron, cobalt, nickel, copper, chromium, vanadium, molybdenum, tungsten, zinc, the platinum group metals, rare-earths and gold. In accordance with this expansion, the number of extractants commercially available for achieving acceptable extraction together with some degree of ion selectivity, have also increased. The general properties and structures of the most common reagent preparations will be discussed later in this chapter, however it is first necessary to give a brief description of the stages of any solvent extraction process in order to facilitate an understanding of the primary features which are of concern in the development of an hydrometallurgical system.

There are three principal stages of solvent extraction⁽²⁴⁾ (Figure (1)) namely extraction, scrubbing and stripping. In the extraction stage an aqueous feed solution containing the metal ion of interest is brought into contact with an organic solvent containing the extractant (or 'ligand'). There are a wide range of industrial designs which perform this task, the most common being batch mixer-settlers, columns and counter-current contactors. Their comparative efficiencies, range of use, design characteristics and principle of operation have been fully reviewed in a collected volume⁽²⁵⁾ but details of this topic are beyond the scope of this work.

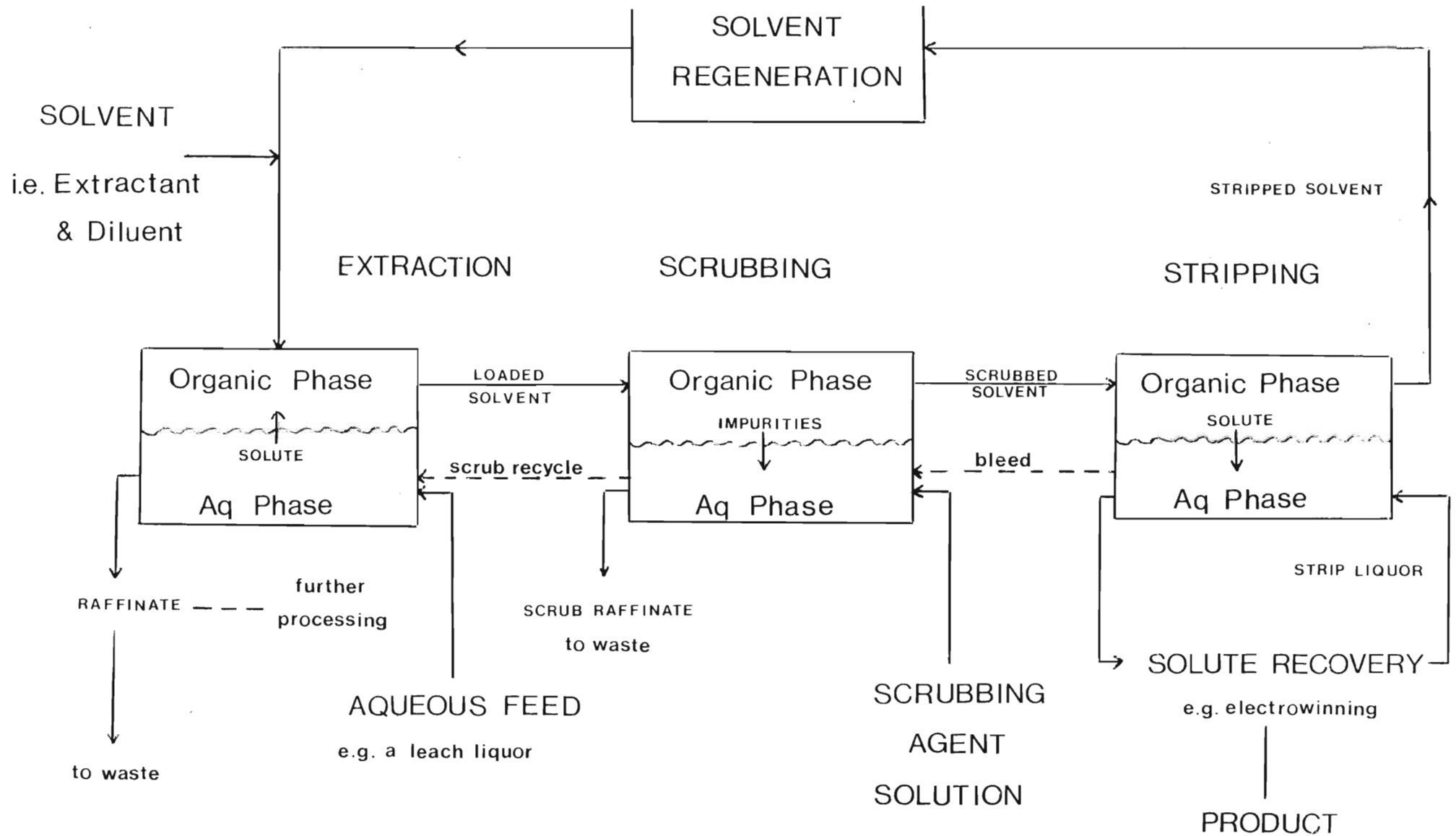


Figure (1). Flow diagram of the solvent extraction process. Dotted lines indicate alternative routes.

Usually, but not always (as is the case with the extractant tributyl phosphate, TBP), the extractant is dissolved in a 'diluent'- an organic medium which: (i) is mutually soluble with the extractant, (ii) has low volatility and a high flash point, (iii) possesses high solvency for any extracted metal-ligand species, (iv) is insoluble in the aqueous phase and (v) is cheap and readily available. Extractants are usually dissolved in a suitable diluent (commonly kerosene-type solvents) to reduce their viscosity and hence improve their ease of handling, improve dispersion (hence extractant availability) and the rate of coalescence during settling, reduce the tendency to form emulsions when brought into contact with an aqueous solution (most extractants are highly surface-active and tend to emulsify under the vigorous agitation conditions used), and to provide a concentration of the active ligand which extracts the metal species in an economically viable manner. The extractant is a material which is capable of combining chemically with the metal ion in the aqueous phase or at the interface to give a complex which is soluble in the diluent. Sometimes extractants on their own are inefficient and consequently other chemicals are added. The use of modifiers for example (Section 3.7), can greatly enhance the extractant properties of the organic phase system by increasing the solubility of the extractant and metal-ligand species and by changing interfacial properties. The products from the extraction stage are the organic solvent containing metal-loaded ligand, unreacted ligand and diluent and an aqueous raffinate; the aqueous phase remaining after extraction of the desired solute. This phase could either go to waste or to further processing.

The loaded solvent from the extraction stage is then usually 'scrubbed' by treatment with fresh aqueous phase to remove contaminants co-extracted during the extraction stage. The scrubbed organic solvent is then 'stripped' of the loaded metal-ion by contact with an appropriate stripping agent-usually a concentrated base or acid. During this process the metal ion is quantitatively removed from the ligand into the 'strip-liquor' and the extractant is cycled to a regeneration stage.

In solvent extraction, the 'extractant' is the active substance responsible for the transfer of a solute from one phase to the other. There are a number of criteria to consider in the choice of a suitable extractant viz.

- (i) The ability to extract the metal with acceptable yield and at the required pH,
- (ii) To be selective for the required metal and to reject undesired metals,
- (iii) To have acceptable rates of extraction, scrubbing and stripping,
- (iv) It must be soluble in aliphatic and aromatic diluents and have low solubility in the aqueous phase and
- (v) It must be stable i.e. capable of withstanding many months of recycling in a solvent extraction circuit without degrading.

Very often these requirements are incompatible and usually some are compromised in order to achieve a balance between them.

There are a plethora of commercial products available on the market at present and it has become convenient to classify

them^(20,26,27) according to their type or on the basis of the chemical reactions involved in the extraction process. There are three broad categories of extractants:

(i) Those which involve compound formation. This class of extractants can be further divided into two sub-classes, namely chelating and acidic extractants. The latter include those with reactive groups such as $-\text{COOH}$, $>\text{POOH}$ and $-\text{SO}_3\text{H}$, while the former include a host of oximes with the active group $\text{R}-\text{C}(\text{OH})-\text{C}(\text{R}')-\text{CR}''=\text{NOH}$ or substituted hydroxy/nitrogen heterocycles,

(ii) Those which involve ion-association. In commercial solvent extraction processing, this class of extractant is limited to primary (RNH_2), secondary (R_2NH) and tertiary (R_3N) amines and quaternary ammonium halides (e.g. $\text{R}_4\text{N}^+ \cdot \text{Cl}^-$),

(iii) Those which involve solvation of the metal ion. There are two main groups of extractants which are used in this area: organic reagents containing carbon-oxygen bonds, such as ethers, esters, ketones and alcohols, and those containing oxygen or sulphur bonded to phosphorus: the alkylphosphates such as tri-n-butyl-phosphate (TBP) and dibutyl-butylphosphonate (TBBP) and the alkyldithiophosphates e.g. the Cyanamid reagent 'Cyanex 471' in which the active reagent is tri-iso-butylphosphine sulphide which is effective in silver and palladium recovery.⁽²⁸⁾

In this work, one of the subclasses of category (i), namely the chelating extractants, are of interest. However before describing the nature of the reactions of these reagents, it is first necessary to give a description of the metal ion of concern to this work, its range of uses, methods employed for

the separation of the metal from its ores, some aspects of the geological occurrence of the metal and its economic importance.

1.1 The Uses, Mineral Origins and Traditional Procedure for the Recovery of Germanium from Multi-element Acidic Leach Liquors

Germanium is a grey-white metalloid with a high refractive index (approximately 4,1) and an electrical resistivity of 47,0 Ω cm (at 20°C) which is typical of semiconductors (resistivity silicon = 48,0 Ω cm). Purified to levels of 99,9999%, the metal currently fetches approximately US \$ 4000/kg (cf. gold US \$12000/kg). The applications of germanium and its oxide, GeO_2 , in the electronics industry and computer technology have been responsible for its classification as a 'strategic element' in terms of its role in defense systems.⁽²⁹⁾ Zone-refining techniques have led to production of crystalline germanium for use as a semiconductor element with an impurity of only one part in 10^{10} . Sometimes the metal is doped with arsenic or gallium producing a transistor element with many electronic applications. With tellurium, germanium forms a Ge-Te alloy with marked thermoelectric properties and as the magnesium salt magnesium germanate, it is a useful phosphor in fluorescent lamps. The metal and its dioxide are transparent to the infrared and are used in extremely sensitive infrared detectors. In addition, the high refractive index of GeO_2 has made it a useful component of glasses used in wide-angle camera lenses,

microscope objectives and optical fibres. The dioxide also has applications as a catalyst in the processing of polyester fibre.^(30,31) Certain germanium compounds have a low mammalian toxicity but high activity against certain bacteria rendering them useful as chemo-therapeutic agents.

Very few minerals contain more than 5% of germanium.

Renierite, a zinc-copper ore containing 6-8% Ge is mined extensively in Kipushi in Zaire and accounts (Table (1)) for about 27% of the total annual world production. The ore sphalerite (ZnS), is now the principal source of germanium although its concentration in this ore is usually less than 1%. The germanium is recovered as a by-product of the sulphuric-acid leach process and must be removed prior to zinc electrowinning because it seriously interferes with the electrolysis process. Another important source of germanium is the flue dust resulting from the burning of coal. The recovery of germanium from this source involves a number of conversion reactions which result in the formation of germanium tetrachloride.^(32,33)

	Mined Output (tons)	Smelter Output (tons)
Belgium	-	12,0
France	-	11,0
West Germany	-	10,0
Italy	10,0	11,0
Japan	-	13,0
Namibia	9,0	-
USA	16,0	16,0
USSR	9,0	9,0
Yugoslavia	-	1,0
Zaire	24,5	-
Others	21,6	-
World Total	90,7	92,0

Table (1). World production of germanium in 1977.⁽³⁴⁾

In the Southern African region there are two principal sources of germanium for exploitation; the Tsumeb Lead-Copper-Zinc-Silver deposit in South West Africa/Namibia and the coal reserves of Eastern Botswana. At Tsumeb, germanium is mined as the hypogenic materials germanite: $\text{Cu}_3(\text{GeFe})(\text{S,As})_4$ and renierite: $\text{Cu}_3(\text{Fe,Ge,Zn})(\text{S,As})_4$ and partly as briartite: $\text{Cu}_2(\text{Fe,Zn})\text{GeS}_4$ and Mawsonite: $(\text{Cu,Ge})_7(\text{Fe,Zn})_2(\text{Sn,As})\text{S}_{10}$.

Trace quantities of germanium are also mined as the ores summarised in Table (2). During the period 1954-1963, a germanium enriched concentrate from the Tsumeb deposit, assaying 0,2-0,5% Ge, yielded in excess of 50 tons of GeO_2 , which at the current price of US \$4000/kg, represents revenue of US \$200 million (equivalent to US \$20 million per annum).

Ore	Germanium Content
Tennanite	60 - 700 ppm
Enargite	500 ppm
Chalcocite	≤ 50 ppm
Galena	≤ 70 ppm
Willemite	0,05 - 0,13% m/m
Olivenite-Adamite	$\leq 0,28\%$
Mimetite	≤ 500 ppm
Duftite-Bayldonite	$\leq 0,11\%$

Table (2). Germanium content of some of the ore deposits at Tsumeb⁽³⁵⁾ in Namibia.

The second important source of germanium for the Southern African region are the coal deposits of Botswana and the fume from zinc smelters, (spent coal which usually contains high concentrations of zinc and other metals from the ore besides the metals originally present in the coal). Table (3)

summarises the composition of a sample of fume from a zinc smelter located at Tsumeb using coal from the Morupule coal field in Botswana, determined in this work by ICP-MS (VG Plasmaquad). The abundances shown are therefore indicative of the composition of the coal and metals picked-up from the ore during smelting. Even though the level of germanium is small (2,6 ppm), a preconcentration process could render the recovery of this source economically viable.

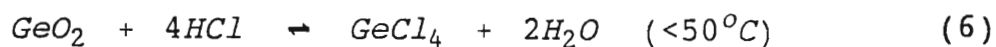
The recovery and refining of germanium from a smelter fume and the final production of electronic-grade GeO_2 is a fairly well established route. Usually, germanium in smelter fume is present as the volatile monosulphide which is first leached with sulphuric acid to dissolve the germanium and then recovered from solution by precipitation with tannin. After

Element	Concentration (ppm)	% of total
B	2,0	0,07
Na	53,9	2,00
Mg	11,2	0,41
Al	3,4	0,12
Ca	25,2	0,92
Cr	0,5	0,02
Mn	0,6	0,02
Fe	25,1	0,91
Cu	10,5	0,38

Element	Concentration (ppm)	% of total
Zn	2379,3	86,69
Ga	0,4	0,02
Ge	2,6	0,10
As	2,9	0,11
Mo	3,0	0,11
Cd	0,9	0,03
Pb	220,5	8,04
Bi	0,7	0,03
Others	2,0	0,07

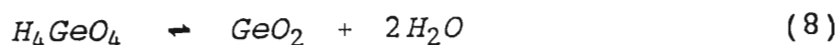
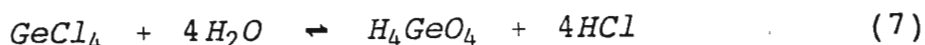
Table (3). Composition of a sample of fume from the Tsumeb zinc smelter. Source of coal: Morupule coal field, Botswana. Quantitation by ICP-MS of a nitric acid digest.

conversion to the oxide by ashing, a concentrate containing 5-20% germanium as GeO_2 is produced. This concentrate is fed to a converter containing 5,5-7,8 M HCl which converts the germanium to the volatile tetrachloride (b.p. $83,1^\circ\text{C}$) viz.

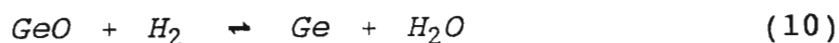
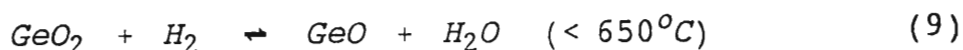


The tetrachloride is then fed, along with chlorine gas, into a distillation column from which reasonably pure GeCl_4 is

condensed. This product is then hydrolysed to GeO_2 (Equations (7) and (8)), which is then removed by filtration, washed, dried and calcined.



If pure metal is required, the dioxide is reduced by hydrogen in a two step process (Equations (9) and (10)), the first of which requires strict temperature control because GeO sublimes at 700°C .



The final procedures in the production of intrinsic semiconductor grade germanium are premelting and zone-refining.

1.2. Separation Procedures for the Recovery of Germanium in Aqueous Solution

The inherent complexity of the procedure described above and in particular the need for a multistep process, has led separation technologists into investigations of separation methods for the recovery of germanium from acidic leach liquors. Liquid-liquid extraction and resin separation methods have been the most widely studied. Various extractants such as long chain amines^(36,37), phosphinic acids⁽³⁸⁾, alkylphosphoric acids^(39,40), 8-hydroxyquinoline^(41,42), hydroxamic acids⁽⁴³⁾ and

alkylpyrocatechol⁽⁴⁴⁾ have been studied as well as many ion exchange resins e.g. Dowex 1⁽⁴⁵⁾, AN-31⁽⁴⁶⁾, AV-16G⁽⁴⁷⁾, EDE-10P⁽⁴⁸⁾, AN-2F, AV-17⁽⁴⁹⁾ and Amberlite XE-243⁽⁵⁰⁾, however the low loading capacity of these resins and extractants as well as their high cost and restrictive mode of use has limited their application.

Until recently, the most promising extractants for the preparative solvent extraction recovery of germanium were the α -hydroxyoxime compounds. In particular, Lix 63 (5,8-diethyl-7-hydroxy-6-dodecanone oxime, Table (4) structure(a)), which has been commercially available since 1963, is a chelating ligand which constituted a major advance in attempts to develop a copper-specific extractant. It has also been extensively studied as a reagent suitable for germanium extraction^(51,52) and has been tested at pilot-plant level.

A number of other chelating extractants, namely Kelex 100, Lix 64N, Lix 34, Lix 54, SME 529 and Acorga P 17 N⁽⁵³⁾ - see Table (4) for structures, as well as some acidic extractants e.g. D₂EHPA⁽⁵³⁾ and D₂EHDTPA^(53,54) (Table (4)), have also received some attention in the literature, however it is the 7-alkylated-8-hydroxyquinoline reagents, of which Kelex 100 is an example, which are of current interest.

Prior to 1976, Kelex 100 was a β -unsaturated 7-alkylated-8-hydroxyquinoline (Table(4), structure (b)) and was marketed by Sherex chemicals. Today, Kelex 100 is manufactured by Schering AG and possesses a significantly altered 7-alkyl side-chain (Figure (2)).

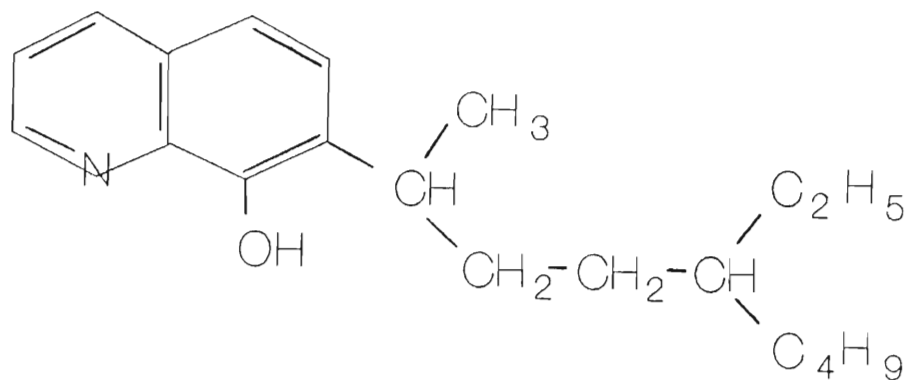
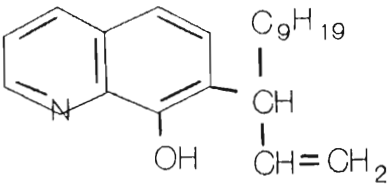
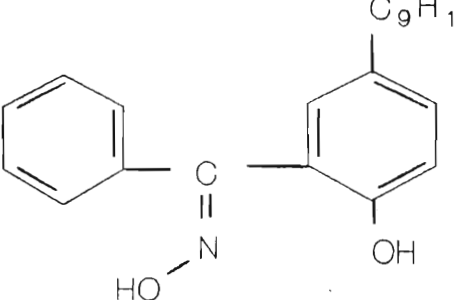
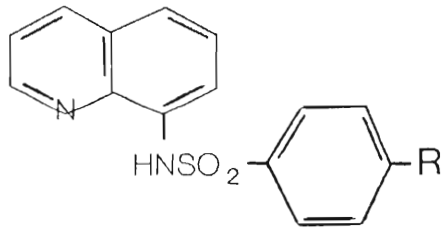
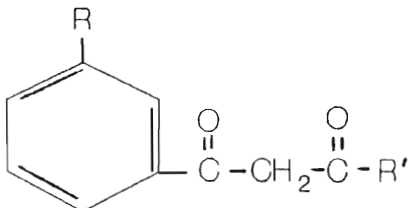


Figure (2). Post 1976 Kelex 100, 7-(4-ethyl-1-methyloctyl)-8-hydroxyquinoline.

Extractant	Formula	Supplier
Lix 63 a	$ \begin{array}{ccccccc} & & \text{C}_2\text{H}_5 & & \text{C}_2\text{H}_5 & & \\ & & & & & & \\ \text{H}_9\text{C}_4 & - & \text{CH} & - & \text{C} & - & \text{CH} & - & \text{CH} & - & \text{C}_4\text{H}_9 \\ & & & & & & & & & & \\ & & & & \text{HO-N} & & \text{OH} & & & & \end{array} $	Henkel
Kelex 100 (Pre-1976) b		Sherex
Lix 64N c	 <p>+ 1 % v/v Lix 63</p>	Henkel
Lix 34 d		Henkel
Lix 54 e		Henkel

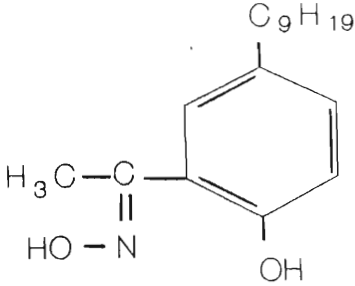
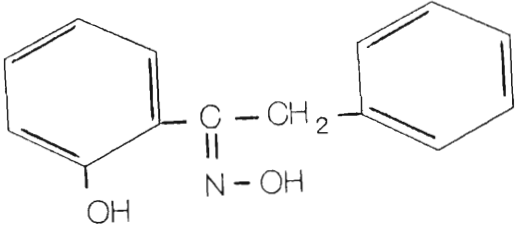
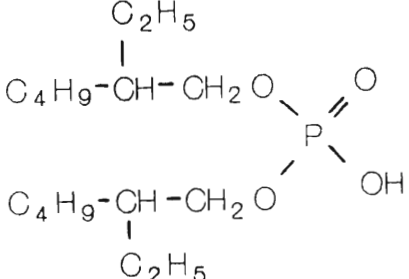
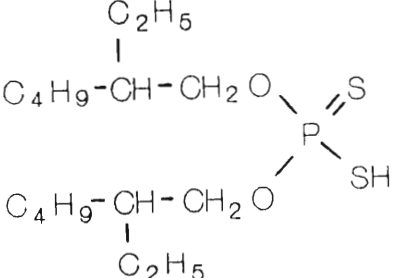
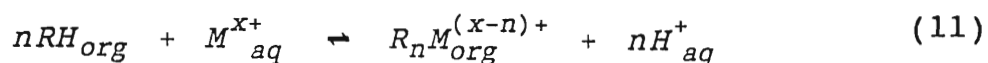
Extractant	Formula	Supplier
SME 529 f		Shell
Acorga P17N g		Imperial Chemical Ind
D2EHPA h		Mobil
D2EHDTPA i		No bulk supplier

Table (4). Some of the chelating (a-g) and acidic (h,i) extractants with application in germanium recovery by solvent extraction. 'Lix' = Liquid ion exchange reagent.

Kelex 100 is a bidentate hydrogen-donor ligand which, when used as an extractant, attaches to the metal ion via lone pairs of electrons on the nitrogen and phenolic oxygen according to the general equation:



where RH is the protonated form of the ligand and R_nM is the chelated metal ion with n ligands per metal and is extracted into the organic phase e.g. for Cu^{2+} , the organic-soluble metal-ligand adduct formed according to Equation (11) is:

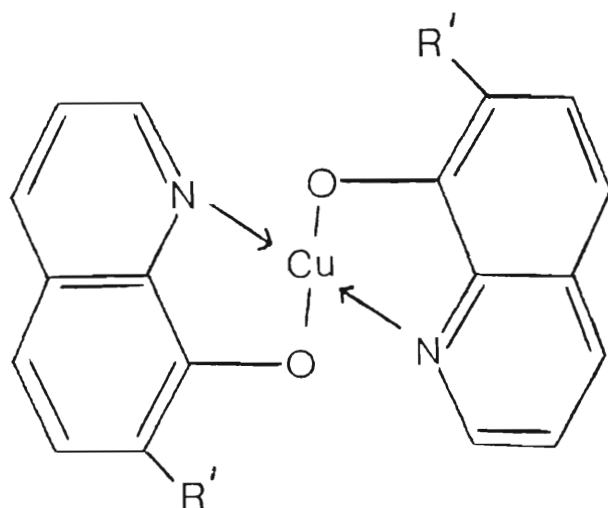


Figure (3). Structure of the charge-neutral complex CuR_2

R : Kelex 100 anionic species.

Over the last twenty or so years, Kelex 100 in one form or another has been used effectively in the quantitative recovery of Cu^{2+} (55-60), Co^{2+} (56,61), Ni^{2+} (62,63), Fe^{3+} (56,64) and Ge^{4+}

(53,65) and some selectivity tests have been performed with copper/iron feeds.⁽⁶⁶⁾

The principal aim of this study is to investigate the characteristics of the solvent extraction of germanium by three 7-alkylated-8-hydroxyquinoline reagents, namely Lix 26, TN 01787 and TN 02181. The first of these reagents is manufactured by Henkel and has been available commercially since 1979. It is supplied as an amber liquid of high viscosity (approximately $3,6 \times 10^{-3} \text{ N s m}^{-2}$ at 25°C) and containing 72% active ligand⁽⁶⁷⁾ with 28% reaction by-products and diluent. Lix 26 is essentially unproven as an effective reagent for germanium apart from one paper⁽⁶⁸⁾ which details only equilibrium data and provides no kinetic analysis of the extraction process nor any description of the effect of important parameters such as pH, ionic strength, ligand and germanium concentration, effect of added modifiers and the nature of the diluent etc., on the observed rate of germanium extraction. Although the identity of the active ligand in Lix 26 is not published, analytical work detailed in Chapter 2 of this thesis has identified the active constituent to be mainly an α -unsaturated straight chain C_{12} hydrocarbon chain at the 7-position of 8-hydroxyquinoline.

TN 02181 and TN 01787 are research formulations produced by Schering AG, and are also 7-alkyl derivatives of 8-hydroxyquinoline (Figure (4)). Briefly, TN 02181 possesses a β -unsaturated $\text{C}_{12}\text{H}_{23}$ 7-alkyl side chain and comprises a number of isomers, while TN 01787 is the α -unsaturated analogue of

post-1976 Kelex 100 (Figure (2)).

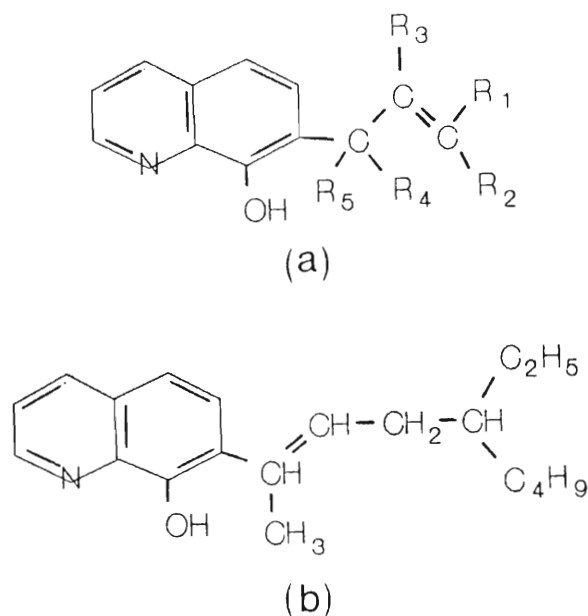


Figure (4). Structures of (a) TN 02181 and (b) TN 01787.
(Registered Patents of Schering AG, Germany)

A full description of these reagents, their purity and the nature of known impurities is presented in Section 2.2.1. To date, these products are untested in any metal extraction application, thus this work is the first publication of a possible commercial use of these reagents.

In this study, the most important goal is the proposal of a mechanistic model for the solvent extraction of germanium by the 7-alkylated-8-hydroxyquinoline reagents discussed above. The mechanism should account for at least qualitatively, but where possible quantitatively, the most important parameters which affect the rate of extraction and the equilibrium percentage extraction.

1.3. General Description of an Elementary Kinetic Model for Metal Extraction by Chelating Ligands

The classical mechanism for metal chelate extraction, Figure (5), requires partition of the chelating agent, HL, from the organic phase into the aqueous phase where it ionizes.

Following sequential stepwise chelate formation the neutral metal-chelate partitions back into the organic phase. The scheme allows for the removal of the metal ion via four concurrent pathways viz. complexation of M^{n+} with neutral ligand, HL and ligand anion L^- both in the aqueous phase and at the liquid-liquid interface.

BULK ORGANIC

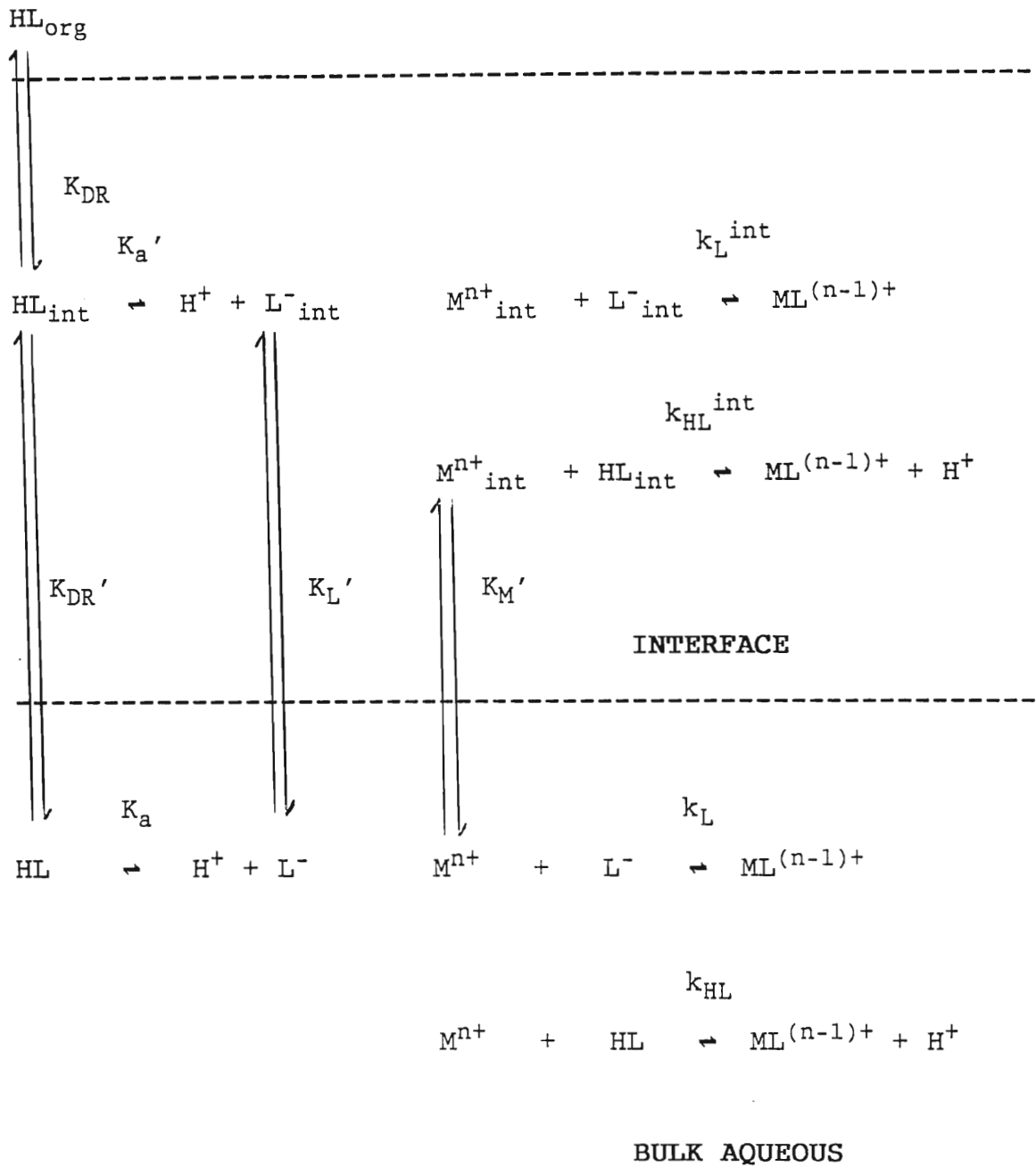


Figure (5). Classical scheme for the solvent extraction of a metal-ion, M^{n+} , by an organic-soluble ligand, HL.

Such a scheme yields a set of equations which can be manipulated to give a relationship between the rate of removal of M^{n+} from the aqueous medium, the bulk aqueous phase pH and bulk organic concentration of un-ionised ligand HL and the various equilibrium constants appropriate to the model i.e. assuming that the metal ion coordinates with a single ligand molecule:

$$-\frac{d[M^{n+}]}{dt} = k_{obs}[M^{n+}][HL] \quad (12)$$

k_{obs} : observed rate constant

Ignoring back reactions , the total rate of removal of metal from aqueous solution is:

$$-\frac{d[M^{n+}]}{dt} = (k_L^{int}[M_{int}^{n+}][L_{int}^-] + k_{HL}^{int}[M_{int}^{n+}][HL_{int}]) + k_L[M^{n+}][L^-] + k_{HL}[M^{n+}][HL] \quad (13)$$

Defining the distribution of ligand, ligand anion, metal ion and the acid dissociation equilibria in the interface and bulk organic and aqueous phases as follows:

$$K_{DR} = \frac{[HL]_{org}}{[HL_{int}]} \quad (14)$$

$$K'_{DR} = \frac{[HL_{int}]}{[HL]} \quad (15)$$

$$K'_a = \frac{[H^+][L_{int}^-]}{[HL_{int}]} \quad (16)$$

$$K_a = \frac{[H^+][L^-]}{[HL]} \quad (17)$$

$$K'_L = \frac{[L_{int}^-]}{[L^-]} \quad (18)$$

$$K'_M = \frac{[M_{int}^{n+}]}{[M^{n+}]} \quad (19)$$

and substituting Equations (14) - (19) into (13) where appropriate gives:

$$\begin{aligned} -\frac{d[M^{n+}]}{dt} = [M^{n+}][HL]_{org} & \left(\frac{K_L^{int} K'_M K'_a}{K_{DR}[H^+]} + \frac{k_{HL}^{int} K_M}{K_{DR}} \right. \\ & \left. + \frac{k_L K_a}{K_{DR}^{//}[H^+]} + \frac{k_{HL}}{K_{DR}^{//}} \right) \quad (20) \end{aligned}$$

where
$$K_{DR}^{//} = \frac{[HL]_{org}}{[HL]}$$

Equation (20) demonstrates that for the model considered, the rate of extraction of the metal is not only dependent upon the ligand concentration, but is also a function of the pH. k_{obs} in Equation (12) is therefore a combination of the constants K'_M , K'_a , K_{DR} , K_a and $K_{DR}^{//}$.

The important factor in the model shown in Figure (5) is the role which is played by the interface. Prior to the mid-70's, all chemical kinetic studies of metal-chelate extraction were interpreted with apparent success using a two-phase model which viewed the chemical reactions occurring entirely in the bulk aqueous phase. Clearly such a model would require a reasonable degree of reagent solubility in the aqueous phase to be credible and thus a problem with interpreting the kinetic behaviour of proprietary reagents such as Lix 63: aqueous solubility 0,006 g/l, Lix 65N: solubility approximately 0,006 g/l and Kelex 100: solubility <0,001 g/l, was encountered. For example, insertion of the value of the distribution constant for Kelex 100 of $10^{4,70}$ for K_{DR} into Equation (20) renders the last two terms in the brackets insignificant in comparison with the first two. In the absence of any interfacial terms, it would thus be almost impossible to give an adequate (and credible) reason for any observed extraction without invoking some 'other' means by which extraction may proceed.

For the last two decades, kineticists have adopted some form of three phase model analogous to the one of Figure (5) in order to give a precise description of the kinetic processes which are rate limiting. The advantage of employing such a model is that it is not specific as regards the locale of the reaction and therefore embraces all the possibilities of the extraction mechanism, viz. reaction in a homogeneous aqueous phase or a heterogeneous reaction, or a combination of both. To date the triphasic model has been successful in rationalizing observed rate data of a host of solvent extraction systems, however

there are problems associated with the manner in which investigators have approached their kinetic studies of solvent extraction mechanisms and a brief assessment of the common methods employed in this regard is presented below.

The manner in which separation chemists and engineers have regarded solvent extraction has been chiefly to consider it as a classical mass-transfer process in which the primary source of 'resistance' to the mass-transfer is the diffusion of species from one phase to another. This disregards chemical reaction rate constants. In order to simplify the interpretation of their data, these workers favour experiments in which the interfacial area is well-known and relatively small. Fixed interfacial area assemblies^(59,69-73), thus have one disadvantage over high-dispersion designs in that the reaction is assumed to be either diffusion or interfacially-controlled. If the extraction rate is diffusion-controlled, it will depend on the interfacial area and the concentration of the slow-diffusing species whereas if interfacial chemical reactions are rate controlling, the significant parameters are the interfacial area, interfacial concentration of reacting species, the rate constant for the slow reaction step and the molecular orientation of the reactive species at the interface- this latter property being indicated by interfacial physical chemical phenomena such as the interfacial tension. Under conditions in which the interfacial reaction is rate-determining, the composition of the interface will be essentially that of reactants only.

Most fixed interface experiments have been performed in either:

- (i) a Lewis Cell⁽⁷²⁾ which is designed such that the

phases in contact with one another are stirred separately at a rate which ensures the replenishment of active ligand to and removal of products of the reaction from the interface or,

(ii) a rising (or falling) drop apparatus in which droplets of one phase are allowed to rise or fall through a vertical column containing the second phase.^(70,71) In the most practical contactors (termed 'single file' contactors), a steady flow of individual solution droplets (either ligand-containing solvent or metal-containing aqueous solution) are allowed to descend from a fine-bore burette fitted with a teflon needle valve, which provides a reproducible and slow rate of addition, through a column containing the other phase. Typically, columns are of the order of 5-7 cm in diameter and of variable length. Droplets are allowed to collect at the base of the column and samples of the loaded organic can be removed as required. Reaction at the droplet interface occurs in three different stages: (1) during formation at the nozzle; (2) during rise or fall and (3) during coalescence at the base of the column and at the micro-interface which is established there. Like the Lewis Cell apparatus, droplets are of known size and hence interfacial area and thus the rate of interfacial mass transfer per unit interfacial area can be accurately calculated.

The current body of opinion is that for technique (i), the vigour of stirring is severely limited by the requirement that the interface remain static and it is doubtful that diffusion effects are completely eliminated if this experimental prerequisite is adhered to, while technique (ii) has been

criticized for not overcoming diffusion effects in the droplet i.e. the droplet is a sphere which, during its descent (or ascent) encounters reactant at the phase boundary. Mass transfer and diffusion are strongly enhanced when there is internal circulation of material within the drop, however once a monolayer of, for example, ligand has formed at the droplet surface, such internal circulation is reduced or even prevented and in this way unreacted metal may never, during the course of the lifetime of the droplet, encounter a ligand species. Moreover, there are doubts as to whether the boundary monolayer is renewed at a rate which is indicative of the reaction occurring at the phase boundary or whether observed rates are a function also of the restricted diffusion of chemical species to the reactive sites.

In conclusion of this discussion of fixed interface kinetic studies, it is noteworthy that in each of these designs, quite different hydrodynamic conditions are created compared with practical mixer devices. While the droplet contactor at least emulates mass-transfer conditions applicable to vigorous mixing on a micro-scale i.e single drops, there are limitations to the predictability of data acquired in this way in that the hydrodynamic conditions are dimensionally inappropriate.

In view of the limitations inherent in fixed-interface designs, most workers employ a high-speed mixing assembly for carrying out kinetic studies of solvent extraction. Under conditions of vigorous shaking^(74,75) or high-speed stirring⁽⁷⁶⁾, mass transfer diffusion rates in metal-chelate solvent extraction processes are much greater than chemical

reaction rates. The observed kinetics are therefore indicative of the slower i.e. rate-determining chemical reaction. The trend at present then for the study of extraction kinetics involves vigorous shaking or stirring of the two phases. Such experiments reach the fastest possible extraction rates regardless of whether the rate-determining step in the mechanism involves a **homogeneous** chemical reaction, in which the important parameters will be the solubility of the reactants, their distribution coefficients, ionization constants and phase volume or a **heterogeneous** reaction at the interface. For the former, high dispersion reduces the time required for mass-transfer processes so that diffusion effects are not involved in the observed reaction rate (and rate equations), while for the latter, high dispersion maximizes the interfacial surface area and therefore the rate of extraction.

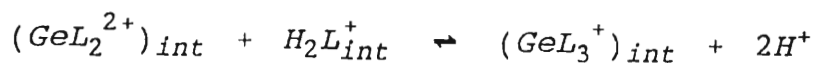
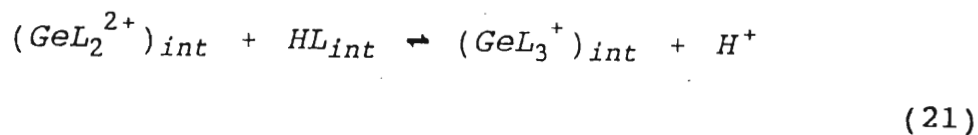
In this work, the solvent extraction kinetics of germanium by 7-alkylated-8-hydroxyquinoline reagents is studied via the use of three experimental assemblies, namely a Lewis Cell arrangement, a mechanical shaker and an AKUFVE apparatus, the last two of these methods create conditions of maximum surface area and high dispersion. In essence, the AKUFVE apparatus, which comprises a mixer and a centrifuge which separates the phases after contact and which allows for on-line manual sampling, is no more than a convenient form of shaker, however results presented in this work demonstrate some differences in the kinetics and equilibrium extraction obtained, thus raising questions vis-à-vis the validity of data obtained with this assembly.

The greatest problem associated with kinetic studies in vigorous-stirring assemblies is the uncertainty attached to the interfacial area. Most workers operate their extraction systems at a very high (but constant) speed in order to overcome any diffusion effects and under these conditions, the interfacial area is an unknown, large, but essentially constant parameter. A knowledge of the parameter would certainly be a useful inclusion in any kinetic model, particularly when considering a scale-up operation. The Microporous Teflon Phase Separator (MPTS) is a recent innovation^(77,78) which permits sampling of the organic phase, via a teflon separator, while it is still intimately in contact with the aqueous phase during vigorous-stirring conditions. One of the advantages of this system is that it facilitates an approximation of the interfacial area during mixing. Unfortunately such apparatus was not available in the course of this work.

There are a number of important parameters omitted on the kinetic scheme of Figure (5). Certain physical characteristics such as the interfacial tension, viscosity and dielectric strength have implications for the rate of extraction-as do the chemical influences of ionic strength of the aqueous medium, nature of the organic diluent, concentration of ligand and the presence of impurities in the commercial reagent. Moreover, the kinetics of extraction and equilibrium yields of metal can be improved by the addition of organic modifiers which are so specific in their effect that they cannot be incorporated in the model. The relevance of all these effects is discussed in this work with particular emphasis placed upon general quantitative treatment of data in order to create a

generally applicable kinetic model.

It is clear that in any multi-step reaction process, the observed kinetics yield information only of the slowest process. In this work, a majority of the studies of effects of the parameters, discussed *vide ut supra*, on the extraction kinetics of germanium were performed at very low pH i.e. sulphuric acid concentration of 1,5 M in the germanium-containing aqueous phase. It is demonstrated in this work that, at this pH, germanium extracts as an ion-association tri-ligand chelate $GeL_3^+ HSO_4^-$, where L is any of the ligands Lix 26, TN 02181 or TN 01787, in two discrete reaction regimes: a fast initial rate which accounts for a high percentage of the total extraction and a slower subsequent reaction regime. It is proposed that the rate-determining step in the formation of this species is the stereochemically-controlled reaction of a GeL_2^{2+} precursor with a molecule of neutral ligand at the interface in the slow reaction regime and with a protonated ligand moiety in the fast regime (Equations 21).



A molecular modelling program, Alchemy⁽⁷⁹⁾, was utilised for the calculation of energy-minimized structures of the chelates and intermediates and to describe other interactions (such as those between ligand molecules and modifiers). One such

structure is shown in Figure (6) and this illustrates the stereochemical constraints intrinsic to Equation (21) - the germanium ion, which is not visible in the spacefill diagram, is enclosed by the 8-hydroxyquinoline chelate centres which are in turn surrounded by the hydrophobic Lix 26, 7-alkyl side chain envelope. The stereochemical constraints mentioned above are apparent in Figure(6): for the reaction given by Equation (21) to occur, the incoming ligand must be correctly oriented with regard to the N and O chelate centres and it must also overcome Van der Waals repulsion energies and steric effects in order to bind. Furthermore, both the GeL_2^{2+} precursor and incoming monomer are restricted translationally since the aqueous phase cannot accommodate the hydrophobic side chains of these molecules.

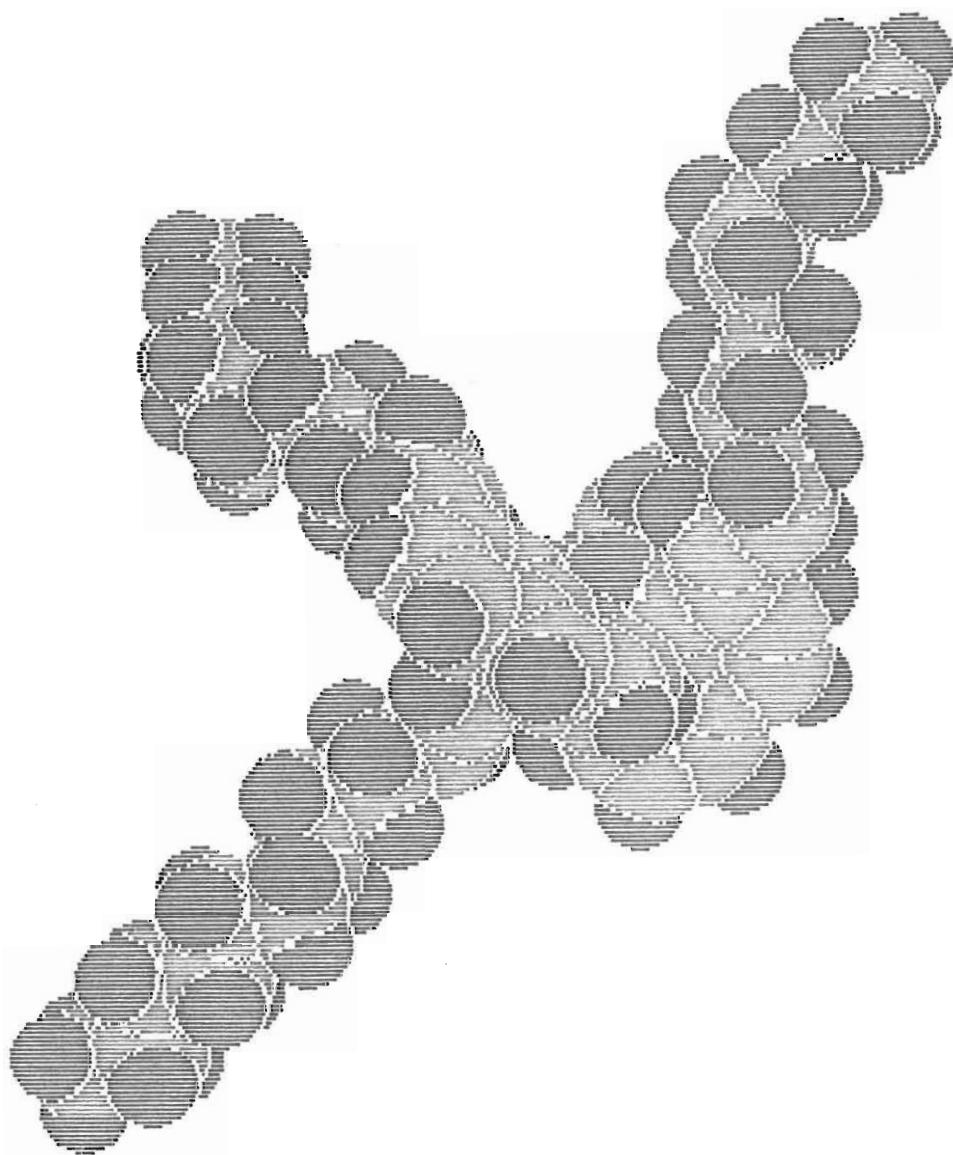


Figure (6). The Alchemy minimized tri-ligand Lix 26-germanium chelate. The oxygen (in red) and nitrogen (in blue) donor atoms of two ligand molecules are just visible. The germanium ion is obscured by the chelate centres.

In summary, the aims of this research are:

- (1) To assess the techniques available for rapid and accurate quantitative analysis of germanium in aqueous solution,
- (2) To elucidate the major contributing parameters to the kinetics of germanium extraction, including those which disfavour chelation,
- (3) To emphasize throughout, the role which is played by the interface during extraction,
- (4) To compare and contrast the behaviour and efficiency of three ligand formulations Lix 26, TN 02181 and TN 01787,
- (5) To give a visual representation, in two dimensions, of the energy minimized structures of the ligand monomers, impurities and germanium-ligand chelates and therefore predict the conformation of these molecules as they exist at the interface,
- (6) To propose an holistic kinetic model for germanium extraction (based on the three-phase model of Figure (5)), which includes all equilibria, partition effects and various physical phenomena appropriate to the system such as interfacial tension, dielectric constant etc.,
- (7) To recommend which of the ligand reagents is the most suitable, on kinetic and equilibrium percentage extraction criteria for germanium extraction (within the limits of the experimental conditions tested in this work) and
- (8) To present an overview of the relevant literature pertaining to developments which have been made over the last 20 years in the interpretation of kinetic data

appropriate to solvent extraction and to discriminate between the models which have been presented on the grounds of the experimental configurations used.

The Chapter which follows, summarises the experimental methods performed and describes the various practical assemblies which were utilised for solvent extraction studies of germanium.

CHAPTER 2

EXPERIMENTAL

This section of the thesis consists of four broad categories:

- (1) Details of chemicals used in experiments (Section 2.1).
- (2) Procedures for the isolation, purification and identification of the components of the 'as-supplied' alkylated-8-hydroxyquinoline ligand reagents (Section 2.2).
- (3) Analytical methods for the quantification of aqueous phases containing germanium (Section 2.3).
- (4) Experimental techniques for the investigation of the kinetics and equilibria relating to the solvent extraction of germanium and the appropriate procedures for the measurement of physical properties of the extraction kinetics (Sections 2.4 and 2.5).

The section which follows immediately details the chemicals used in this work and is followed by procedures for the purification of the ligand reagents tested and data relating to the identification of the active constituents of the commercial reagents.

2.1. Materials

Details of chemicals used in this work are listed below in the order; name, chemical grade, supplier, percentage assay and any other relevant information.

2.1.1. Chemicals For Solvent Extraction and Stripping Experiments

Germanium Dioxide (Electronic)	Aldrich	Assay 99,999%
Heavy Distillate (Suitable for use in testing petroleum products by Institute of Petroleum and American Standards and Testing of Materials methods)	BDH	Density 0.78g/l
Hexane (AR)	Saarchem	Assay min 98%
8-Hydroxyquinoline (AR)	Riedel-de Haën	Assay min 99%
Sodium Hydroxide (AR)	Kleber	Assay min 98%
Sodium Perchlorate (LAB)	BDH	Assay min 97%
Sodium Sulphate (LAB)	Kleber	Assay 99,2%
Sulphuric Acid (LAB)	Saarchem	Assay 97-98%
Toluene (AR)	Kleber	Assay 99,4%

The ligand preparations used in this work are listed below. The purities and characteristics of these reagents are further discussed in Section 2.2.

<u>Ligand</u>	<u>Supplier</u>	<u>Percentage Purity</u>
Lix 26	Henkel	72
Kelex 100	Schering AG	84-87
TN 02181	Schering AG	84
TN 01787	Schering AG	87

2.1.2. Chemicals For Preparing Buffered pH Solutions

Hydrochloric Acid (LAB)	Saarchem	Assay min 32%
		Density 1,16 g/ml
Potassium Chloride (AR)	Merck	Assay min 99,5%
Potassium Dihydrogen Phosphate (AR)	BDH	Assay min 99,5%

Potassium Hydrogen Phthalate (LAB)	BDH	Assay min 99,5%
Potassium Nitrate (AR)	BDH	Assay min 99,5%
Sodium Hydroxide (AR)	Kleber	Assay 98%

2.1.3. Chemicals For Phenylfluorone UV Determination of Germanium

Ethanol (Absolute)	Saarchem	Assay 99%
Gelatine (Microbiological)	Holpro	
Phenylfluorone	Merck	Assay 98,5%
Sulphuric Acid (LAB)	Saarchem	Assay 97-98%

2.1.4. Chemicals For Germanium Titration With Mannitol

Mannitol (AR)	BDH	Assay 99%
p-Nitrophenol (LAB)	Aldrich	Assay 98-99%
Phenolphthalein (AR)	PAL	Assay 99%
Sodium Hydroxide (AR)	Kleber	Assay 98%
Sodium Tetraborate (LAB)	Holpro	Assay 98%

2.1.5. Chemical Modifiers Used in Extraction Experiments

Benzyl Alcohol (AR)	Saarchem	Assay 99,5%
n-Butanol (ARISTAR)	BDH	Assay 99,9%
n-Octanol (AR)	Merck	Assay 99%
n-Pentanol (LAB)	Saarchem	Assay 98%
n-Propanol (GC)	Merck	Assay 99%

2.1.6. Chemicals For Thin Layer Chromatography

Acetone (AR)	Saarchem	Assay 99,5%
Aluminium Sulphate (LAB)	Saarchem	Assay 97%
Carbon Tetrachloride (AR)	Saarchem	Assay 99,5%

TLC Plates : Qualitative : Merck Silica gel 60 aluminium foil
without fluorescent indicator,
layer thickness 0,2 mm

Quantitative : Merck Silica gel 60, glass plate
20 cm x 20 cm without fluorescent
indicator, layer thickness 2 mm

2.1.7. Chemicals For Column Chromatography

Acetone (AR)	Saarchem	Assay 99,5%
Carbon Tetrachloride (AR)	Saarchem	Assay 99,5%
Silica Gel	Merck	Particle Size 0,04 - 0,063 mm (230-400 mesh)

2.1.8. Chemicals For Acid-Wash Purification of Ligand Preparations

Hydrochloric Acid (LAB)	Saarchem	Assay min 32%
Sulphuric Acid (LAB)	Saarchem	Assay 97-98%
Toluene (AR)	Kleber	Assay 99,4%

2.1.9. Chemicals For Zinc Extraction Trials

Zinc Metal	Merck	Assay 99,9%
Zinc Sulphate (AR) Heptahydrate	BDH	Assay 99,5%

2.1.10. Addresses of Chemical Suppliers

Aldrich Chemical Company Inc.	BDH Chemicals Ltd
1001 West Saint Paul Ave	Broom Rd
Milwaukee	Poole, Dorset
Wisconsin 53233	BH 12 4NN
USA	England

Henkel Corporation
Suite 104
1844 West Grant Rd
Tucson, AZ 85745-1273
USA

Holpro Analytics (Pty) Ltd
1 Snell St
Micor
Johannesburg
South Africa

Kleber Chemicals (Pty) Ltd
P.O. Box 12018
Jacobs, 4026
South Africa

E. Merck
250 Frankfurterstrasse
D-6100 Darmstadt
Germany

Riedel-De-Haën AG
Wunstorfer Straße 40
P.O. Box
D-3016 Seelze
Hannover
Germany

Saarchem (Pty) Ltd
P.O. Box 144
Muldersdrift
1747
South Africa

Schering AG
Postfach 15 40
D-4709
Bergkamen
Germany

Sigma Chemical Corporation
P.O. Box 14508
St. Louis
Mo, 63178
USA

2.2. Reagent Purity, Techniques For Purification , Isolation and Identification of the Active Ligand Components and Impurities

2.2.1. Description of the Ligand Preparations

The structure of the 'active' ligands in the Schering research products TN 02181 and TN 01787 are given in Figure (7) below:

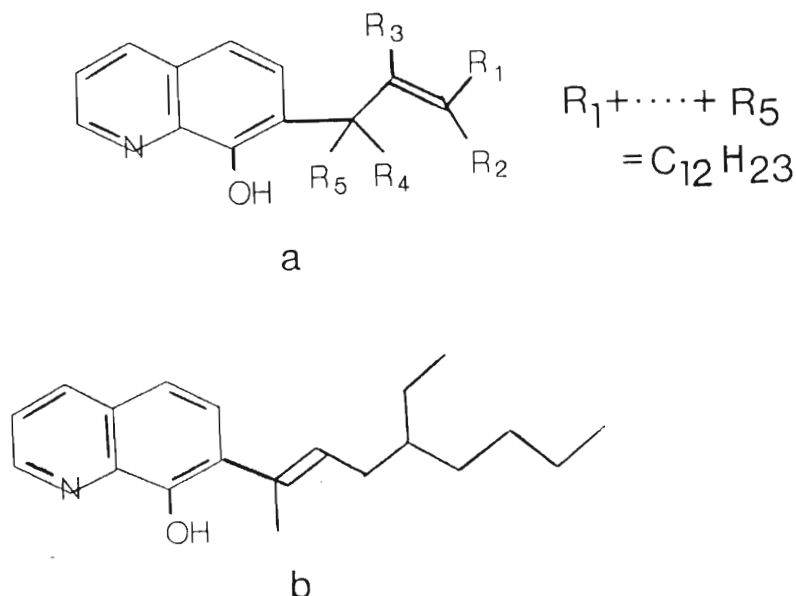


Figure (7). Structures of (a) TN 02181 ; 7-alkyl = $C_{12}H_{23}$ (β - dodecenyl) and (b) TN 01787 ; 7-alkyl = $C_{11}H_{21}$ (α - undecenyl).

TN 02181 is a special grade of another research product produced by Schering AG labelled 'TN 01911'. The preparation is supplied with no diluent and comprises a mixture of several isomers with an average of 12 carbon atoms in the β - unsaturated side chain. Consequently, the suppliers cannot determine the percentage of active compounds by GC analysis⁽⁸⁰⁾. The sample is reported⁽⁸⁰⁾ to have an 8-

hydroxyquinoline content of 0,2% m/m and a copper-loading of 97,3 g/kg which is 95,2 % of the theoretical yield assuming the formation of a 2:1 ligand:Cu complex. The copper-loading is an indication of the purity of the ligand preparation and entails the potentiometric evaluation of the quantity of copper consumed from a phthalate-buffered CuSO_4 solution, by an exact mass of the ligand preparation dissolved in isopropanol⁽⁸¹⁾. The copper consumption is recorded as g copper/ kg ligand. For the figure quoted above, it would not be unreasonable to assume that TN 02181 is as pure as the specification given for Kelex 100 of 84-87% m/m⁽⁸¹⁾ which has a copper loading of 90-97 g/kg.

TN 01787 is the α -unsaturated precursor of Kelex 100. GC analysis of the sample by the suppliers yielded the following average percentage composition (Table (5)) for this product.

% by mass (determined by GC)	Component
0,7	8-hydroxyquinoline
0,4	7-octenyl-8-hydroxyquinoline
0,9	C ₂₂ - ketone
88,0	7-undecenyl-8-hydroxyquinoline (2 isomers)
2,7	unsaturated furoquinolines
7,4	'higher compounds', possibly also furoquinolines and some 5,7-dialkyl-8-hydroxyquinoline derivatives

Table (5). Percentage composition and identity of the components of TN 01787⁽⁸⁰⁾.

The copper loading for this product is quoted⁽⁸⁰⁾ as 101,3 g/kg (94,7 % of theoretical), indicating a slightly higher purity than TN 02181. Again, the extractant was supplied containing no added diluent.

Unlike the Schering research products discussed above, Lix 26 (Henkel), has been commercially available since 1979 and has already assumed great importance in the hydrometallurgy of copper⁽⁸²⁾, however chemical specifications for the product have not been established⁽⁸³⁾. The product is approximately 72%

pure, the remaining 28% being reaction by-products and diluent⁽⁶⁷⁾.

An obvious prerequisite for an investigation of the kinetics of solvent extraction of a metal ion, in this case germanium, by a ligand preparation is a knowledge of the exact structures of the extractant molecule(s) and any component impurities. It was therefore necessary to undertake an investigation of purification routes for Lix 26.

To facilitate a clear perspective of the magnitude of this undertaking, it is worth summarizing the details of the chemical route to the industrial scale preparation of 7-alkylated-8-hydroxyquinoline extractants and to identify the side products which arise during the synthesis. The scheme outlined in Figure (8) summarises the relevant details as best as can be deciphered from chemical patents⁽⁸⁴⁾.

The procedure comprises four stages : two aldol condensations (steps 1 and 3) and two catalysed hydrogenation reactions (steps 2 and 4). For the scheme depicted, structures I and II correspond to the active constituents of TN 01787 and Kelex 100 respectively. The preparation of TN 02181 and Lix 26 would involve substituting an alternative aldehyde into step(1) of the process.

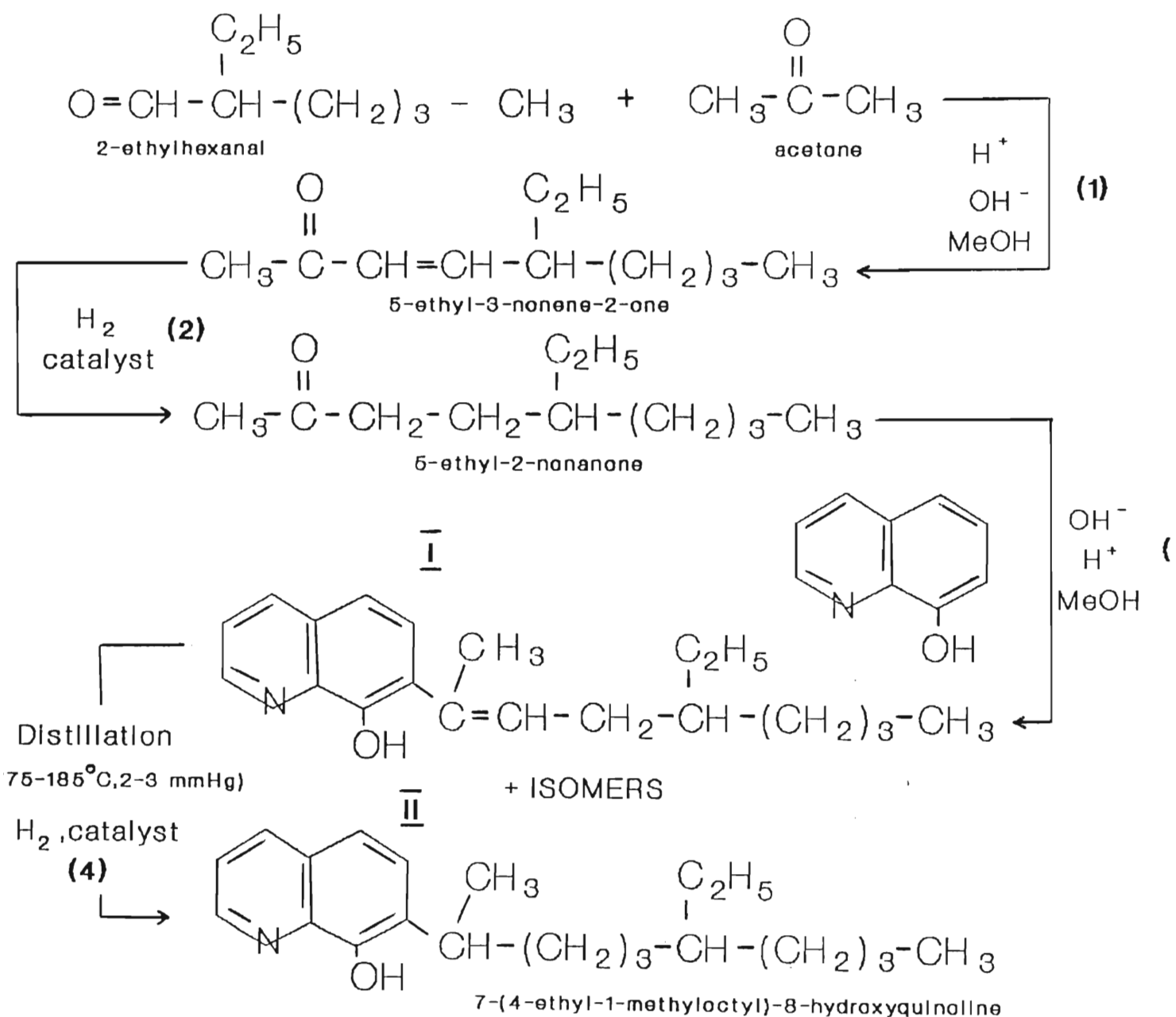
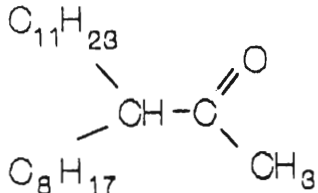
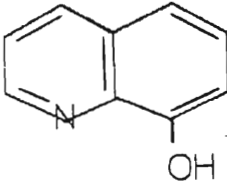
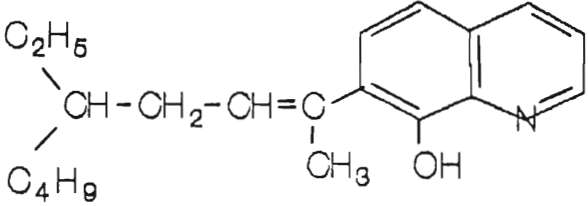
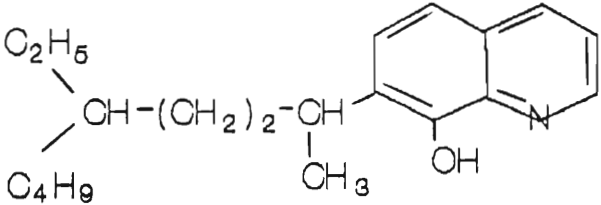
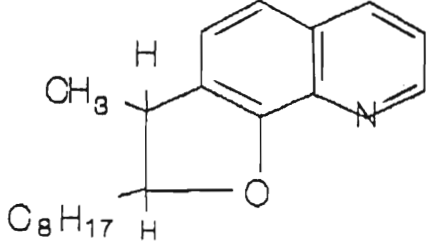
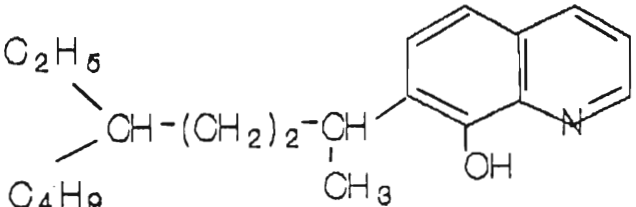
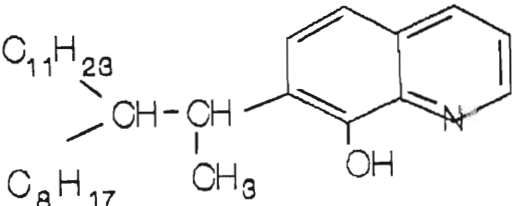


Figure (8). Preparative route for the synthesis of 7-alkylated-8-hydroxyquinoline extractants.

Two recent reports^(85,86) have dealt with the identification and quantification of the impurities in Kelex 100. In particular, Gareil *et al.*⁽⁸⁶⁾ identified twelve products in a sample of commercial grade Kelex 100 by submitting fractions collected from an LC column (Spherisorb-phenyl 5 μ m) to a mass spectrometer. The structures of these impurities and their approximate percentage by mass in the commercial product, are listed in Table(6).

Molecular weight	Approx % by mass	Structure
(1) 324	< 0,1 %	
(2) 145	0,5 %	
(3) 172	< 0,1 %	$\text{CH}_3\text{-CH(OH)-CH}_2\text{-C}_8\text{H}_{17}$

Molecular weight	Approx % by mass	Structure
(4) 257	1 %	 <p>Chemical structure showing a quinoline ring system with a hydroxyl group (OH) at position 5. The ring is substituted at position 1 with a side chain: C_2H_5 and C_4H_9 are attached to a CH group, which is double-bonded to a $\text{CH}=\text{C}$ group. The $\text{C}=\text{C}$ double bond is also substituted with a CH_3 group.</p>
(5) 297	0,5 %	 <p>Chemical structure showing a quinoline ring system with a hydroxyl group (OH) at position 5. The ring is substituted at position 1 with a side chain: C_2H_5 and C_4H_9 are attached to a CH group, which is single-bonded to a $(\text{CH}_2)_2$ group, which is then single-bonded to a CH group. The CH group is also substituted with a CH_3 group.</p>
(6) 297	0,5 %	 <p>Chemical structure showing a quinoline ring system with a hydroxyl group (OH) at position 5. The ring is substituted at position 1 with a side chain: a CH group is bonded to a CH_3 group and a C_8H_{17} group. The CH group is also bonded to a hydrogen atom (H).</p>
(7) 299	82 %	 <p>Chemical structure showing a quinoline ring system with a hydroxyl group (OH) at position 5. The ring is substituted at position 1 with a side chain: C_2H_5 and C_4H_9 are attached to a CH group, which is single-bonded to a $(\text{CH}_2)_2$ group, which is then single-bonded to a CH group. The CH group is also substituted with a CH_3 group.</p>
(8) 453	3 %	 <p>Chemical structure showing a quinoline ring system with a hydroxyl group (OH) at position 5. The ring is substituted at position 1 with a side chain: a CH group is bonded to a $\text{C}_{11}\text{H}_{23}$ group and a C_8H_{17} group. The CH group is also bonded to a hydrogen atom (H). The C_8H_{17} group is also bonded to a CH_3 group.</p>

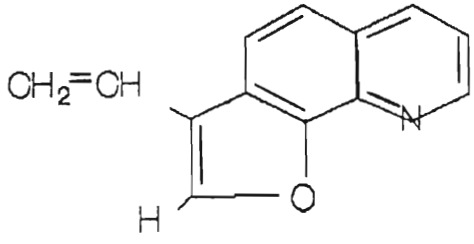
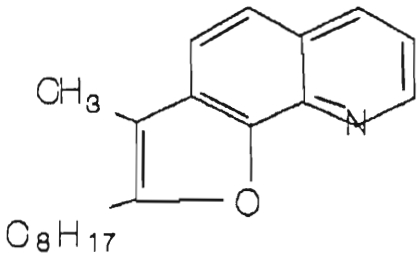
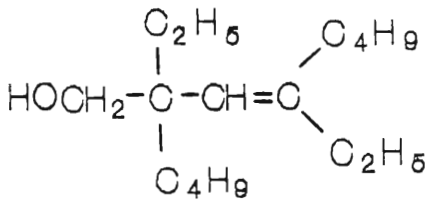
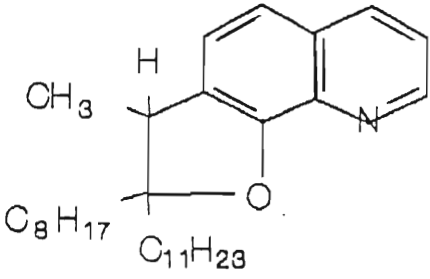
Molecular weight	Approx % by mass	Structure
(9) 295	4,5 %	
(10) 195	~ 8 %	
(11) 240	< 0,1 %	
(12) 451	0,2 %	

Table (6). The structure of the impurities and their approximate percentage in commercially available Kelex 100.⁽⁸⁶⁾

It is important to note that some of these products may actively complex metal ions and subsequently extract them into

an appropriate organic medium (structures 4,5,7 and 8), while others are unlikely complexing agents (structures 6,9,10 and 12 are furoquinoline derivatives with bonded oxygen atoms and therefore not amenable to chelate formation- cases do, however, exist where such oxygen atoms bond to metal ions), but may or may not play an active role in germanium extraction.

The sections (2.2.2) which follow describe procedures which were performed for the purification of Lix 26, primarily to facilitate the elucidation of the structure of the active component, but also to determine at least qualitatively, the presence of any of the impurities *vide ut supra*. Data is also presented for the separation of the components of the TN research formulations.

2.2.2. Thin Layer and Column Chromatographic Separation of Reagent Components

Procedures for the chromatographic separation of the components of Kelex 100 by silica gel plates and columns have been reported by Ashbrook^(87,88) and were modified for use in this study. Section 2.2.2.1 will describe the procedure and results obtained for **qualitative** separation of the components of Lix 26 and the TN research products. Section 2.2.2.2 will detail the procedure used for the bulk-purification of the reagents to facilitate the taking of nmr, infra-red, ultraviolet and MS spectra of those components which were adequately resolved by this technique.

2.2.2.1. Thin Layer Chromatography

TLC plates used for qualitative studies were Merck aluminium foil silica gel 60 without fluorescent indicator, layer thickness 0,2 mm. Preparative plates were of the same composition but of 2 mm thickness. Samples were dissolved in carbon tetrachloride, spotted onto the plate, dried and eluted with carbon tetrachloride. The plates were developed with a 1 M solution of $\text{Al}_2(\text{SO}_4)_3$ which stains all reagent components green/yellow. Figure (9) shows the resolution of the components of the three reagents on the TLC plate. R_f values for the components shown in Figure (9) are given in Table (7).

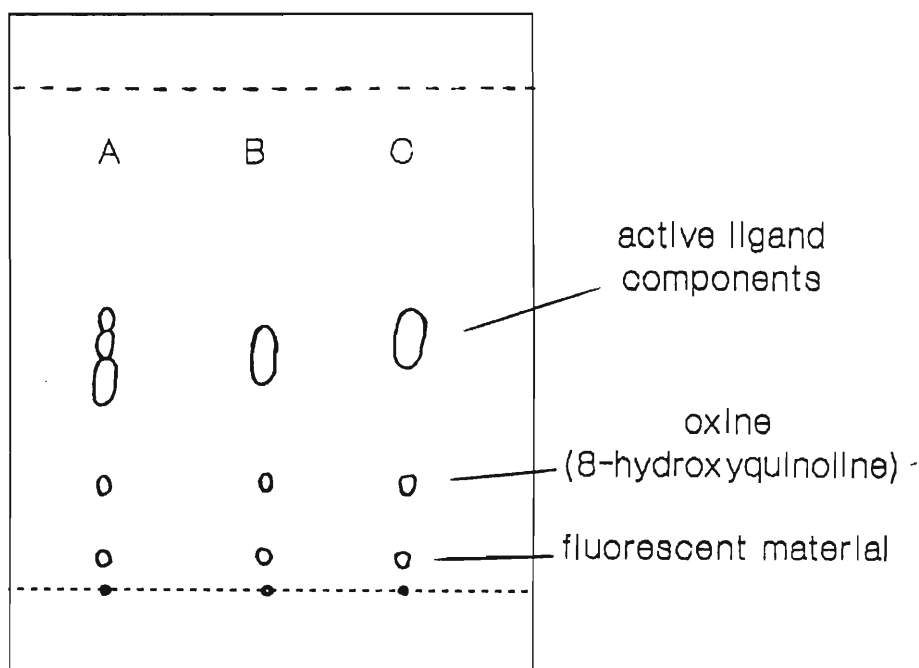


Figure (9). Resolution of the components via TLC of (A) TN 01787, (B) TN 02181 and (C) Lix 26. Mobile phase : CCl_4 .

The presence of oxine in these extractants was confirmed by the R_f value on the TLC plate compared with a plate run with pure 8-hydroxyquinoline and by spectra (uv, ir, nmr and MS) obtained by scraping a preparative plate as described further in this section. The dark fluorescent material in the reagents adhered strongly to the silica gel and is further discussed in the section dealing with column chromatography. Single spots were visualized for the active components of both TN 02181 and Lix 26, however plates for TN 01787 indicated the presence of three components which are identified via their GC/MS spectra in Section 2.2.2.3.

Component	R_f Value		
	TN 01787	TN 02181	Lix 26
Fluorescent Material	0,03	0,02	0,02
8-hydroxyquinoline	0,18	0,21	0,21
Active Ligand(s)	0,38	0,46	0,54
	0,53		
	0,64		

Table (7). R_f values of the components of the ligand preparations separated by TLC.

To facilitate the isolation of sufficient active Lix 26 for spectral analysis, preparative TLC plates (Merck silica gel 60, layer thickness 2 mm) were spotted with larger quantities of a carbon tetrachloride solution of the reagent and eluted

with carbon tetrachloride. The silica was scraped from the plate over three regions between $R_f : 0,35 - 0,54$; $R_f : 0,15 - 0,25$ and $R_f : 0,01 - 0,04$; corresponding to the active ligand, 8-hydroxyquinoline and the fluorescent compound respectively. The combined scrapings from three such chromatographic runs were refluxed for two hours in dichloromethane. Hot methanol is also recommended⁽⁸⁸⁾ for component elution but was found to be unsatisfactory for the tenacious fluorescent compound. The brown solution obtained was filtered and the solvent allowed to evaporate. Infrared spectra were obtained by redissolving a small quantity of each component in AR carbon tetrachloride and recording the spectra in a liquid cell (NaCl windows, 0,1 mm pathlength) with a Pye-Unicam SP-300 Infrared Spectrophotometer. Figure (10a) and (10b) show the infrared spectra for 8-hydroxyquinoline and the Lix 26 active component respectively. The stretching frequencies characteristic of 8-hydroxyquinoline are identified, with possible assignments in Table (8).

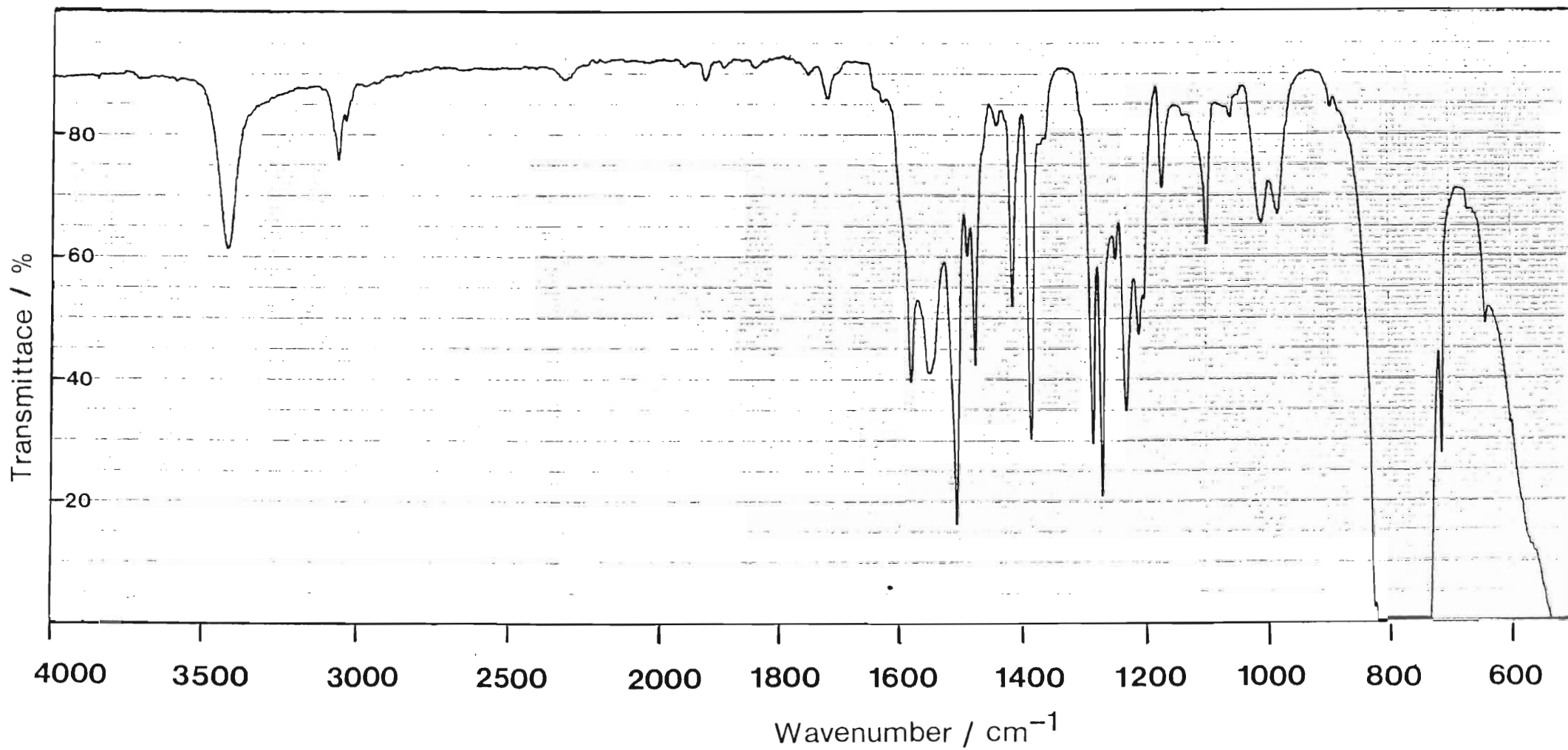


Figure 10(a). Infrared spectrum of 8-hydroxyquinoline in carbon tetrachloride. Liquid cell: NaCl windows; path length 0,1 mm. Pye-Unicam SP-300 IR Spectrophotometer.

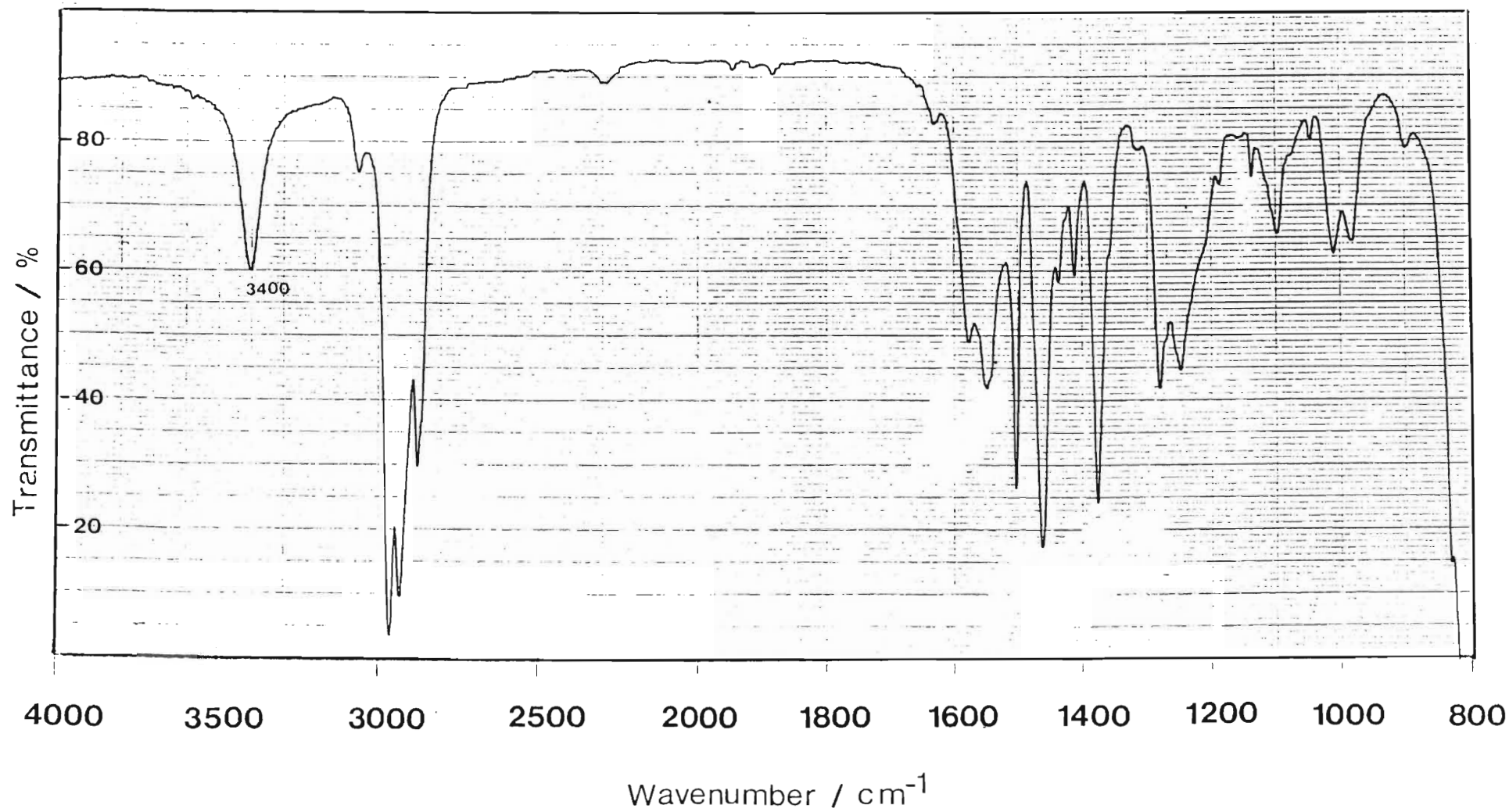


Figure 10(b). Infrared spectrum of the active component of Lix 26 in carbon tetrachloride, separated from its constituent impurities by preparative TLC. Liquid cell: NaCl windows; path length 0,1 mm. Pye-Unicam SP-300 IR Spectrophotometer.

Frequency / (cm^{-1})	Group	Remarks
3400 (s)	H-bonded OH	Ph-OH stretching involved in intramolecular bonding ^(11,12)
3060 (m)	$\begin{array}{c} \text{H} > \text{C} = \text{C} < \text{H} \\ \text{H} > & < \text{H} \end{array}$	C - H stretching
1580 (s) 1500 (s)	Aryl - H	Aromatic C - H stretching
1480 - 1660	$\begin{array}{c} > \text{C} = \text{N} - \\ - \text{C} = \text{C} - \end{array}$	Difficult to identify due to variations in intensity and similarity in frequency to aromatic C = C stretch
1410 (s)	- O - H	O - H bending
1110 (s)	C - O	C - O stretching

Table (8). Characteristic Infra-red stretching frequencies of 8-hydroxyquinoline (NaCl liquid cell : CCl_4 solvent).

The spectrum of Lix 26 differs in the following respects, resulting from the olefinic C-C, C=C and C-H groups in the 7-alkyl chain of the 8-hydroxyquinoline moiety:

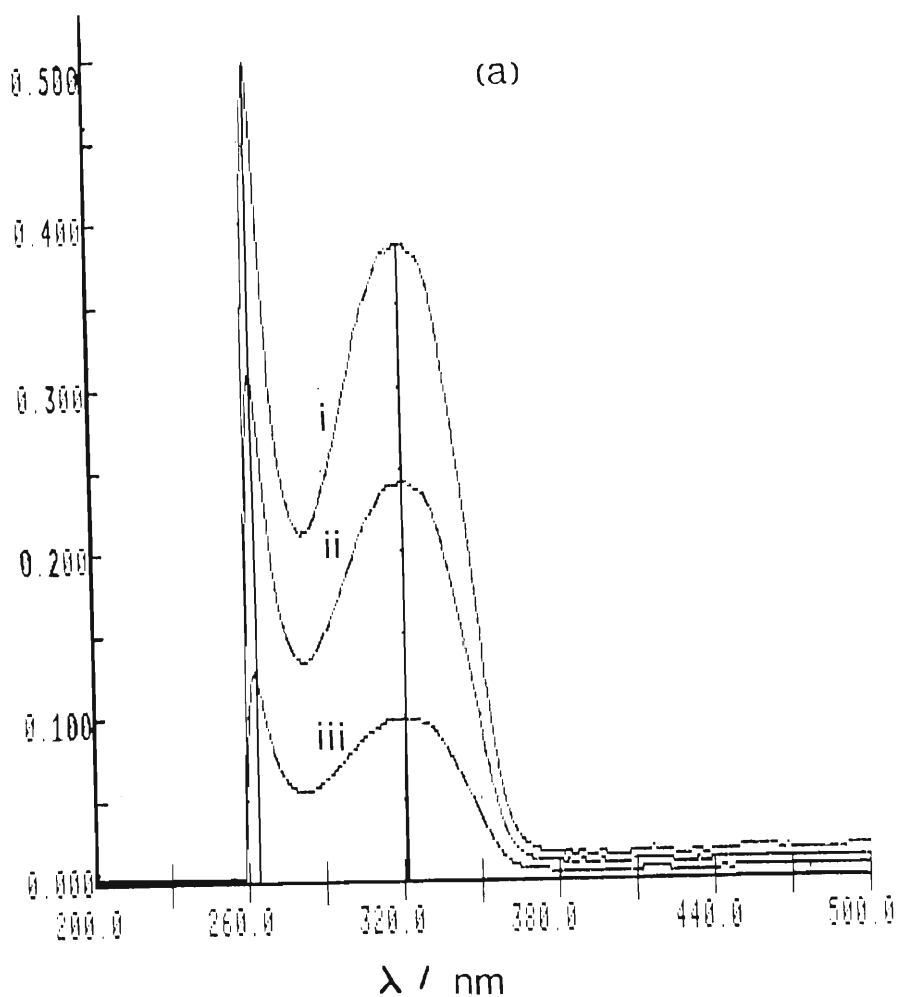
- (1) strong olefinic absorption frequencies at 2930, 2960 ($>\text{CH}_2$ and $-\text{CH}_3$ stretch), and at 2880 cm^{-1} ($>\text{C}-\text{H}$ stretching),
- (2) C-H deformations at 1470 cm^{-1} , obscuring the C=N and $-\text{C}=\text{C}-$ absorptions and
- (3) loss of resolution in the region $1200 - 1300 \text{ cm}^{-1}$.

It is not apparent from the spectrum whether the 7-alkyl substituent is unsaturated or saturated because the appearance of such a peak would be obscured by the much stronger bands of saturated C-H groups occurring below 3000 cm^{-1} .

The uv spectrum for the active Lix 26 moiety was recorded in CCl_4 by a Varian Model DMS-300 Double Beam UV/VIS Spectrophotometer and is shown in Figure (11b) with maxima at 262,1 and 320,0 nm. 8-hydroxyquinoline (Figure (11a)) has a similar spectrum with maxima at 264,7 and 321,7 nm.

A Varian CFT-20 80 MHz NMR Spectrometer was used for recording the ^1nmr of the isolated ligand. Figure 12 (a) and (b) show the spectra obtained for 8-hydroxyquinoline and the active Lix 26 ligand respectively in deuteriochloroform. The integrated proton signal for 8-hydroxyquinoline gave a ratio of 1:2:4 corresponding to the single proton of the hydroxide group at position 8 ($\delta_{8,2}$), the two protons at the 2 and 7 position ($\delta_{7,8}$ and $\delta_{7,6}$ respectively) and the four equivalent aromatic protons at the 3,4,5 and 6 positions (approx $\delta_{6,7} - \delta_{7,2}$). It will be shown that 7-alkylation of this structure (Lix 26 below) results in the shifting of the proton signals at positions 6 and 8. Other signals for the 8-hydroxyquinoline parent structure remain essentially unchanged.

Absorbance



Absorbance

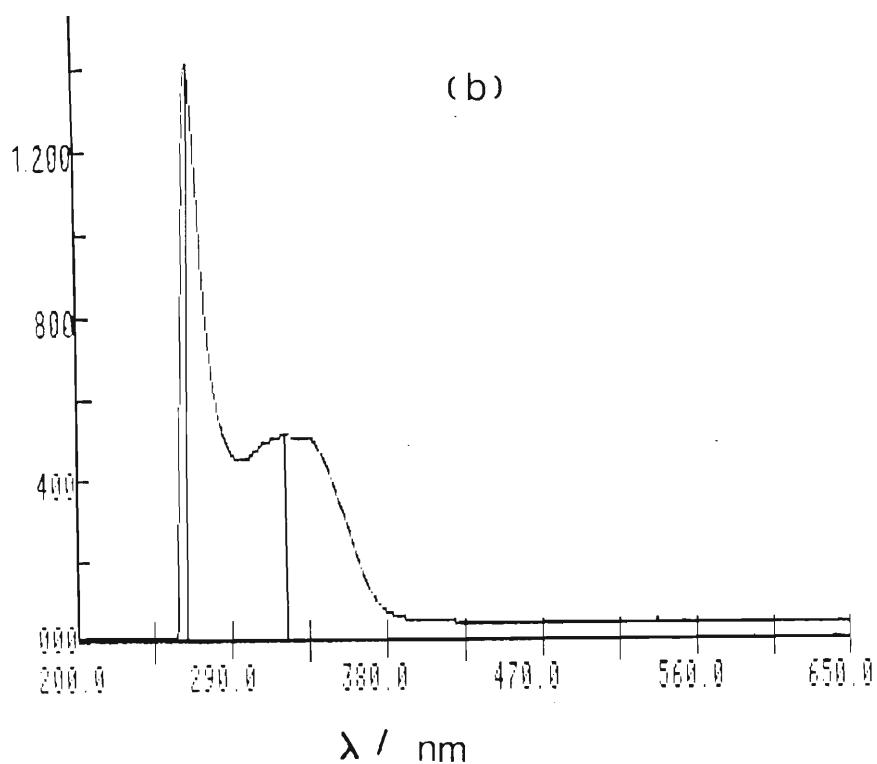


Figure (11). (a) UV/Vis spectrum of 8-hydroxyquinoline in CCl_4 in concentrations of (i) $6,90 \times 10^{-3}$ M (ii) $3,45 \times 10^{-3}$ M and (iii) $1,72 \times 10^{-3}$ M, uv maxima at 264,7 and 321,7 nm. (b) UV/Vis spectrum of the active component of Lix 26 in CCl_4 , (approx 0,1 g in 100 ml) separated via preparative TLC from other constituent impurities.

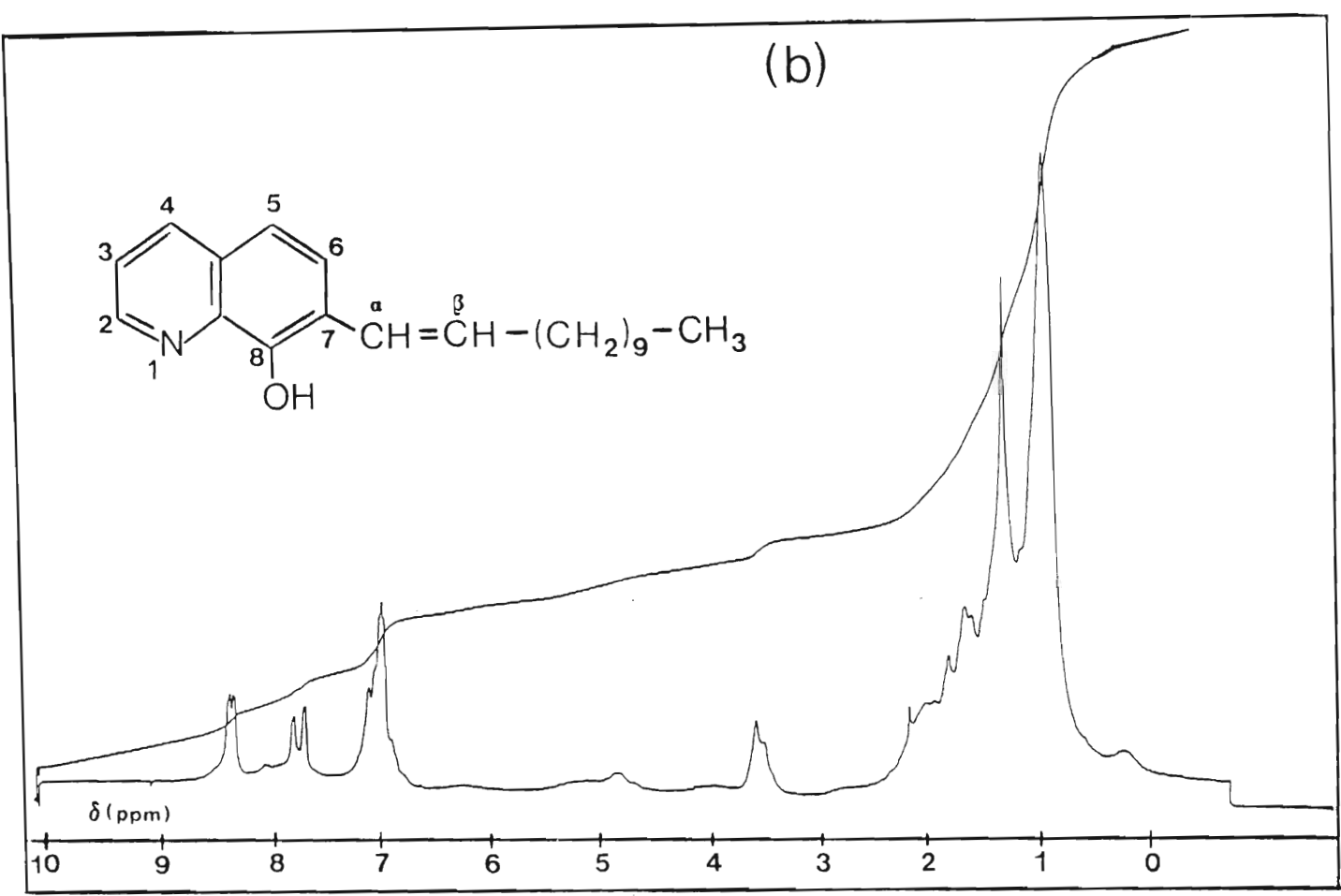
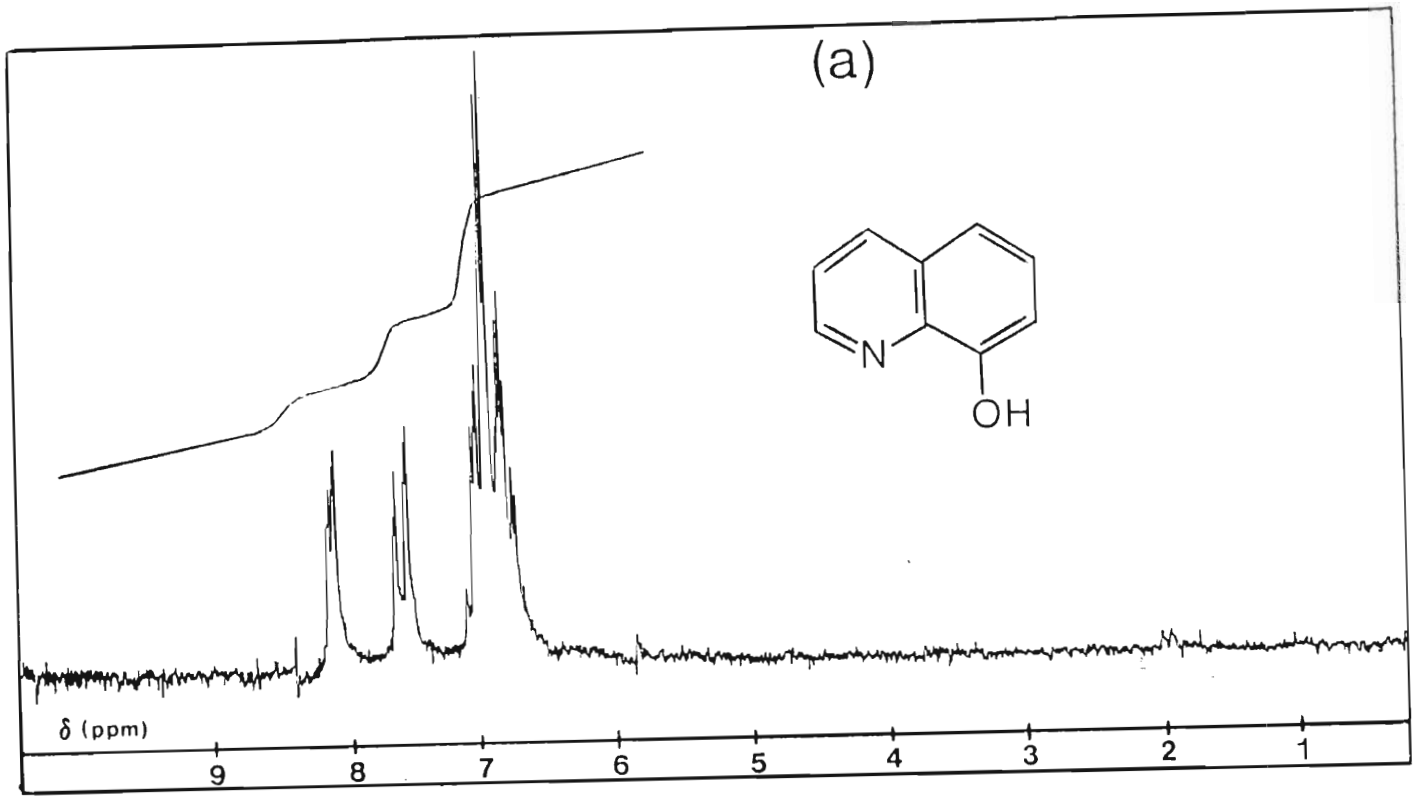
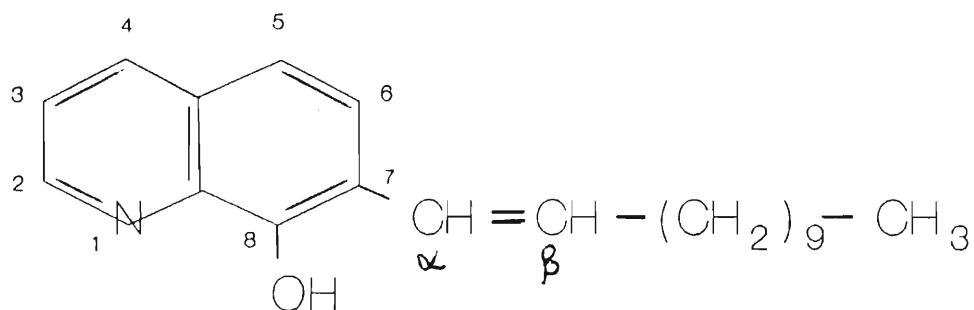


Figure (12). ¹nmr spectra of (a) 8-hydroxyquinoline and (b) the active Lix 26 ligand. Both spectra were obtained in deuteriochloroform with a Varian CFT-20, 80 MHz NMR Spectrometer.

Section 2.2.2.3 describes GC/MS data obtained for Lix 26, where a straight-chain α -unsaturated group is proposed for the structure of the 7-alkyl substituent viz.



The ratios for the proton responses, chemical shifts and possible assignments to the spectrum of Figure (12b) are given in Table (9).

Chemical Shift (ppm)	Integrated Proton Signal	Assignment : Proton(s) at position indicated
~ 1,0	21	olefinic protons
3,7	1	β proton
4,8	1	α proton
7,0	3	equivalent aromatic protons 3,4 & 5
7,8	1	2-position proton
8,4	2	OH and 6-position proton

Table (9). Chemical shifts and possible assignments of the ^1nmr spectrum of Lix 26.

Spectra obtained for the dark fluorescent compound in an analogous manner to those for the Lix 26 active component, isolated from the preparative TLC plate were very poor. The ^1nmr and i.r. spectra particularly, were diffuse and uninterpretable indicating a high level of impurity of this component. It is likely that the sample isolated comprised of a number of the impurities which were listed in Table (6). Ashbrook⁽⁸⁸⁾ showed via a qualitative analysis of the dark fluorescent material isolated from Kelex 100, that iron comprised a major metallic constituent and suggested that the component was a thermal degradation product. The presence of the metal is suggested to arise from pick-up from the vessels in which the extractant is produced. A.A analysis of the impure ligand preparation supplied to this laboratory indicated an iron content of approximately 7-8 ppm.

The section following details a procedure which could be more useful for purifying the ligand reagent solutions in bulk than the scraping of preparative TLC plates.

2.2.2.2. Purification of Sample Components Via Low Pressure Column Chromatography

The success of this technique and the resolution of the components which is obtained depend upon a number of factors for instance, column performance is sensitive to the sample loading and also to the rate of elution. The apparatus required (Figure (13)) consists of a flat-bottomed glass tube (400mm x 20mm i/d) with a teflon-sealed screwtop and 5mm glass capillary connected via rubber tubing to a small air

compressor. The flow controller valve was used to regulate the elution rate from the column. Glass wool was packed into the neck above the burette tap followed by a 5mm layer of sand. Merck silica gel 60 (230-400 mesh) pre-swollen in a 96:4 CCl_4 : acetone eluent was packed into the column under pressure. Still *et al.*⁽⁸⁹⁾, in a report detailing the optimization of chromatographic parameters for the separation of any general admixture, suggest a sample loading of 160-360 mg onto a column of 20mm diameter in order to achieve resolution of components which give $\Delta R_f \geq 0,1$ on qualitative TLC plates. For this sample loading, they recommend that 200-400 ml of eluent are required and that typical fraction sizes are 10-20 ml. The conditions which were used in this laboratory for the bulk purification of Lix 26 and the TN products in accordance with the above recommendations are summarised below:

Sample Loading	:	approx 200 mg
Flow Rate	:	6,5 \pm 0,3 ml/min
Volume of Eluent	:	400 ml
Fraction Size	:	5 ml

Fractions collected were spotted onto TLC plates and components identified by their R_f values. For Lix 26, the active component eluted first in fractions 25-45, while for TN 01787, the active ligand component eluted between fractions 30-41. For both chromatographic separations, the fluorescent compound, identifiable as a dark stain, remained bound to the silica packing at the top of the column but could be eluted with acetone or by refluxing the silica with dichloromethane. TLC analysis of this residue gave only the fluorescent spot on the plate. Chromatographic separations attempted for TN 02181 by this method were unsuccessful.

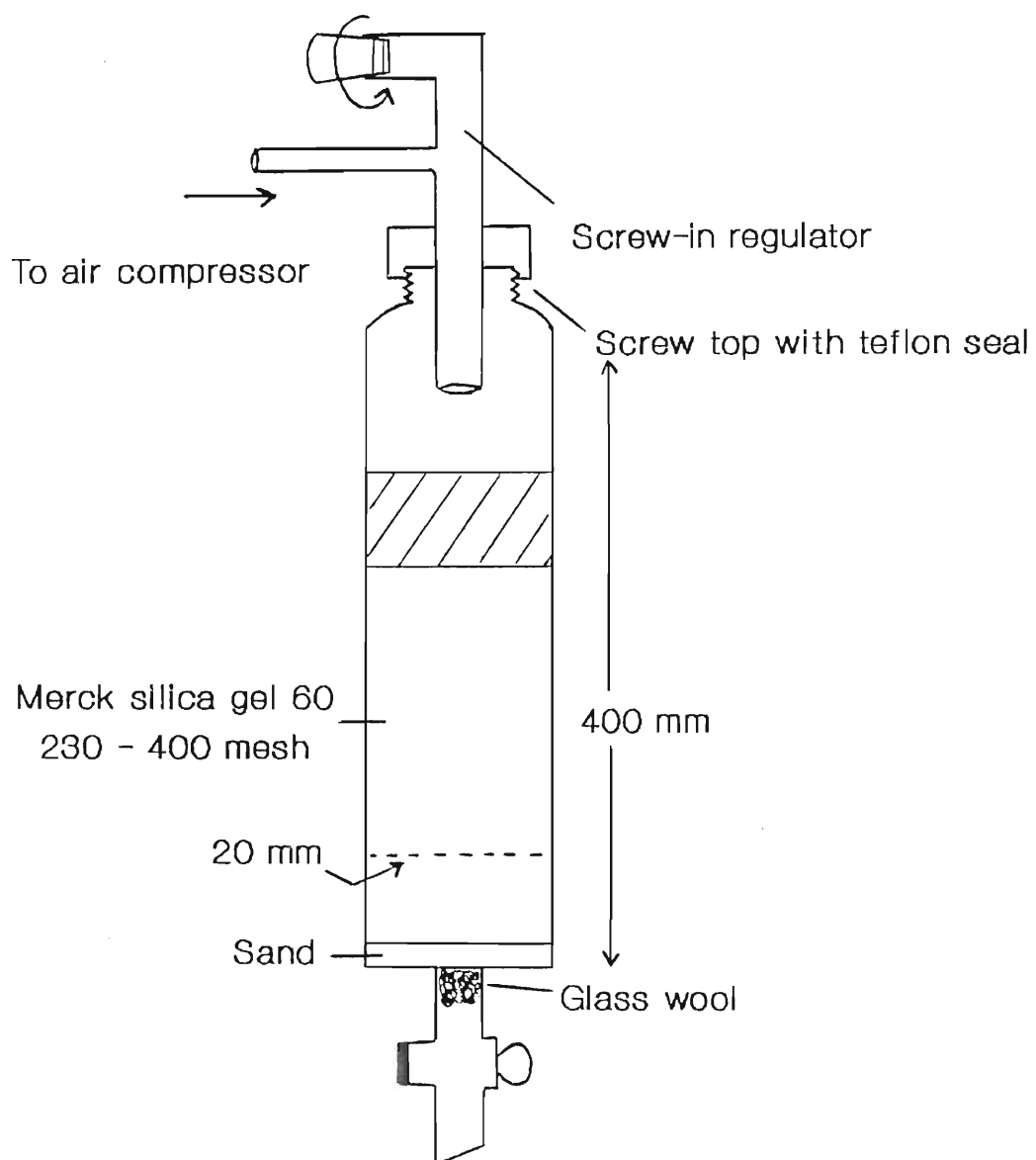


Figure (13). Column chromatography apparatus.

GC/MS is a powerful technique for the separation and identification of the components of a mixed sample and is described next.

2.2.2.3. GC/MS Analysis of the Components of Lix 26, TN 02181, TN 01787 and Kelex 100.

Provided a column can be identified which adequately resolves the components of a chemical mixture, GC/MS analysis provides a powerful tool for structure determination and was utilized as a technique in this work to a) elucidate the structure of, or at least the nature of the predominant component of Lix 26, (b) to confirm the structure of TN 01787 and as far as possible TN 02181 and (c) to identify the major impurities in the reagents as-supplied.

For all analyses a Hewlett-Packard 5890A Gas Chromatograph and Model 5988A Mass Spectrometer was used with 70 eV ionizing energy, ion source temperature 250°C with monitoring in the region 40-400 amu. The best resolution of the reagent components was offered by an HP-1 Crosslinked Methyl Silicone Gum (12m x 0,2mm ; 0,33 μ m particle size). Samples were prepared by dissolving approximately 0,3-0,4 g of material in 100 ml AR CCl₄ followed by dilution to obtain a solution of concentration of approximately 0,05 g/100 ml CCl₄.

Figure (14) shows the gas chromatogram and mass spectrum of the abundant ions for 8-hydroxyquinoline. Table (10) summarises the m/z values and possible assignments of the molecular ions.

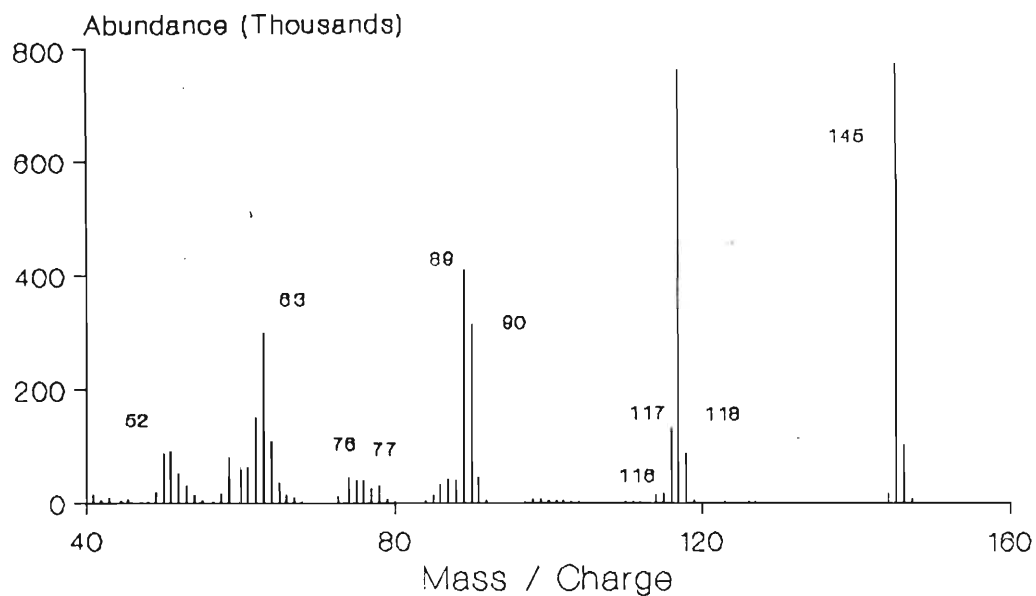
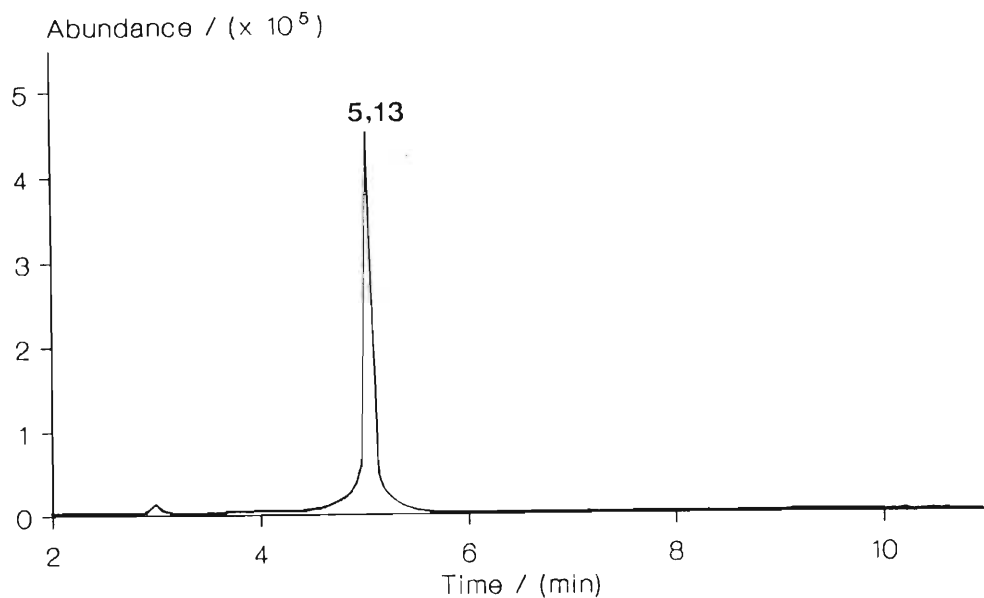


Figure (14). GC spectrum and mass spectrum for 8-hydroxyquinoline in CCl_4 . HP-1 Crosslinked methyl silicone gum column packing; ion source temperature 250°C ; 70 eV ionizing energy. m/z data are given in Appendix A(1).

m/z	Possible Assignment	Comments
145,25	Base Peak C_9H_7NO	
144,25	$C_9H_6NO^+$	- H
126,15	$C_9H_5N^+$	- OH
118,10	$C_8H_6O^+$	-HCN
117,10	$C_8H_5O^+$	-CH ₂ N
116,10	$C_8H_4O^+$	-CH ₃ N
90,10	$C_7H_6^+$	-C ₂ HNO
89,10	$C_7H_5^+$	-C ₂ H ₂ NO
77,00	$C_6H_5^+$	benzene ring fragments
76,00	$C_6H_4^+$	
72,70	$C_9H_6NO^{2+}$	metastable ion
63,00	$C_5H_3^+$	benzene ring fragments
62,00	$C_5H_2^+$	
58,50	$C_8H_6O^{2+}$	metastable ion
57,50	$C_8H_5O^{2+}$	metastable ion
52,00	$C_4H_4^+$	benzene fragment

Table (10). m/z Values and fragmentation pattern for 8-hydroxyquinoline.

Figure (15) shows the GC/MS data obtained for Lix 26. The mass-to-charge ratio for the base peak of 311,30 suggests a

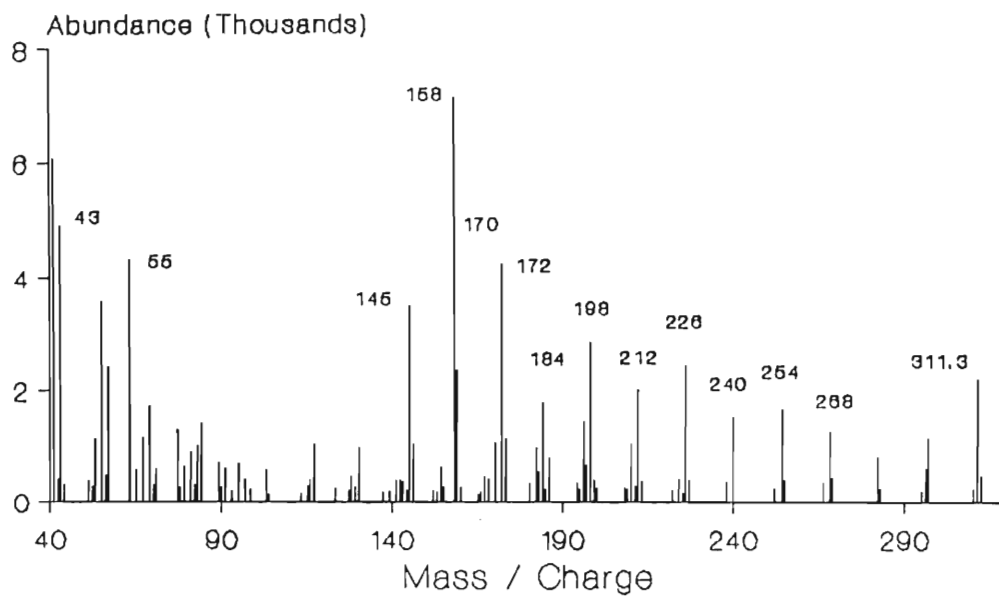
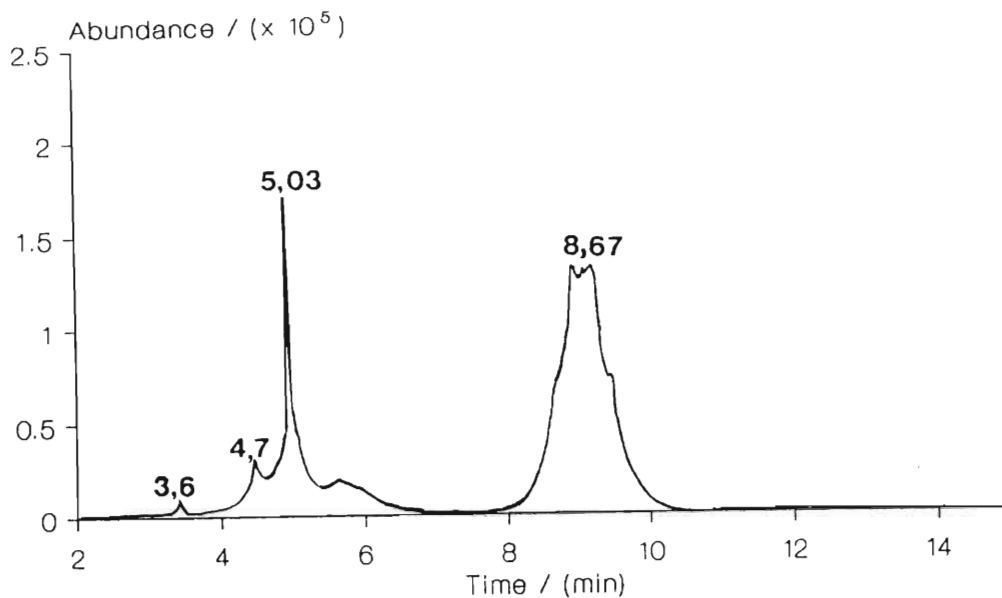
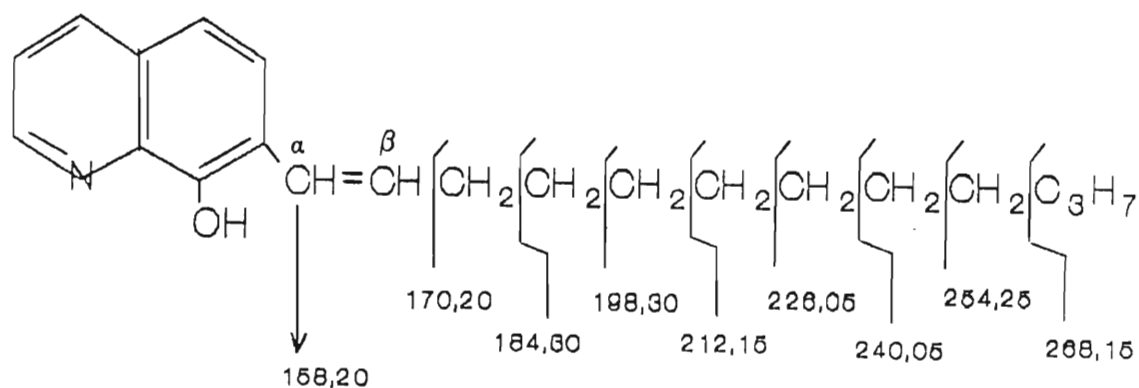
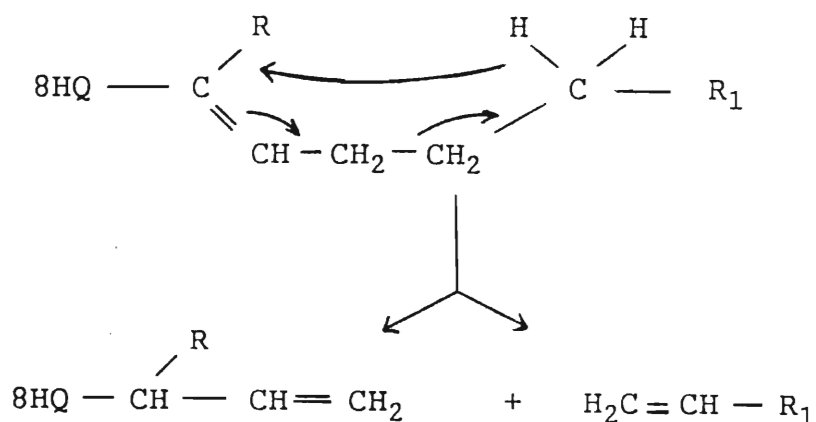


Figure (15). GC spectrum and mass spectrum for Lix 26 in CCl_4 . Experimental conditions as for Figure (14). m/z data for the peaks shown in the GC spectrum are given in Appendix A(2).

$C_{12}H_{23}$ group at the 7-alkyl position of 8-hydroxyquinoline and this implies that the alkyl group must be unsaturated. Free oxine is evident in the GC spectrum at 5,03 min and possesses the characteristic fragmentation pattern previously described. In comparison with other commercial preparations (see later), it is apparent that Lix 26 contains much greater quantities of free oxine. Quantitative GC performed in this work estimates the oxine of Lix 26 to be of the order of 3-5% by weight (Kelex 100 has a maximum 1,5% by weight of oxine). Impurities in the gas chromatograph at approximately 3,6 and 4,7 min with m/z base peaks of 132,2 and 205,0 respectively, cannot be identified on the basis of the current knowledge of the procedure for 7-alkylated-8-hydroxyquinoline manufacture (Section 2.2.1). However, the following fragmentation pattern is suggested by the MS data of Figure (15) for the peak eluting at 8,67 min which represents the active Lix 26 ligand.



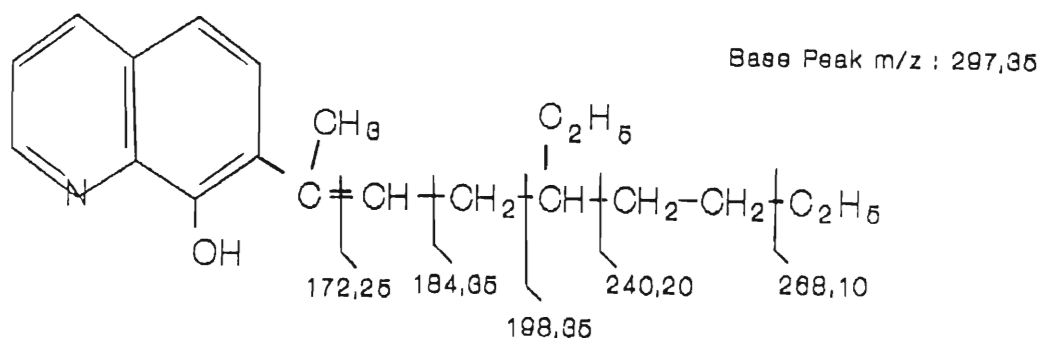
The intense signal at $m/z = 158,20$ suggests rearrangement of a proton at the double bond giving $R-CH_2^+$ and explaining the loss of one $m/z = 12$ unit corresponding to the carbon in the β position. It should be noted that the mass spectrum of any unsaturated 7-alkyl group becomes complex because the molecule is amenable to the McLafferty rearrangement viz.



8-HQ : 8-hydroxyquinoline

These rearrangement products subsequently fragment and produce a number of intermediate ionization products.

Figure (16) shows the separation obtained on the column for TN 01787 with the active component eluting at approximately 8,67 minutes. The fragmentation scheme given below is one which is consistent with MS data recorded.



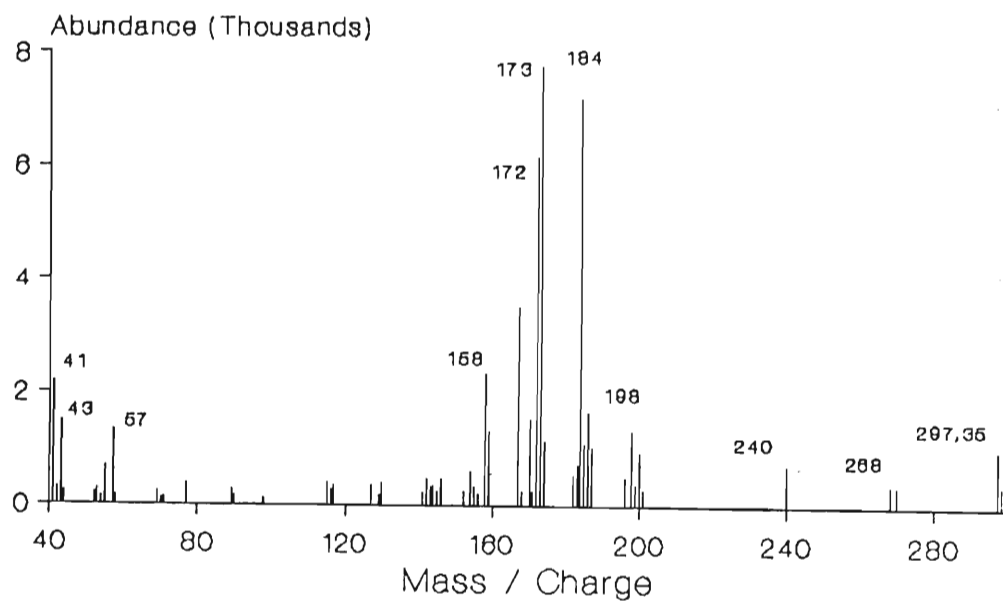
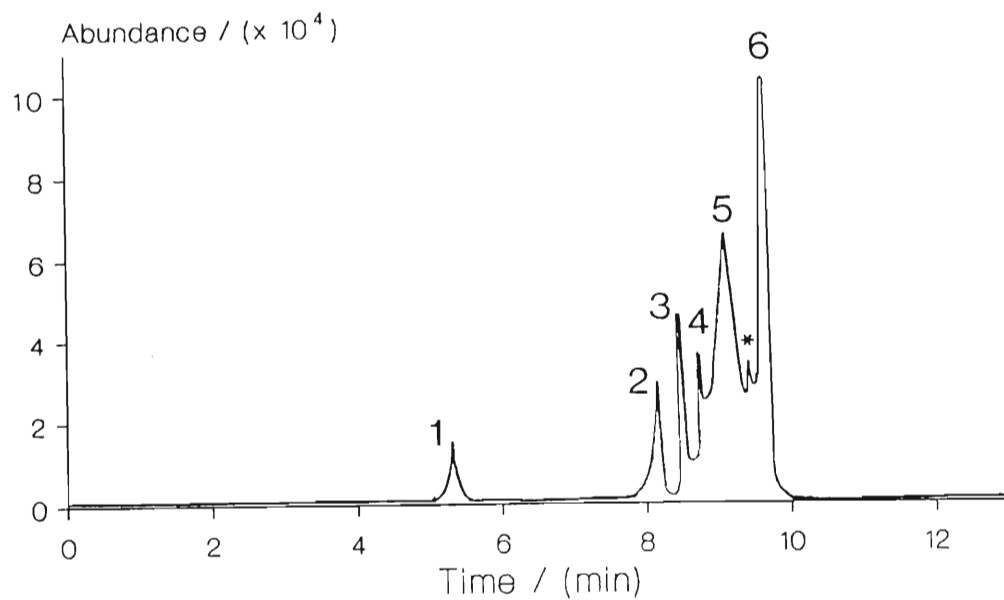
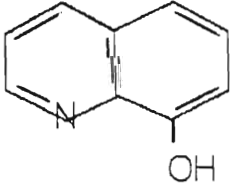


Figure (16). GC spectrum and mass spectrum for TN 01787 in CCl_4 . Experimental conditions as for Figure (14). m/z data for peaks 2-6 are given in Appendix A(3).

Again, rearrangement of the β -proton and the electrons in the alkene bond occur giving $R-CH^+-CH_3$ ($m/z = 172,25$) and this is followed by the loss of $-CH_2$ to give the intense $m/z = 158,25$ signal. The fragmentation pattern for 8-hydroxyquinoline then proceeds.

In Section 2.2.1, it was mentioned that the industrial-scale manufacture of 7-alkylated-8-hydroxyquinoline derivatives results in the formation of a number of side-products: of particular note are the furoquinolines which would not react with metal ion because the oxygen atom is involved in bonding (see comments p.50). Whether or not these impurities play an active role during extraction is uncertain and if they were purified in sufficient quantity they could make an interesting study. Inspection of the gas chromatogram for TN 01787 indicates the presence of six discrete peaks. Possible identities of these components, based on molecular weights and fragmentation patterns (Appendix A(3)) are given in Table (11) below:

Peak	Retention Time (mins)	m/z	Structure Assignment
1	5,10	145	

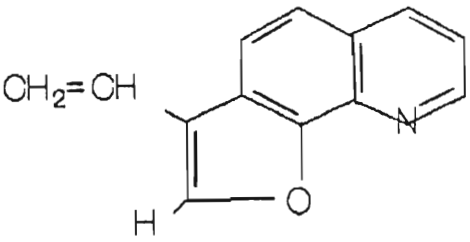
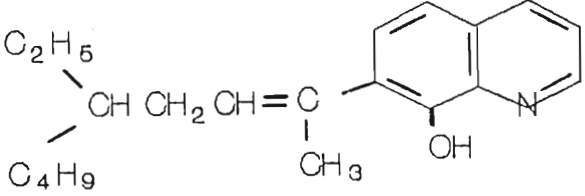
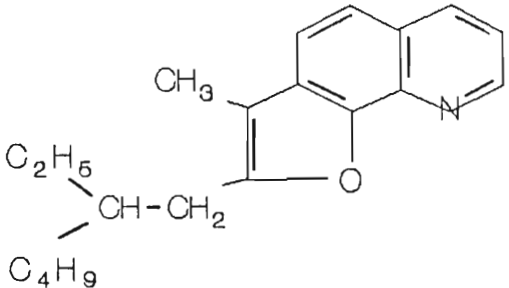
Peak	Retention Time (mins)	m/z	Structure Assignment
2,3	8,14 / 8,40	195	 <p>CH₂=CH H</p>
4,5	8,67	297,35	 <p>C₂H₅ C₄H₉ CH CH₂ CH = C CH₃ OH</p>
6	9,38	295,25	 <p>CH₃ C₂H₅ C₄H₉ CH-CH₂</p>

Table (11). Retention times, molecular weights and possible identities of the major constituents of TN 01787.

The order of elution shown in Figure (16) and the above assignments are similar to those determined by Demopoulos and Distin⁽⁸⁵⁾ for Kelex 100, the saturated analogue of TN 01787 (refer to Figure (8)). In addition, these authors suggest the following structure (Figure (17)) for the small peak indicated by an asterisk in the chromatogram, eluting at approximately 9,10 minutes.

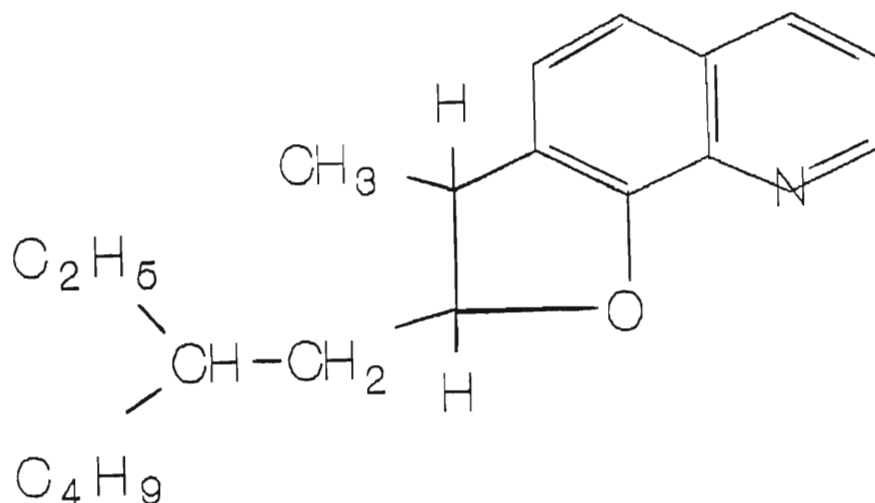


Figure (17). Proposed structure for one of the furoquinoline impurities in TN 01787.

The GC separation achieved for Lix 26 and TN 01787, was not obtained for TN 02181 and this is attributed to the number of isomers which make up the chemical formulation of this product. Although the spectrum was found to be complex (Figure (18)), an attempt was made to identify as best as possible, the chemical structures of the constituents which account for the two major peaks at 8,81 and 9,10 minutes ($m/z = 297,35$ and $311,47$ respectively). The m/z values of the predominant fragments of the former are outlined in the scheme below:

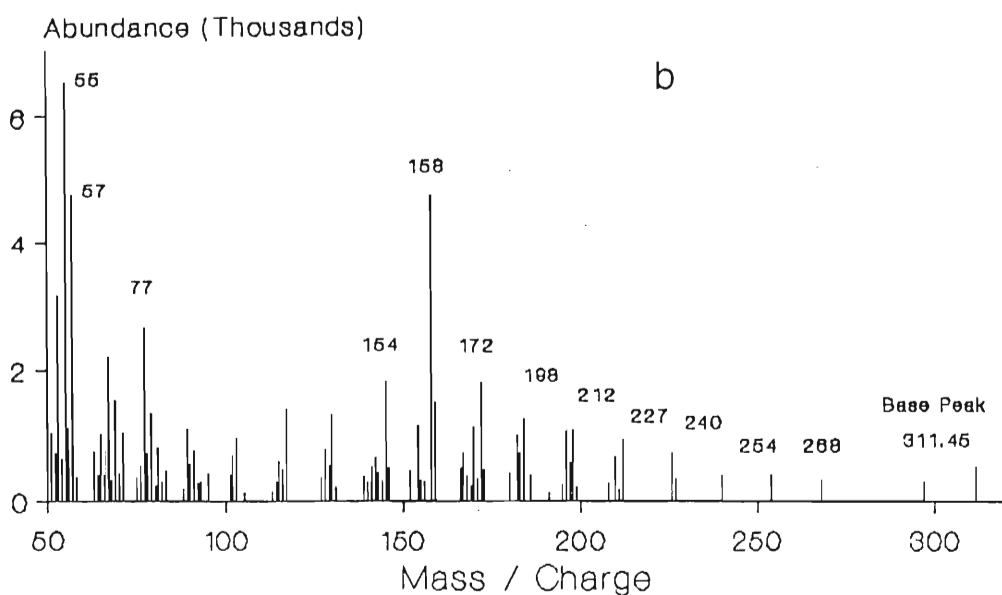
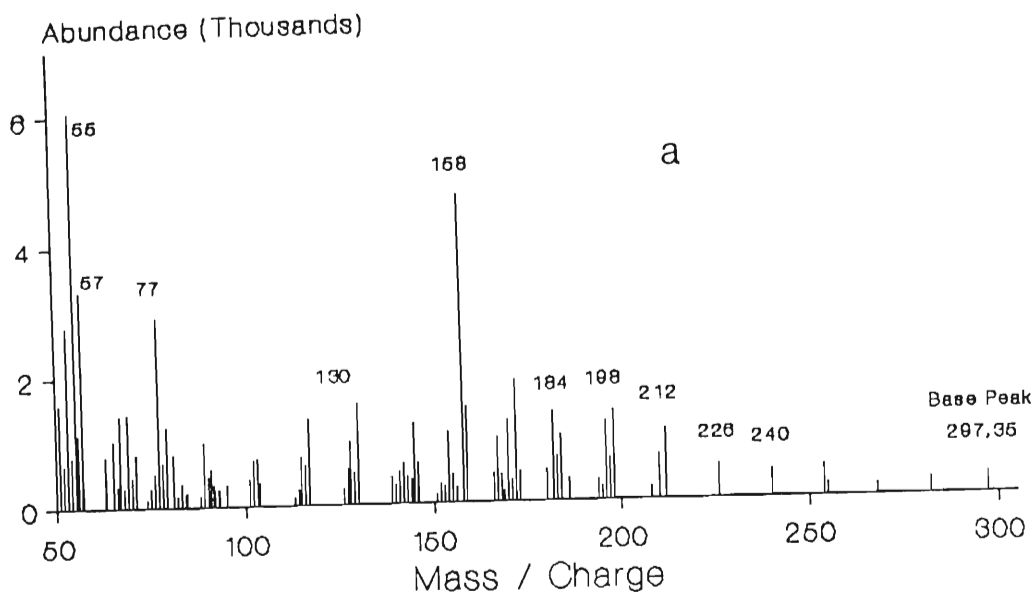
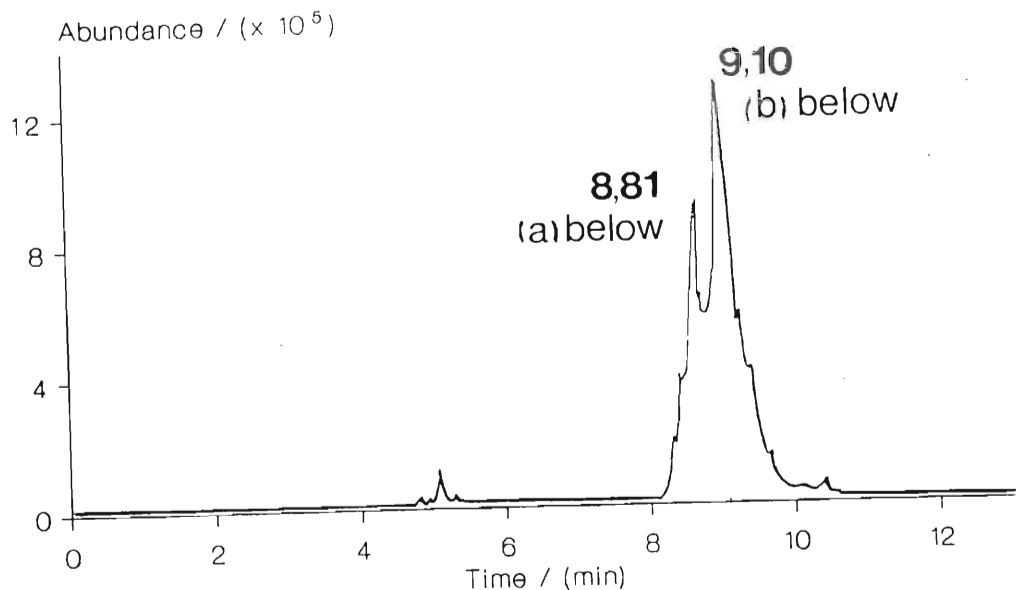
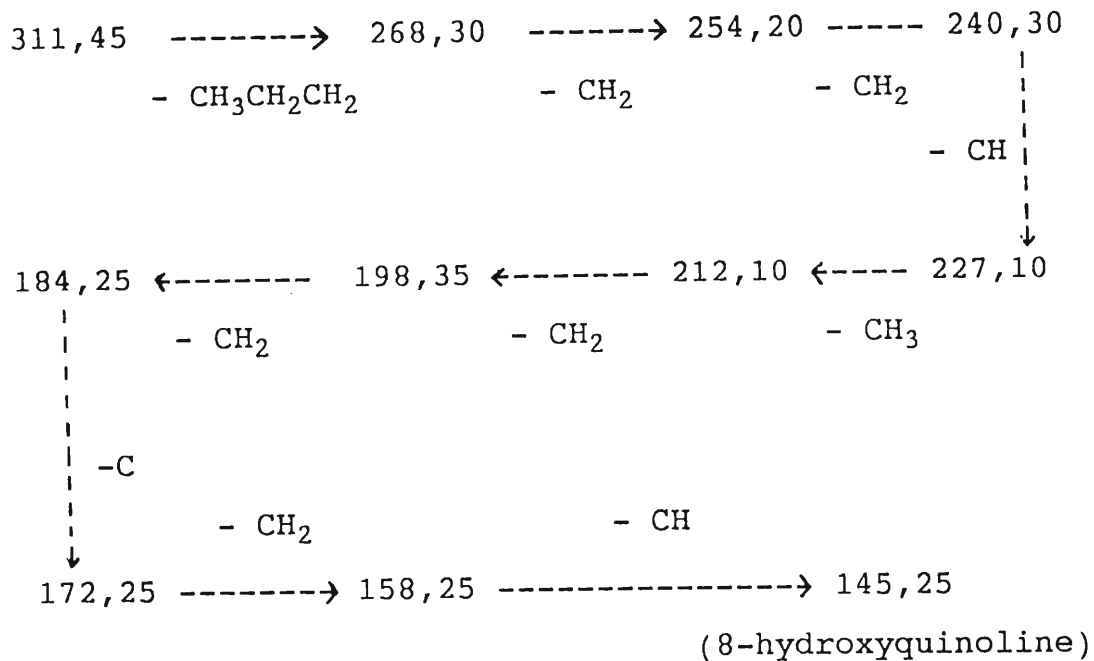
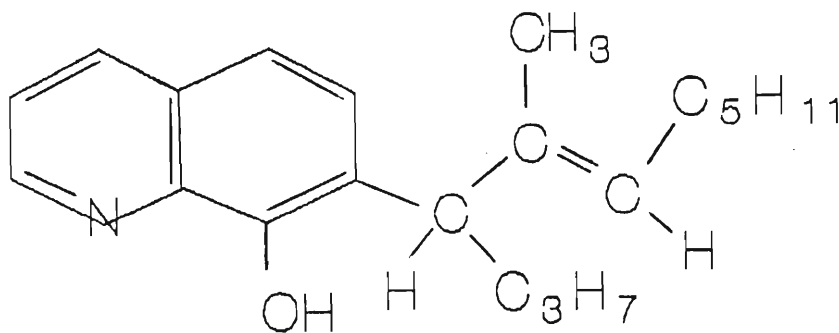


Figure (18). GC spectrum and mass spectra for the components eluting at (a) 8,81 min and (b) 9,10 min for TN 02181. Experimental conditions as for Figure (14). m/z data for the two peaks

(Base Peak)



Given that rearrangements occur about the double bond, one structure which would be consistent with this fragmentation pattern is,



Although the GC chromatogram indicated that this isomer was present in greater quantity in the reagent than any others, the incomplete separation obtained did not enable an

estimation of the relative quantity of this predominant isomer. The evidence given here however, does confirm that the alkyl side-chain is chiefly an $C_{12}H_{23}$ unsaturated moiety.

The peak eluting at 8,81 minutes could be the furoquinoline of Figure (17). The constituent has a molecular weight of 297,35 and the M/S abundant molecular ions are at $m/z = 198,35$ and $184,45$, corresponding to the loss of the C_8H_{17} and adjacent CH_2 group respectively on the five-membered furoquinoline ring.

Besides the techniques for the purification of and identification of the reagents described in this section of the work, a number of other purification techniques, most of which have been published, proved to be less successful and will be described in the next section.

2.2.2.4. Other Techniques for the Purification of 7-alkylated-8-hydroxyquinoline Extractants.

There are two broad categories of purification routes suggested in the literature. The first, reported by Fleming⁽⁵⁹⁾, involves reacting an acetate-buffered solution of $CuCl_2$ with an ethanolic solution of Kelex 100. The copper complex so formed is recrystallized from hot butanol, dissolved in ether and the copper extracted with a 20% solution of sulphuric acid. After 3-4 'strips', the ether is evaporated leaving the pure reagent. Attempts to purify Lix 26 by this route in this laboratory proved unsuccessful. The copper-complex did not 'crystallize' as such but formed a dark sludgy mass which was difficult to manipulate. The sludge was

treated via the subsequent steps described above and the final product spotted onto a TLC plate as per Section 2.2.2.1. The technique was repeated a number of times, altering the number of 'recrystallization' and acid stripping steps. No purification was discernable from the developed TLC plates.

The second technique for purification suggested in the literature involves acid conditioning of the reagent. Flett *et al.*⁽⁵⁷⁾ used Kelex 100 which was first conditioned by shaking the as-received reagent with acid and then with water before diluting as required for their studies of copper complexation. Lakshmanan and Lawson⁽⁶¹⁾ purified Kelex 100 by shaking a toluene solution of the reagent several times with 1 M hydrochloric acid until the aqueous extract no longer showed an absorption peak in the uv at 212 nm. Since 8-hydroxyquinoline protonates at a pH of $4,99 \pm 0,04$ ⁽⁹⁰⁾, the authors were presumably monitoring the distribution of free oxine into the acidic aqueous phase. After washing the organic phase, the solvent was evaporated and the 'purified' Kelex 100 was dried *in vacuo* over silica gel. The same purification route has also been reported elsewhere^(81,91).

In accordance with the above procedure, 50 ml of the impure Lix 26 reagent was dissolved in 100 ml AR toluene and shaken vigorously by a wrist-action shaker (Gallenkamp) with 150 ml of 1 M hydrochloric acid. After fifteen minutes the aqueous phase was removed and sampled and the organic phase contacted with a fresh acid solution. The free oxine in the aqueous raffinate was monitored by recording the u.v absorbance of the solution at 220, 260, 315 and 360 nm versus an 1 M HCl blank. The monitoring wavelengths coincide with the maxima of 8-

hydroxyquinoline in acid (Figure 11a). Figure (19) summarises the absorption data obtained at two of the monitoring wavelengths for 45 strip cycles and indicates that the acid-wash procedure does **gradually** remove free oxine from the organic phase. It is not clear, however, how selective the procedure is and whether it is exclusively free oxine which is removed. Given the number and variety of impurities in Lix 26 (and of the TN products), it is not inconceivable that some of these are also removed in small quantity with each contact. Attempts to purify Kelex 100 via the same procedure yielded a comparable result. The method was therefore abandoned as a route for purification and raises some question as to exactly what is defined as 'pure' by authors who have subsequently utilised the conditioned reagent for kinetic and equilibrium studies and interpreted their data with this premise.

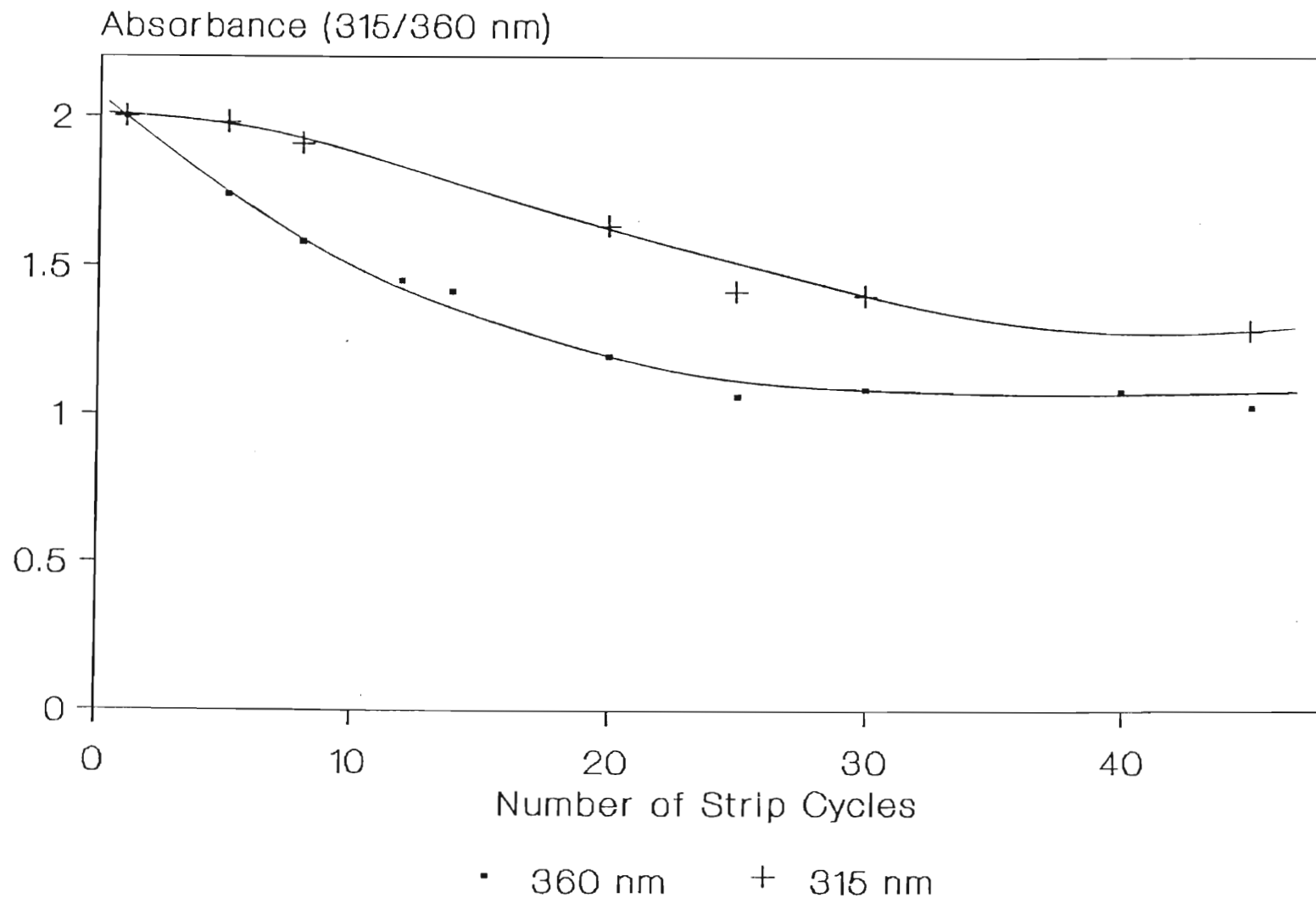


Figure (19). Absorbance of the aqueous phase at two wavelengths (315 and 360 nm) after contact with a Lix 26/toluene solution as a function of the number of strip cycles. Organic phase : 50 ml (≈ 50 g) Lix 26 in 100 ml AR toluene. Aqueous phase : 150 ml H₂O

The toluene solution of acid-washed Lix 26 was rotary evaporated *in vacuo* to remove the solvent and retained for comparison of extraction kinetics and equilibrium extraction of germanium with the as-received reagent. An interesting contrast in behaviour is presented in Section 3.8 of this work.

In this section of the thesis the nature of the active constituents and impurities in the ligand preparations supplied, have been discussed. The development of an accurate, precise and rapid technique for the routine quantification of germanium in aqueous solution was vital to the execution and interpretation of the kinetic and equilibrium data reported in this thesis and is detailed in the section following.

2.3. Techniques for the Quantification of Germanium in Aqueous Solution

Of the plethora of techniques available for germanium quantification, titrimetric, colorimetric, atomic absorption and to a lesser extent gravimetric methods are the most widely reported upon.

Germanic acid (H_3GeO_4^-) is a very weak acid ($\text{pK}_a = 8,59^{(92)}$) and therefore it is impossible to titrate it directly via alkalimetric methods. However, when a polyhydric alcohol is added to a solution of germanium dioxide, a complex monobasic acid is formed with $\text{pK}_a = 4,92^{(93)}$ which is readily titrated by alkali. The most popular titration method involves

determination via strong base of the complex monobasic acid formed when mannitol is added to the germanium-containing analyte^(53,65,94,95). Other polyhydric alcohols used in an analogous manner include glucose⁽⁹⁶⁾ and fructose⁽⁹⁷⁾. The relative simplicity of the procedure and the sharp end point appear to be the properties which have precluded less convenient and inherently more difficult titrimetric methods. Nazarenko⁽⁹⁴⁾, has given a full account of these less preferred methods.

The simplest gravimetric determinations of germanium describe methods for the quantification of germanium by precipitation as GeS_2 or GeO_2 . Fano and Zanotti⁽⁹⁸⁾ describe a procedure in which germanium is precipitated by tannin from a weak oxalic acid/oxalate system and report an error of $< 1\%$ in their determination of the metal in thermoelectric alloy samples containing tellurium and selenium in addition to germanium.

There are a number of documents which report upon methods for the atomic absorption determination of germanium in solution⁽⁹⁹⁻¹⁰³⁾, however as described later in this section, the technique necessitates careful control of the conditions for thermal atomization and access to some quite sophisticated apparatus.

The colorimetric determination of germanium with various chromophoric ligands has been widely reported upon. Methods involving determination of germanium as germanomolybdic acid and germanomolybdenum blue complexes^(94,95,104,105) and as the o-chlorofluorene complex⁽¹⁰⁶⁾ are common. Other colorimetric

procedures besides these have been reviewed by Nazarenko⁽⁹⁴⁾, but by far the most common reagent used for the colorimetric determination of germanium is phenylfluorone, 2,3,7-trihydroxy- 9-phenyl-3H-xanthen-3-one^(51,53,94,107-111) shown in Figure (20). In strong acid medium (in which germanium is present mainly as Ge^{4+} with some $[\text{Ge}(\text{OH})]^{3+}$ - see Section 3.4.5 for the speciation of germanium in aqueous solution), phenylfluorone complexes germanium in a 2:1 ligand:metal ratio via the 2 and 3 oxygen donor atoms⁽⁹⁴⁾, to form a yellow/orange complex which absorbs strongly at 510 nm.

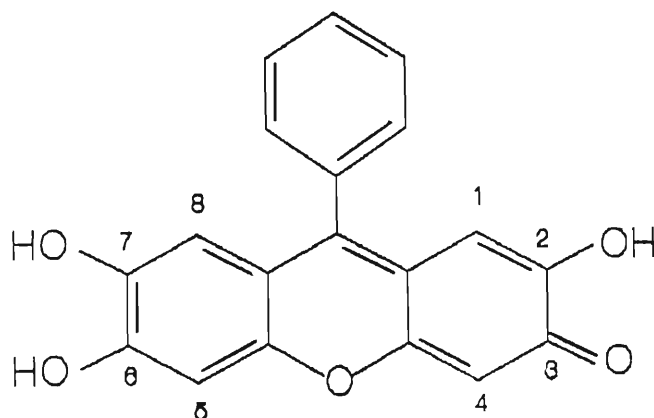


Figure (20). Structure of phenylfluorone, 2,6,7-trihydroxy-9-phenyl-3-H-xanthen-3-one.

In order to develop a routine quantification procedure for germanium, three of the abovementioned techniques viz. titration of the germanomannitol complex, atomic absorption and colorimetric with phenylfluorone, were investigated. The details and results of these techniques are presented in Sections 2.3.1 to 2.3.3.

2.3.1. The Quantification of Germanium by Mannitol Titration.

For this determination, a 10 ml aliquot of an alkaline solution of GeO_2 , prepared by dissolving exactly 2,8817 g of GeO_2 in approximately 800 ml deionized water and utilising a few drops of NaOH solution to assist solubilization and then cooled and diluted to 1 litre, was weakly acidified with 2-3 drops of 1 M sulphuric acid, boiled for 10 minutes to expel carbon dioxide and cooled under protection of soda-lime. The solution was then neutralised by a standard 0,1 M NaOH solution to the yellow p-nitrophenol end-point. 0,5-0,7 g of mannitol was added (this is a sufficient excess of polyol for determinations in which the 10 ml aliquot contains between 1 and 50 mg germanium⁽¹¹²⁾) and the monobasic acid complex so formed was titrated with the 0,1 M NaOH solution to a phenolphthalein end-point (a 'lilac colour'). A small quantity of mannitol was again added and if the solution became decolourised, the titration was resumed to the lilac end-point. The quantity of base added after the addition of mannitol corresponds to the amount of germanium present in the aliquot. In the titration, 1 ml of 0,1 M NaOH is equivalent to 7,26 mg Ge or 10,46 mg GeO_2 . Table (12) summarises the results obtained for six replicate determinations.

Vol NaOH (ml)	[Ge] g/l	% Error
30,68	2,175	8,75
30,58	2,168	8,40
30,50	2,163	8,15
30,56	2,167	8,35
30,59	2,169	8,45
30,61	2,170	8,50
Average	2,169 ± 0,004	8,43 ± 0,20

Table (12). Results for the acidimetric mannitol titration of germanium. [Ge] = 2,000 g/l :
 [NaOH] = $9,768 \times 10^{-3}$ M. Aliquot of germanium solution = 10 ml (\equiv 20 mg Ge).

As these results demonstrate, the mannitol titration procedure is precise, but the relative error is unacceptably high ($8,43 \pm 0,20$ %) and well in excess of the error reported by Kol'tgof and Stenger⁽¹¹³⁾ of $\leq 1\%$. In addition, the end-point is obscure because it necessitates the identification of the appearance of a 'lilac' colour against the yellow background of the para-nitrophenol end-point.

2.3.2. The Colorimetric Quantification of Germanium by Phenylfluorone.

2.3.2.1. Experimental Procedure

The following solutions were required for this determination:

- (i) 1:1 H_2SO_4 prepared by dissolving 250 ml concentrated sulphuric acid in 250 ml deionized water.
- (ii) A 5,0 g/l gelatine solution prepared by dissolving 0,5 g gelatine in approximately 50 ml deionized water with gentle heating. This reagent was always freshly prepared.
- (iii) A 0,1 g/l phenylfluorone solution prepared by dissolving with careful heating, 0,05 g phenylfluorone in 100-200 ml absolute ethanol containing 5 ml 2,5 M H_2SO_4 , cooling and diluting to 500 ml with ethanol.
- (iv) Standard germanium solutions prepared by dissolving, with heat, 0,1441 g GeO_2 in approximately 300 ml water, utilising a few drops of NaOH solution to assist solubility. This solution was diluted to 500 ml giving a stock in which 1 ml \equiv 0,200 mg Ge \equiv 200 mg/l Ge.

A Beer's Law calibration curve was prepared for the germanium-phenylfluorone complex by adding 1,3,5,8,10,12 and 15 ml of germanium stock solution (iv) from a burette, to clean 25 ml volumetric flasks. 1,4 ml 1:1 H_2SO_4 , 1,0 ml gelatine solution and then 5,0 ml phenylfluorone solution were added in that order to each flask with shaking after each addition. The flasks were diluted to the mark with deionized water and allowed to stand for 90 minutes. The absorbance of each solution at 510 nm was determined against a similarly prepared blank using a Varian Model DMS-300 UV/VIS Double-Beam Spectrophotometer. The calibration curve of Absorbance (510 nm) vs [Ge] in mg/l shown in Figure (21), is linear over a range of germanium concentration of 0 - 0,60 mg/l and has a least squares slope of 1,144 $\text{l}\cdot\text{mg}^{-1}$. Accordingly, germanium solutions for analysis in this work were diluted to give

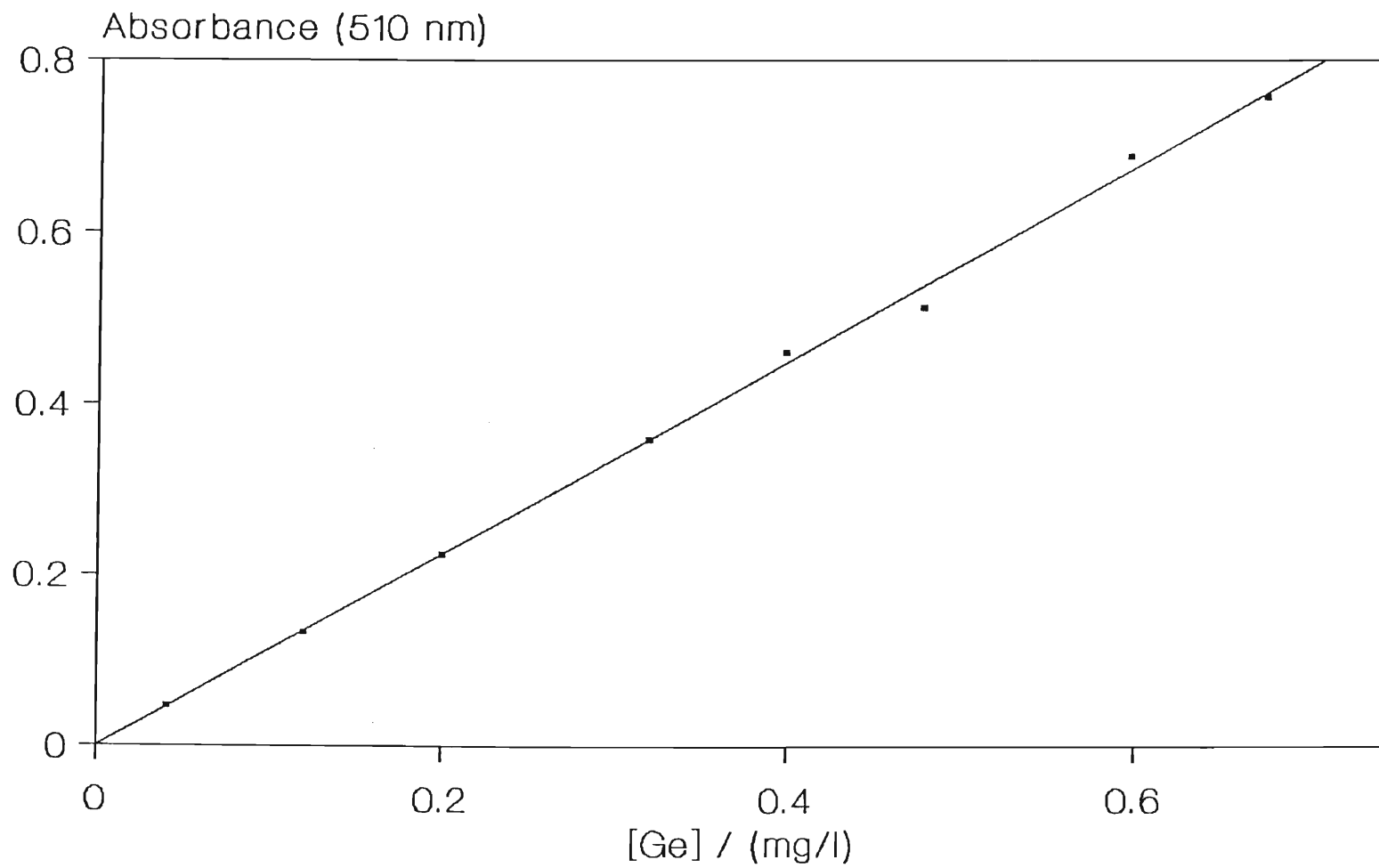


Figure (21). Calibration curve for the germanium-phenylfluorone complex at 510 nm.

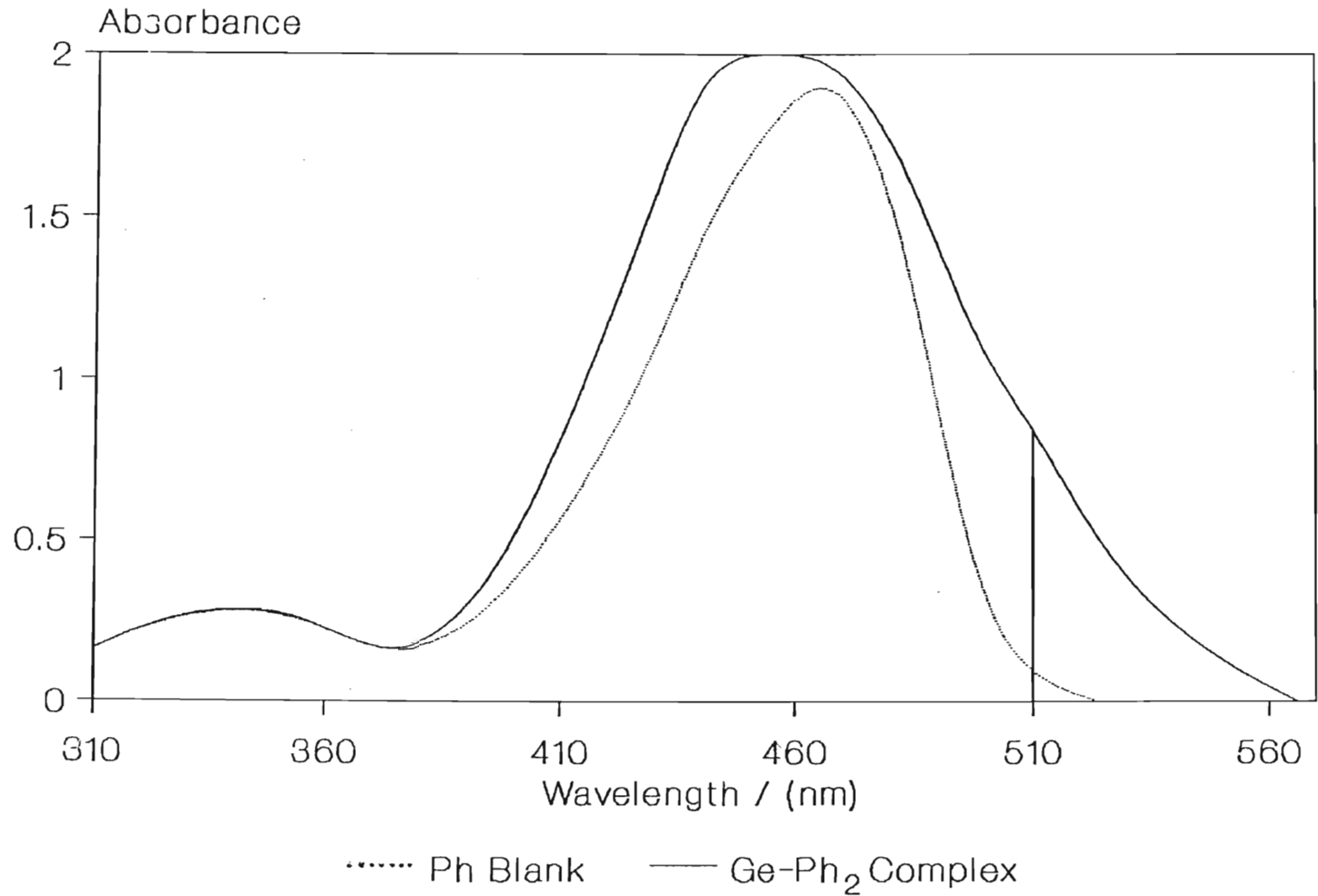


Figure (22). The UV/VIS spectra of the germanium-phenylfluorone complex, GePh₂, and phenylfluorone.

absorbances in this linear range and germanium concentrations were calculated using this extinction coefficient.

Figure (22) shows the uv-visible spectra for the phenylfluorone blank and the 12 ml standard germanium solution and demonstrates that the difference in extinction between the two solutions is at a maximum at 510 nm and is therefore the most suitable monitoring wavelength.

2.3.2.2. Accuracy and Precision of the Phenylfluorone Technique and Associated Microanalysis.

The method of sampling of the aqueous phases of experiments designed for studying the effects of various parameters upon the kinetics of solvent extraction of germanium are discussed in Section 2.4 of this work, but some comment is appropriate here. In order to preserve the aqueous : organic phase ratio during extraction runs and to simplify the calculation of germanium concentration remaining in the aqueous phase following some period of ligand extraction during which a number of samples for analysis are taken, it was necessary to sample no more than 100-200 μ l of the aqueous phase. It was therefore essential to implement a microanalysis method for germanium quantitation via the phenylfluorone technique. For most analyses, a 25-50 μ l sample (Volac High Precision Micropipette R880A) was used to quantitate germanium. Testing the precision and accuracy of the phenylfluorone technique would therefore also give an indication of the same parameters for the micro-sampling. Table (13) summarises the absorbance data for ten samples in which 25 μ l aliquots of a solution of

exactly 0,6000 g/l Ge (prepared by dissolving 0,8645 g GeO₂ in 1 litre solution), were taken. These results give $[\text{Ge}]_{\text{ave}} = 0,584 \pm 0,004$ g/l which represents a relative error of $2,67 \pm 0,67\%$. This compares favourably with an error of $2,90 \pm 0,33\%$ obtained by electrothermal atomization atomic absorption analysis of a set of solutions (discussed further in Section 2.3.3) and is therefore of an equivalent precision and accuracy to a technique generally accepted as suitably accurate for germanium quantification. Unfortunately, the electrothermal technique is not generally available to most laboratory workers. These data also confer an acceptable degree of confidence upon the micropipetting technique utilised in sampling.

Sample	Absorbance ₅₁₀
1	0,669
2	0,668
3	0,668
4	0,674
5	0,669
6	0,670
7	0,667
8	0,657
9	0,672

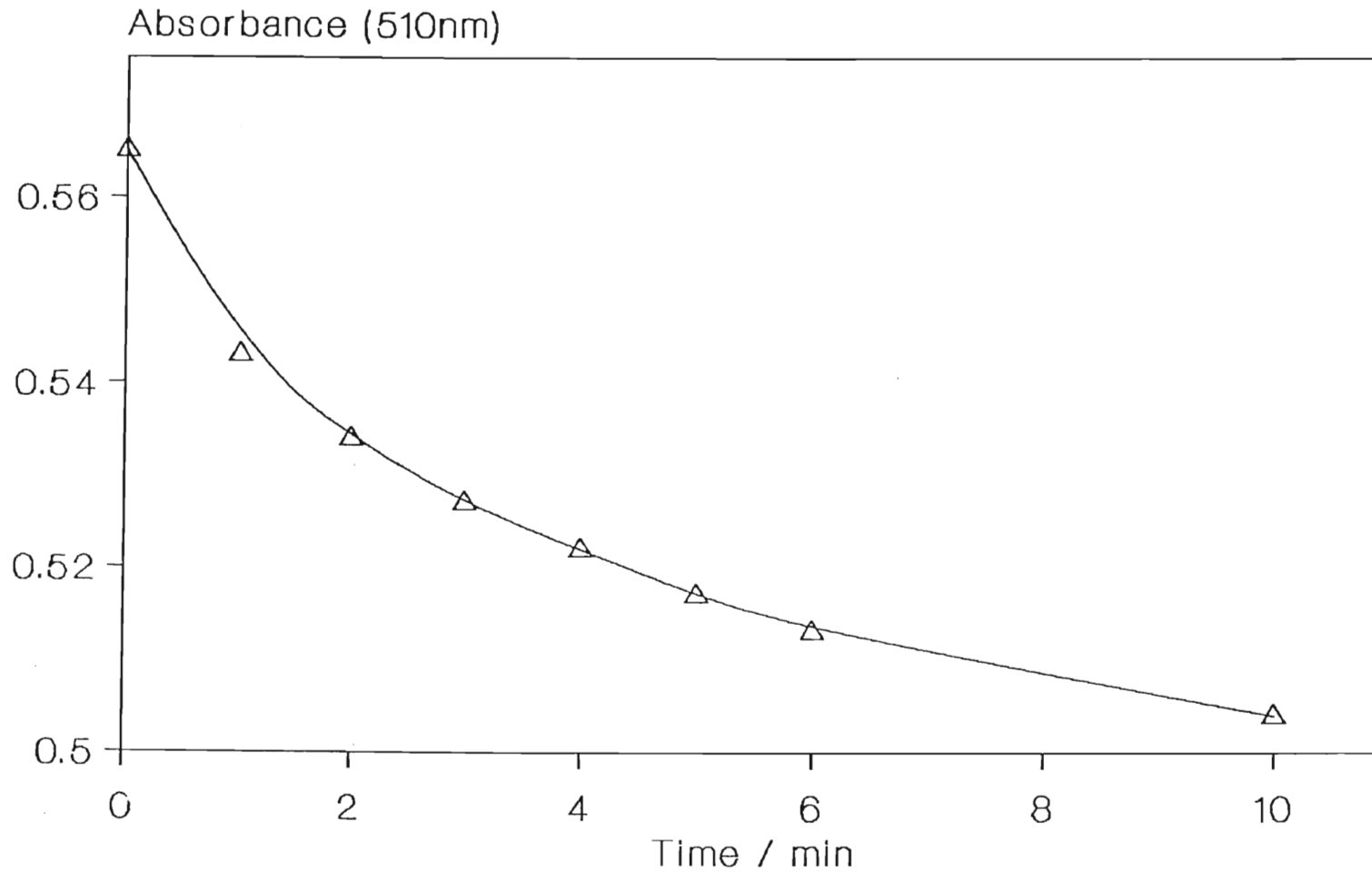
Sample	Absorbance ₅₁₀
10	0,664
Average	0,668 ± 0,004

Table (13). Results for the phenylfluorone determination of germanium. $[\text{Ge}]_{\text{actual}}$ (by weight) = 0,6000 g/l , aliquot for analysis = 25 μl .

2.3.2.3. The Stability of the Germanium-Phenylfluorone Complex.

The yellow/orange germanium-phenylfluorone complex is stable provided sufficient gelatine is present in solution⁽⁹⁴⁾. Pedrosa and Paul⁽¹⁰⁸⁾ employed a phenylfluorone procedure in which a buffer solution and ethanolic solution of phenylfluorone were added to the germanium-containing test solution, allowed to stand for four minutes, further acidified and then read immediately versus a similarly prepared blank at 525 nm. Figure (23) shows the change in absorbance with time following the four minute period for a solution containing approximately 0,62 mg/l germanium treated exactly according to the method reported. It is obvious from these data (and that from 3 other solutions of a lower initial germanium concentration not shown), that this procedure would invariably furnish spurious data and it is suggested that the germanium-phenylfluorone complex precipitates out unless a protective colloid such as gelatine is added to the solution. Figure (24) shows the change in absorbance of the germanium-phenylfluorone complex with time when the procedure used includes gelatine.

In order to obtain the kinetic plot shown, the time was noted after the addition of ligand simultaneously to the blank and germanium-containing solution (approx 0,200 g/l Ge). Both solutions were immediately placed in the double-beam spectrophotometer and the difference in absorbance at 510 nm obtained with time. It is clear from this plot that a minimum of 90 minutes is required for equilibration prior to absorbance measurements. Such solutions were found to be stable (absorbance unchanged) for up to 50 hours.



Method : Pedrosa and Paul⁽¹⁰⁸⁾

Figure (23). The visible absorption stability of the germanium-phenylfluorone complex at 510 nm if prepared in solution in the absence of a polyol (method of Pedrosa and Paul⁽¹⁰⁸⁾). $[Ge]_{initial} \sim 0,62 \text{ mg/l}$.

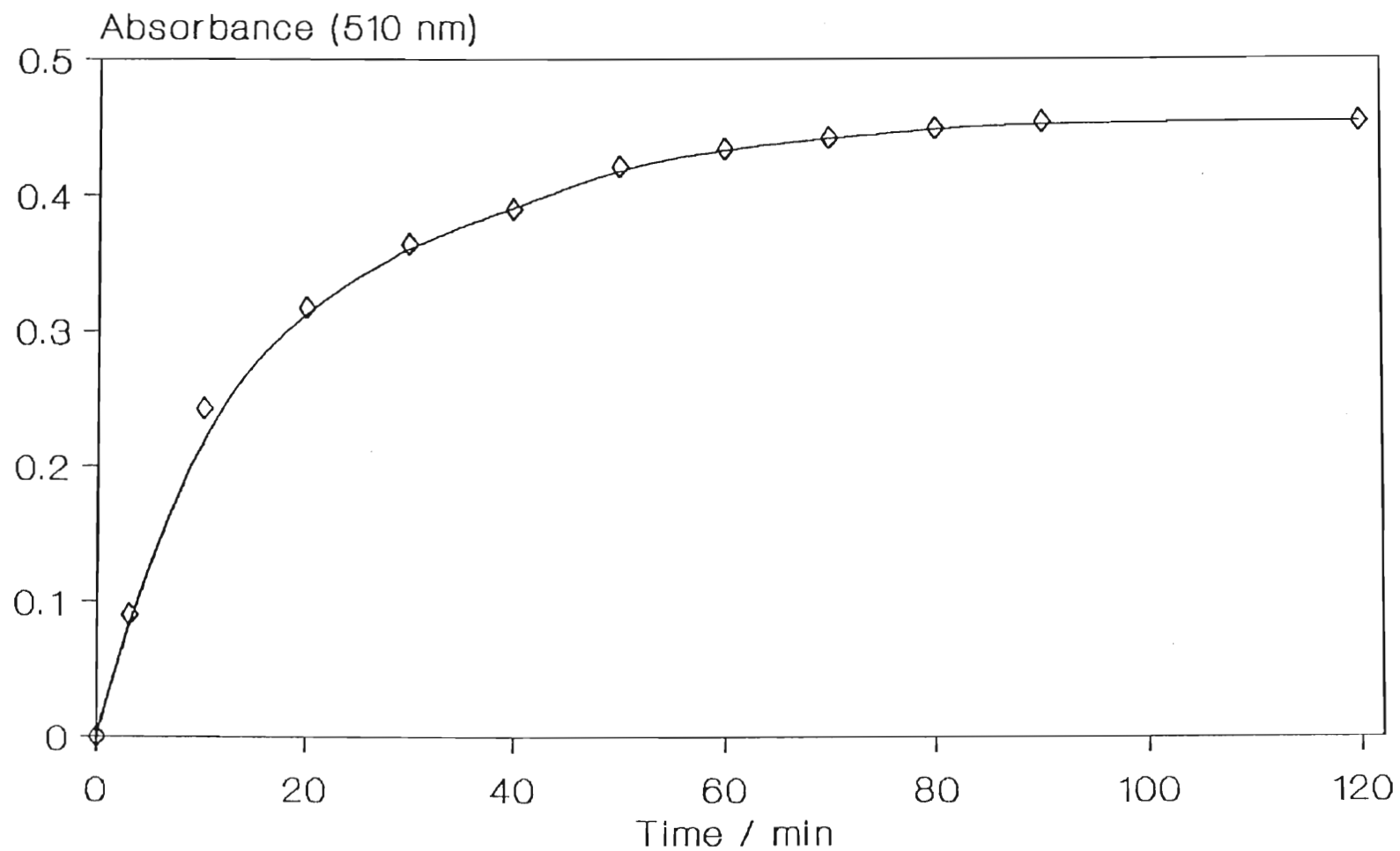
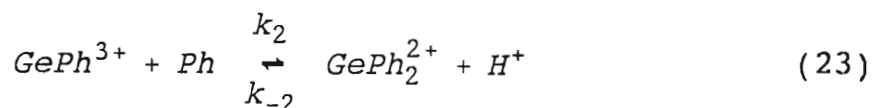
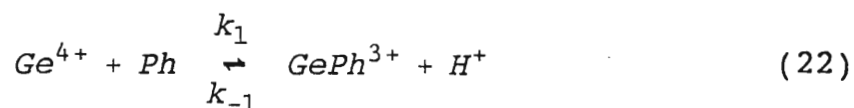


Figure (24). Absorbance at 510 nm as a function of time for the formation of the germanium-phenylfluorone complex.

2.3.2.4. The Kinetics of the Phenylfluorone Complexation Reaction.

The form of Figure (24) suggests typical first-order (or pseudo-first-order) kinetics and this implies that the reaction must proceed via a single rate-determining step, that is to say a fast initial attachment of one ligand molecule to a Ge^{4+} (or germanium hydroxy species), to form GePh^{3+} (Ph : phenylfluorone), followed by a slower step to form GePh_2^{2+} (which is charge balanced by two hydroxyl groups i.e. $\text{GePh}_2(\text{OH})_2$) viz.



Ph : Phenylfluorone

In Chapter 1, the nature of the rate-determining step in the chelation of germanium by alkylated 8-hydroxyquinoline reagents was proposed to be the stereochemically controlled attachment of the third ligand to the GeL_2^{2+} intermediate at the aqueous/organic interface. The stereochemical bulk of a phenylfluorone ligand which approaches a GePh^{2+} precursor molecule is also proposed to be the controlling influence in the rate determining step. Figure (25) illustrates the mechanism by which the incoming second ligand is hindered by the proximity of the ligand already bonded to the central germanium atom.

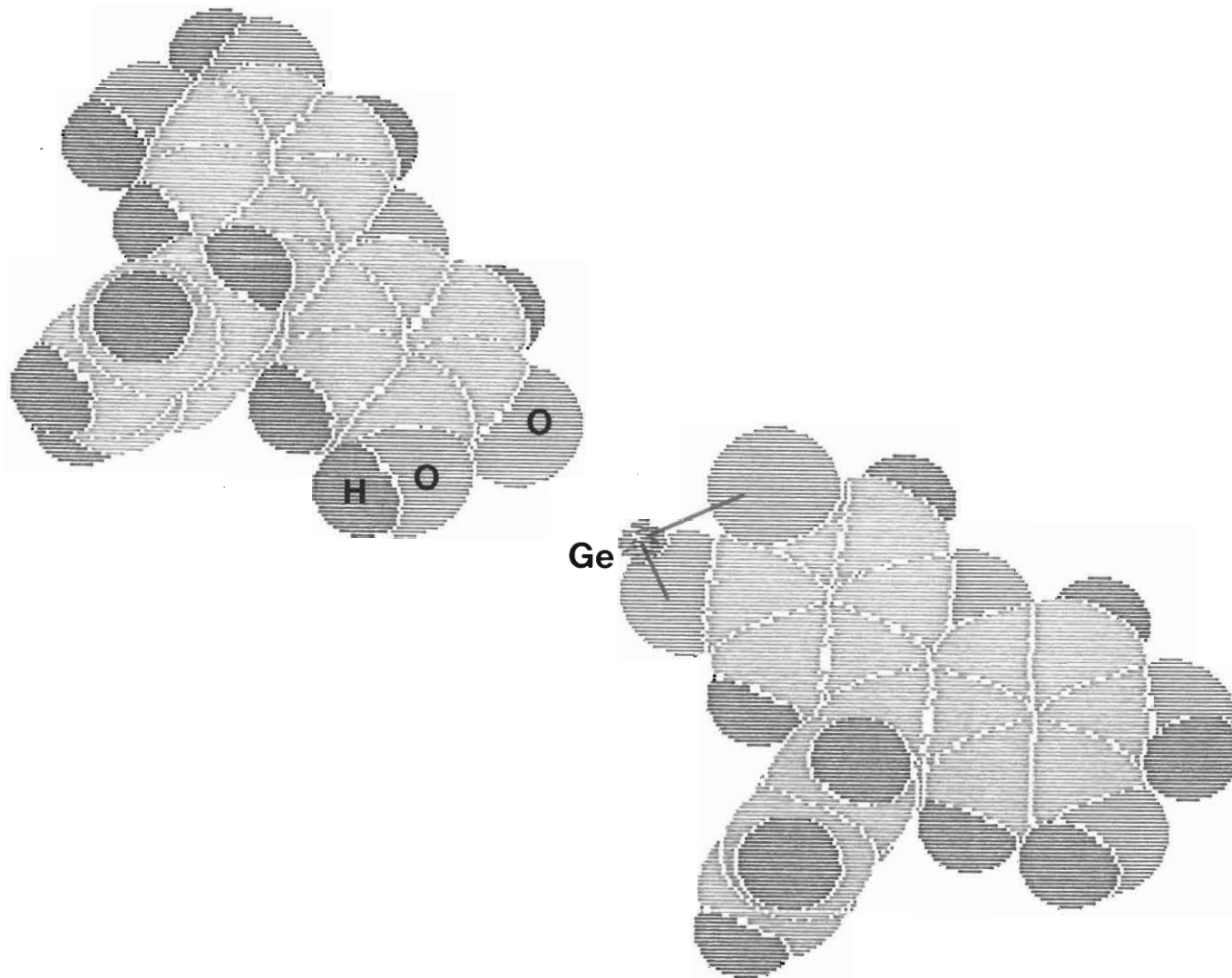


Figure (25). Pictorial representation of the stereochemically-hindered reaction between phenylfluorone and the GePh_3^+ intermediate.

If the back-reaction of Equation (23) is negligible (K_{eq} high), then the rate-determining step for the complexation is given by Equation (24),

$$Rate = k_2 [GePh^{3+}] [Ph] \quad (24)$$

and since for all determinations, ligand was present in large excess (i.e. $> 10^2$ - fold), then the pseudo-first-order Equation (25) follows:

$$Rate = k_2' [GePh^{3+}] \quad (25)$$

and therefore,

$$k_2 = \frac{k_2'}{[Ph]} \quad (26)$$

Figure (26) shows a first order plot of $\ln (A_{510}^{\infty} - A_{510}^t)$ versus time, where A_{510}^{∞} and A_{510}^t are the absorbances of the germanium-phenylfluorone complex at equilibrium and at some intermediate time respectively, which is linear with slope $-8,5 \times 10^{-4} \text{ s}^{-1}$, hence $k_2' = 8,5 \times 10^{-4} \text{ s}^{-1}$. Inserting $[Ph] = 6,24 \times 10^{-5} \text{ M}$ (the concentration of 5 ml of 0,1 g/l phenylfluorone diluted to 25 ml) into Equation (26) gives $k_2 = 13,6 \text{ mol}^{-1} \text{ dm}^3 \text{ s}^{-1}$.

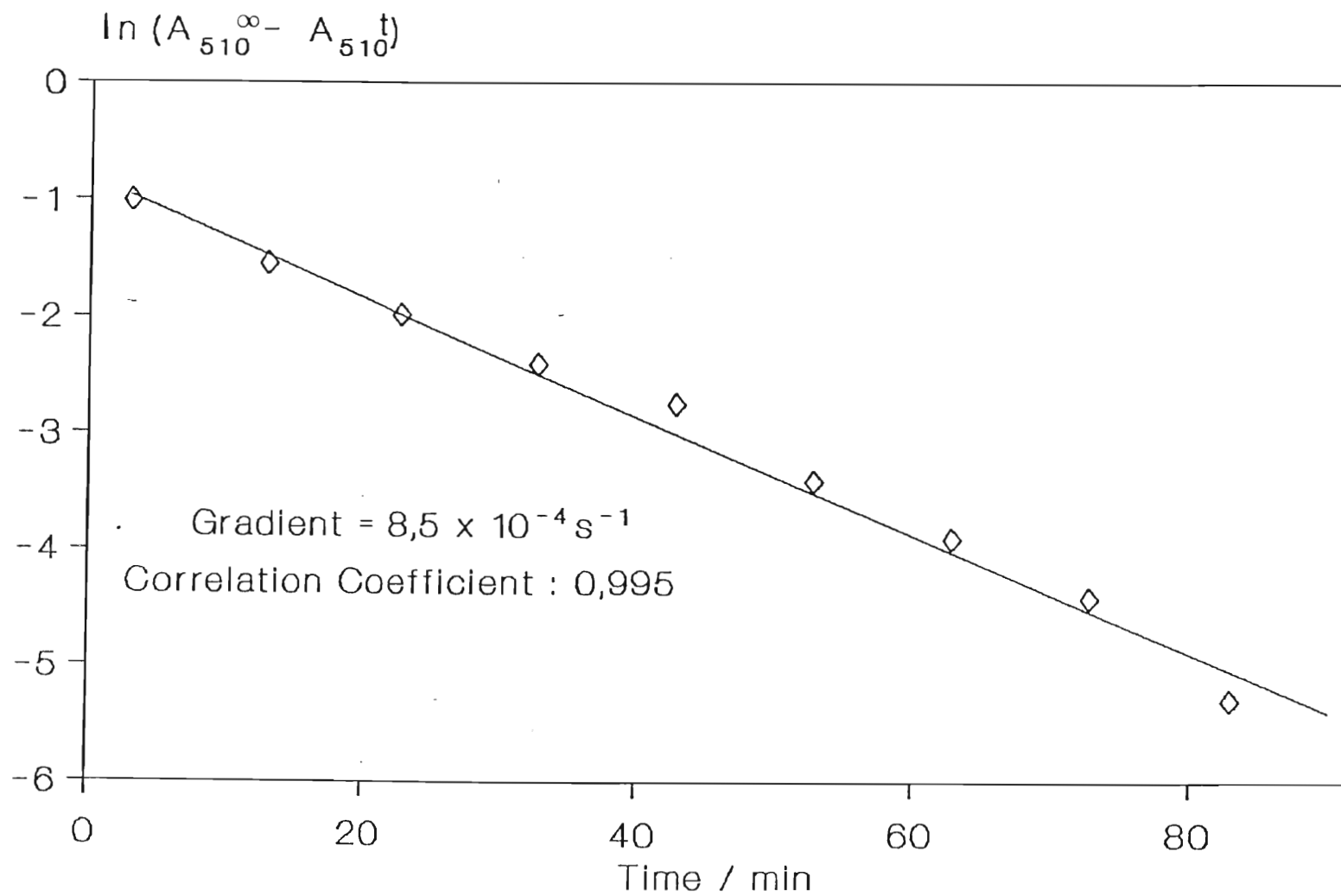


Figure (26). First order kinetic plot of $\ln(A_{510}^{\infty} - A_{510}^t)$ as a function of time for the formation of GePh_2^{2+} .

The kinetic modelling program CAKE, Version 3,0⁽¹¹⁴⁻¹¹⁶⁾ was used to predict the reduction in germanium concentration and the yields of GePh^{3+} and GePh_2^{2+} with time using the above value for k_2 and a value of $k_1 \geq 20,0 \text{ mol}^{-1} \text{ dm}^3 \text{ s}^{-1}$, (the results are similar if a greater value for k_1 is utilised). Given the medium in which the phenylfluorone reaction is carried out viz. ethanol/water containing gelatine, it is not surprising that no equilibrium or formation constant data is available in the literature. The low solubility of the fluorones, in general, has rendered an accurate measurement of stability constants virtually impossible. Nazarenko and Biryuk⁽¹¹⁷⁾ determined the value of $\log K_{\text{eq}}$ in 4% ethanolic medium for the salicylfluorone complex of Ti^{4+} , formula $\text{Ti}(\text{OH})_2(\text{H}_2\text{L})_2$ where L = salicylfluorone shown in figure (27a) below, to be 26,19. Besides this single value there are no quoted values for metal chelates of the fluorone type available in the literature. However, values of K_{eq} are available for a number of metal ions with the monodentate ligand 1-hydroxyxanthone⁽¹¹⁸⁾, which is similar to the fluorone structure (Figure (27b)). Selected values of K_{eq} and the medium in which the constant was measured are given in Table (14).

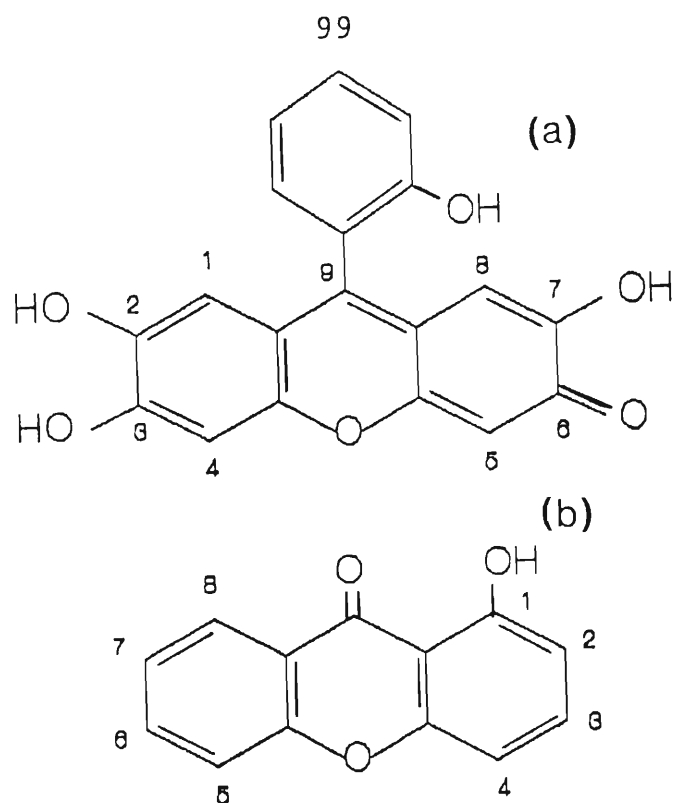


Figure (27). Structures of (a) Salicylfluorone : 9-(o-hydroxyphenyl)-2,3,7-trihydroxy-6-fluorone and (b) 1-hydroxyxanthone.

Metal ion	Medium	log K_{eq}
Al^{3+}	50% ethanol, 0,1 M $NaClO_4$	10,37
Cu^{2+}	50% ethanol, 0,1 M $NaClO_4$	8,92
Fe^{3+}	50% ethanol, 0,1 M $NaClO_4$	13,05
Th^{4+}	50% ethanol, 0,1 M $NaClO_4$	11,89
Co^{2+}	50% ethanol, 0,1 M $NaClO_4$	5,88

Table (14). Values of log K_{eq} for various metal ion complexes (ML) of 1-hydroxyxanthone.⁽¹¹⁸⁾

It is worth noting that the smaller, highly electropositive ions viz: Al^{3+} , Fe^{3+} and Th^{4+} have the largest values of K_{eq} while the values for Cu^{2+} and Co^{2+} are significantly smaller. This effect has been interpreted by Pearson⁽¹¹⁹⁾ in his 'Principle of Hard and Soft Acids and Bases'. RO^- (where R = xanthone) is a 'hard base' and Al^{3+} , Fe^{3+} and Th^{4+} are 'hard acids', whereas Cu^{2+} and Co^{2+} are 'borderline'. Since the molecular structures of 1-hydroxyxanthone and phenylfluorone are similar and the values of K_{eq} for the former were measured in a partially alcoholic medium, it is proposed that the equilibrium constant for the formation of GePh^{2+} (in which Ge^{4+} and phenylfluorone are 'hard') is of the order of the higher values quoted in Table (14), i.e. $\log K_{\text{eq}}$ approximately 10-12. Since $K_{\text{eq}} = k_1 / k_{-1} = 10^{10} - 10^{12}$, the value of the reverse rate constant is negligibly small if $k_1 = 20,0 \text{ mol}^{-1} \text{ dm}^3 \text{ s}^{-1}$.

Figure (28) shows the manner in which the concentrations of Ge^{4+} , GePh^{3+} and GePh_2^{2+} are predicted to change by CAKE for the starting conditions given in the legend of the figure. If it is assumed that the total observed absorbance of the germanium-phenylfluorone solution at 510 nm is a function of both GePh^{3+} and GePh_2^{2+} i.e. $A_{510}^t \propto (A_{510}\text{GePh}^{3+} + A_{510}\text{GePh}_2^{2+})$, then the total concentration of these species yield the computed curve of Figure (29). Reasonable kinetic fit is indicated by this plot. Notwithstanding the assumptions required to obtain this result, the pseudo first-order kinetics and associated rate constants proposed in this work give rationalisation of the observation made by other authors that the reaction between phenylfluorone and germanium is

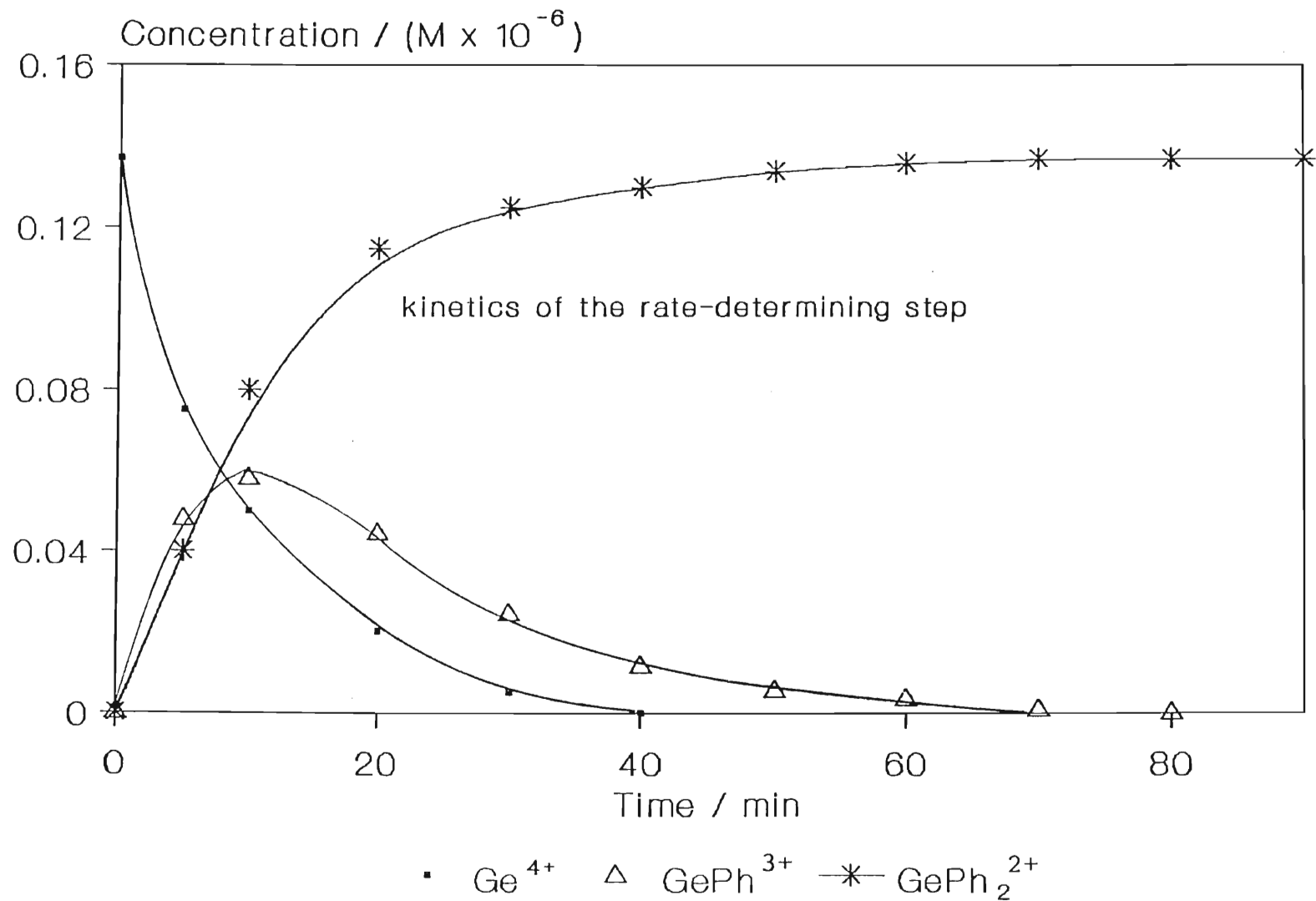


Figure (28). The yields of Ge^{4+} , GePh^{3+} and GePh_2^{2+} predicted by CAKE as a function of time. $[\text{Ge}]_{\text{initial}} = 1,37 \times 10^{-7} \text{ M}$; $[\text{Phenylfluorone}]_{\text{initial}} = 6,24 \times 10^{-5} \text{ M}$; $k_2 = 13,6 \text{ mol}^{-1} \text{ dm}^3 \text{ s}^{-1}$.

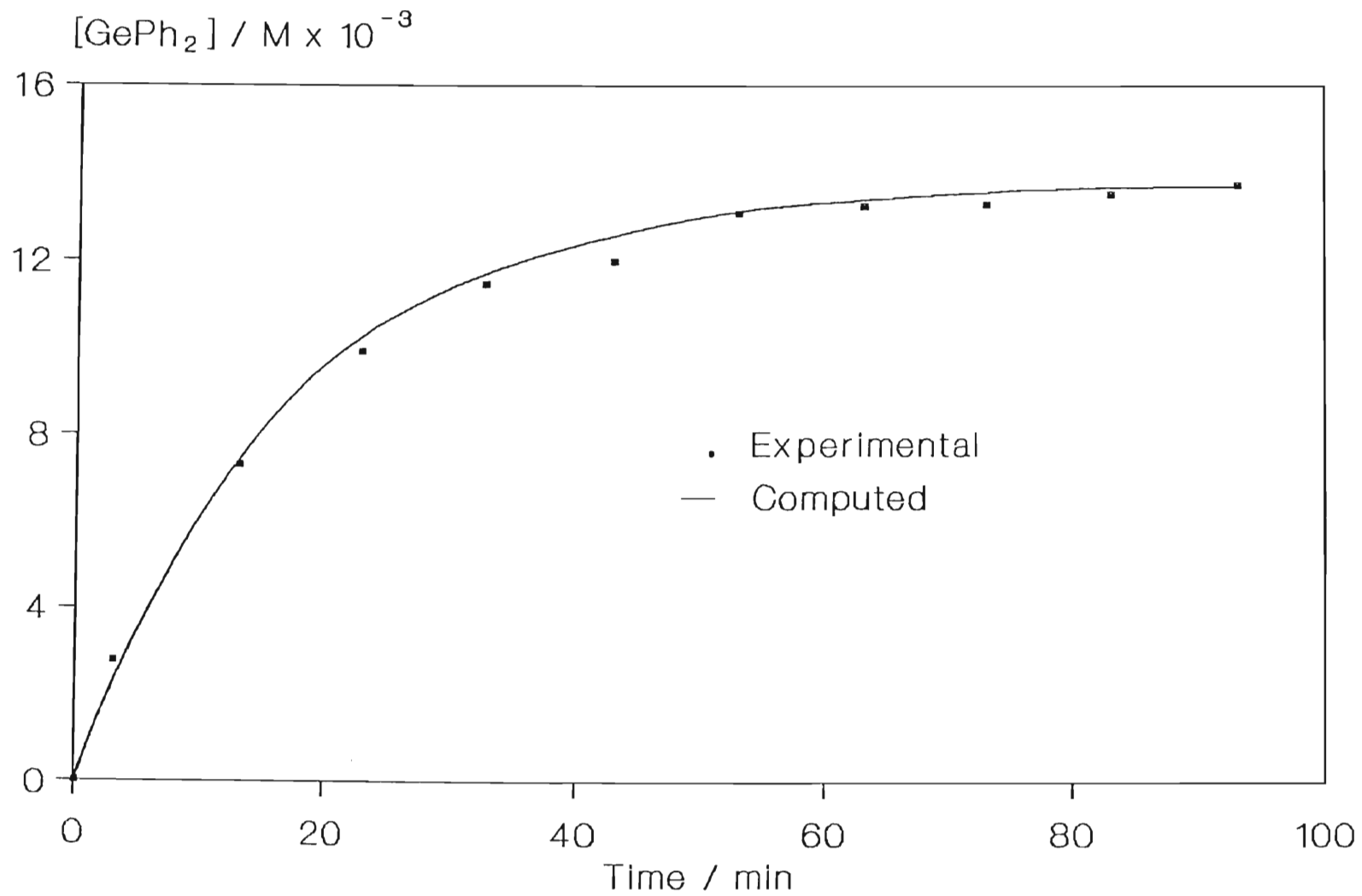


Figure (29). The yield of GePh_2 predicted by CAKE as a function of time assuming that $A_{510}^t \propto (A_{510}\text{GePh}^{3+} + A_{510}\text{GePh}_2^{2+})$.

2.3.3. Quantification of Germanium in Aqueous Solution by Atomic Absorption Spectroscopy.

The determination of germanium by atomic absorption spectroscopy is intrinsically an attractive technique because minimum sample preparation is required for analysis and excellent sensitivity and reproducibility are reported by some authors^(99,100,103). A study was therefore undertaken to determine the applicability of the technique to the analysis of aqueous germanium-containing samples.

A calibration curve for germanium was obtained at 265,2 nm using a Varian Model 1475 A.A Spectrophotometer and hollow cathode germanium lamp, for a set of standards in the concentration range 40-800 ppm, prepared by weight from GeO_2 and using a little hydroxide to aid solubility. A gas mixture of acetylene/nitrous oxide was used with a reducing flame. Over the range of germanium concentration quoted, a linear calibration curve was obtained. Table (15) summarises the concentrations of a number of samples determined by interpolation of the calibration curve and in addition, the actual (determined by weight) concentrations in ppm.

The low accuracy indicated by Table (15) has been attributed^(101,102) to the formation of highly stable oxide species which preclude the efficient production of germanium atoms. Even the use of a graphite furnace does little to improve the sensitivity of the method since reduction of GeO_2 to GeO occurs in the presence of carbon⁽¹⁰²⁾ and GeO begins to

sublime at ca. 1000°C. Since germanium atoms are not produced

Sample	[Ge] determined by A.A at 265,2 nm (ppm)	[Ge] _{actual} (ppm)	% Error
1	438	654	33,0
2	380	580	34,5
3	355	473	24,9
4	265	358	26,0

Table (15). Percentage error obtained for the direct determination of germanium by Atomic Absorption Spectroscopy. .

below approximately 3000°C (because of the large dissociation energy of the Ge-O bond), large errors are incurred. To overcome these difficulties, a procedure involving electrothermal atomization A.A. Spectroscopy (ETA-AAS) of the sample has been developed, with a detection limit of 0,8 µg/l, by workers at the Council For Mineral Technology, South Africa⁽¹²⁰⁾. Although this technique was not available in this laboratory, some germanium samples were quantitated by this procedure in order to establish some comparison in accuracy with the phenylfluorone technique. The results are outlined in Table (16).

Sample	[Ge] _{actual} (ppm)	Phenylfluorone (ppm)	% Error	*ETA-AAS (ppm)	% Error
1	2000,00	1981,00	0,95	1935,00	3,25
2	30,88	31,04	0,52	30,00	2,85
3	3,09	3,10	0,32	3,01	2,59

Table (16). Comparison of the relative error in germanium quantification via the phenylfluorone and ETA-AAS technique. * Determinations performed at the Council For Mineral Technology, South Africa.

The relative error of $0,60 \pm 0,32\%$ for the phenylfluorone technique versus $2,90 \pm 0,33\%$ for the ETA-AAS method imparts credibility to the spectrophotometric procedure, which has been adopted as routine in this laboratory.

In Chapter 1, an overview was given of the experimental techniques which have been devised by various workers to study the kinetics and equilibrium solvent extraction of metal ions by ligands soluble in aqueous immiscible diluents. The section following details the essential features of the techniques which have been utilised in this work to investigate the effects of various physical and chemical parameters upon the kinetics of solvent extraction of germanium by the ligands which were discussed in detail in Section 2.2.

2.4. Experimental Techniques for the Study of the Extraction Kinetics of Germanium in Quasi Steady-State and Vigorously-Stirred Systems

As the title above suggests, this section of the work will be divided into two parts, first the description of the apparatus, experimental technique and sampling for a system in which the interface between the aqueous and organic phases in contact is static and of known and reproducible area and second for systems designed to maximize the interfacial area between the phases in contact i.e. vigorously-stirred assemblies.

2.4.1. Experiments For The Study of Mass Transfer Across a Quiescent Interface.

It has been shown⁽¹²¹⁾ that when a chemical reaction occurs at a solid-liquid interface, then the process will be chemically controlled if the reaction is slow, diffusion-controlled if the reaction is fast and of some intermediate complex nature if the chemical reaction rate is of the same order as the diffusion rate. A similar state of affairs applies to the mass transfer with reaction of chemical species across a liquid-liquid interface and in order to investigate the unsteady-state transfer of solutes between phases, Lewis⁽⁷²⁾ designed a transfer cell (Figure (30)) in which the degree of turbulence of two phases in contact could be accurately controlled. The

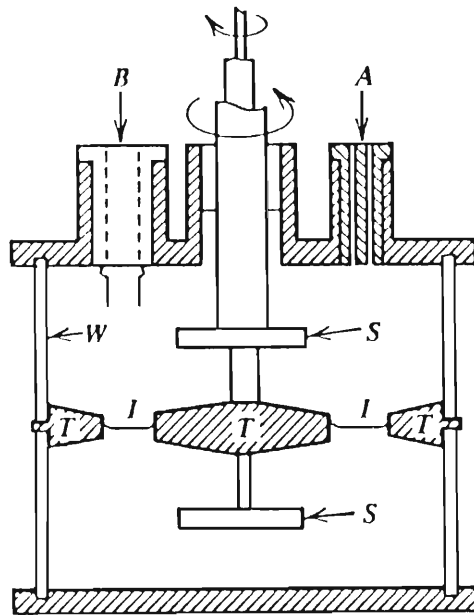


Figure (30). Original design of the Lewis cell⁽⁷²⁾. A : filling and sampling plug; B : polyethylene plug with electrodes; S : Impellers (flat); T : Stator baffles; W : Cylindrical glass wall; I : Annular interface.

cell was provided with horizontal baffles to give an annular interface and the stirrers were mounted on separate shafts, concentric with the support for the central baffle and driven at accurately controllable speeds. The central baffles were bevelled to enable drops of either phase accidentally introduced into the other to roll to the interface. All experiments were carried out at stirring speeds which would ensure the replenishment of chemical species to and from the interface without disturbing its quiescent nature.

Since the first experiments carried out by Lewis on the transfer of uranyl nitrate between water and various solvent systems⁽¹²²⁾, the original cell design has undergone a number of modifications and has been used to calculate mass transfer coefficients and elucidate the mechanisms of a number of solvent extraction processes^(59,73,123-128). The apparatus which was employed in this study is based upon the original design described by Lewis and essential design features are shown in the cross-section of Figure (31).

The reaction cell itself comprises a glass cylinder (114 mm internal diameter x 127 mm long, 5 mm wall with ground glass ends), tightly sealed via four cell retaining bolts into 5 mm annular channels (5 mm depth) of an upper and a lower teflon base plate. Both plates incorporate removable vertical baffles designed to reduce the build-up of eddy currents and vortices at the cell walls. The region between the baffles shown in Figure 31(a) constitutes the reaction zone or interface with geometrical area of exactly 103,9 cm². The dual phase impeller (Figure 31(b)) was driven by a Heidolph Model W77/18 overhead

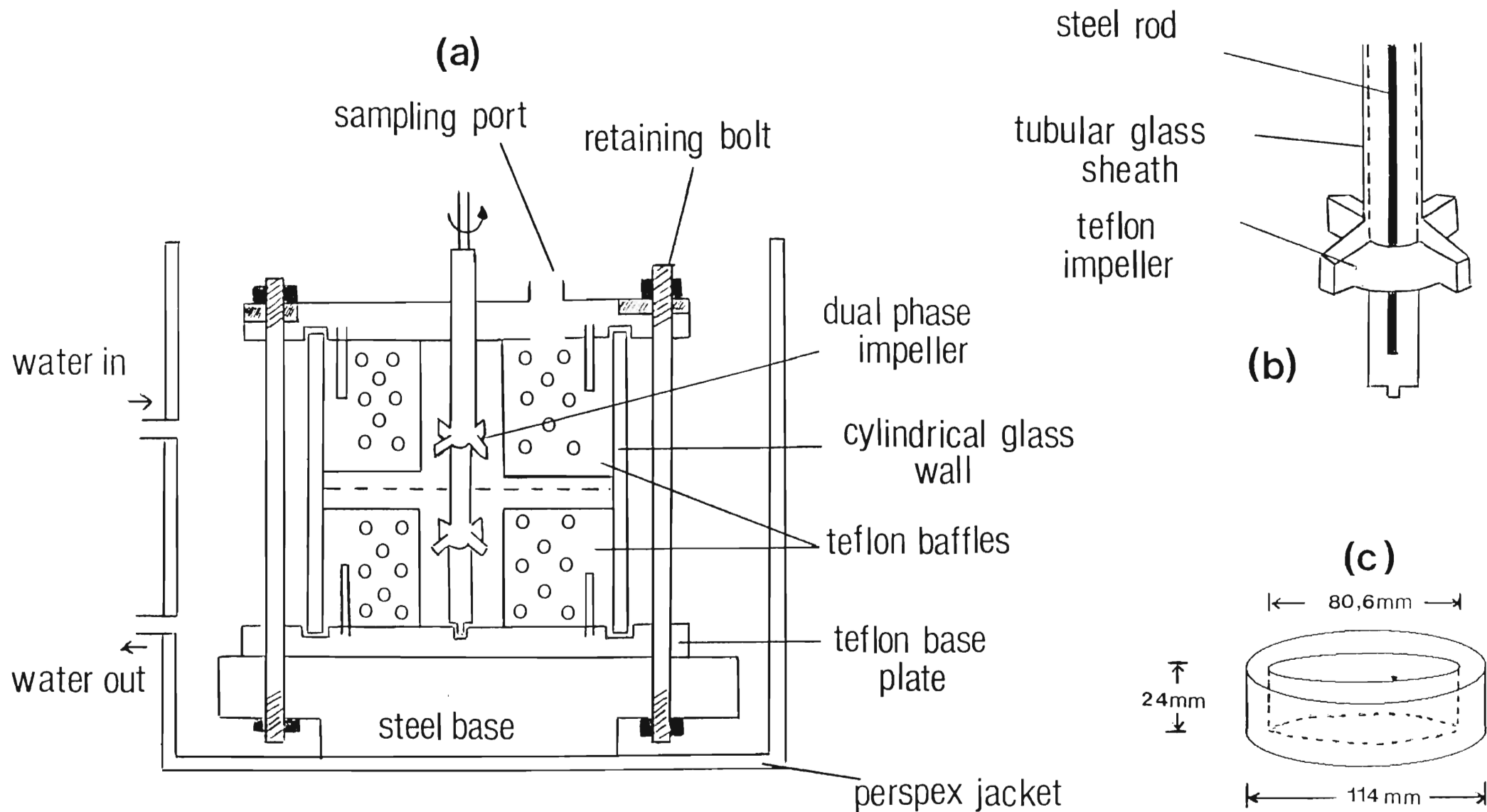


Figure (31). a) Essential design features of the adapted Lewis arrangement used for fixed-interface kinetic studies, b) Detail of the dual phase impeller, c) Teflon insert with approximately half the original interfacial area.

AC Stirrer. Temperature was held constant at $25^{\circ}\text{C} \pm 0,1^{\circ}\text{C}$ by circulating water from a Grant Model DP50 water bath through the perspex jacket which encloses the entire assembly.

In order to determine the relationship between the rate of extraction and the area of the interface, a tight-fitting teflon annular ring (Figure 31(c)) was inserted into the interfacial region. The cross-sectional area of this insert reduced the available reaction area by just less than a half to $50,3 \text{ cm}^2$.

For all extraction experiments reported in this work with this apparatus, the following procedure was adopted:

- (a) The cell assembly was tightly bolted together and water at 25°C allowed to circulate through the outer jacket for a few minutes to check for leaks.
- (b) Exactly 630 ml of germanium-containing aqueous phase was introduced via the sampling port into the cell using a long-necked funnel. This volume was found to fill the cell to a point mid-way between the baffles. The aqueous phase was allowed to equilibrate to 25°C for 30 minutes.
- (c) Exactly 550 ml of ligand-containing toluene solution at 25°C was then introduced into the cell by carefully pouring the solution into a funnel with a small bore and an outlet close to the interfacial region. As the cell filled with the organic solution, the funnel was gradually raised. This procedure was found to reduce 'splashing' of the interface to a minimum. The volume of organic phase specified ensures that this phase rises approximately 1 cm into the sample port, therefore

leaving no void between the upper phase and the teflon seal - this can be a source of turbulence⁽⁷²⁾.

(d) The dual-phase impeller was switched on and the time noted.

(e) Small samples of the aqueous phase were obtained at time intervals by carefully lowering a 1 ml pipette into the centre of the aqueous phase and withdrawing approximately 0,5-1,0 ml of solution.

(f) Germanium concentration in the aqueous phase was monitored with time via phenylfluorone quantification (Section 2.3.2.1).

The time for extraction to attain the equilibrium value depends upon the initial concentration of the ligand in the upper organic phase. For most kinetic runs reported in this work, sampling was continued for 48 hours, but for slow experiments, the extraction process was monitored for periods exceeding 72 hours.

The overhead stirrer was calibrated to produce a constant speed of 80 rpm \pm 2 rpm and was periodically checked for consistency. This speed was shown (Section 3.1.2) to be on the plateau of an observed rate constant vs impeller speed plot, indicating the preservation of the quiescent nature of the interface.

2.4.2. Procedures For The Investigation of Solvent Extraction Kinetics of Vigorously Stirred Systems.

In Chapter 1, brief descriptions of a number of assemblies

were given which have been used by various investigators to measure rate constants for solvent extraction systems and for the most part the choice of method would appear to be merely a matter of preference since they all operate on different principles. In this work, two devices were used to study liquid-liquid extraction kinetics, the first, which will be described next, utilizes a high speed centrifuge to separate light and heavy phases (organic and aqueous respectively) after contact in a mixing chamber, while the second and simplest operates in a manner similar to a batch mixer-settler in that samples of the aqueous phase are taken by allowing the phases in contact to separate for a short period of time. The latter technique was used extensively in this work.

2.4.2.1. The AKUFVE Solvent Extraction System

The acronym AKUFVE is an abbreviation in Swedish for 'Apparatus for Continuous Measurement of Partition Factors in Solvent Extraction'. The assembly was developed during 1962-1967⁽¹²⁹⁻¹³⁵⁾ to improve the accuracy and rapidity of measurement of solvent extraction distribution factors. The apparatus allows for the continuous monitoring of the distribution of dissolved species between immiscible phases since samples can be channelled to optical devices such as a u.v spectrophotometer^(132,136) but is also amenable to off-line sampling. The accuracy achieved in distribution ratio measurements which is of the order of $< 1\%$, has made the AKUFVE useful for the determination of equilibrium constants⁽¹³⁷⁻¹³⁹⁾, extraction isotherms⁽¹⁴⁰⁻¹⁴⁴⁾, thermodynamic constants^(138,145-147) and studies of solvent extraction reaction kinetics^(55,57,148-152).

The principle of the AKUFVE is illustrated in Figure (32). The aqueous and organic phases are vigorously stirred in the mixing chamber by an adjustable overhead stirrer. The two-phase mixture passes down (1) to a continuous flow centrifuge in which absolute phase separation takes place, i.e. the outgoing light and heavy phases are completely free from droplets of one another. The pure phases then pass along (2) and (3) through measuring devices for flow and then, if required, through detectors. Typically either the aqueous phase or the organic phase or both are connected to a continuous-monitoring uv-spectrophotometer or if the metal ion of interest is radioactive, to a scintillation counter^(131,153). Alternatively, the phases can be sampled manually via outlets (8) and (9). The liquids then flow through heat exchangers back into the mixing chamber. The heat exchangers are necessary because heat develops in the mixing chamber and as a result of the acceleration and retardation of liquids in the centrifuge. The heart of the AKUFVE system is the H-centrifuge, shown in detail in Figure (33) and *in situ* in Figure (34), labelled (14). The technical data for the system used in this study is given in Table (17) below. It is characterised by a high speed of rotation (up to 14 000 rpm), short hold-up time (0,3 - 5 seconds) and efficient phase separation. Tests have shown that absolute phase separation by the H-centrifuge is achieved for most liquid-liquid systems and that none of the phases leaving it contain entrained droplets of the other phase^(129,130,154). If this were not the case, the on-line measurement of, for example the absorbance and therefore concentration of a species in the aqueous phase at a particular wavelength, would be complicated if just a little, say benzene, were flowing through the uv cell.

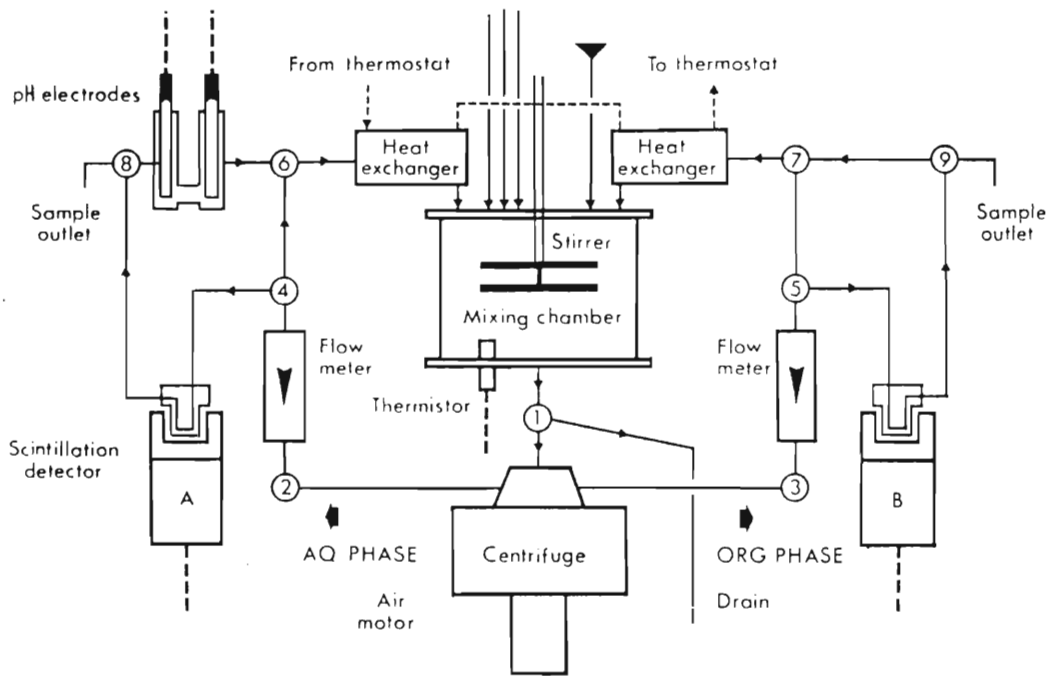


Figure (32). Diagram of the AKUFVE liquid flow system. The pH electrodes and scintillation detector shown are optional. (252)

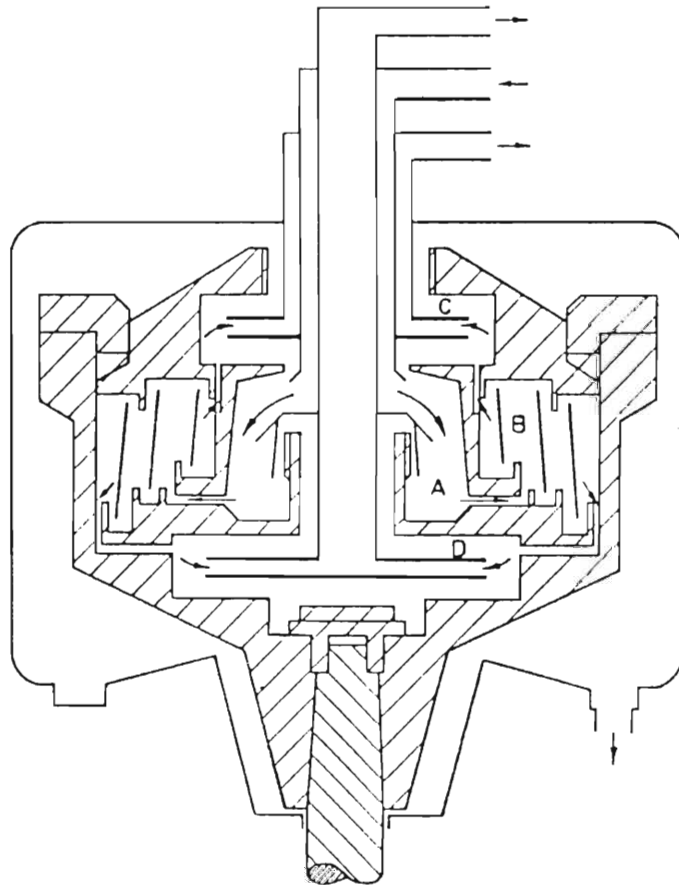


Figure (33). The principle of operation of the H-centrifuge. (A) : Inlet chamber, (B) Separation volume, (C) and (D) are collecting chambers with pump wheels. (After H. Reinhardt and J. Rydberg, Chem.Ind., April 1970, 488.)

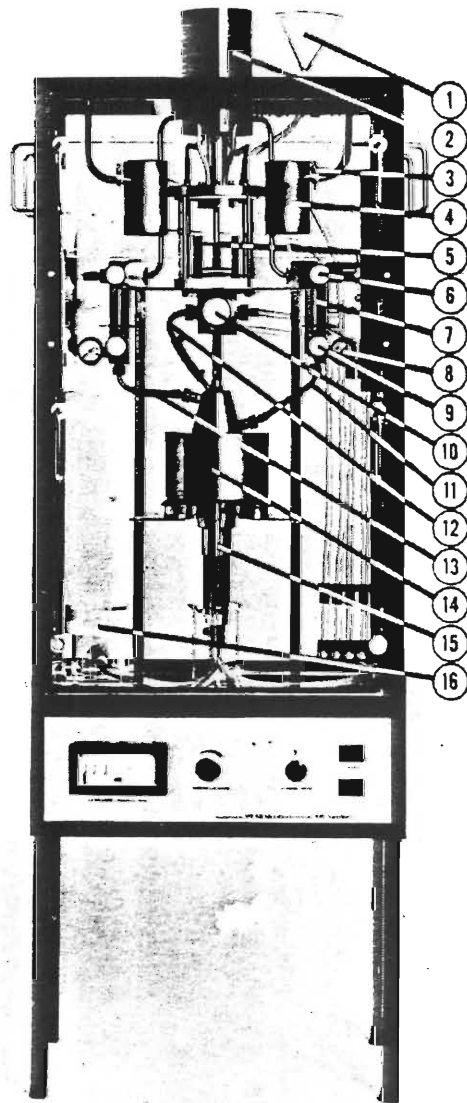


Figure (34). The AKUFVE system with H-33tr centrifuge. (1) main feed inlet; (2) stirrer motor; (3) sampling valve; (4) heat exchanger; (5) mixer; (6) valve 'detector or mixer'; (7) flowmeter; (8) pressure guage; (9) throttling valve; (10) valve 'centrifuge or drain'; (11) centrifuge outlet, light phase; (12) centrifuge inlet; (13) centrifuge outlet, heavy phase; (14) centrifuge; (15) centrifuge air motor; (16) silencer.⁽²⁵²⁾

Parameter	
Flow Capacity (Benzene/water) $\ell \text{ hr}^{-1}$	300
Bowl Volume, ℓ	0,12
Hold-Up Time, seconds	1,5
Rotational Speed (max)	
No Liquid Flow, rpm	22 000
Maximum Liquid Flow, rpm	14 000
Maximum Air Consumption, $\text{m}^3 \text{ min}^{-1}$	0,45
Motor Power (Mixer), W	500

Table (17). Technical data for the H-centrifuge of the AKUFVE apparatus, type H-33tr.

Briefly, the H-centrifuge operates as follows: (refer to Figure (33)). The organic/aqueous mixture enters centrally into the centrifuge and is accelerated to the rotational speed in the inlet chamber (A). After acceleration, the mixture is forced into the separation volume (B), which comprises eight sector-shaped chambers arranged symmetrically about the axis and separate from one another. In this chamber the droplets have a 'zig-zag' motion imposed by peripheral partition walls and interspersed baffle ridges. The separated phases are discharged from an upper collecting chamber, (C)- the organic phase, and from a lower one (D)- the aqueous phase, by pump wheels of various types which maintain an adequate pressure and avoid excessive frothing of the liquids. Power to the

centrifuge is provided by an pneumatic air motor driven by compressed air. For this work, a Balma Model VD2, 50 litre 2HP Air Compressor was used, outputting approximately 3-Bar of compressed air.

It is worth noting, that the developers of the AKUFVE apparatus were extremely careful in their choice of materials for the components of the assembly. Table (18) summarises the materials used for the various components of the AKUFVE which are in contact with the liquid phases flowing through the apparatus, (refer to Figure (34) for component labels). All of the materials listed in this table are considered to be as innocuous as possible to any extraction process involving metal ions and passive to the action of strong acids, alkalis and solvents.

The following procedure was adopted for kinetic experiments performed with this apparatus in this work. Numbers in brackets refer to the components of Figure (34):

- (a) 300 ml of germanium-containing aqueous phase was charged into the mixing chamber (5) and mixed at a setting of '3' - approximately 1250 rpm.
- (b) Air output from the compressor was set at approximately 3 Bar. This causes the centrifuge to spin at a rate of approximately 8500 rpm.
- (c) Valve (10) was turned to 'centrifuge' and the aqueous contents of the mixer allowed to circulate through the instrument; Water at exactly $25^{\circ}\text{C} \pm 1^{\circ}\text{C}$ was circulated through the heat exchanger units (4).

Component	Material
<u>Mixing Chamber</u> (5)	
Reaction cylinder	Glass
Top/Bottom Lid	Teflon sealed into titanium
Inlet/Outlet Joints	Teflon or Viton
Stirrer Blade	Titanium
<u>H-Centrifuge Baffles</u> (14)	Titanium
<u>Flow System</u>	
Throttling Valve (9)	
Valve Body	Titanium
Valve Needle	Teflon
Pressure Gauge Membrane (8)	Teflon
Flowmeter (7)	
Cavity	Glass
Floating Ball	Tantalum
Heat Exchanger (4)	Titanium

Table (18). Materials of the components of the AKUFVE apparatus.

(d) 300 ml of ligand-containing toluene, pre-equilibrated to 25°C was added after temperature equilibration of the aqueous phase and the time noted when all the organic had been added.

(e) At time intervals, valve (6) on the aqueous side was turned from 'mixer' to 'detector'. This directed approximately 2 ml of aqueous phase into an L-shaped side-arm from which a 200 μ l sample was taken. The valve was then returned to the 'mixer' position, thus returning the small isolated volume back into the bulk. Aliquots (25 μ l) of the sample were analysed for germanium as described previously (Section 2.3.2.1)

(f) The organic phase was not sampled and the valve controlling the flow of this phase was left in the 'mixer' position.

There are a number of points worth mentioning for future users of this instrument:

(1) Air pressure to the centrifuge must be carefully monitored. Under load, the centrifuge decelerates initially and the air pressure required to maintain the centrifuge at a speed which maintains absolute phase separation is increased. If the air pressure is allowed to fall below approximately 2 Bar (see Figure (35a)) which translates to a centrifuge speed of approximately 6400 rpm, the phases are incompletely separated and an entire experimental run may need to be discarded.

(2) The centrifuge generates a vortex effect and phases leaving the unit do so with turbulence. This effect is exacerbated by the points noted in (1) above. Laminar flow can be achieved if both throttling valves (9) are left fully open.

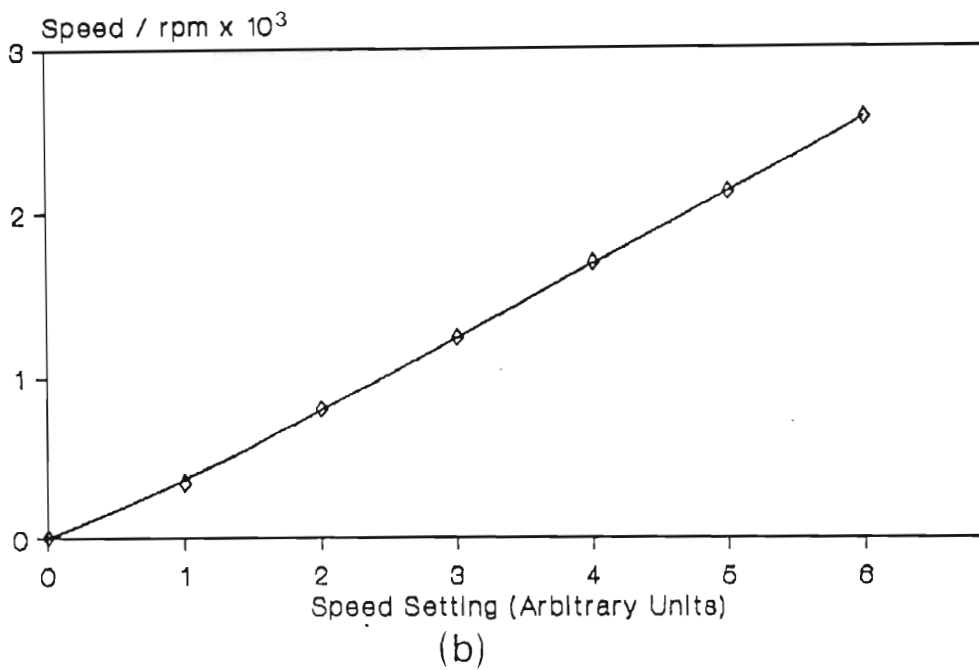
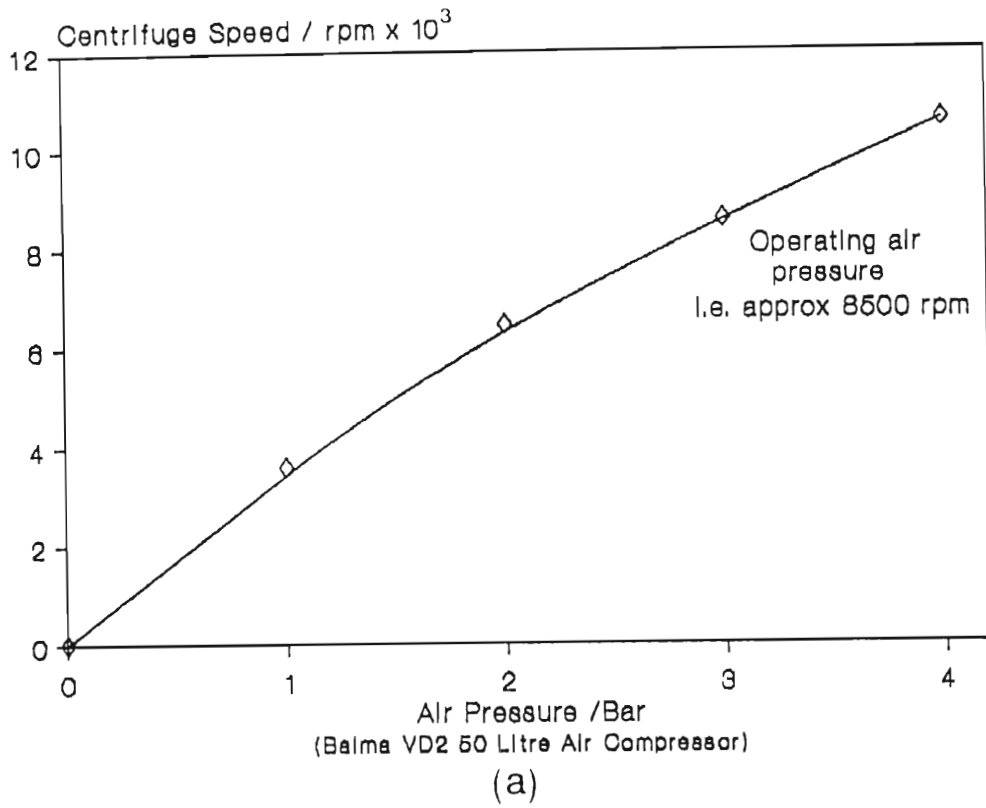


Figure (35). a). AKUFVE centrifuge speed under load as a function of air pressure, b). AKUFVE mixer setting versus actual speed.

(3) Figure (35b) shows the relationship between the stirrer speed setting of the mixer on the unit and the actual speed of the stirrer under load (450 ml water in the mixing chamber). It has been shown⁽¹⁵⁵⁾, that provided this setting is greater than '2', which correlates with a stirrer speed of approximately 800 rpm, then the rate of reaction is constant. For all experimental runs reported in this work, a setting of '3' was selected.

Because of the ability to carefully control the temperature of experiments with the AKUFVE apparatus, some experiments were performed to investigate the effect of temperature upon the rate of extraction of germanium by the various ligands which have been discussed, in order to facilitate the calculation of the enthalpy of reaction via an Eyring (Arrhenius-type) plot. For these experimental runs, all conditions as described already prevailed except the temperature of the water passing through the heat exchanger was varied over the range 15-45°C.

2.4.2.2. The Investigation of Liquid-Liquid Solvent Extraction Kinetics With a Simple Mechanical Shaker.

The preceding section described an assembly which allowed for the continuous on-line monitoring of the extraction kinetics and distribution data for liquid-liquid extraction systems. If, however, (i) phase separation is rapid when the phases in contact cease to be agitated, (ii) stable emulsions are not formed during contact, (iii) the rate of agitation of the phases is such that the observed rate of reaction is

chemically-controlled and not diffusion-controlled, (iv) an uncontaminated sample can be obtained from the aqueous phase, (v) the rate of exchange of solute across the static interface is slow, (vi) the movement of the device used to shake the liquid mixture is reproducible and (vii) the extraction kinetics are sufficiently slow, then the most convenient and rapid technique for the determination of rate and equilibrium data is the use of a mechanical shaker. The use of such devices by other workers is well represented in the literature for equilibrium, distribution and kinetic studies^(51,53,61,62,65,76). Besides the inherent simplicity of the method, one advantage of using a simple shaking apparatus is that it behaves in a similar manner to conventional batch mixer-settlers.

For all experimental runs performed in this work, whether for determining the equilibrium percentage germanium extraction or investigating the kinetics of extraction under various conditions, a Gallenkamp wrist-action shaker was used. Extraction and stripping experiments were carried out at room temperature ($21^{\circ}\text{C} \pm 1^{\circ}\text{C}$), by shaking the mixture of organic and aqueous phases (total volume 200 ml) in pear-shaped 500 ml flasks. For most runs, the phase ratio was 1:1, although some experiments were performed to optimize stripping and extraction phase ratios. Kinetic runs were timed from the addition of the last quantity of ligand-containing organic solution to the germanium-containing aqueous solution. The shaker was operated at the maximum setting of approximately 770 oscillations per minute (opm). Single extraction experiments performed at 500 opm and 1300 opm (Griffin Model 760S Flask Shaker), produced no change in the rate of reaction

It is assumed therefore that all runs were operated under conditions in which the diffusion of species would not be a limiting factor. Sampling of the aqueous phase involved stopping the shaker, allowing phase separation to occur, withdrawing an aqueous sample of approximately 0,2-0,3 ml and restarting the shaker. In most cases, phase separation was of the order of 5-10 seconds, however if chemical modifiers i.e. alcohols, were added to the organic phase, separation times were extremely rapid (< 5 seconds). If stable emulsions formed, aqueous samples were obtained by dispensing 0,3 ml of emulsified mixture into an Eppendorf vial and separating the phases by centrifugation with a Hettich Model 2021 microlitre centrifuge. Less than one minute was usually required in order to obtain 2 x 25 μ l samples for phenylfluorone analysis.

The mechanical shaker was used to investigate the effect of a number of parameters upon the kinetics and equilibrium percentage extraction of germanium by the ligand preparations of concern to this study, which were naturally varied one at a time. Accounts of the necessary experimental details are given in the sections which follow.

2.4.2.2.1. Preparation of Ligand and Germanium Solutions.

Germanium solutions were prepared by dissolving 0,9365 g (for 0,65 g/l Ge) or 0,2881 g (giving 0,20 g/l Ge), GeO_2 in approximately 700 ml deionized water with heating. For the higher concentration, a few drops of a saturated NaOH solution were added to the hot solution to assist solubility. Ligand solutions were prepared, and will henceforth be specified as

such, by **mass**. Where necessary, results will be presented in which the concentration has been calculated by adjusting weighed quantities for the purities specified in Section 2.2.1.

2.4.2.2.2. Adjustment of Aqueous Phase pH.

For studies on the effect of aqueous phase pH upon the extraction kinetics of germanium, buffered solutions were prepared for values of $\text{pH} \geq 0,24$ (the pH of 0,5 M H_2SO_4). Buffering is considered necessary at high pH because a proton is released for each ligand molecule which coordinates with the germanium ion. Table (19) enumerates the preparation of buffers utilised for this study in the pH range 1-7. All prepared buffer solutions were checked against a combination glass electrode calibrated against three (pH 4,0, 7,0 and 9,0) standard buffers (BDH Clark and Lub's Solutions, all specified $\pm 0,02$ pH units accuracy). For values of $\text{pH} < 0$, i.e. 1,0 M and 1,5 M H_2SO_4 , pH was calculated using a value of $K_2 = 1,2 \times 10^{-2} \text{ M}^{(156)}$ for sulphuric acid.

Buffer Contents	pH	Ionic strength Adjusted with:
(1) 62,5 ml (a) + 167,5 ml (b)	1,00	KCl
(2) 62,5 ml (a) + 16,25 ml (b)	2,00	KCl
(3) 125,0 ml (c) + 55,75 ml (d)	3,00	KNO ₃
(4) 207,5 ml (e) + 42,5 ml (f)	4,00	KNO ₃
(5) 80,0 ml (e) + 170,0 ml (f)	5,00	KNO ₃
(6) 125,0 ml (g) + 14,0 ml (h)	6,00	KNO ₃
(7) 125,0 ml (g) + 72,8 ml (h)	7,00	KNO ₃

Table (19). Components for the preparation of buffered germanium solutions. Volume : 250 ml, Mass GeO₂ = 0,2341g (≡ 0,65 g/l Ge), Ionic Strength = 0,5 M.

Key to Buffer Contents:

(a) 0,2 M KCl, (b) 0,2 M HCl, (c) 0,1 M Potassium hydrogen phthalate, (d) 0,1 M HCl, (e) 0,2 M CH₃COOH (f) 0,2 M CH₃COONa, (g) 0,1 M KH₂PO₄, (h) 0,1 M NaOH

2.4.2.2.3. The Effect of Free 8-Hydroxyquinoline On Germanium Extraction.

8-hydroxyquinoline is very soluble in acidic media due to protonation of the tertiary amine group which occurs at pH ≤ 4,99⁽⁹⁰⁾. 8-hydroxyquinoline is known to complex germanium and under certain conditions, extracts the metal ion into a suitable diluent. Since all of the ligand preparations of interest to this work contain free oxine (which may be as much

as 3-5% m/m in the relatively impure Lix 26 reagent), a detailed study was undertaken to determine the effect upon extraction of adding free oxine to Lix-containing solutions as well as separately dissolved in toluene. The distribution of the impurity between toluene and an aqueous phase containing 1,5 M H_2SO_4 , was also investigated in order to indicate in which phase the reagent resides during extraction. The following 8-hydroxyquinoline solutions were prepared to facilitate these studies:

(a) Solutions in the concentration range $6,89 \times 10^{-4}$ - $5,51 \times 10^{-5}$ M oxine in 1,5 M H_2SO_4 for the preparation of a uv-calibration curve (monitoring wavelength 360 nm). A least squares value of $1,724 \times 10^3 \text{ mol}^{-1} \text{ dm}^3 \text{ cm}^{-1}$ was obtained for ϵ_{360} from the resulting Beer's Law plot (correlation coefficient 0,9998).

(b) Toluene solutions containing 0,1 - 40,0 g/l ($6,89 \times 10^{-4}$ - $2,76 \times 10^{-1}$ M) 8-hydroxyquinoline

(c) Solutions containing 10 and 30 g/l oxine in 50 g/l Lix 26/toluene.

Both (b) and (c) were contacted with aqueous phases containing approximately 0,65 g/l Ge in 1,5 M H_2SO_4 . The aqueous phase was analysed for germanium via the phenylfluorone procedure already described. The possibility of extraction by oxine at pH values approaching the pK_a of the hydroxyl group ($9,66 \pm 0,03^{(90)}$), was also investigated by contacting toluene solutions containing 17 g/l 8-hydroxyquinoline with germanium-containing aqueous phases with initial pH values of 8,60 and 11,10, prepared by adjustment of 100 ml germanium solutions with a dilute NaOH solution. The results of this study are reported in detail in Section 3.3.2.

2.4.2.2.4. The Effect of Ionic Strength on Germanium Extraction Kinetics.

The effect of ionic strength upon the kinetics of germanium extraction was investigated by dissolving the quantities of Na_2SO_4 detailed below into 100 ml of an 0,65 g/l germanium-containing solution in 0,5 M H_2SO_4 . The pH of the aqueous phase (approx 0,24) and a reasonably low ligand concentration (50 g/l Lix 26), were selected as being conditions which would retard the observed extraction rate sufficiently enough to permit quantitative comparison of the resulting data. Ionic strengths were calculated as below:

$$I_m = \frac{1}{2} \sum_i m_i z_i^2 \approx I_c = \frac{1}{2} \sum_i c_i z_i^2 \quad (27)$$

I_m : Molal ionic strength

m_i : molality of species i

z_i : charge on species i

Since $1 \text{ mol kg}^{-1} \approx 1 \text{ mol litre}^{-1}$, I_m is approximated to I_c above hence ionic strengths are reported in units of mol dm^{-3} in this work.

Mass Na ₂ SO ₄ added to 100 ml solution (g)	[Na ₂ SO ₄] in solution / M	I _c
0	-	0,715
7,102	0,50	2,215
14,204	1,00	3,715
22,726	1,60	5,515
35,510	2,50	8,215

Table (20). Solution preparation for investigating the effect of ionic strength on extraction kinetics. [H₂SO₄] = 0,5 M.

2.4.2.2.5. The Effect of the Aqueous/Organic Phase Ratio.

The ratio of the volume of the metal-containing aqueous phase to the ligand-containing organic phase (abbreviated a:o) is a parameter which is necessary for the hydrometallurgical development of any solvent extraction process. In principle, it is advantageous to contact as large a volume of aqueous phase as possible with the minimum volume of organic phase which will carry the metal-loaded ligand. Moreover, the ligand concentration in the organic phase is reduced, for economic reasons, to a quantity which gives an acceptable percentage extraction in a single pass of a multiple counter-current or batch mixer-settler extractor. This is of course, within the realm of chemical process design and outside the scope of this work, however, a:o data has been obtained in anticipation of

this development and is reported upon in Section 3.16. Table (21) below details the a:o ratios which were investigated: in each case the total volume remained constant. Aqueous phases contained the quantity of germanium equivalent to an $8,954 \times 10^{-3}$ M solution (i.e. constant moles in the aqueous phase) in 1,5 M H_2SO_4 , whilst organic phases were adjusted to give a quantity of Lix 26 equivalent to 75 g/l reagent in toluene in each solution.

	A	B	C	D	E	F
Volume aqueous (ml)	50	75	100	125	150	175
Volume organic (ml)	150	125	100	75	50	25
Ratio a:o	1:3	3:5	1:1	5:3	3:1	7:1

Table (21). Aqueous : Organic phase ratios investigated to determine optimal conditions. [Ge] = molar equivalent of 0,65 g/l : [Lix 26] = quantity equivalent to 75 g/l in toluene.

Under the conditions investigated therefore, the molar quantities of germanium and Lix 26 were constant and the only variable was the phase volumes.

2.4.2.2.6. Choice of Diluent.

In solvent extraction, the term 'diluent' refers to the organic liquid in which the extractant and modifier (discussed in the next section) are dissolved to form the 'solvent'. In

the majority of cases, the diluent comprises the major portion of the solvent. Proper selection of the diluent and modifier can be almost as important as selecting the extractant because of the effects, both physical and chemical, which the diluent and modifier can exhibit. The general requirements of a diluent are that it: (i) be insoluble in the aqueous phase, (ii) be mutually soluble with an extractant and modifier, (iii) possess high compatibility with an extracted metal species, thus minimising both the problem of third-phase formation and low loading capacity of the solvent, (iv) have low volatility, (v) have low surface tension and (vi) be cheap and readily available. The functions of the diluent are to decrease the viscosity of the extractant, to provide a suitable concentration of extractant as may be required for a particular objective, to decrease the emulsion-forming tendencies of the extractant (most extractants are surface-active and emulsify with agitation) and finally to improve the dispersion characteristics of the ligand. A number of studies have been considerably illuminating in respect of the close association between extractant behaviour and diluent nature⁽¹⁵⁷⁻¹⁵⁹⁾ and in particular correlations have been detailed between extractant performance and the viscosity, polar nature and solvency power of the diluent. In this work, the effect upon extraction performance by four diluents viz. toluene, hexane, BDH 'Heavy Distillate' and Paraffin (i.e. kerosene) were investigated. The comparison in behaviour was made by ascertaining their effect upon the kinetics and equilibrium extraction of germanium of concentration 0,65 g/l in 0,5 M H₂SO₄ by 50 g/l Lix 26 in the diluents specified. The measurement of viscosity and dielectric constant of these

solutions are discussed in Sections 2.5.3 and 2.5.2 respectively.

2.4.2.2.7. The Effect of Chemical Modifiers.

The addition of a modifier (usually aqueous-insoluble alcohols) to overcome third phase and emulsion tendencies in a solvent system is a common practice in solvent extraction. As with extractants and diluents, modifiers should be very soluble in the organic phase, insoluble in the aqueous phase, readily available and cheap. Usually the amount of modifier required in a solvent is of the order of 2-5% v/v, but some systems demonstrate improved extraction characteristics with modifiers present in much larger quantity, 10% or more. As with diluents, the choice of modifier is not indiscriminate: selection is based upon the nature of the diluent and extractant.

In this work, the abilities of five modifiers to enhance the extraction characteristics of the ligand reagents have been determined, viz. benzyl alcohol, n-octanol, n-butanol, n-pentanol and n-propanol. Although only one of these (n-octanol), has been generally reported upon in the literature^(53,160), the intention in this work was merely to establish a trend amongst an homologous series of aliphatic alcohols and to compare their efficacy with an aromatic alcohol.

For all five alcohols, 10% v/v solutions of alcohol were prepared by adding 10 ml of the alcohol to 90 ml of a 50 g/l ligand/toluene solution, therefore diluting the ligand reagent

to 45 g/l. The 100 ml composite solvents were shaken with 100 ml $\sim 0,65$ g/l Ge in 0,5 M H_2SO_4 , aqueous samples were taken and analysed for germanium.

For n-octanol, further studies were performed to determine the effect of increasing the modifier from 5-100% by volume, upon the extraction characteristics of an extremely dilute solution (14 g/l) of Lix 26 in 'BDH Distillate' (see Section 2.4.2.2.6). Equilibrium percentage extraction data for all five modifiers was also obtained for Lix 26 in this diluent (14 g/l Lix 26, BDH Distillate, 10% v/v modifier).

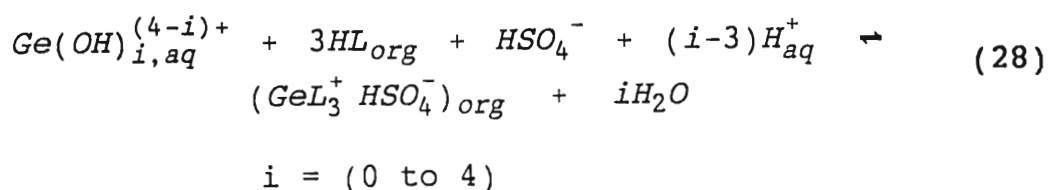
Modifiers also seem to influence the ability of a strip solution such as sodium hydroxide to remove chelated metal and this is dealt with in full in Section 2.4.2.2.9.

2.4.2.2.8. Studies With 'Purified Reagents'.

The 'acid-washing' procedure for purification of 7-alkylated-8-hydroxyquinoline extractants was discussed in Section 2.2.2.4, where it was concluded that the method did indeed remove free oxine from the extractant, but it was also suggested that the method may result in the gradual extraction of other reagent components. To ascertain whether this treatment subsequently affected the rate of germanium extraction by Lix 26, the extraction characteristics of 50 g/l solutions of as-supplied and acid-washed Lix 26 both dissolved in toluene were compared. Aqueous phases contained $\sim 0,65$ g/l Ge in 1,5 M H_2SO_4 .

2.4.2.2.9. Investigation of the Kinetics of 'Stripping' Germanium-Loaded Ligand.

Stripping is the reverse reaction to extraction. The choice of stripping reagent is dependent upon the stability of the extracted species and is usually either a strong acid or base. Inspection of Equation (28) below, indicates that if $i = 0, 1$ or 2 then a lowering of the aqueous phase pH should favour the left-hand-side of the equilibrium, i.e. the metal is stripped from the ligand.



In practice however, this method of stripping has been shown to be inefficient⁽⁶⁵⁾, however contact with a solution of high pH has been shown to be effective for germanium stripping from Kelex 100⁽⁶⁵⁾ according to Equation (29):



The study of the stripping kinetics and the factors which have an effect upon the process usually attracts a research effort of an equivalent magnitude to the extraction process. In this study, only the most important aspects relating to the stripping phenomenon have been investigated.

For all stripping experiments, aliquots of germanium-loaded (usually 100 ml) ligand solution were contacted with a quantity of sodium hydroxide solution. The increase in concentration of germanium in the alkaline aqueous phase with time, was monitored by sampling from the shaker as previously described and determining the concentration of metal via phenylfluorone. In this way, the following stripping characteristics were investigated:

- (i) The rate of stripping versus [NaOH] over the range 0,5 - 5,0 M.
- (ii) The influence, if any, of a modifier present in the organic phase, on the stripping rate,
- (iii) The determination of an optimum a:o ratio. Table (22) below summarises the details of experiments performed to establish this parameter.

	1	2	3	4
Volume loaded organic (ml)	40	40	40	40
Volume alkaline aqueous (ml)	40	80	120	200
Ratio a:o	1	2	3	5

Table (22). Ratio of volume of strip solution to germanium-loaded organic phase for the determination of an optimum a:o ratio. $[\text{Ge}]_{\text{org}} \sim 0,65 \text{ g/l}$, $[\text{Lix } 26] = 50 \text{ g/l}$ in toluene. $[\text{NaOH}] = 1 \text{ M}$.

2.4.2.2.10. Investigation of the Selectivity of the Ligand Reagents for Germanium.

In Chapter 1, semi-quantitative ICP-MS data was given for the metal composition of the fume from a zinc smelter and it was noted that the levels of germanium present could render a germanium extraction process economically viable if plant leach liquors were subjected to some pre-concentration process. Additionally, germanium often occurs in zinc ores in sufficient quantity to interfere with the electrowinning process. A study was therefore undertaken to determine the selectivity of the 7-alkylated-8-hydroxyquinoline ligands for germanium over zinc under various conditions. Cote and Bauer⁽⁵³⁾, achieved excellent selectivity with Kelex 100: in a mixed aqueous feed containing 1,22 g/l germanium, 81,5 g/l ZnSO₄ and 150 g/l H₂SO₄, 87% of the germanium and only 0,1% of the zinc were transferred to the organic phase.

The following experiments (Table (23)) were performed to examine the selectivity of the ligand reagents towards germanium.

Organic Phase (100 ml)	Aqueous Phase (100 ml)
(1) 50 g/l Lix 26 TN 01787 } in toluene TN 02181 }	~ 0,58 g/l Zn ²⁺ in 1,5 M H ₂ SO ₄
(2) 50 g/l Lix 26 in toluene	~ 0,58 g/l Zn ²⁺ buffered at pH 2,5

Organic Phase (100 ml)	Aqueous Phase (100 ml)
(3) 50 g/l Lix 26 in toluene	(i) ~ 0,65 g/l Ge + ~ 0,65 g/l Zn ²⁺ (ii) ~0,65 g/l Ge + ~ 6,50 g/l Zn ²⁺

Table (23). Details of experiments performed to investigate the selectivity of 7-alkylated-8-hydroxyquinoline extractants for germanium over zinc.

Phases were shaken together as described previously, and aqueous samples taken at regular time intervals. (1) and (2) in Table (23) would test whether Zn²⁺ (added as ZnSO₄·7H₂O; 0,58 g/l zinc is the molar equivalent of 0,65 g/l germanium), is extracted at all at low and at a higher pH. Experiment (3) would indicate the selectivity for germanium in the presence of a 1:1 and 1:10 Ge:Zn mass ratio and any interference with the germanium extraction process. Germanium concentration in the aqueous phase was determined as described in Section 2.3.2.1. Determinations of the germanium in stock solution 3(ii) yielded identical data to that of solutions containing no zinc, indicating that the presence of zinc does not interfere with the phenylfluorone determination. Zinc concentration was monitored by atomic absorption spectroscopy. Standards in the concentration range 0,2 - 2,0 µg/ml were prepared by multiple dilution of a 1000 µg/ml zinc stock, (1,0000 g zinc metal dissolved in 40 ml 1:1 HCl and diluted to 1 litre). Absorbances were determined on a Varian Model 1475 AA Spectrophotometer at 213,9 nm using an acetylene/air flame. A linear calibration curve was obtained

over the range of zinc concentration determined. Zinc-containing samples from extraction runs were diluted as necessary (50 μ l diluted to 25 ml) to obtain concentrations within the linear range of absorbance.

2.4.2.2.11. Determination of the Uptake of Acid into Ligand Organic Phases by Lix 26, TN 02181 and TN 01787.

In Section 3.4.6. of this work, it is postulated that the initial rate at which germanium is extracted by 7-alkylated-8-hydroxyquinoline reagents is related to the quantity of sulphuric acid which is 'extracted' into the organic phase. Distribution isotherms for sulphuric acid between the aqueous and organic phase were therefore determined by vigorously shaking together, 100 ml quantities of toluene solutions of the ligand reagents of varying concentration, with 100 ml of aqueous phase containing approximately 1,5 M H_2SO_4 for 24 hours. Following phase separation, 10 ml aliquots of the residual aqueous phase were titrated with an approximately 1,0 M solution of freshly-prepared NaOH, which was standardised before each determination with a standard solution of 0,9905 M $HClO_4$.

2.5 Techniques for the Investigation of Physical Parameters Important in the Study of Solvent Extraction

The rate of mass transfer of a solute across a phase boundary is a function of a number of chemical and physical effects and it must be mentioned here that altering a chemical parameter would invariably modify one or more physical characteristics of the system. It is usually necessary to invoke physical phenomena to explain, at least partially, the course of chemical events and vice versa. In studies involving mass transfer across a phase boundary by a surface-active species, four parameters warrant investigation:

- (a) the interfacial tension ($\gamma \text{ Nm}^{-1}$),
- (b) the relative dielectric constant of the ligand-containing solution (ϵ_c^r) and the effect upon ϵ_c^r of adding modifiers,
- (c) the viscosity of the diluent/ligand solution and the relationship between viscosity and $[\text{HL}]$ and
- (d) the possibility of aggregation of the extractant molecules in the organic phase to form polymeric species of the type $(\text{HL})_2$ etc. The existence of such species would reduce the availability of the ligand in the form which chelates with metal ion.

The procedures for measuring these properties are outlined in the sections which follow.

2.5.1. The Measurement of Interfacial Tension.

The interfacial tension ($\gamma \text{ N m}^{-1}$), is one of the most easily measured interfacial properties and it is well known that changes in this property result in changes in the mass transfer rates of solutes across an aqueous/organic interface. Indeed, the **distribution** of an extractant is usually not affected by the extent of shaking or stirring of the aqueous and organic phases present in a system, but is affected by the interfacial tension. Accordingly, much attention has been given to the role of the interface in solvent extraction studies^(59,91,161-169) and the trends which emerge from interfacial tension measurements have been reconciled on a qualitative basis with solvent extraction data.

In this study, a White Electrical Instrument Co Ltd Du Nuöy Tensiometer with 4 cm circumference platinum ring was used for all interfacial tension measurements. The dimensions of the platinum ring and the calibration of the tensiometer, were checked by comparing the average surface tension for water at 21°C with the value quoted in the literature (measured $71,4 \pm 0,7 \times 10^{-2} \text{ N m}^{-1}$: literature $71,6 \pm 0,2 \times 10^{-2} \text{ N m}^{-1}$ - reference (156)). All measurements were made in a 60 mm depth flat-bottomed dish containing equal volumes (25 ml) of aqueous phase and ligand-containing organic phase. To ensure that the platinum ring was completely hydrated and free of oil-droplets, the ring was suspended in the lower aqueous phase and the organic phase carefully added from a pipette from above. The phases were then allowed to equilibrate for 15 minutes in the dish prior to the measurement of the

interfacial tension. The 15-minute equilibration time was established by monitoring the interfacial tension for 20 hours for an aqueous phase at pH 3,3 and ionic strength 0,5 M and an organic phase containing 0,68 g/l Lix 26 in AR toluene. No change in γ was observed after 5 minutes.

Measurements of γ were made over a range of concentration of the ligand reagents of interest to this work and at varying values of aqueous pH, but at a constant ionic strength of 0,5 M. Na_2SO_4 was used to maintain the ionic strength, the pH of the aqueous phase was adjusted by the addition of concentrated H_2SO_4 or a saturated solution of NaOH. Values of γ were recorded as N m^{-1} . The glass dish and platinum ring were cleaned with hot chromic acid prior to each measurement.

2.5.2. Dielectric Constant Measurements.

Interaction of the diluent with the extractant and chelated metal ion complex can result in lower (or higher) extraction coefficients for metal ions. The formation of an 'extractant-diluent' species in the organic phase produces a lower concentration of the free extractant with a consequent decrease in extraction coefficient⁽¹⁷⁰⁾. Most of the usual diluents that are considered for use in solvent extraction processes are of the kerosene type, with relative dielectric constants, ϵ_c^r between 2 and 3. The value of ϵ_c^r is of course affected by the addition of modifiers. In general, there is usually some correlation between the value of ϵ_c^r , the characteristics of extraction by a ligand and the charge status of the extracted species. If the metal-ion chelate is

charge-balanced e.g. $\text{Co}(\text{D}_2\text{EHPA})_2$, then extraction of the species is favoured by low dielectric constant. De⁽¹⁷¹⁾, for example noted that for the extraction of various metal ions with a high molecular weight carboxylic acid, SRS-100, extraction was favoured by diluents such as benzene which has a low dielectric constant. In this work, it is proposed that at low pH, the extracted species is of the form GeL_3^+ (plus a counterion for electroneutrality:-in sulphuric acid medium this would be HSO_4^-) and therefore charged, which suggests that a diluent with a high value of ϵ_c^r would favour extraction. It was recognized that two of the parameters investigated in this work may have some effect upon ϵ_c^r , viz. the addition of alcohol modifiers to a ligand/diluent solution and an increasing ligand concentration in the diluent and therefore appropriate studies of the change in dielectric constant of these systems were performed.

Values of ϵ_c^r were calculated from capacitance measurements obtained with a Wayne Kerr Automatic Component Bridge Model B605 and a variable parallel plate capacitor. With the capacitor connected and suspended in an empty 100 ml beaker, the bridge was 'trimmed' in air and the capacitance of air thence recorded, giving $C_0 = 106,38 \pm 1,00$ pF. The capacitor was then suspended in 50 ml (i.e. sufficient to completely cover the capacitor), of the solvent of interest containing ligand, modifier or both. Values of ϵ_c^r were recorded in pF or nF for a number of solutions of ligand in various diluents and for the ligand/modifier solutions investigated in this work. Care was taken to ensure that glassware and the capacitor were

free of contaminants prior to all measurements. Dielectric constant values quoted in this work are all relative to air, calculated from:

$$\epsilon_c^r = \frac{C_r}{C_o} \quad (30)$$

where C_r is the capacitance of the solution of interest and C_o is the capacitance of air.

2.5.3. Measurement of Solution Viscosity.

One of the reasons for dissolving a ligand reagent in a suitable diluent is to lower the viscosity (η). The influence upon mass transfer of lowering viscosity requires no elaboration, but it must be expected that increasing the quantity of ligand in the diluent will affect the viscosity and this could be manifest in the extraction data. Very often, changes in extraction behaviour are noted when the ligand is present in very large excess and although this is usually interpreted in terms of maximal population of the interface by the ligand (usually referred to as the Excess Interfacial Population Density, EIPD), viscosity effects cannot be ignored.

Viscosity determinations were made with an Ostwald U-tube viscometer (with side-arm) suspended in a water bath at 25°C. The time taken, for solutions of varying reagent concentration in toluene, to pass between the marks above and below the bulb of the apparatus were recorded. η_{solution} was calculated from

Poiseuille's Law using η_{toluene} and the timed passage of toluene viz.

$$\eta_{\text{solution}} = (\eta_{\text{toluene}} \times t_{\text{soln}}) / t_{\text{tol}}$$

where t_{soln} and t_{tol} are the times for the passage of the solution and pure toluene through the viscometer respectively. All measurements of viscosity reported in this work have units of N s m^{-2} .

2.5.4. Investigation of Extractant Aggregation by Infra-Red Spectroscopy.

The aggregation of extractants such as the alkyl-phosphates⁽¹⁷²⁾, carboxylic and sulphonic acids^(173,174) and the β -hydroxyoximes⁽¹⁷⁵⁾ via hydrogen-bonding, to form polymeric species such as $(\text{HL})_2$ etc., may affect extraction kinetics by lowering the availability of the form of the extractant which chelates the metal ion. The extent of self-association is expected to increase with increasing extractant concentration. In view of these comments, it was thought possible that Lix 26, TN 02181 and TN 01787 could aggregate and therefore an appropriate investigation was initiated. Dimerization of organic molecules can usually be detected by the disappearance and shifting of one -OH band on the infra-red spectrum and the appearance of another as the concentration of the organic molecule decreases⁽¹⁷⁶⁾. In general, a sharp band at 3570 cm^{-1} is characteristic of free -OH stretch, while a broad band at 3350 cm^{-1} is associated with hydrogen-bonding (either intra- or intermolecular). If intermolecular bonding is present, then the intensity of the band at 3350 cm^{-1} decreases faster than

the concentration i.e. a Beer's Law plot is not linear, and the free -OH band at 3570 cm^{-1} becomes more pronounced as more -OH moieties are free to stretch in their normal mode.

Infrared Spectra were obtained for all three extractants and for 8-hydroxyquinoline in spectra-grade CCl_4 using a Pye-Unicam Model SP3-300 Infrared Spectrophotometer and a liquid cell with NaCl windows and a 0,1 mm pathlength. Solutions were scanned over the range $2000\text{-}4000\text{ cm}^{-1}$.

The visualization of chemical phenomena in three dimensions can be revealing in the development of a rationale for *a priori* studies of chemical events which have stereochemical implications. The next section describes a chemical-modelling program which was used to create a visual awareness of the ligand molecules and the chelates formed with germanium.

2.6. The Alchemy Modelling Program⁽⁷⁹⁾.

Very little information exists on the size, shape and conformation of extractant molecules in the literature^(177,178). The Alchemy program^(179,180), can be used to build 3-dimensional representations of molecules, manipulate structures, measure various molecular parameters such as distances between bonded and non-bonded atoms and bond angles and conduct empirical energy minimization routines.

In this study, Alchemy was utilised as a tool to facilitate:

- (i) the three dimensional visualization of the ligand molecules of interest, in order to compare their

conformations and to allow a qualitative perception of their orientation at an aqueous/organic interface,
(ii) the determination, via the minimization routine, of the most stable molecular conformation,
(iii) the calculation of an approximate two-dimensional geometric surface area for comparison with areas calculated via interfacial tension measurements and
(iv) a visual comparison of the germanium-ligand chelates formed during the complexation reaction.

It was envisaged that a comparison of the ligands themselves and of the metal-ligand chelates, would allow predictions to be made vis-à-vis which of the extractants would be likely to be the most efficient. Also the stereochemical constraints applicable to the formation of the GeL_3^+ species would facilitate a qualitative description of the nature of the rate-determining step during extraction.

Since the assertions drawn from the Alchemy models are reliant upon the minimization routine utilised by the program, some comment regarding the calculation of the minimum potential energy is in order.

The program calculates the minimum energy as a sum of five terms viz.

$$E = E_{str} + E_{ang} + E_{tor} + E_{vdw} + E_{oop} \quad (31)$$

where the subscripts in Equation (31) are the bond-stretching, angle-bending, torsion deformation, Van der Waals interactions and out-of-plane bending energies in kcal mol^{-1} (but are converted to kJ mol^{-1} in this work). The terms in Equation

(31) are defined as follows:

$$E_{str} = \sum_{i=1}^{N \text{ bonds}} k_i^d / 2 \cdot (d_i - d_i^o)^2 \quad (32)$$

where d_i : length of the i^{th} bond (\AA)

d_i^o : equilibrium length for the i^{th} bond (\AA)

k_i^d : bond stretching force constant

(kcal/mol \AA^2)

$$E_{ang} = \sum_{i=1}^{N \text{ angles}} k_i^\theta / 2 \cdot (\theta_i - \theta_i^o)^2 \quad (33)$$

where θ_i : angle between two adjacent bonds (degrees)

θ_i^o : equilibrium value for the i^{th} angle (degrees)

k_i^θ : angle bending force constant

(kcal/mol degree²)

$$E_{tor} = \sum_{i=1}^{N \text{ tors}} \frac{k_i}{2} \cdot (1 + \text{sign}(\text{per}_i) \cos(|\text{per}_i| \omega_i)) \quad (34)$$

where ω_i : torsion angle (degrees)

k_i : torsion angle force constant

(kcal/mol degree²)

per_i : periodicity

$\text{sign}(\chi) = -1$ ($\chi < 0$)

1 ($\chi \geq 0$)

$$E_{vdw} = \sum_{i=1}^{N \text{ atoms}} \left(\sum_{j>i}^{N \text{ atoms}} E_{ij} \left[\frac{1,0}{a_{ij}^{12}} - \frac{2,0}{a_{ij}^6} \right] \right) \quad (35)$$

where E_{ij} : Van der Waals constant (kcal/mol)

a_{ij} : $r_{ij} / (R_i + R_j)$

r_{ij} : distance between atom i and atom j (Å)

R_i : Van der Waals radius of the i^{th} atom

E_{vdw} is the sum of the 1st - 4th and more distant non-bonded interactions.

$$E_{oop} = \sum_{i=1}^{N \text{ oop}} k_i^{\delta} / 2 \cdot d_i^2 \quad (36)$$

where k_i^{δ} : Out-of-plane bending constant for atom type δ (kcal/mol degrees²)

d_i : length of the i^{th} bond

Perhaps the only major criticism of the applicability of the Alchemy program to this work is the use of **crystal data** by the program. Although there are some indications that solid-state data is of the same order as constants measured in the liquid state, it is important to appreciate that the calculation of the Van der Waals energy term in particular (Equation (35)), does not include a term for medium permittivity, nor does it account for the possibility of hydrogen-bonding between molecules and/or molecules and solvent.

Since germanium is not included in the libraries which accompany the software, the following parameters were incorporated into the Atomdef.tab file of the program:

Atomic Number : 32
Bonding Geometry : Octahedral
Electronegativity : 1,8
Van der Waals Radius : 0,53 Å.

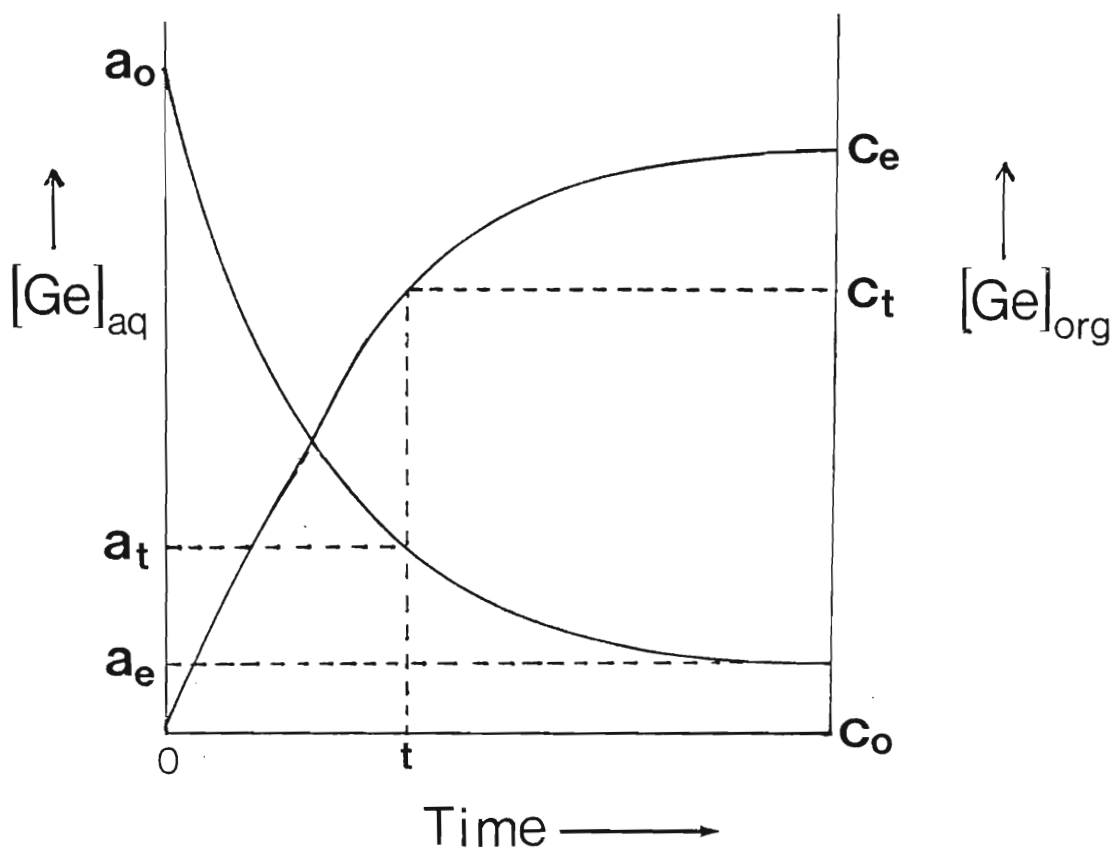
CHAPTER 3RESULTS AND DISCUSSION

Chapter 2 described the experimental procedures which have been used in this work to facilitate the development of an extraction model for germanium by 7-alkylated-8-hydroxyquinoline extractants. Three experimental methods were described for the acquisition of kinetic and equilibrium data appropriate to the extraction process, two of which involve mass transfer in vigorously-stirred systems and one in which the transfer of metal occurs across a quasi-static interface of definite geometrical area. Since the last mentioned yields information which establishes the location of the rate-determining step during extraction, which is necessary for the subsequent discussion, data obtained with the Lewis Cell apparatus will be presented first.

3.1. The Kinetics of Germanium Extraction Across a Quiescent Interface: The Lewis Cell.

3.1.1. Kinetic Analysis: The Relationship Between the Mass-Transfer Coefficient and Volume/Area.

The extraction of germanium by ligand and the approach of the system to equilibrium can be presented diagrammatically as follows:

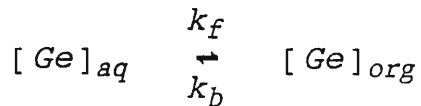


where : a_0 , a_t and a_e represent the aqueous concentrations of germanium initially, at some time t and at equilibrium respectively and c_0 , c_t and c_e represent the same variables in the organic phase.

The concentration of germanium in excess of that present at equilibrium in the aqueous phase is given by Equation (37):

$$[Ge]_{aq}^t = a_t - a_e = c_e - c_t \quad (37)$$

The net forward reaction for the process:



is,

$$-\frac{d[Ge]}{dt} = k_f a_t - k_b c_t \quad (38)$$

At equilibrium, $-\frac{d[Ge]}{dt} = 0$,

hence from Equation (38),

$$k_f a_e = k_b c_e \quad (39)$$

From Equation (37),

$$a_t = a_e + [Ge] \quad \text{and} \quad c_t = c_e - [Ge] \quad (40)$$

(note that the subscript 'aq' and superscript 't' of [Ge] have been dropped for simplicity).

Rearranging Equation (39) in terms of k_b gives:

$$k_b = k_f a_e c_e^{-1} \quad (41)$$

Inserting Equations (40) into (38) gives:

$$-\frac{d[Ge]}{dt} = k_f(a_e + [Ge]) - k_b(c_e - [Ge]) \quad (42)$$

and substituting for k_b from (41):

$$\begin{aligned} -\frac{d[Ge]}{dt} &= k_f(a_e + [Ge]) - k_f a_e c_e^{-1} (c_e - [Ge]) \\ &= k_f[Ge] + k_b[Ge] \end{aligned} \quad (43)$$

If no germanium is present in the organic phase initially, then $c_o = 0$ and $c_e = a_o - a_e$. Inserting this result in Equation (43) and using Equation (41) gives:

$$-\frac{d[Ge]}{dt} = k_f[Ge] + \frac{k_f a_e [Ge]}{(a_o - a_e)}$$

and hence,

$$-\frac{d[Ge]}{dt} = k_f[Ge] \left(\frac{a_o}{(a_o - a_e)} \right) \quad (44)$$

Rearranging (44), separating variables and integrating the process to a time t which is remote from equilibrium gives:

$$-\frac{(a_o - a_e)}{a_o} \int \frac{(a_t - a_e)}{(a_o - a_e)} \frac{d[Ge]}{[Ge]} = \int_{t=0}^{t=t} k_f dt \quad (45)$$

and therefore,

$$k_f t = \frac{(a_o - a_e)}{a_o} \ln \frac{(a_o - a_e)}{(a_t - a_e)} \quad (46)$$

The expression for the reverse rate constant k_b , can be obtained in an analogous way by substituting for k_f from (41) into (43) giving,

$$k_b t = \frac{a_e}{a_o} \ln \frac{(a_o - a_e)}{(a_t - a_e)} \quad (47)$$

Equations (46) and (47) are generally applicable for the kinetics of extraction of germanium (and back-extraction) from the aqueous phase, except that as equilibrium is approached, the function given by Equation (46) becomes very sensitive to small changes in a_t .

In the Lewis Cell, the rate of extraction is slow, hence studies are carried out far from equilibrium. Under these conditions $a_o - a_e \approx a_o$ and (46) simplifies to:

$$k_f t = \ln \frac{a_o}{a_t - a_e} \quad (48)$$

Equation (48) can be manipulated to yield k_f in terms of the concentration of germanium in the organic phase i.e. from Equation (37), $a_t = c_e - c_t + a_e$ giving,

$$k_f t = \ln \frac{a_o}{c_e - c_t} \quad (49)$$

and since $c_e = a_o - a_e \approx a_o$ at a time far from equilibrium then,

$$k_f t = \ln \frac{a_0}{a_0 - c_t} \quad (50)$$

If the above assumptions are correct and the rate of extraction is first order in germanium concentration then plots of $\ln a_0/(a_0 - c_t)$ versus time would be linear with slope equal to k_f .

The rate of transfer of germanium from the bulk aqueous phase to the aqueous/organic interface, j ($\text{mol cm}^{-2} \text{s}^{-1}$), is given by Fick's First law i.e.,

$$j = k' (c_{int} - c) \quad (51)$$

k' : mass transfer coefficient (cm s^{-1}).

$(c_{int} - c)$ is the concentration gradient of germanium from the bulk aqueous phase to the interface.

However the transfer rate is also given by,

$$j = \frac{V}{A} \cdot \frac{dC}{dt} \quad (52)$$

where V : Volume of the aqueous phase (cm^3)

A : Area of the interface in the Lewis Cell (cm^2)

dC/dt : Concentration time gradient from the bulk to the interface.

If equilibrium exists at the interface, then the interfacial concentration of metal ion is constant and essentially equal to the saturation or equilibrium value i.e. $c_i = c_e$.

Equating (51) and (52) and integrating between the limits $(a_t - a_e)$ and $(a_0 - a_e)$ i.e. inserting aqueous phase variables as defined previously, gives:

$$k' = \frac{V}{At} \ln \frac{(a_o - a_e)}{(a_t - a_e)} \quad (53)$$

and hence, following the rationale as above,

$$k' t = \frac{V}{A} \ln \frac{a_o}{a_o - c_t} \quad (54)$$

and therefore the slope of a $\ln a_o/(a_o - c_t)$ versus time plot gives $k'A/V$. Since in this work $A = 103,9 \text{ cm}^2$ and $V = 630 \text{ cm}^3$, such plots yield values of the mass transfer coefficient in cm s^{-1} .

3.1.2. The Effect of Impeller Speed Upon the Rate of Extraction.

The possibility that the mass transport of reactants or products controls the rate of reaction was examined by altering the velocity of the dual phase impeller from 40-120 rpm, while all other parameters were kept constant i.e.

Aqueous Phase : 630 ml ~ 0,65 g/l Ge in 1,5 M H_2SO_4

Organic Phase : 550 ml 75 g/l Lix 26 in AR toluene

Temperature : $25^\circ\text{C} \pm 1^\circ\text{C}$

Impeller Speed : Variable

Figure (36) depicts the observed decrease in germanium concentration in the aqueous phase over a period of 62 hours. The kinetic plot obtained from Equation (50) is shown in Figure (37), with a least squares slope of $1,72 \times 10^{-5} \text{ s}^{-1}$. The forward rate constant for the reaction is therefore $1,72 \times 10^{-5} \text{ s}^{-1}$ and the mass transfer coefficient k' , is

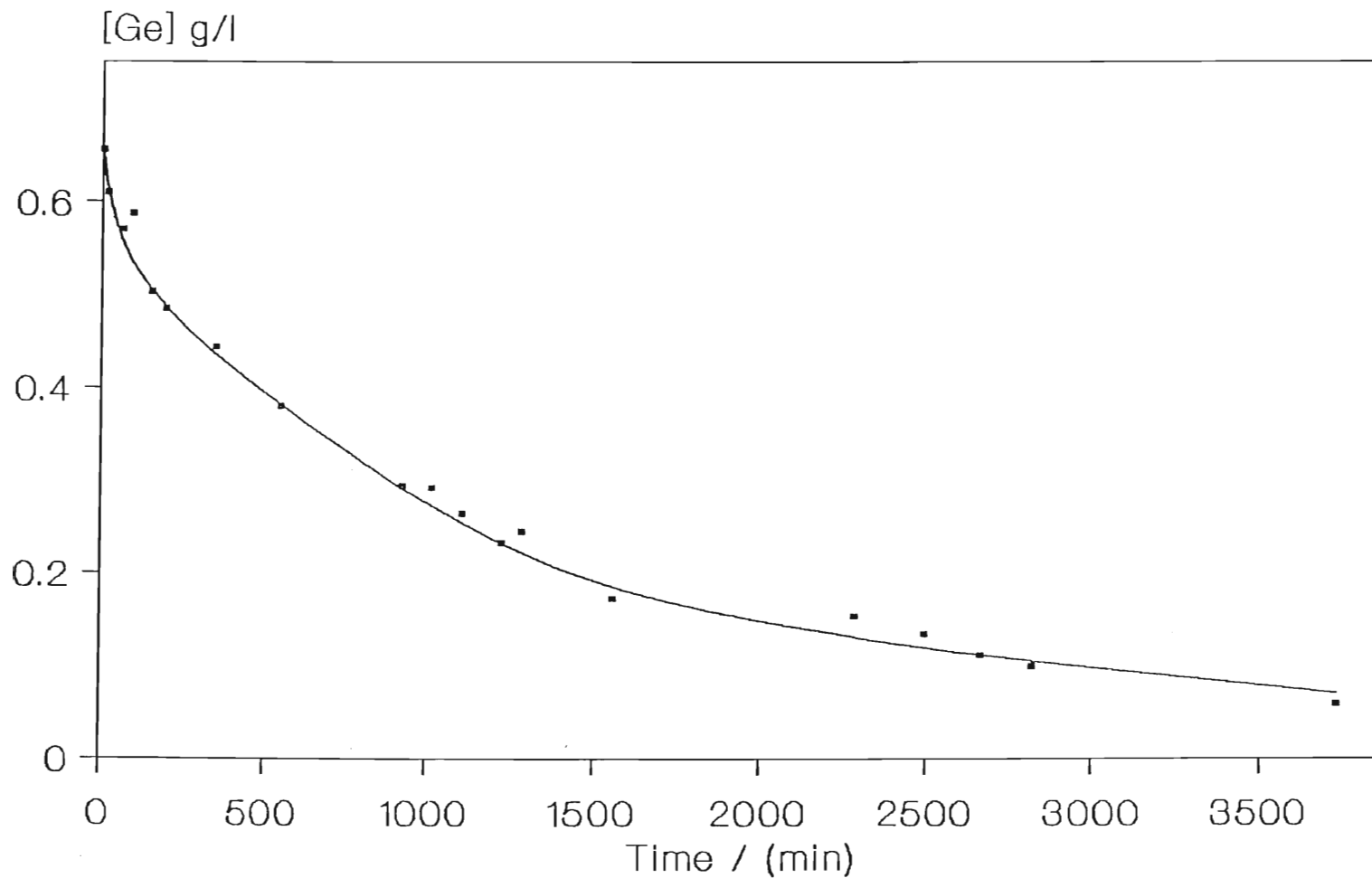


Figure (36). Extraction kinetics of germanium in the Lewis Cell assembly. Aqueous phase : 630 ml ~ 0,65 g/l Ge in 1,5 M H_2SO_4 Organic phase : 550 ml 75 g/l Lix 26 in AR toluene ; Temperature : 25°C ; Impeller speed : 80 rpm ; Interfacial area : 103,87 cm^2 .

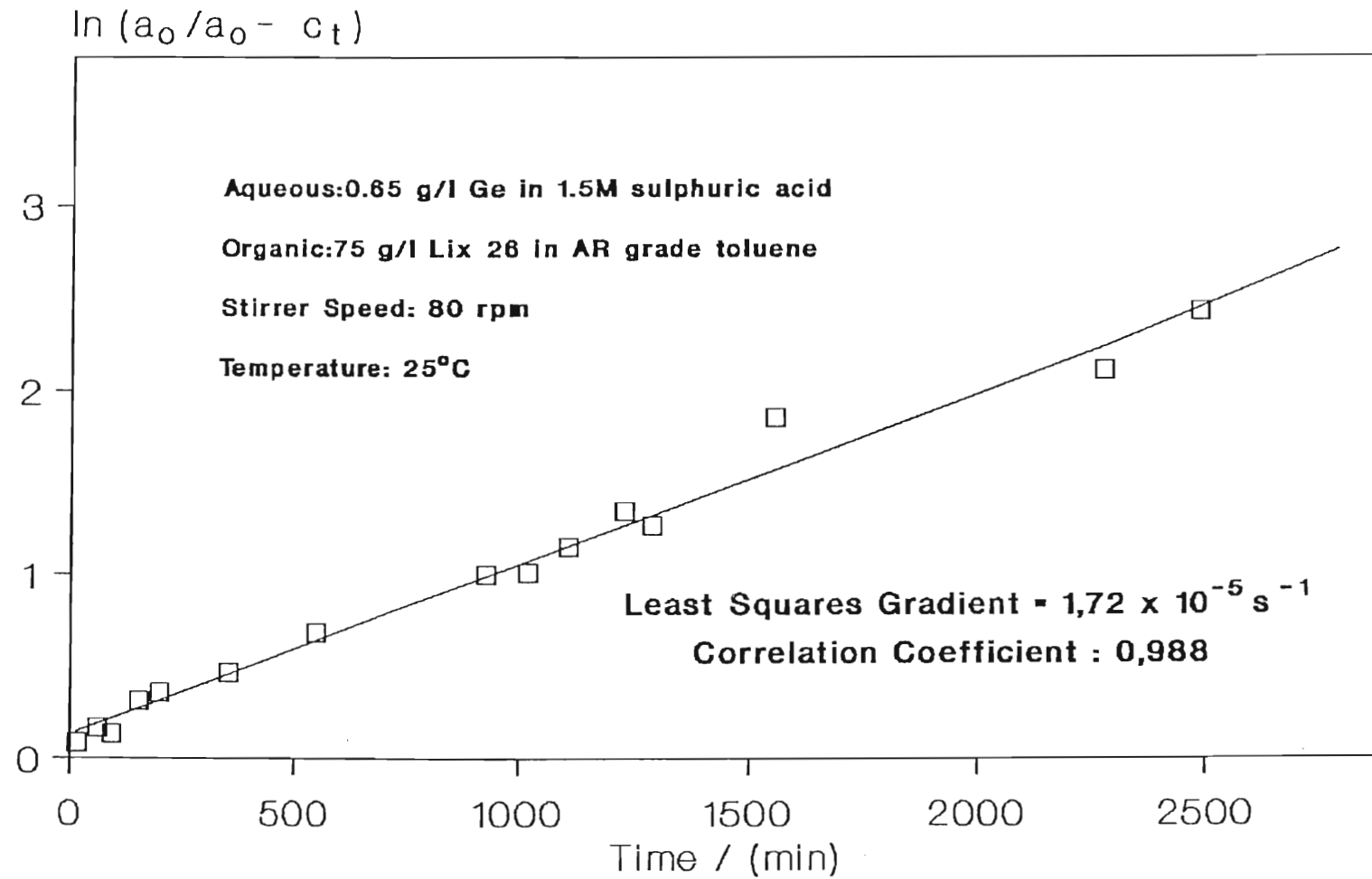


Figure (37). First order kinetic plot (Equation 50) for germanium extraction in the Lewis Cell. a_0 : concentration of germanium in the aqueous phase initially; c_t : concentration of germanium in the organic phase at time t .

$1,05 \times 10^{-4} \text{ cm s}^{-1}$. Very little has been published regarding values of k' for metal-ion transfer into toluene under non-turbulent conditions, however, Fleming⁽⁵⁹⁾ measured k' for the transfer of Cu^{2+} from aqueous solutions to chloroform solutions of Lix 64N using a Lewis Cell with varying interfacial area and obtained values of approximately $7,2 \times 10^{-5} \text{ cm s}^{-1}$. For the transfer of acetic acid from aqueous solution into toluene, Lewis⁽¹⁸¹⁾, using his original cell design, determined values of k' for a range of initial solute concentrations, temperatures and stirring speeds, which are conveniently reported as Reynold's Number, Re , as opposed to rpm in order to correlate observed rates with the modes of turbulence exhibited by fluids. In the transition flow region $2000 < Re < 5000$ (for laminar flow $Re < 2000$), values of k' in the range $1,7 \times 10^{-5} - 8,3 \times 10^{-4} \text{ cm s}^{-1}$ were measured at 20°C for low initial solute concentration ($\leq 60 \text{ g/l}$). The values of k' obtained in this work (approximately $1,0 \times 10^{-4} \text{ cm s}^{-1}$ under non-turbulent conditions) are of the same order as the values quoted by Fleming and within the range of values obtained by Lewis, although it is worth noting that the higher values quoted in the above range (as measured by Lewis) apply to mass transport **without** reaction i.e. interfacial absorption and subsequent partition is the measured effect whereas in this work the mass transfer coefficient is an indication of partition effects and the rate limiting reaction of metal at the interface.

The data in Table (24) below and plotted in Figure (38) show the relationship between impeller velocity and the observed

rate constant for the appearance of germanium in the organic phase and the mass transfer coefficient calculated from the appropriate plots.

Impeller velocity /rpm	Observed Rate Constant / s ⁻¹	# Mass Transfer Coefficient / cm s ⁻¹
40	1,75 x 10 ⁻⁵	1,06 x 10 ⁻⁴
	1,90 x 10 ⁻⁵	1,15 x 10 ⁻⁴
60	1,80 x 10 ⁻⁵	1,09 x 10 ⁻⁴
80	1,72 x 10 ⁻⁵	1,05 x 10 ⁻⁴
80 (½ interfacial area)*	9,40 x 10 ⁻⁶	1,07 x 10 ⁻⁴
	9,19 x 10 ⁻⁶	1,04 x 10 ⁻⁴
100	1,79 x 10 ⁻⁵	1,08 x 10 ⁻⁴
120	3,97 x 10 ⁻⁵	2,41 x 10 ⁻⁴

Table (24). Rates of mass transfer across the quiescent interface of the Lewis Cell (some repeat runs are shown). Area of the interface = 103,87 cm² except * for which Area = 50,27 cm²:- phase ratio constant but aqueous volume = 570 ml, organic volume = 485 ml. (# calculated from Equation (54)).

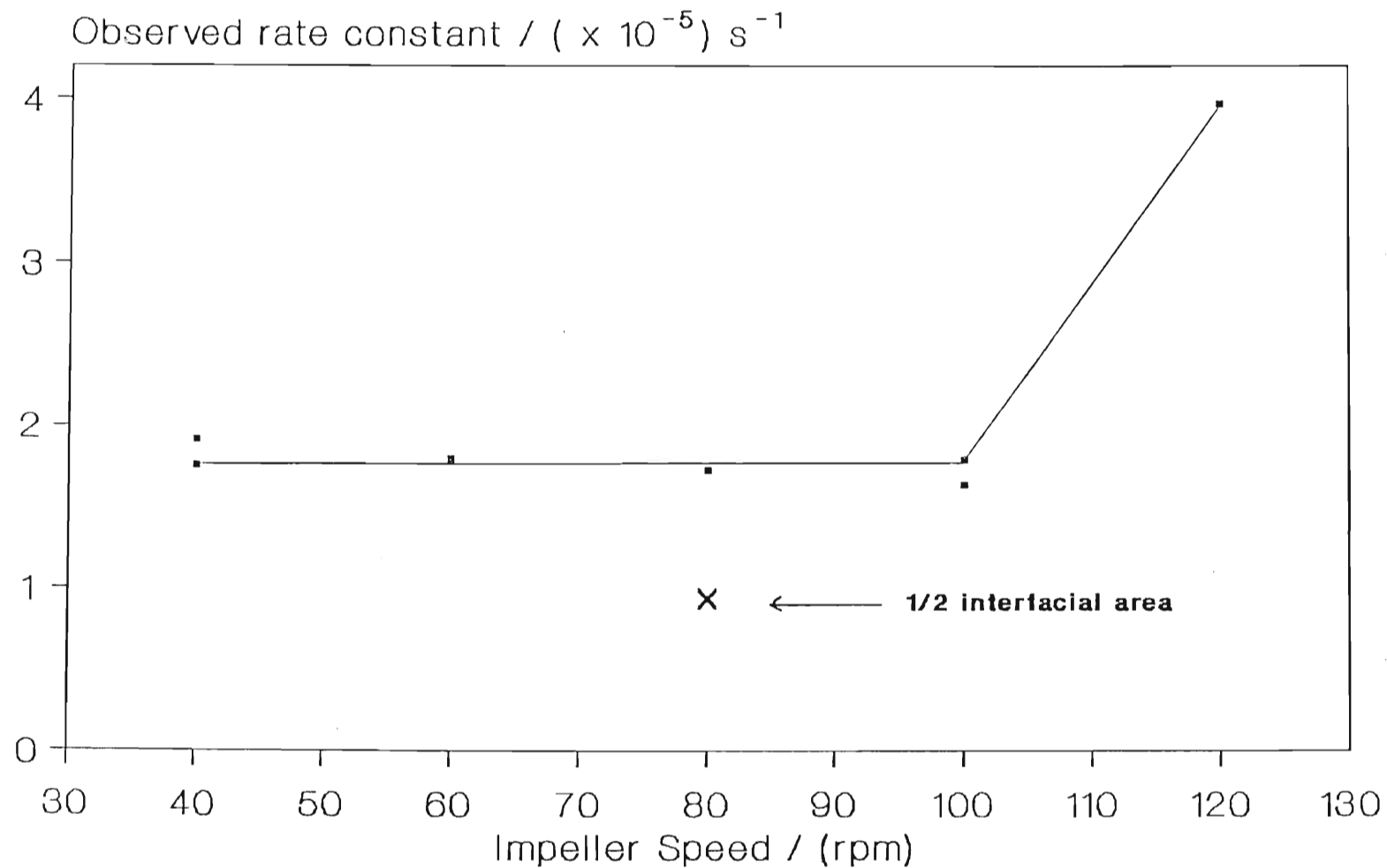


Figure (38). Observed rate constant versus impeller speed for the Lewis Cell. Aqueous phase : 630 ml ~ 0,65 g/l Ge in 1,5 M H₂SO₄ ; Organic phase : 550 ml 75 g/l Lix 26 in AR toluene ; Temperature : 25 °C ; The data point at half interfacial area (50,27 cm² as opposed to 103,87 cm²) was obtained with aqueous phase = 570 ml and organic phase =485 ml. Values of k_{obs} were

It is apparent from the data shown in Figure (38) and Table (24) that the observed rate constant for germanium extraction by Lix 26 from the aqueous phase is independent of impeller velocity between 40 and 100 rpm: this suggests that chemical reaction limits the rate of extraction in this impeller speed region, whereas the increasing rate thereafter suggests destruction of the quiescent interface and the onset of turbulent behaviour where, although the chemical reaction still limits the rate, the surface area increases to a larger but uncertain value.

In any solvent extraction process involving solute transfer with reaction at a phase boundary, the rate of reaction can be controlled by one or more of the following:

- (1) Diffusion of the active species (germanium and ligand) to and from the interface,
- (2) Transfer of material across the interface (in both directions),
- (3) A chemical reaction in either phase or
- (4) A chemical reaction at the interface.

The data presented here would appear to suggest that in the linear region of impeller speed discussed, the rate determining process is (4) above, since (1) - (3) would be expected to increase the observed extraction rate constant with the increasing rate of stirring of the phases in contact. Thus the data are consistent with non-diffusional control of reactants and products at stirrer speeds in the range 40-100 rpm.

The data at 80 rpm for two different interfacial areas suggests a linear relation between reaction rate and interfacial area (a plot of k_f vs Area passes through the origin and has slope $1,47 \times 10^{-7} \text{ s}^{-1} \text{ cm}^{-2}$). This is in agreement with the conclusions made by Flett *et al.*⁽¹⁵⁰⁾, who investigated rates of extraction of Cu^{2+} by Lix 65N and Lix 63 in toluene and Roddy *et al.*⁽¹⁸²⁾, who measured rates of extraction of $\text{Fe}^{(3+)}$ by di-(2-ethylhexyl) phosphoric acid (D2EHPA) in octane- see Table (4) for structures of these ligands. These workers concluded, from data sets obtained in a similar manner to those of this work and from their observation of the linear dependence of observed rates on interfacial area, that for the systems studied, reaction in a homogeneous aqueous phase could be excluded as a possibility for the site of the rate determining process i.e. the interface was concluded to be the site of reaction and mass transfer. It must be noted that although the work of this thesis arrives at the same conclusion, this does not imply that the kinetic mechanisms are the same. This is an important result and it is unequivocally established by the data in Figure (38) and Table (24) i.e. the location of the rate determining step during germanium extraction by alkylated-8-hydroxyquinoline ligands is the interface. The low expected aqueous solubility of the active component ($< 0,001 \text{ g/l}$ ⁽¹⁸³⁾ for Kelex 100), in Lix 26, TN 02181 and TN 01787 lends support to this.

3.1.3. The Effect of Ligand Concentration on the Extraction Kinetics of Germanium in the Lewis Cell.

The effect of bulk organic ligand concentration upon germanium extraction was investigated with the set of starting conditions detailed in Section 2.4.1. A stirrer speed of 80 rpm was selected for all experiments because it is within the linear range previously discussed (Section 3.1.2) and therefore excludes any mass transfer effects due to agitation and destruction of the quiescent interface.

Table (25) summarises the values of rate constants calculated graphically from plots similar to Figure (37).

	[HL] /(g/l)	log [HL]	[HL] _{corr} /(g/l)	log [HL] _{corr}	k _{obs} / (s ⁻¹)	log k _{obs}
Lix 26	50	1,70	36	1,56	8,78x10 ⁻⁶	-5,06
	75	1,88	54	1,73	1,72x10 ⁻⁵	-4,76
	100	2,00	72	1,86	2,96x10 ⁻⁵	-4,53
	125	2,10	90	1,95	3,75x10 ⁻⁵	-4,43
TN 01787	50	1,70	42	1,62	4,44x10 ⁻⁶	-5,35
	62,5	1,80	52,5	1,72	7,34x10 ⁻⁶	-5,13
	75	1,88	63	1,80	2,32x10 ⁻⁵	-4,64
	100	2,00	84	1,92	6,01x10 ⁻⁵	-4,22
	125	2,10	105	2,02	6,45x10 ⁻⁵	-4,19

	[HL] /(g/l)	log [HL]	[HL] _{corr} /(g/l)	log [HL] _{corr}	k _{obs} / (s ⁻¹)	log k _{obs}
TN 02181	50	1,70	44	1,64	6,91x10 ⁻⁶	-5,16
					7,42x10 ⁻⁶	-5,13
	75	1,88	66	1,82	1,75x10 ⁻⁵	-4,76
					1,91x10 ⁻⁵	-4,72
	100	2,00	88	1,94	1,63x10 ⁻⁵	-4,78
					1,47x10 ⁻⁵	-4,83
	125	2,10	110	2,04	1,71x10 ⁻⁵	-4,76
					1,89x10 ⁻⁵	-4,72

Table (25). Values of k_{obs} calculated from plots utilising Equation (50). $[HL]_{corr}$ is the active-component-corrected concentration of the reagents, using active component percentages as follows: Lix 26 \approx 72%⁽⁶⁷⁾, TN 01787 \approx 84%⁽⁸⁰⁾, TN 02181 \approx 88%⁽⁸⁰⁾ all v/v%. Repeat runs are included in the table for TN 02181 and indicate the reproducibility of kinetic data arising from the use of the Lewis Cell.

Since all kinetic results yielded straight lines using Equation (50) (correlation coefficient, $r > 0,98$ in all instances), it can be assumed that the observed kinetics are first-order in germanium. This was confirmed via the half-life method; $t_{1/2}$ was essentially constant (Table (26)) for all kinetic runs.

[Ge] _{aqueous} / g/l	log [Ge]	t _½ / min	log t _½
0,656	-0,183	820	2,91
0,328	-0,484	830	2,92
0,164	-0,785	870	2,94

Table (26). Half-life data taken from Figure(36). Gradient of log t_½ vs log[Ge] plot = -0,05, hence apparent reaction order with respect to germanium = 1,05, suggesting first order kinetic behaviour with respect to [Ge].

Figure (39) shows plots of log k_{obs} vs log [HL] for the three reagents of concern to this work. Apparent reaction orders with respect to ligand were obtained from the gradient of the linear portions of these plots as follows:

<u>Reagent</u>	<u>Apparent Reaction Order</u>
Lix 26	1,76
TN 02181	2,11
TN 01787	3,77

There are a number of features of interest in Figure (39):

(i) For each of the ligand solutions, there is a region in which the kinetics are linearly dependent upon the concentration. However the range of concentration over which linearity is observed is different. For both TN 01281 and TN 01787, the plots level off at 75 g/l and 100 g/l respectively. This result is consistent first with the result that the active ligand tended to accumulate at the interface, therefore maximally populating the surface and resulting in a constant observed rate (see also Section 3.2.1.2.) and second with

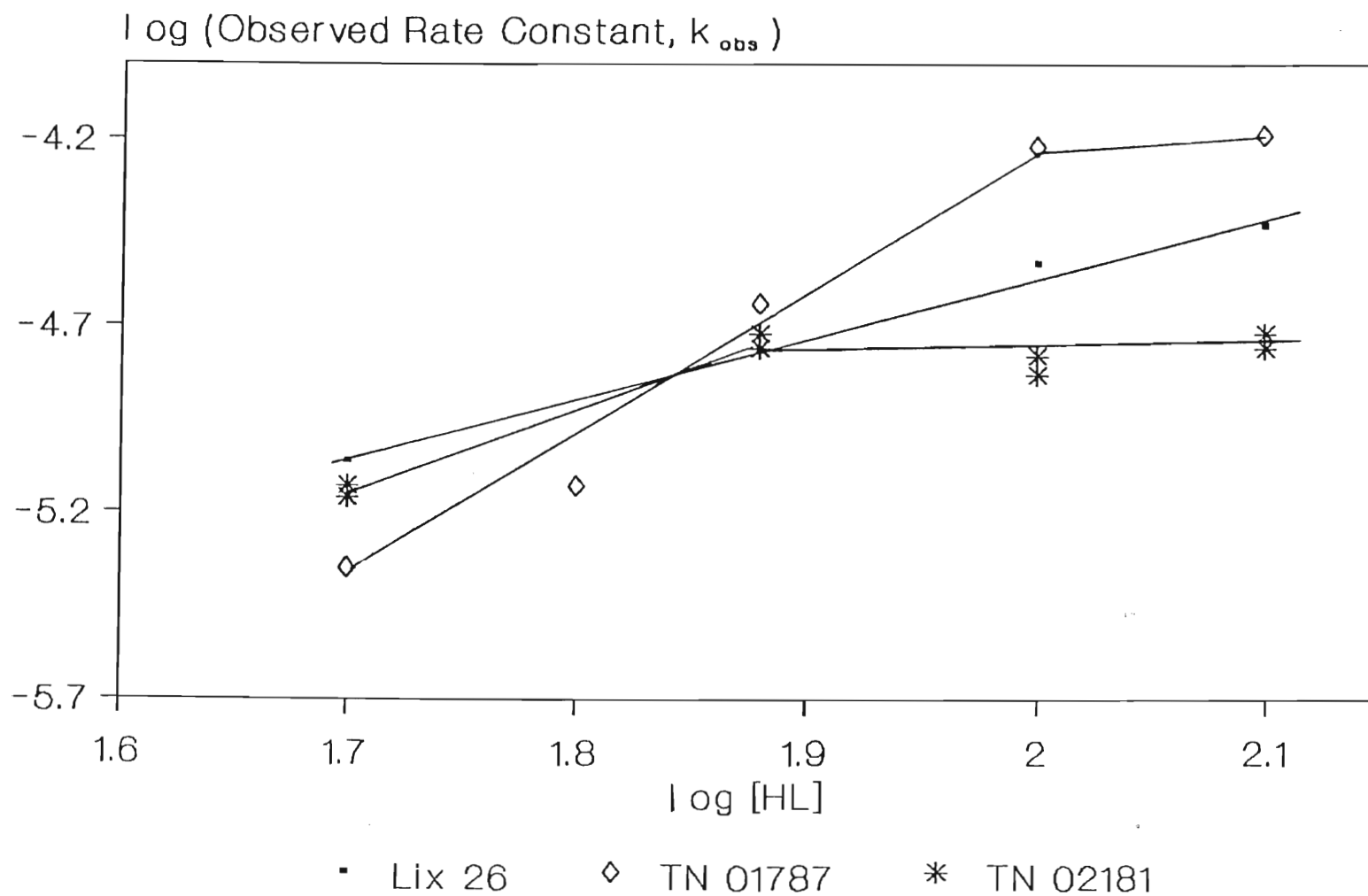


Figure (39). $\log k_{\text{obs}}$ versus $\log[\text{HL}]$ for Lix 26, TN 02181 and TN 01787 in the Lewis cell. Gradients of linear portions of curves are:

HL	Gradient
Lix 26 .	1,76
TN 01787 ◇	3,77
TN 02181 *	2,11

the assertion made by Van der Zeeuw⁽¹⁶³⁾ who noted, following extensive studies of the extraction of Cu^{2+} by β -hydroxyoximes, that the reaction order with respect to HL in the formation of ML_n could be anything from zero to n depending upon the reagent concentration and nature of the diluent. Preston and Luklinska⁽¹⁸⁴⁾ noted similar behaviour for these reagents. The significance of the excess interfacial population density (EIPD) is usually invoked in order to correlate effects such as these and will be fully discussed in Section 3.11.2.3 which details the interfacial tension data obtained in this work.

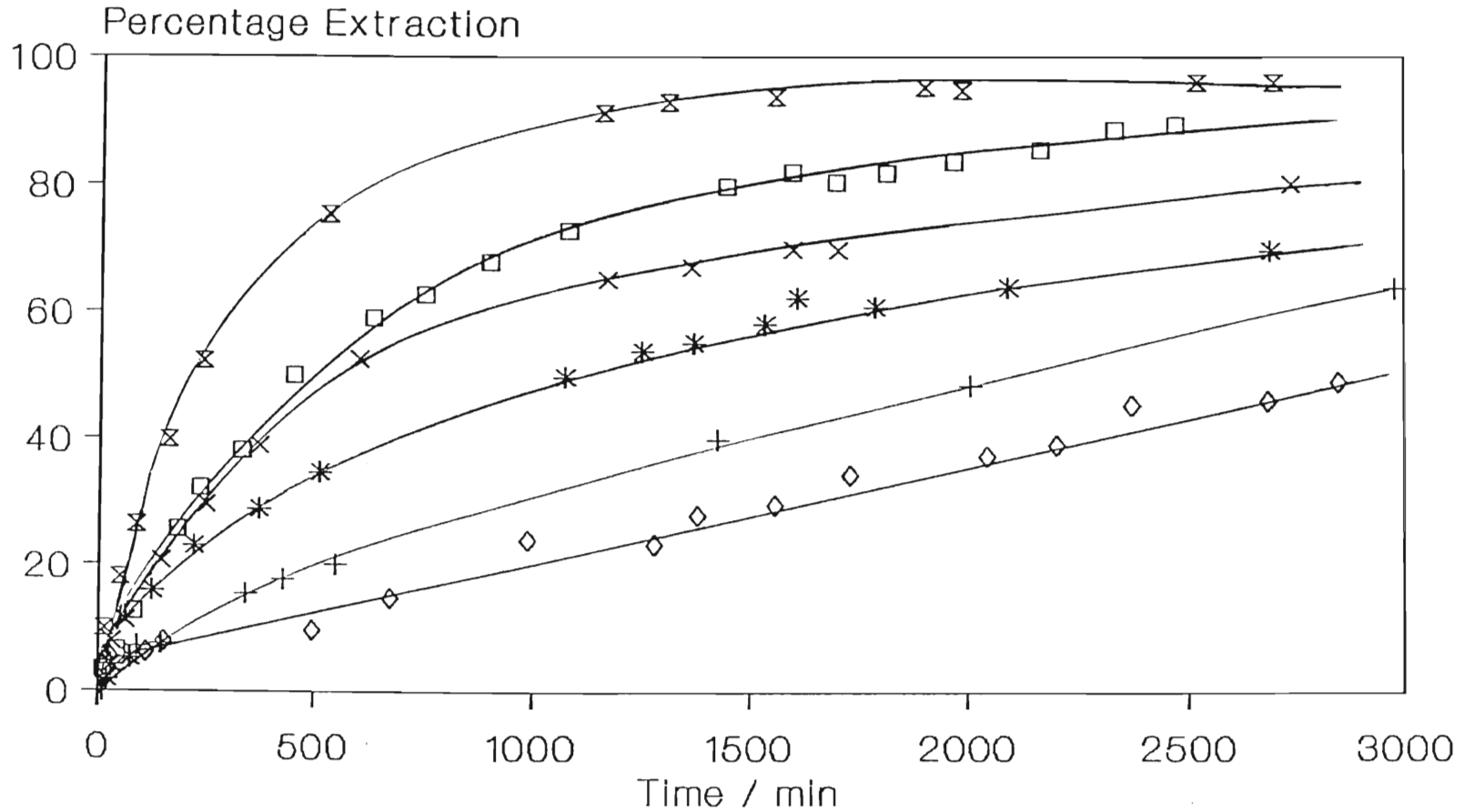
(ii) There are very noticeable differences between the reaction orders of the three ligands in the linear region and there is a curious cross-over in extraction efficiency at approximately $\log [\text{HL}]_{\text{org}} = 1,85$.

Figure (40) shows percentage extraction versus time data at two concentrations, viz. 50 g/l and 100 g/l. At high ligand concentration, the order of extraction efficiency is:

TN 02181 < Lix 26 < TN 01787

whilst at the lower ligand concentration:

TN 01787 < TN 02181 < Lix 26.



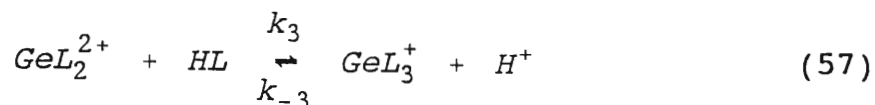
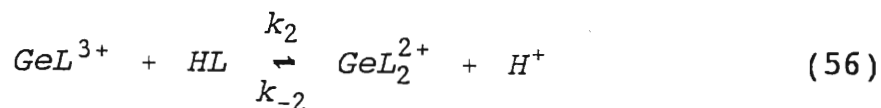
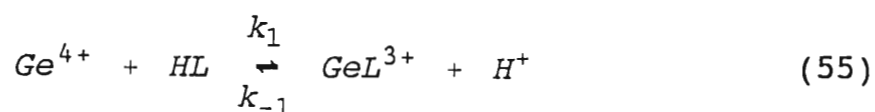
◇ TN 01787 : 50 g/l	⊗ TN 01787 : 100 g/l	* Lix 26 : 50 g/l
□ Lix 26 : 100 g/l	+ TN 02181 : 50 g/l	× TN 02181 : 100 g/l

Figure (40). Percentage extraction versus time in the Lewis Cell for Lix 26, TN 01787 and TN 02181 at concentrations of 50 and 100 g/l in toluene.

There are clearly large differences in the surface behaviour of these ligands or possibly the interaction between either or both of the ligand and metal-chelate products with the diluent. Moreover, it would be expected that these effects would become more prominent in a shaking apparatus where the aqueous:organic contact area is maximized. Comment relating to these differences is therefore reserved until shaking data have been presented (Section 3.2.).

(iii) The absolute values of the reaction orders with respect to [HL] necessitate some comment:

If the salient processes occurring at the interface are the attachment of consecutive ligand species as follows:



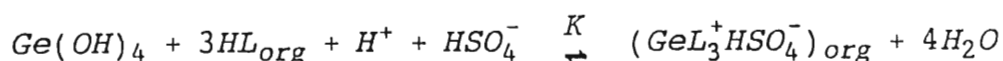
Note: A more representative scheme including all partition effects discussed in Chapter 1, is presented in Section 3.15. All species shown above are assumed to be located at the interface.

The observed reaction rate (i.e. the rate-determining process) in this scheme is proposed to be the stereochemically-hindered addition of the third ligand

(Equation (57)) to the GeL_2^{2+} intermediate- see Section 3.13.2 and thus,

$$\text{Rate} = \frac{d[\text{GeL}_3^+]}{dt} = k_3[\text{GeL}_2^{2+}][\text{HL}] - k_{-3}[\text{GeL}_3^+][\text{H}^+] \quad (58)$$

Marchon *et al.*⁽⁶⁵⁾ estimated a formation constant for germanium complexation with three Kelex 100 molecules viz.



$$K = \frac{[\text{GeL}_3^+\text{HSO}_4^-]}{[\text{Ge}(\text{OH})_4][\text{HL}]^3[\text{H}^+][\text{HSO}_4^-]} : \log K = (6,44 \pm 0,35)$$

Consequently, since $k_{-3} = k_3/K$, the reverse reaction in Equation (58) is unlikely to be significant, especially at low $[\text{HL}]$ where k_{obs} (which is indicative of k_3) is of the order of $1 \times 10^{-5} \text{s}^{-1}$. This simplifies Equation (58) to:

$$\text{Rate} = \frac{d[\text{GeL}_3^+]}{dt} = k_3[\text{GeL}_2^{2+}][\text{HL}] \quad (59)$$

If it is assumed that $[\text{GeL}_3^+]$ and $[\text{GeL}_2^{2+}]$ attain a steady state at the interface and that $[\text{HL}]_{\text{int}}$ is not limiting, then the Steady State Approximation can be invoked for Equations (55) and (56) viz.

$$\begin{aligned} \frac{d[GeL^{3+}]}{dt} &= k_1[Ge^{4+}][HL] - k_{-1}[GeL^{3+}][H^+] \\ &\quad - k_2[GeL^{3+}][HL] = 0 \end{aligned} \quad (60)$$

$$\begin{aligned} \frac{d[GeL_2^{2+}]}{dt} &= k_2[GeL^{3+}][HL] - k_{-2}[GeL_2^{2+}][H^+] \\ &\quad - k_3[GeL_2^{2+}][HL] = 0 \end{aligned} \quad (61)$$

Solving Equation (60) for $[GeL^{3+}]$ gives Equation (62):

$$[GeL^{3+}] = \frac{k_1[Ge^{4+}][HL]}{k_{-1}[H^+] + k_2[HL]} \quad (62)$$

and solving Equation (61) for $[GeL_2^{2+}]$ and inserting Equation (62) where appropriate gives:

$$[GeL_2^{2+}] = \frac{k_2 k_1 [Ge^{4+}] [HL]^2}{(k_{-2}[H^+] + k_3[HL])(k_{-1}[H^+] + k_2[HL])} \quad (63)$$

Finally, substituting Equation (63) in Equation (59) gives:

$$Rate = \frac{d[GeL_3^+]}{dt} = \frac{k_3 k_2 k_1 [Ge^{4+}] [HL]^3}{(k_{-2}[H^+] + k_3[HL])(k_{-1}[H^+] + k_2[HL])} \quad (64)$$

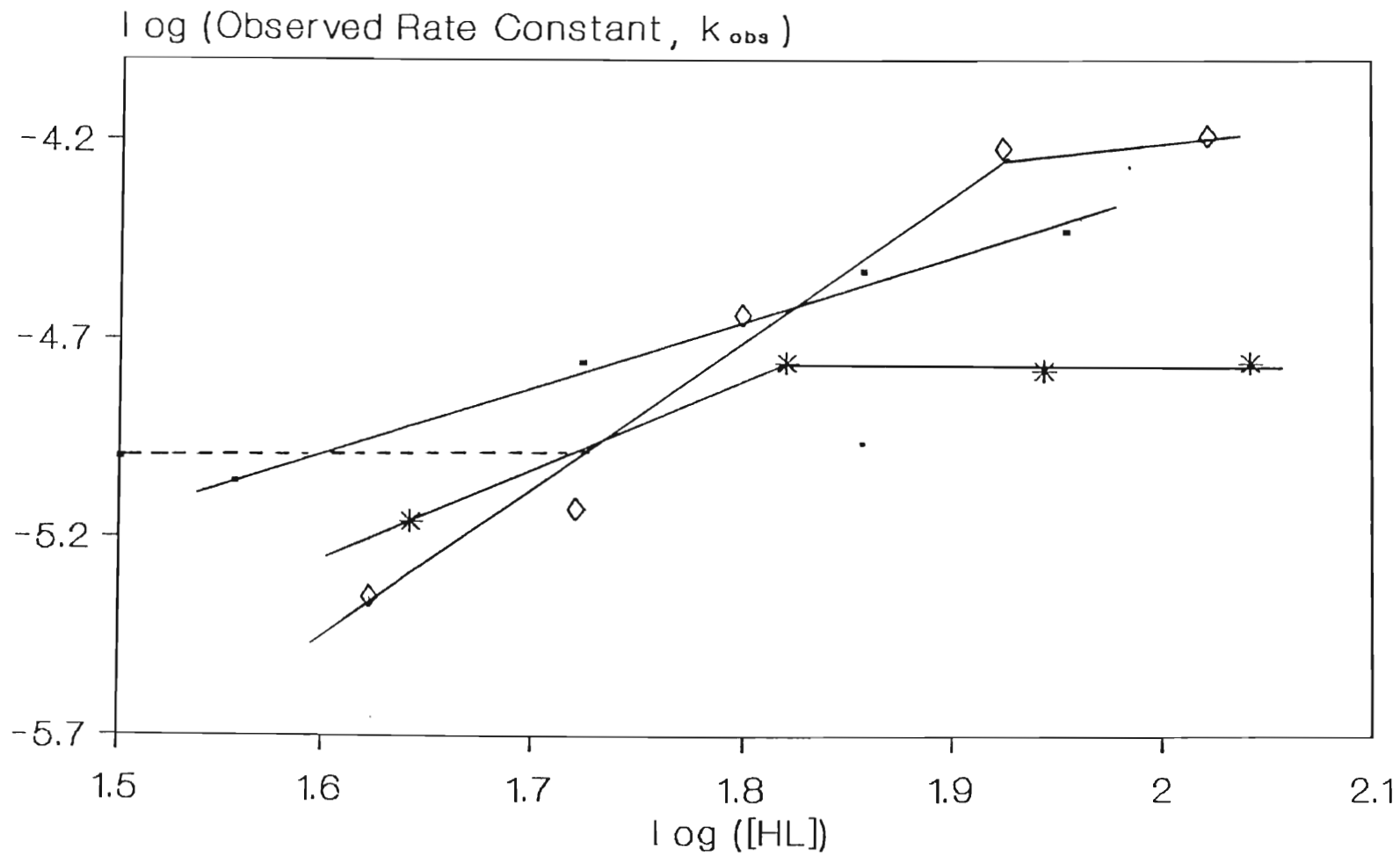
From a purely kinetic viewpoint, since interfacial effects are not included in the rationale of the foregoing discussion, it is possible to conceive of the kinetics of the rate-determining step varying from an order of 1 to 3 with respect to ligand, for at high $[HL]$

(where 'high' refers to circumstances in which the interfacial ligand concentration is at a maximum, although the effects of viscosity, dielectric constant etc., play an important role.), $k_{-2}[H^+] \ll k_3[HL]$ and $k_{-1}[H^+] \ll k_2[HL]$ and therefore, cancelling where possible in Equation (64),

$$\text{Rate} = k_1[Ge][HL]$$

i.e. first order behaviour is expected. At low ligand concentration, higher orders to a maximum of 3 with respect to ligand are anticipated. The values of the orders with respect to ligand for Lix 26 (1,76 for [Lix 26] in the range 36-90 g/l of purity-corrected ligand) and TN 02181 (2,11 for [TN 02181] in the range 44-66 g/l of the purity-corrected reagent), suggest some intermediate complex behaviour and can be rationalized by the interpretation given above (and suggested by Van der Zeeuw⁽¹⁶³⁾), since they both have orders within the range of the two extremes i.e. 1-3, however this rationalization cannot explain the apparent ligand reaction order for TN 01787 of 3,77 (observed in the range of purity-corrected concentration of 42 - 84 g/l). Further comment of this apparent kinetic contradiction is made after presentation of shaking apparatus data in Section 3.2.1.7.

(iv) Figure (41) shows the plot of $\log k_{obs}$ vs $\log[HL]$ for active-constituent corrected reagent concentration. The plot shows how much better, in real terms, Lix 26 is compared with the other two reagents under the conditions which prevail in the Lewis Cell, i.e. at the dotted line shown, the concentrations of ligand required to give an



* TN 02181 ◊ TN 01787 • Lix 26

Figure (41). Log k_{obs} versus log [HL] for active-constituent corrected concentrations of extractants. The dotted line shows the difference in active ligand concentration required to obtain a rate constant of $1 \times 10^{-5} \text{ s}^{-1}$ for the three ligand reagents

observed rate constant of e.g. $1,0 \times 10^{-5} \text{ s}^{-1}$ are:

Lix 26	:	38,0 g/l
TN 02181	:	50,7 g/l
TN 01787	:	52,5 g/l

This is not immediately apparent from Figure (39) and may be of interest to the suppliers of these reagents.

3.1.4. The Relevance of Lewis Cell Extraction Data to Turbulent Systems.

The role of the liquid-liquid interface in mass transfer during extraction has received much attention over the last ten years and remains controversial. There exist two opinions regarding the mechanism of extraction by which ligand molecules chelate metal ions : the two points-of-view can be summarised as:

- (i) The rate of extraction of metal ion in the aqueous phase by the extractant molecule dissolved in the organic phase is reflected by a rate-determining step at the interface and
- (ii) The bulk aqueous phase is the site of the rate-determining step.

It is axiomatic that in any multistep kinetic process, the observed rate correlates with the slowest step in the reaction, thus in order to test the two opinions described above for various metal and ligand systems, workers have been limited in their experimental approach. Those advocating the interfacial mechanism conduct experiments under conditions of well-defined surface area i.e. Lewis Cell arrangements, whereas proponents of the bulk aqueous (homogeneous) mechanism

have utilised high speed arrangements which, until recently^(77,78), have not permitted any measurement of the interfacial area. The work reported in this section concludes that an interfacial mechanism for germanium extraction is appropriate for the alkylated-8-hydroxyquinoline reagents of concern to this work and the low aqueous solubility ($< 0,001 \text{ g/l}^{(183)}$) of the active ligand components gives additional justification to this inference. If the experimental conditions which apply to the Lewis Cell yield observed kinetic data which is a true manifestation of chemical control (i.e. diffusion effects can be ignored), then it might be expected that data acquired from a high speed mixer/shaker apparatus would yield similar results. In view of this rationale, the kinetics of extraction of germanium by Lix 26, TN 02181 and TN 01787 in a high speed mixing apparatus are dealt with in Section 3.2. which follows.

3.2. Factors Affecting the Kinetics of Germanium Extraction in High Speed Mixing Assemblies.

There are a number of parameters which may influence the kinetics and the equilibrium percentage extraction of germanium by 7-alkylated-8-hydroxyquinoline derivatives. Although, in order to elucidate their effect on the systems studied, they will be treated as separate entities in the succeeding discussion, it should be noted that it is usually the case that varying one parameter affects other properties of the system and therefore (perhaps) the validity of conclusions made. For example, a necessary study for kinetic modelling is the effect of pH on extraction, but, altering the pH also:

(i) alters the characteristics of the interface (since species become protonated or deprotonated) which alters the ligand population at the interface and, *inter alia*, the interfacial tension and the resistance to mass transfer, (Section 3.11.2),

(ii) alters the ionic strength of the medium (Section 3.5), which modifies the extraction characteristics measurably in the initial stages,

(iii) determines the nature of the species which is extracted (Section 3.4.5).

The parameters which are discussed are therefore important individual considerations in the construction of an holistic kinetic model (Section 3.15).

3.2.1. The Effect of Ligand Concentration on Extraction Kinetics.

3.2.1.1. Kinetic Treatment

In Section 3.1.1, an equation was derived (Equation (46)) which related the forward rate constant, k_f , for the extraction of germanium from the aqueous phase by a ligand dissolved in an organic phase, to the concentration of germanium in the aqueous phase initially, at some intermediate time and at equilibrium: a_0 , a_t and a_e respectively. Under conditions of vigorous stirring, the equilibrium concentration of germanium in the aqueous phase is rapidly attained and therefore the term $(a_0 - a_e)$ is significant at all stages during extraction. Hence, Equation (46), as written, was used to calculate k_f .

3.2.1.2. Determination of the Order of Reaction With Respect to [Lix 26]

The overall rate for germanium extraction at constant pH, temperature, ionic strength etc., is given by Equation (65):

$$\text{Rate} = k_{obs}[\text{Ge}][\text{HL}]^{\chi} \quad (65)$$

In order to determine the value of constant χ , the ligand concentration in toluene was varied while [Ge] remained constant at approximately 0,62 g/l in 1,5 M H₂SO₄. Volumes, sampling and germanium quantification were as described in Section 2.2.2.1. Table (27) details a typical data set obtained, in this case for 50 g/l Lix 26.

Sample	Time /min	[Ge]/ (g/l)	$\frac{a_0 - a_e}{a_0} \ln \frac{a_0 - a_e}{a_t - a_e}$	% Extraction
Initial	-	0,608	-	-
1	2	0,284	0,771	53,3
2	5	0,184	1,224	69,7
3	10	0,136	1,550	77,3
4	20	0,087	2,057	85,7
5	30	0,058	2,559	90,5
6	45	0,041	3,050	93,3
7	60	0,039	3,128	93,6
8	90	0,024	4,085	96,1

Sample	Time /min	[Ge]/ (g/l)	$\frac{a_0 - a_e}{a_0} \ln \frac{a_0 - a_e}{a_t - a_e}$	% Extraction
9	150	0,017	5,552	97,2
10	360	0,015	$a_t = a_e,$ equilibrium value.	97,5

Table (27). Germanium extraction kinetic data, aqueous phase : 0,608 g/l Ge in 1,5 M H₂SO₄, organic phase : 50 g/l Lix 26 in AR toluene. Vigorous shaking.

Figure (42a) shows the semi-logarithmic plot obtained from these data, while Figure (42b) depicts the percentage of extraction of germanium obtained as a function of time. A number of important features are evident on these plots:

(a) The initial rate of extraction is rapid with $t_{1/2} < 2$ minutes. This is followed (Figure (42a)) by a linear kinetic regime which could be loosely referred to as a slower 'equilibrium' period, followed by deviation from linearity at approximately 60 minutes. Although for other data sets such plots could be higher or lower in the two regions, they all had this basic shape.

(b) The time to attain equilibrium percentage extraction is of the order of 90 minutes, however, if the reagent were to be used industrially in a multistage mixer-settler operation in which aqueous raffinate is contacted with organic phase a number of times, then ten minutes contact would achieve excellent percentage extraction ($\approx 77\%$).

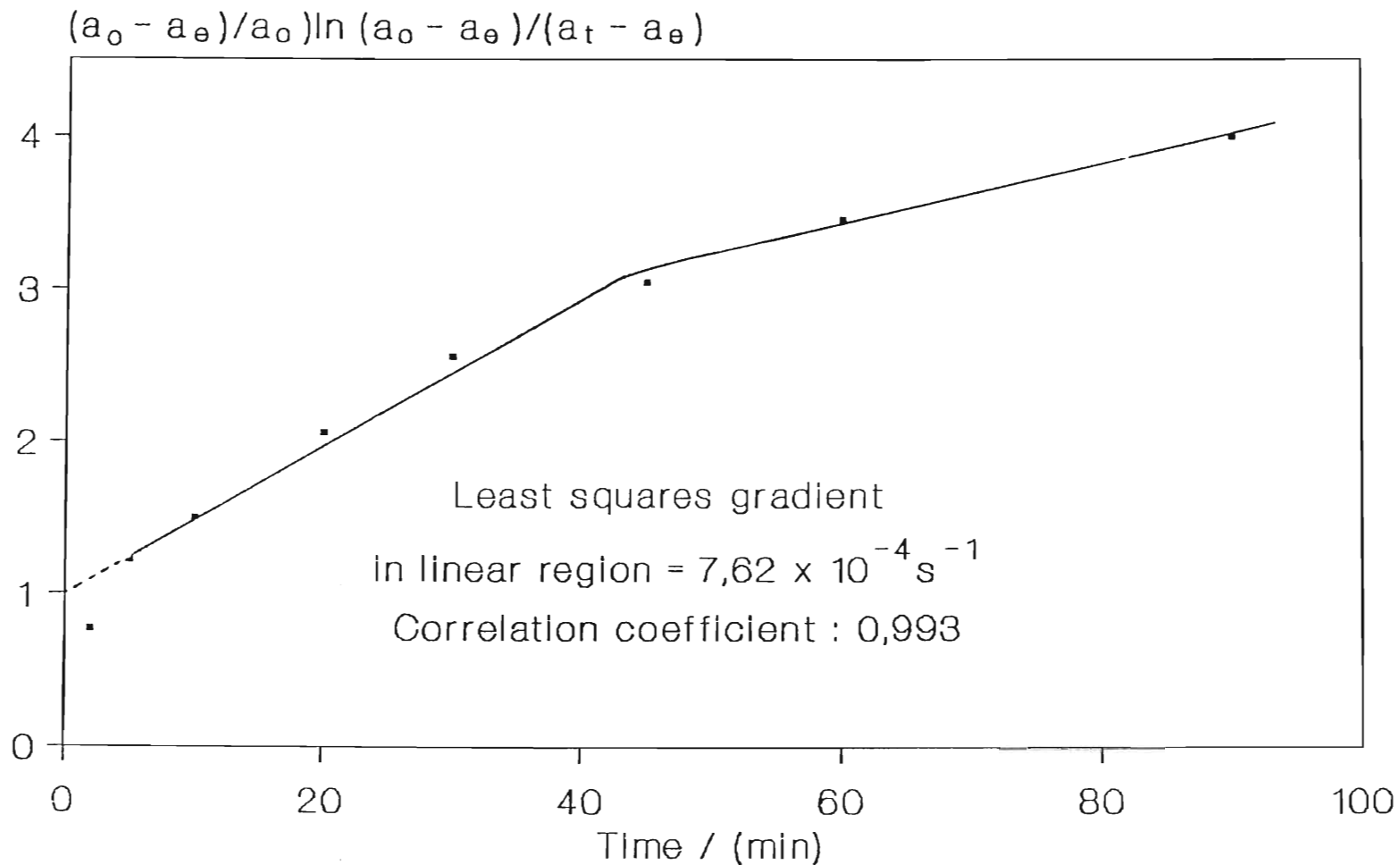
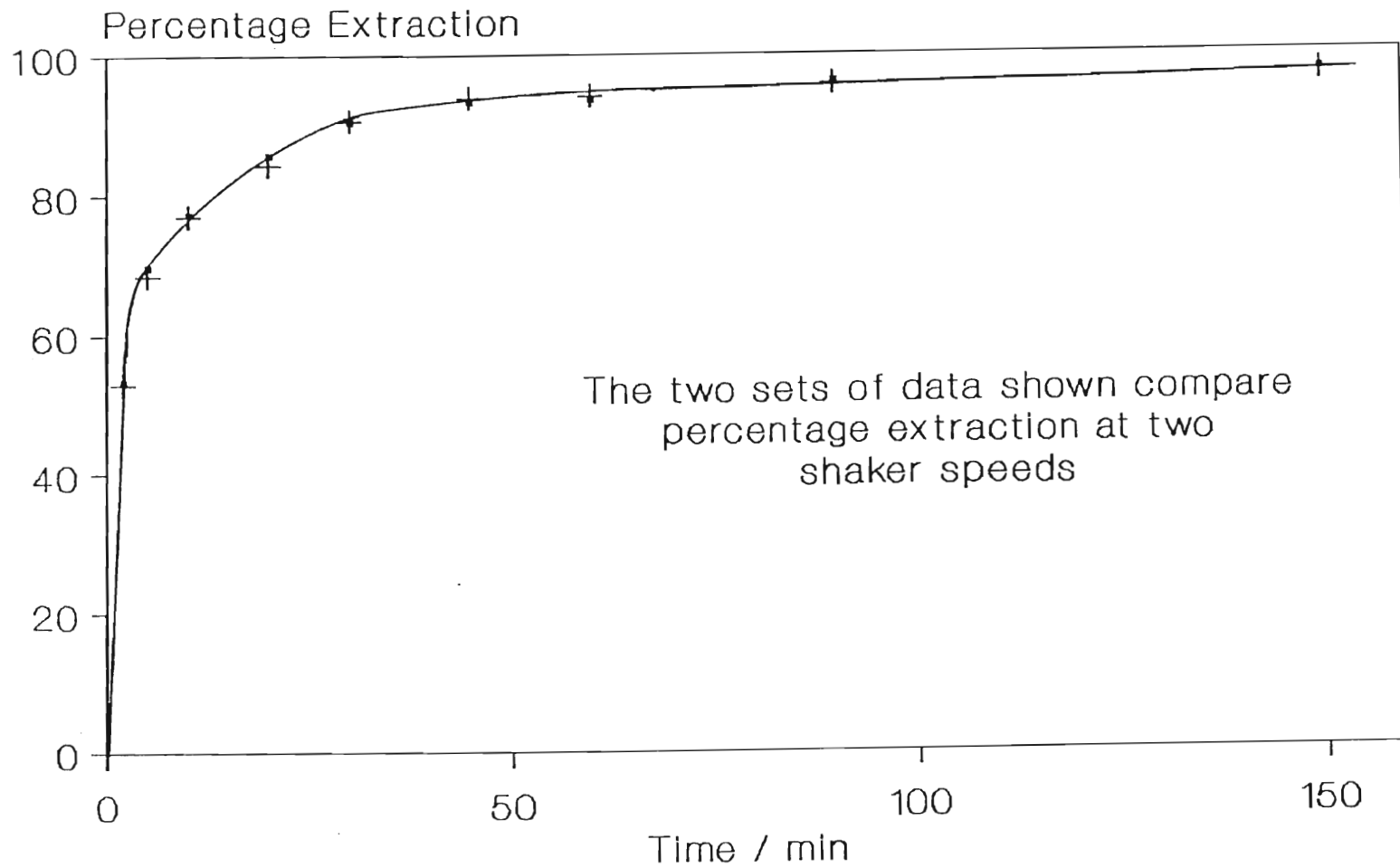


Figure (42a). Kinetics of germanium extraction in the vigorous shaker for 50 g/l Lix 26 in toluene and $\sim 0,62$ g/l Ge in 1,5 M H_2SO_4 . a_0 , a_e and a_t are the concentrations of germanium in the aqueous phase initially, at equilibrium and at some intermediate time. The extrapolation to $t=0$ is the value of a_t used to calculate the quantity of germanium which is extracted in the initial fast reaction regime and is discussed in Section 3.4.6.



▪ 770 oscillations/min + 500 oscillations/min

Figure (42b). Percentage germanium extraction as a function of time for vigorous shaking. Organic phase : 50 g/l Lix 26 in toluene; Aqueous phase : ~ 0,62 g/l Ge in 1,5 M H_2SO_4 . A further set of extraction data obtained at 1300 oscillations per minute produced a concurrent plot with the two shown in the figure but is omitted for simplicity.

(c) A least squares observed rate constant of $7,62 \times 10^{-4} \text{ s}^{-1}$ was calculated for the linear region shown in Figure (42a). The subsequent change in gradient thereafter suggests that as equilibrium is approached, Equation (46) becomes sensitive to small errors and more accurate data is required. It must be noted that plots such as the one in Figure (42a) did not pass through the origin and, except at low ligand concentration, the first point on the plot was excluded from the gradient calculation: the kinetics in this initial very fast regime are discussed later in this section and an interpretation is presented in Section 3.4.6.

(d) A shaking speed of 770 oscillations per minute is sufficient to ensure that the rate of reaction is not limited by diffusion. Two further data sets obtained under the same conditions but with shaking speeds of 500 and 1300 oscillations per minute produced concurrent plots (Figure 42b).

Rate constant values were obtained in an analogous manner for extraction runs performed with Lix 26 in the concentration range 12,5-150 g/l and the results are summarised in Table (28).

[Lix 26] /(g/l)	log [Lix 26]	$k_f(\text{obs}) / \text{s}^{-1}$	log $k_f(\text{obs})$
12,5	1,10	$3,29 \times 10^{-6}$	-5,48
19,0	1,28	$4,66 \times 10^{-5}$	-4,33
25,0	1,40	$1,62 \times 10^{-4}$	-3,79
35,0	1,54	$2,51 \times 10^{-4}$	-3,60
50,0	1,70	$7,62 \times 10^{-4}$	-3,12
75,0	1,88	$1,79 \times 10^{-3}$	-2,75
100,0	2,00	$4,03 \times 10^{-3}$	-2,39
150,0	2,18	$5,41 \times 10^{-3}$	-2,27

Table (28). Kinetic data obtained for the extraction of germanium by Lix 26 in a mechanical shaker. $[\text{Ge}] \sim 0,65 \text{ g/l}$, $[\text{H}_2\text{SO}_4] = 1,5 \text{ M}$. All Lix 26 solutions made up in AR toluene. Phase volumes 100 ml.

A plot of $\log k_f(\text{obs})$ vs $\log[\text{Lix 26}]$ is shown in Figure (43a). The lower plot (approximately 0,65 g/l germanium) shows a number of features of importance to the extraction kinetics:

- (i) For the ligand concentration range 19-100 g/l, a rate equation of the form $\text{Rate} = k_{\text{obs}}[\text{Ge}][\text{Lix 26}]^{2,7}$ is suggested (cf. an order of 1,76 in the Lewis Cell, Section 3.1.3)

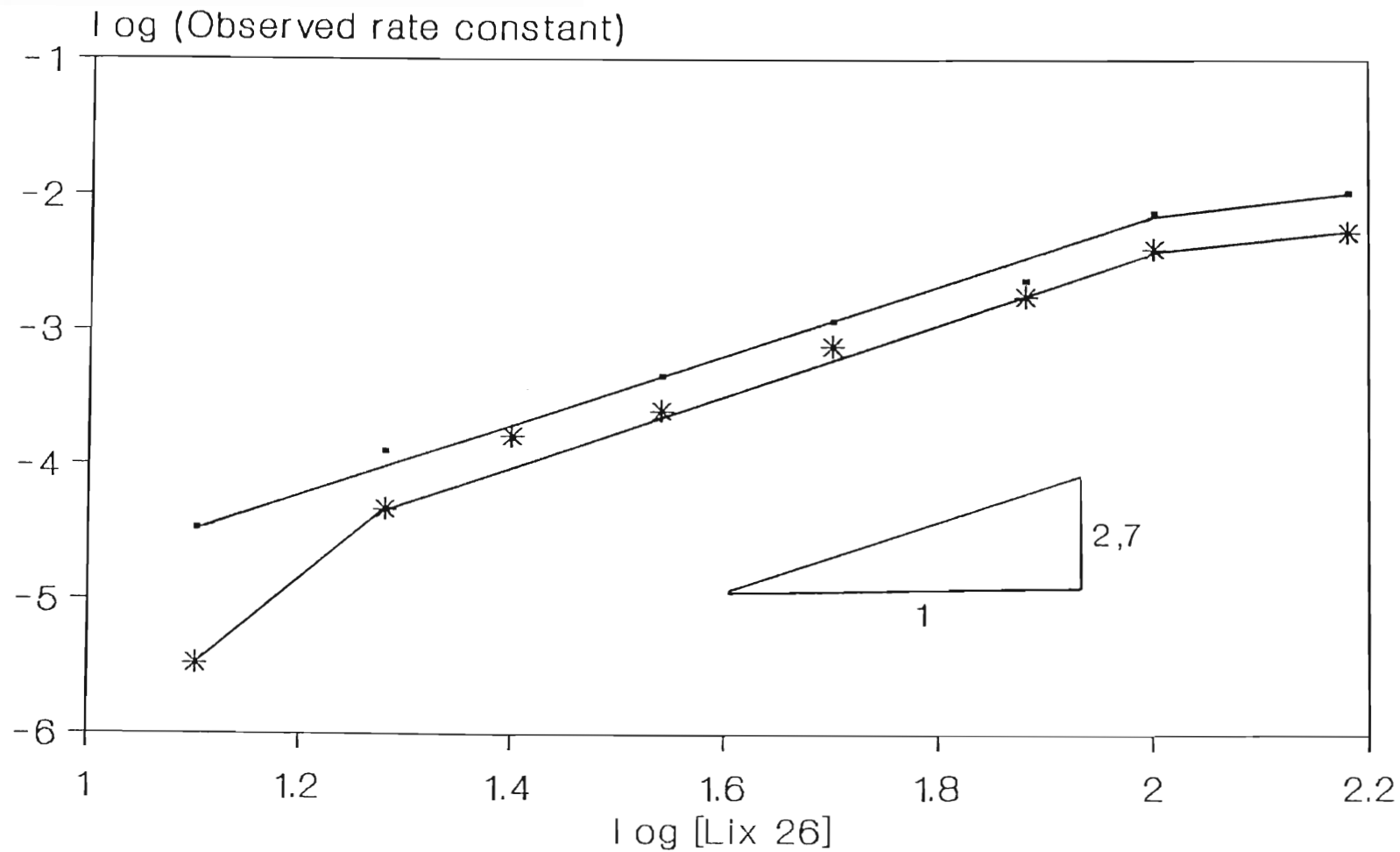


Figure (43a) Plot of Log(Observed rate constant) as a function of log[Lix 26] obtained in the vigorous shaker for concentrations of germanium of 0,65 g/l and 0,20 g/l. Aqueous phases were 1,5 M H₂SO₄ and Lix 26 was dissolved in AR toluene. Least squares gradients in the linear region are 2,7 (lower curve) and 2,6 (upper curve).

(ii) A deviation from linear behaviour is evident at low ligand concentration (< 19,0 g/l Lix 26) for the 0,65 g/l concentration of germanium. At this concentration of germanium ($\sim 8,95 \times 10^{-3}$ M) and assuming that each metal ion consumes 3 ligand molecules, a Lix 26 concentration of $2,69 \times 10^{-2}$ M would apparently be required to complex all of the metal ion. This corresponds to a concentration of approximately 11,6 g/l of impure Lix 26, which suggests that chemical stoichiometric excess is not the only factor which determines the observed deviation of Figure (43a). This deviation is not observed at the lower germanium concentration shown in Figure (43a): for 0,2 g/l Ge, which is equivalent to $2,76 \times 10^{-3}$ M Ge, Lix 26 is in 3,5-fold stoichiometric excess when $[\text{Lix 26}] = 12,5$ g/l, the lowest concentration for which the observed reaction rate was determined. Further discussion of the upper curve of Figure (43a) is presented later in this section.

(iii) The plot levels off at $[\text{Lix 26}] \geq 100$ g/l giving an apparent reaction order with respect to ligand of 0,66. In Section 3.1.3., it was suggested that the order with respect to ligand could conceivably be anything from 1 to 3, although it has been suggested⁽¹⁶³⁾ that orders approaching zero are possible at very high ligand concentrations and this apparent reaction order (0,66) is illustrative of this tendency. There are three plausible causes for the behaviour towards low ligand order dependency:

(a) The interface is maximally populated by ligand molecules above $[\text{Lix 26}] = 100$ g/l and further

ligand loading into the organic phase does not alter ligand availability.

(b) The ligand-containing organic solution becomes increasingly viscous with increasing concentration of ligand reagent (Section 3.11.3). It is proposed that at high concentrations, the viscosity of the organic medium affects the distribution constants of reactive ligand partitioning to the interface and of the products formed at the interface into the organic bulk.

(c) At high ligand concentration, the competition for germanium by free oxine impurity, which partitions to the aqueous phase where it complexes the metal-ion, becomes significant. This possibility is fully investigated in Section 3.3.

Of (a) and (b) above, the first mentioned is most likely to be predominant and is further discussed in Section 3.11.2.2. where interfacial tension data for this system is used to calculate the concentration of Lix 26 which would be required to completely saturate the interface.

Included on the plot of Figure (43a) are the values of $\log k_f(\text{obs})$ for a set of extraction runs for which $[\text{Ge}] = 0,20 \text{ g/l}$. The plot obtained at the lower initial metal concentration shows similar behaviour over the entire range of ligand concentration with a slope in the linear region of 2,60 (cf. a value of 2,7 for the higher germanium concentration - this further supports the inference that the observed rate is first order in germanium concentration). However for the 0,2 g/l system the observed kinetics do not deviate from linearity at low ligand concentration and this can be

attributed to the increased stoichiometric ratio of ligand to metal.

The equilibrium data for the two initial germanium concentrations are shown in Figure (43b). At low ligand concentration, percentage extractions for the 0,65 g/l system are typically lower than the 0,20 g/l system, indicating the higher ligand:metal ratio for the latter, however at approximately 35 g/l ligand, the plots are almost concurrent. At this ligand concentration, the molar ratios of purity-corrected ligand:metal for the two germanium concentrations are approximately 30:1 (0,20 g/l Ge) and 9:1 (0,65 g/l Ge), which, given the 3:1 ratio in the chelate complex which is formed, suggests 10-fold and 3-fold molar excesses of active ligand. Apparently then, a 3-fold molar excess of ligand is required for equivalent germanium extraction yields.

It is apparent from Figure (42a), that germanium extraction by Lix 26 is characterised by two kinetic regimes: a fast initial regime, followed by a slower one which persists until the simple first-order analytical function no longer describes the kinetics adequately- possibly due to the increasing sensitivity to the experimental data of the analytical expression used.

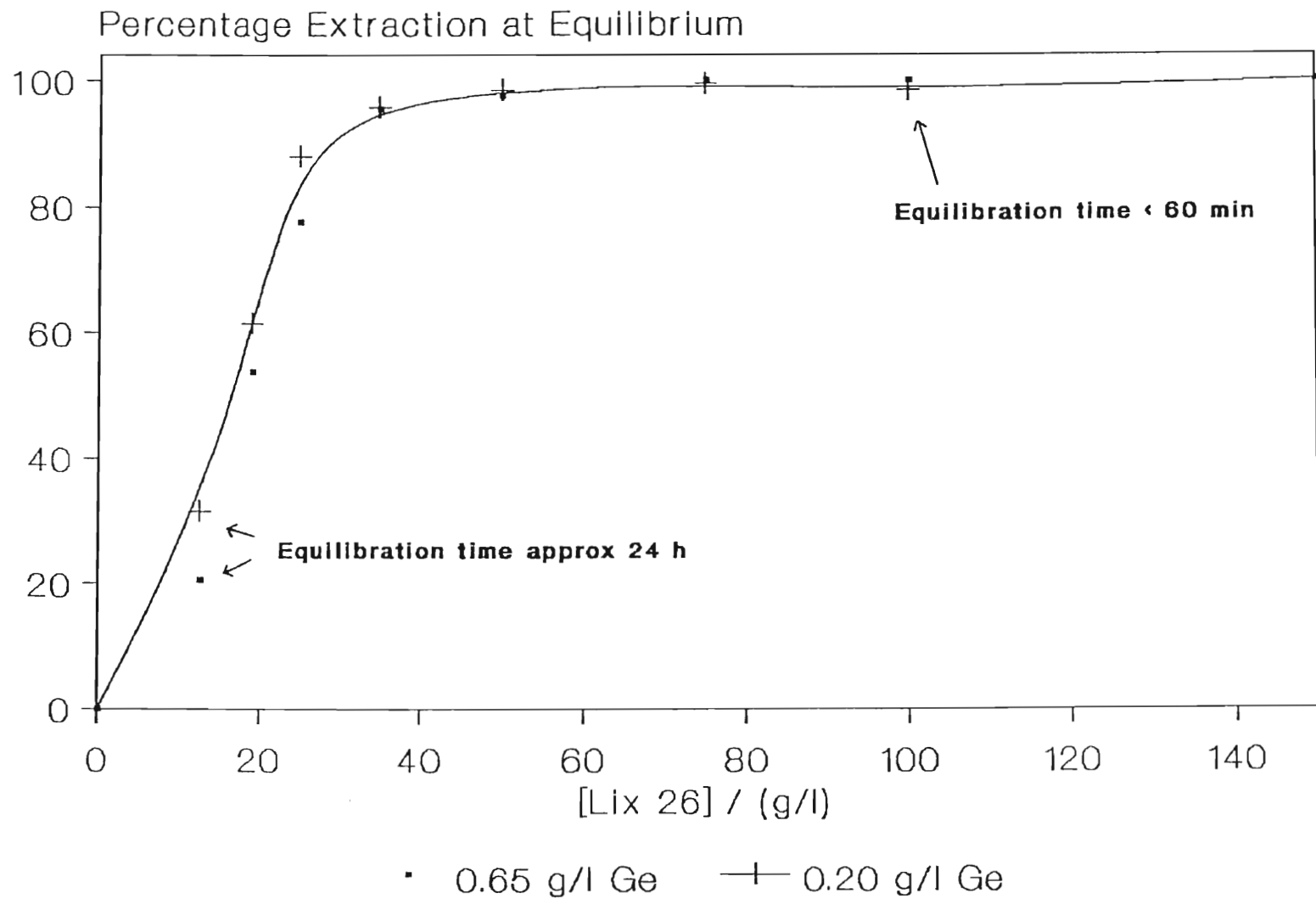


Figure (43b). Comparison of the percentage extraction obtained at equilibrium (i.e. when no further extraction is observed) as a function of Lix 26 concentration for two initial germanium concentrations viz 0,20 and 0,65 g/l. Organic phase : Lix 26 in AR toluene; Aqueous phase : germanium in 1,5 M H_2SO_4 .

Thus far, discussion has centred upon the slower region, however it has been noted previously (p.181), that the first data point on the semi-logarithmic plots did not fit the linear kinetics observed thereafter and it is because of this that the initial region draws attention. In order to determine the order with respect to ligand in this fast kinetic regime, the initial rate method was used. Initial rates were calculated from the plots of $[\text{Ge}]_{\text{aq}}$ versus time in the initial region - usually only the first five minutes of the reaction. Figure (44) shows a plot of $\log(\text{Initial rate})$ versus $\log[\text{Lix 26}]$. In the concentration range 12,5-50,0 g/l of the as-received reagent, an order with respect to ligand of 2,1 is suggested, while for $[\text{Lix 26}] \geq 50$ g/l, the plot levels off with a slope of 0,53 (cf. 0,66 for the slower reaction regime) implying maximal population of the interface by ligand and also suggesting the generation of the other factors contributing to this behaviour as discussed earlier (p.184). The implications of Figures (42a) and (44) for the interpretation of extraction data are as follows:

(i) For all ligand concentrations (12,5-150,0 g/l), the initial rate of extraction of germanium from the 1,5 M H_2SO_4 aqueous phase, is much faster than the subsequent rate which follows typical first-order behaviour. In the range $12,5 \text{ g/l} \leq \text{Lix 26} \leq 50,0 \text{ g/l}$, the order with respect to ligand concentration in the initial kinetic regime is 2,1 compared with 2,7 for the subsequent slower kinetic regime, while for $[\text{Lix 26}] \geq 50,0 \text{ g/l}$, an apparent reaction order of 0,53 prevails for the initial extraction region. Thus the initial rate plot indicates a deviation to very low orders at a concentration very much

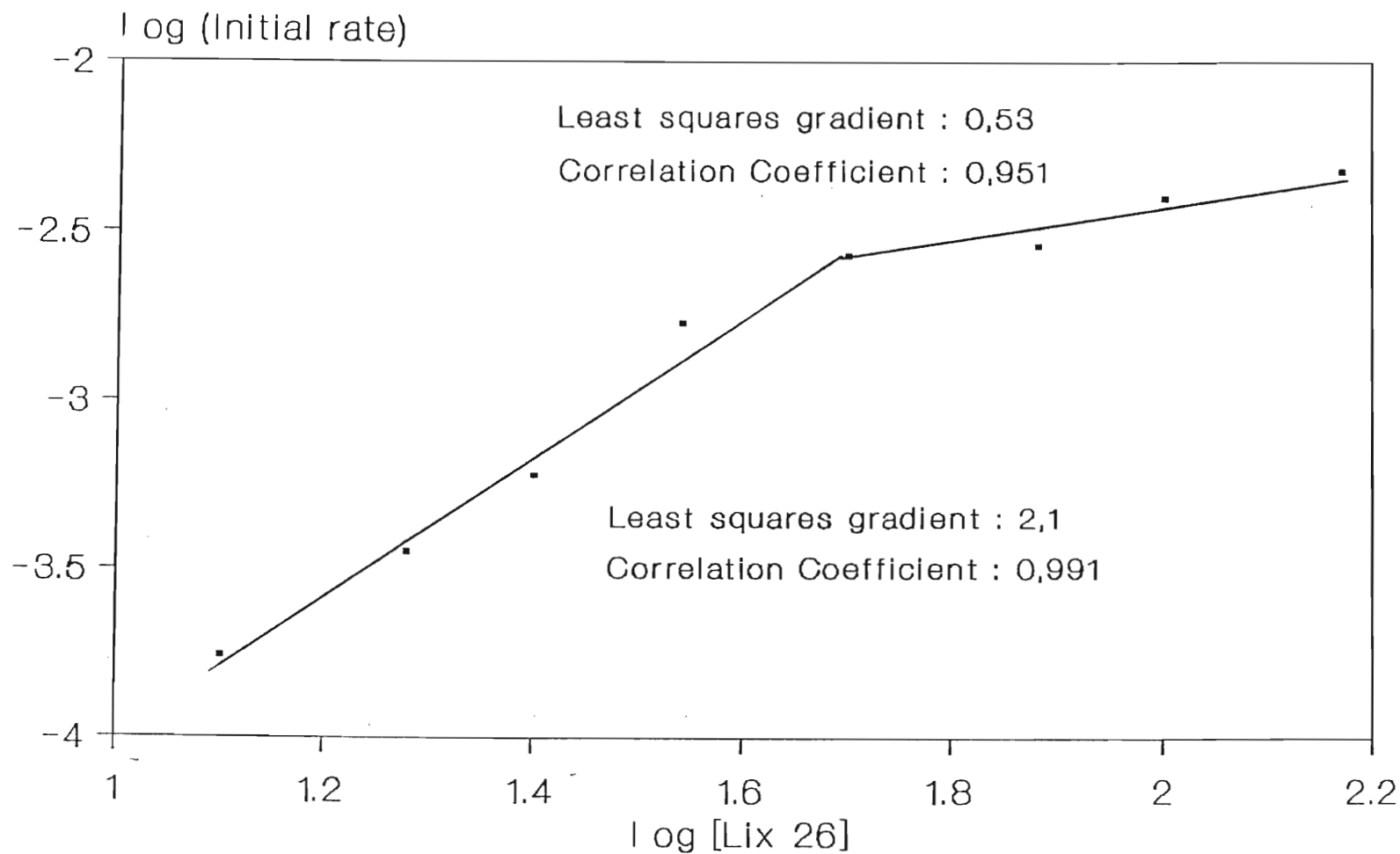


Figure (44). Log(Initial rate) versus log[Lix 26] for germanium extraction by various concentrations of Lix 26 in a mechanical shaker. Aqueous phase : ~0,65 g/l Ge in 1,5 M H₂SO₄; Organic phase : Lix 26 in AR toluene. The least squares gradient for log[Lix 26] ≥ 1,7 = 0,53.

lower than the plot obtained for the kinetics in the slower regime (50,0 g/l compared with 100 g/l). This observation concerning the initial rate suggests that, during the initial stages of reaction at least, the interface is also saturated with ligand. It is interesting to compare the bulk organic ligand concentrations (purity-corrected), with the initial germanium concentration: the 50,0 g/l and 100,0 g/l reagent concentrations correspond to 4-fold and 8-fold stoichiometric excesses respectively.

(ii) Bearing in mind the commercial application of this work it is worth remarking that the data shown in Figure (43a) suggests that, since the interface is fully saturated for $[\text{Lix 26}] \geq 100,0 \text{ g/}$ reagent concentrations greater than this would not be economically efficient.

3.2.1.3. The Apparent Reaction Orders With Respect to Ligand for TN 01787 and TN 02181.

The kinetics of extraction of Schering's two research products, investigated under the same conditions as Lix 26, are summarised in the $\log k_f(\text{obs})$ versus $\log [\text{HL}]$ plot of Figure (45). Orders with respect to ligand of 3,08 and 1,12 are indicated for TN 01787 and TN 02181 respectively. These results indicate therefore that TN 02181 is a more efficient extractant than TN 01787 over the entire ligand concentration range studied. Two points of interest are evident in Figure (45):

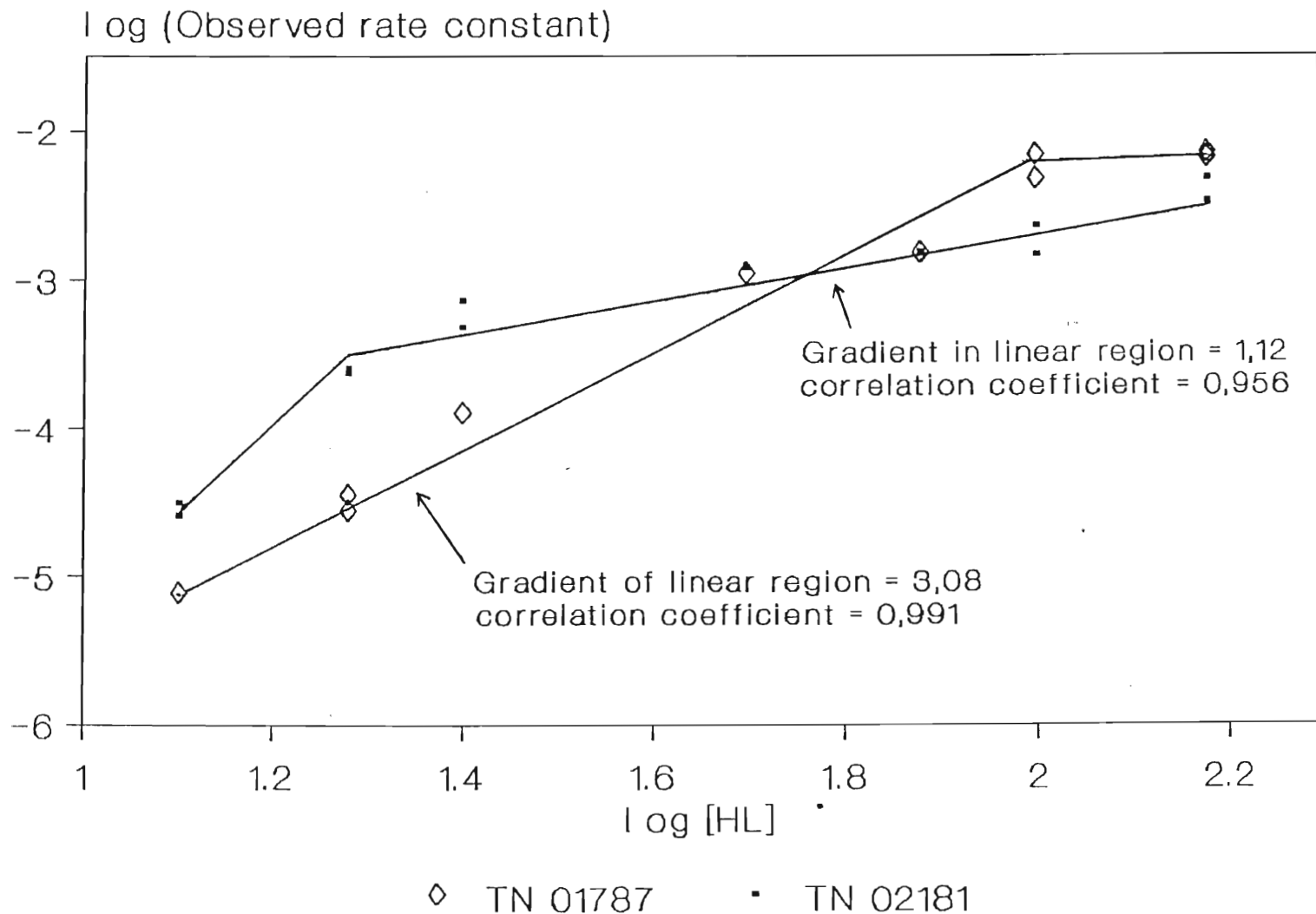
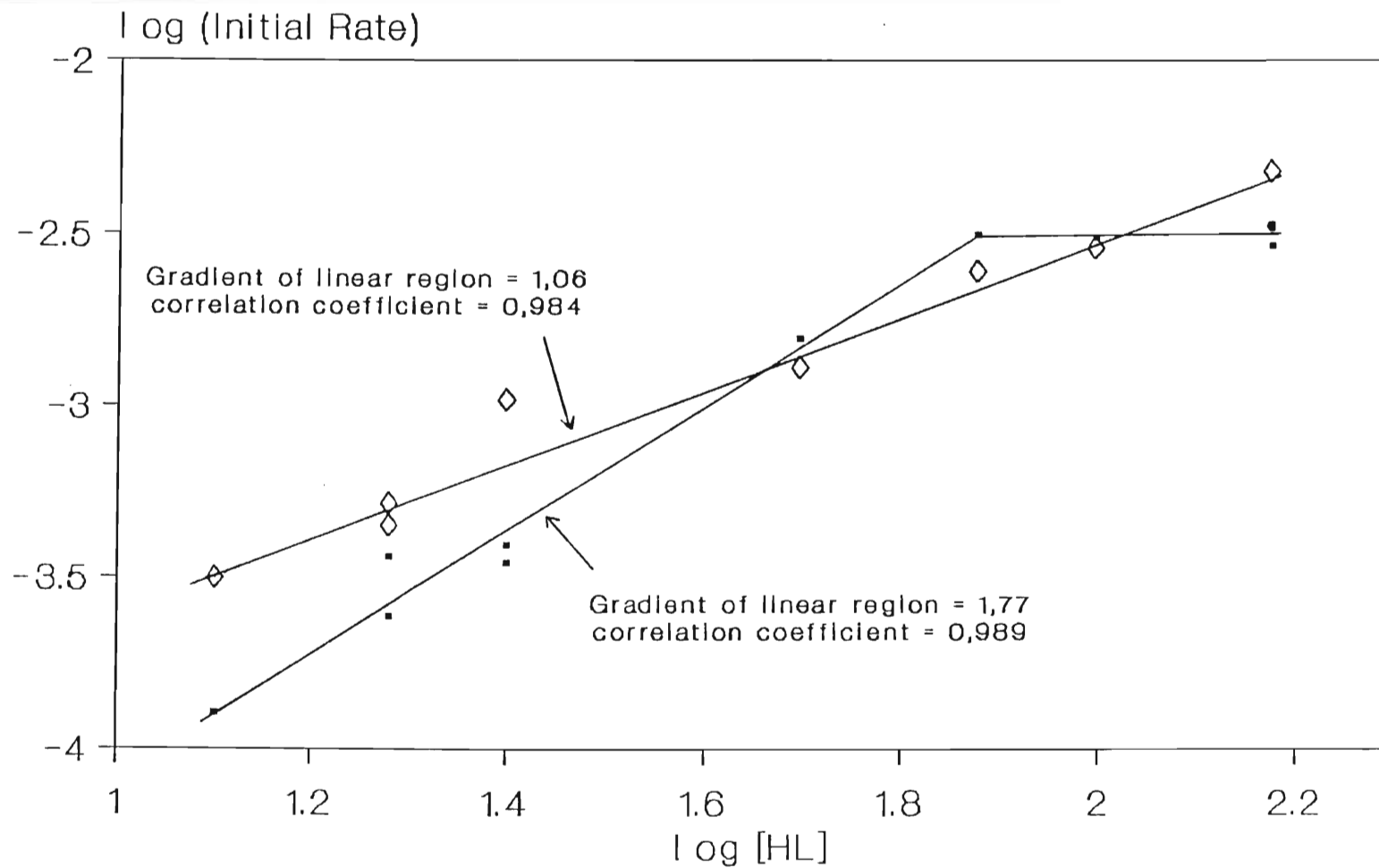


Figure (45). Log(Observed rate constant) versus log[HL] for germanium extraction by TN 02181 and TN 01787 in the slow kinetic regime. Vigorous shaking. Aqueous phase : ~ 0,65 g/l Ge in 1,5 M H₂SO₄; Organic phase : reagents dissolved in AR toluene. Orders with respect to [Ge] and [HL] are 1,12 and 3,08 respectively.

(a) The $\log k_f(\text{obs})$ vs $\log [\text{HL}]$ plot for TN 02181 does not exhibit the deviation from linearity at high concentration which characterises the Lix 26 and TN 01787 systems and,

(b) Of the two sets of data plotted on Figure (45), only that for TN 02181 deviates from linearity at low ligand concentration ($< 12,5$ g/l). This can be partly accounted for by the lower purity of the product (84%) compared with TN 01787 (88%) but it is more likely that differences in their interfacial activity and stability are responsible.

Initial rate data for the two reagents are shown in Figure (46). The behaviour parallels that for Lix 26, viz. lower orders with respect to ligand in this initial rate region (1,06 and 1,77 for TN 02181 and TN 01787 respectively). In the case of TN 02181, the value of 1,06 is not significantly different from the value of 1,12 obtained for the longer time scale, whereas an initial rate somewhat faster than the first-order kinetic regime is indicated for TN 01787. It is interesting to note that while the order with respect to TN 01787 concentration tends towards a value < 1 at high ligand concentration (like Lix 26), this is not a characteristic of TN 02181.



▪ TN 01787 ◇ TN 02181

Figure (46). Log(Initial rate) versus log[HL] for germanium extraction by TN 02181 and TN 01787 in the shaking apparatus. Initial rates were calculated from the gradients of $[Ge]_{aq}$ versus time plots in the initial reaction region. Aqueous phase : $\sim 0,65$ g/l Ge in 1,5 M H_2SO_4 ; Organic phase : TN 02181 or TN 01787 in AR toluene. Ligand orders are indicated.

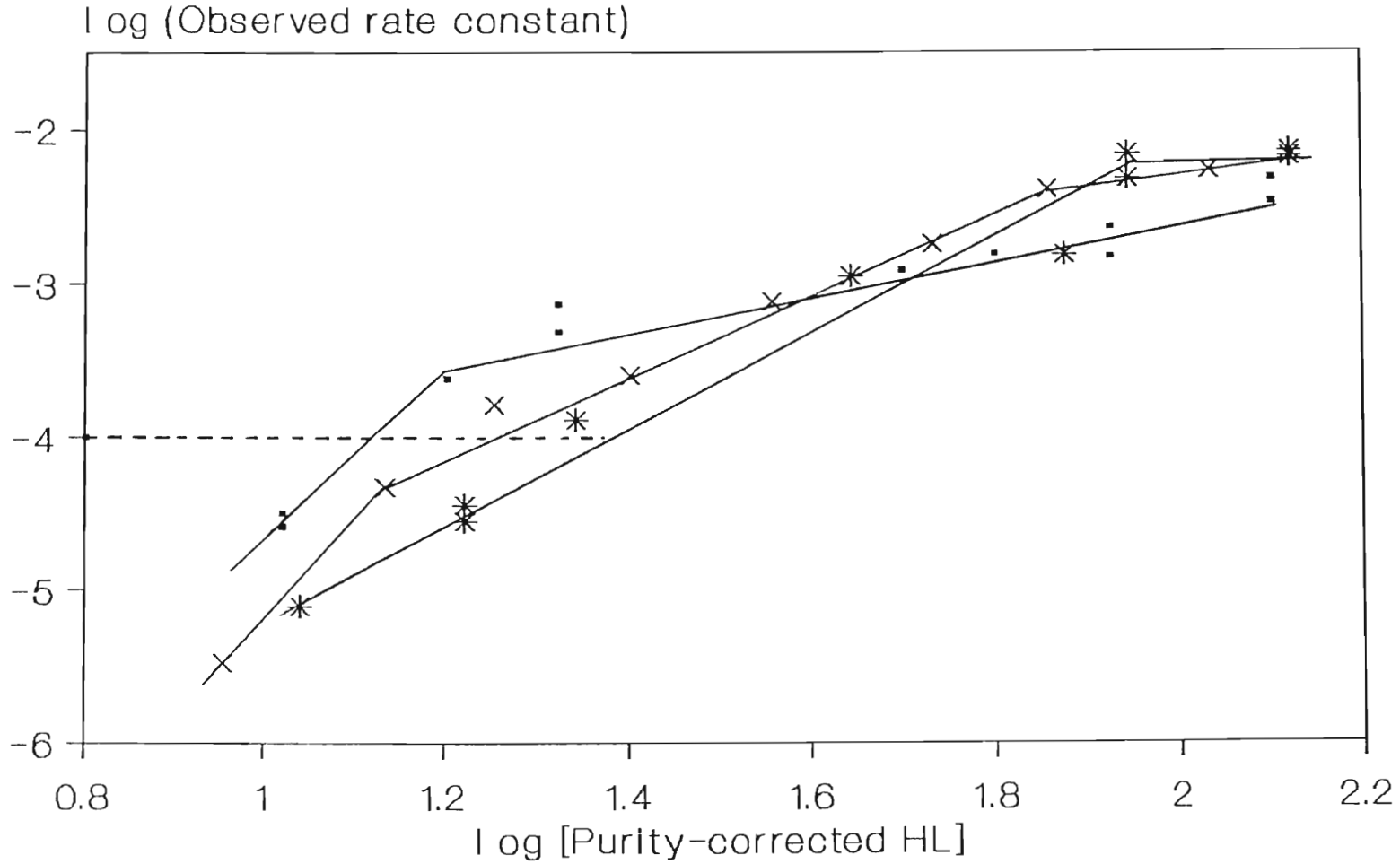
3.2.1.4. A Comparison of the Rate of Germanium Extraction by Lix 26, TN 01787 and TN 02181.

Figure (47) gives a comparison of the observed rate constants for germanium extraction by the title reagents reduced in concentration in accordance with their 'activity'.

For $[HL]_{org} \leq 50,0$ g/l, the order of extraction efficiency indicated by these data is TN 01787 < Lix 26 < TN 02181, while at high ligand concentration, observed rate constants are essentially the same (except that TN 02181 gives a rapid initial rate). An indication of the extraction efficiencies at low pH (1,5 M H_2SO_4) and low ligand concentration ($< 50,0$ g/l), can be gained by comparing the concentrations of ligand required to attain a specified observed rate of germanium extraction (phase ratios, temperature etc. being constant). For example, to obtain an observed rate constant of $1,0 \times 10^{-4} s^{-1}$, the following reagent concentrations are required:

TN 02181	:	14,5 g/l
Lix 26	:	17,4 g/l
TN 01787	:	26,0 g/l

Therefore for low ligand concentration, TN 02181 is more suited for germanium recovery, but the absolute rates at these low ligand concentrations are unlikely to be commercially viable. (This is not strictly true if a chemical modifier is added to the system, see Section 3.7.)



▪ TN 02181 * TN 01787 × Lix 26

Figure (47). Log(Observed rate constant) versus log[HL] (corrected for percentage active constituent) for TN 01787, TN 02181 and Lix 26. The dotted line indicates the concentration of ligand (in g/l) required to obtain an observed rate constant of $1 \times 10^{-4} \text{ s}^{-1}$.

3.2.1.5. The Equilibrium Percentage Extraction of Germanium by Lix 26, TN 02181 and TN 01787

An important parameter in the field of solvent extraction is the percentage extraction obtained with time, particularly at equilibrium (where further time of contact does not improve yields). Often the rate of the extraction process decreases with time so that it is not practical to continue commercial operation to the limit of 'equilibrium'. Figures (48) to (50) summarise the percentage extraction data for the three ligand reagents of concern in this work. On their own these data are useful in determining optimal operating conditions, but of greater value to this study is a comparison of the efficiencies of the ligand reagents at low and at high concentration and *inter alia* the determination of the stoichiometric ratio of ligand to germanium in the extracted complex. Figure (51) compares the extraction efficiencies of the three ligands in terms of percentage extraction. Kelex 100, which was discussed in Chapter 1 is also included. Since at high ligand concentrations, the ratio of $[HL]_{int} : [Ge]_{int}$ is high in all cases, the equilibrium and kinetic data are approximately equivalent for all four extractants. However, distinct differences exist at the low concentration represented in Figure (51) i.e 25 g/l. Since the major difference between these compounds is the position of unsaturation in the 7-alkyl group, the data presented here appears to suggest that this is the determining factor in the kinetic properties of these ligands since for Kelex 100 the 7-alkyl group is saturated and this is the poorest extractant, Lix 26 and TN 01787 are both α -unsaturated and roughly

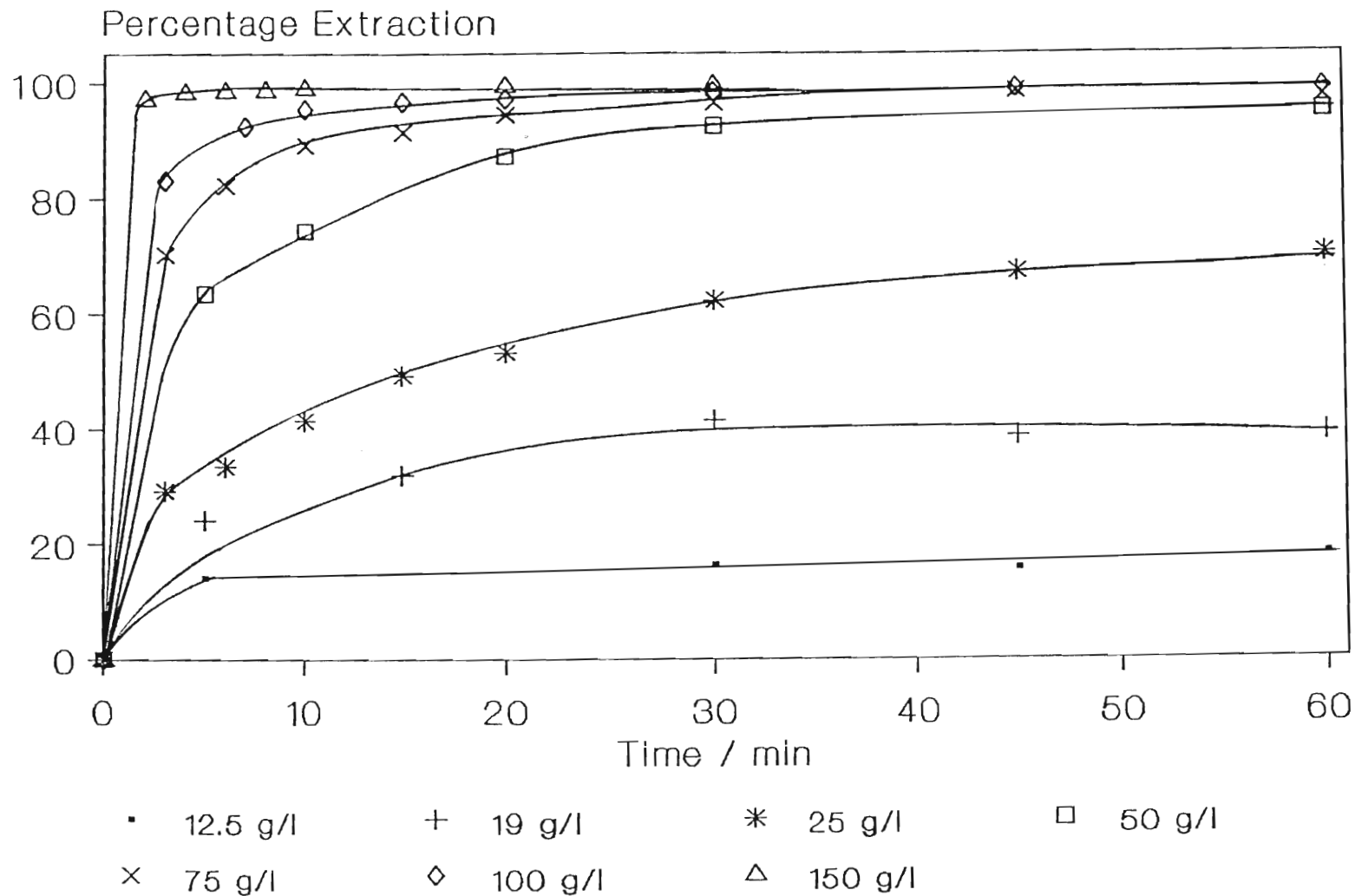


Figure (48). Percentage germanium extraction versus time for TN 02181 solutions of varying concentration obtained with a mechanical shaking apparatus. Organic phase : TN 02181 in AR toluene; Aqueous phase : ~ 0,65 g/l Ge in 1,5 M H₂SO₄. Phase volumes 100 ml.

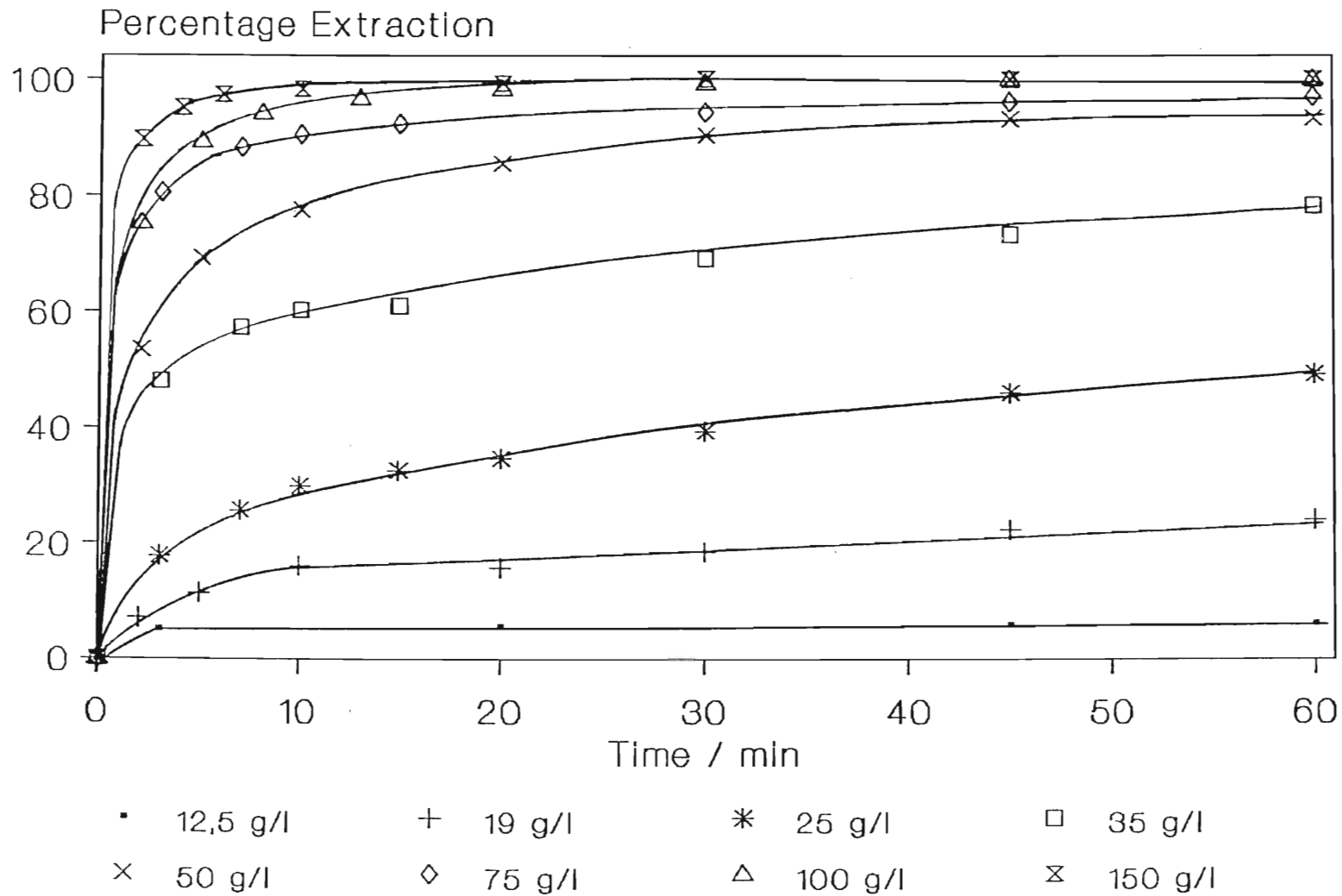


Figure (49). Percentage germanium extraction versus time for Lix 26 solutions of varying concentration obtained with a mechanical shaker. Conditions as for Figure(48).

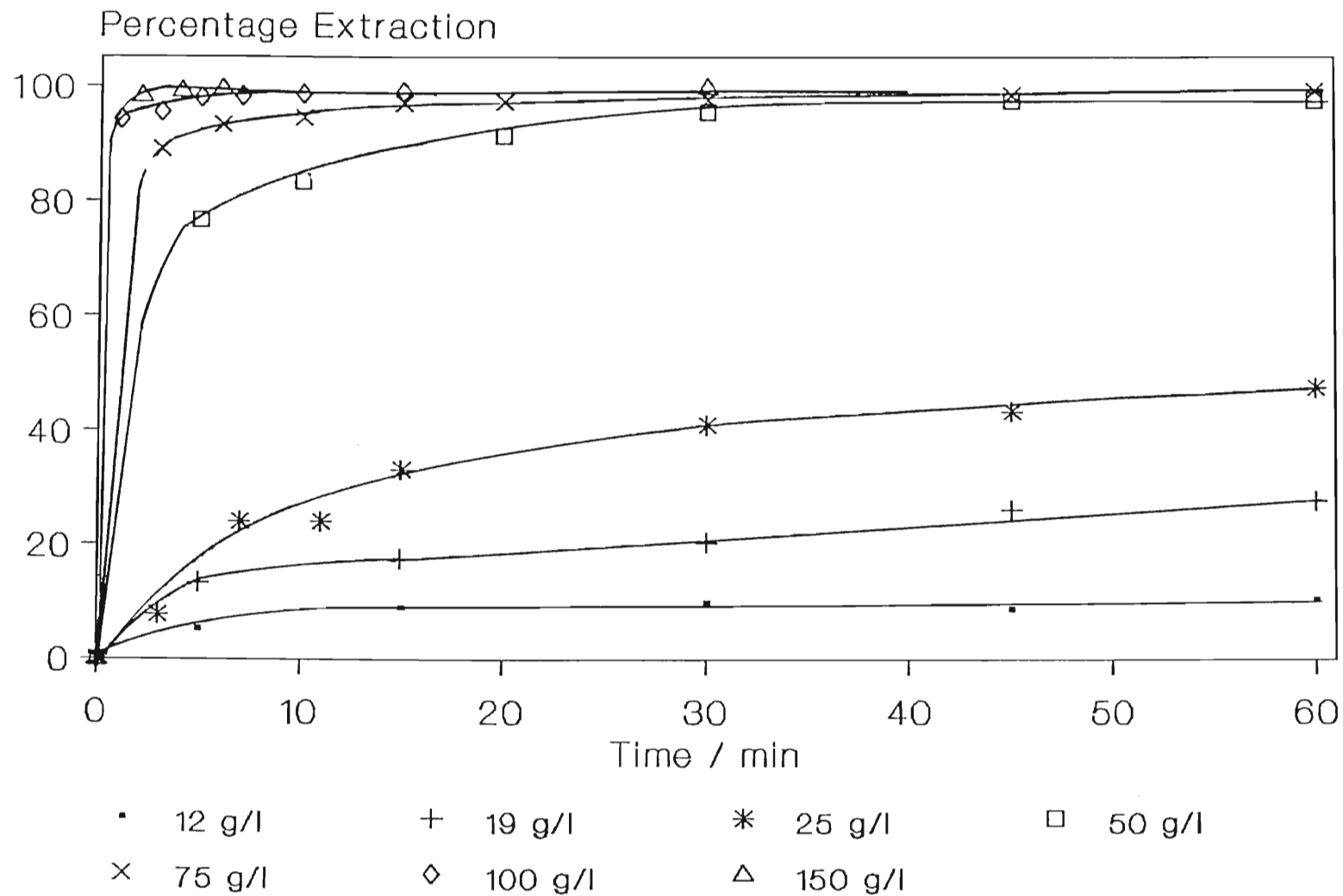
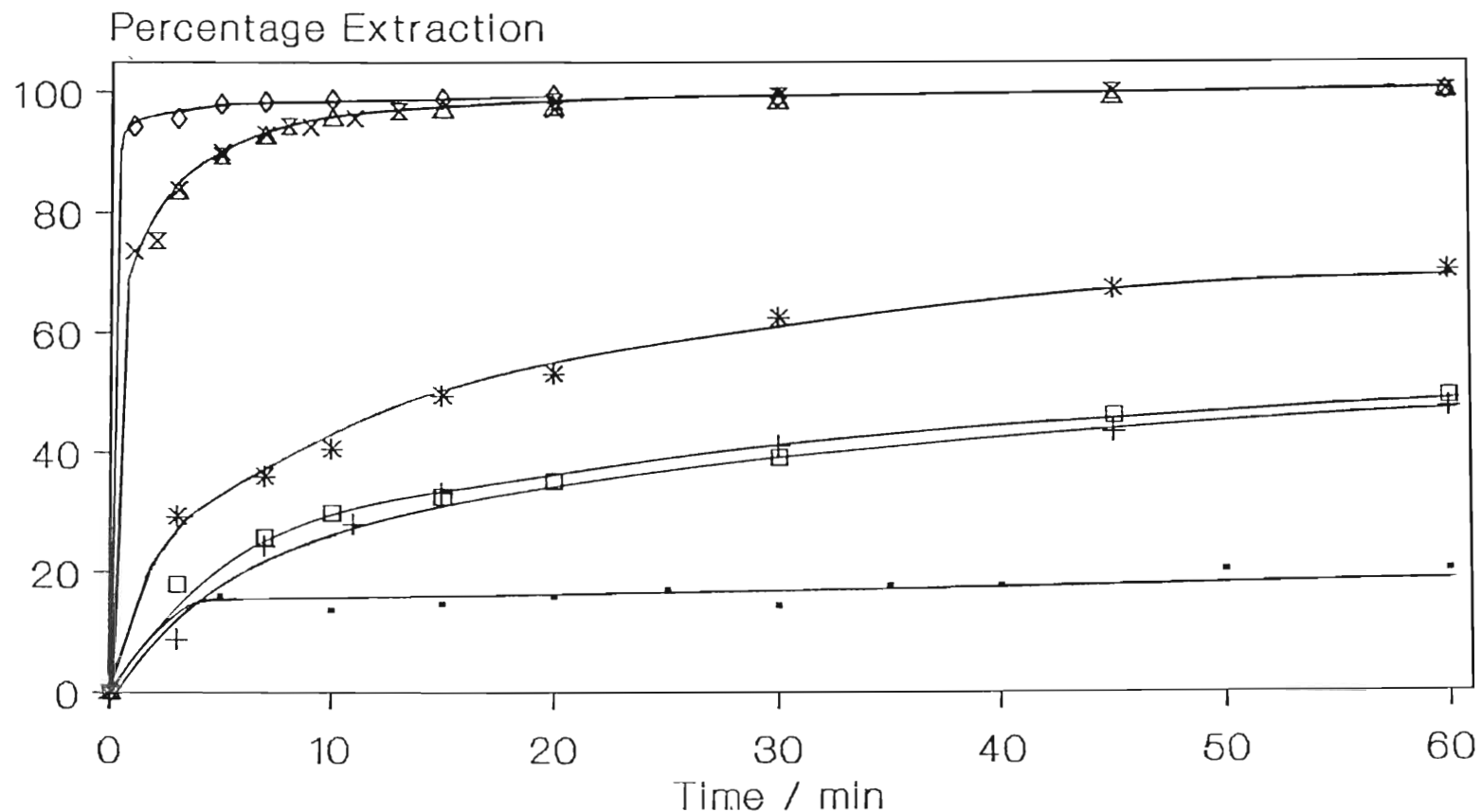


Figure (50). Percentage germanium extraction versus time for TN 01787 solutions of varying concentration. Vigorous shaking, conditions as for Figure (48).



• Kelex 100	+ TN 01787	* TN 02181	□ Lix 26
× Kelex 100	◇ TN 01787	△ TN 02181	⊗ Lix 26

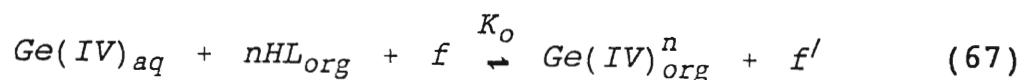
Figure (51). A comparison of the percentage germanium extraction as a function of time by TN 02181, TN 01787 and Lix 26 in a mechanical shaker at two ligand concentrations. The lower curves represent 25 g/l solutions of reagent in toluene whilst the upper curves show the extraction characteristics of 100 g/l solutions. Aqueous phases were ~ 0,65 g/l germanium in 1,5 M H₂SO₄.

equivalent in behaviour while TN 02181 is β -unsaturated and by far the most efficient of the reagents. Correlations between molecular structure, physical size and area and the extraction efficiencies noted in this section are discussed in Section 3.13, where three-dimensional representations of the structures of the energy-minimized ligands are presented.

The second important use of equilibrium data is the determination of the stoichiometry of the extracted metal/ligand complex. If it is assumed that the reactions of ligand, represented in this discussion as HL, with germanium (IV) results in the formation of only one compound $\text{Ge(IV)}^n_{\text{org}}$, then the total concentration of germanium in the organic phase at equilibrium is expressed by $[\text{Ge(IV)}^n_{\text{org}}]$ which represents the organic germanium (IV) species which contains n molecules of ligand per atom of metal. Since the organic phase is the phase into which solute passes, the distribution coefficient, D is merely:

$$D = \frac{[\text{Ge(IV)}^n_{\text{org}}]}{[\text{Ge(IV)}_{\text{aq}}]} \quad (66)$$

The reaction of ligand with germanium (IV) can be written in general as follows:



where f and f' are any species such as H^+ , H_2O , OH^- etc. required to complete the reaction but not additional germanium or ligand species. The equilibrium constant for Equation (67) can thus be written:

$$K_o = \frac{[Ge(IV)_{org}^n][f']}{[Ge(IV)_{aq}][HL]_{org}^n[f]} \quad (68)$$

and inserting (66) into (68) gives:

$$K_o = D \frac{[f']}{[HL]_{org}^n[f]} \quad (69)$$

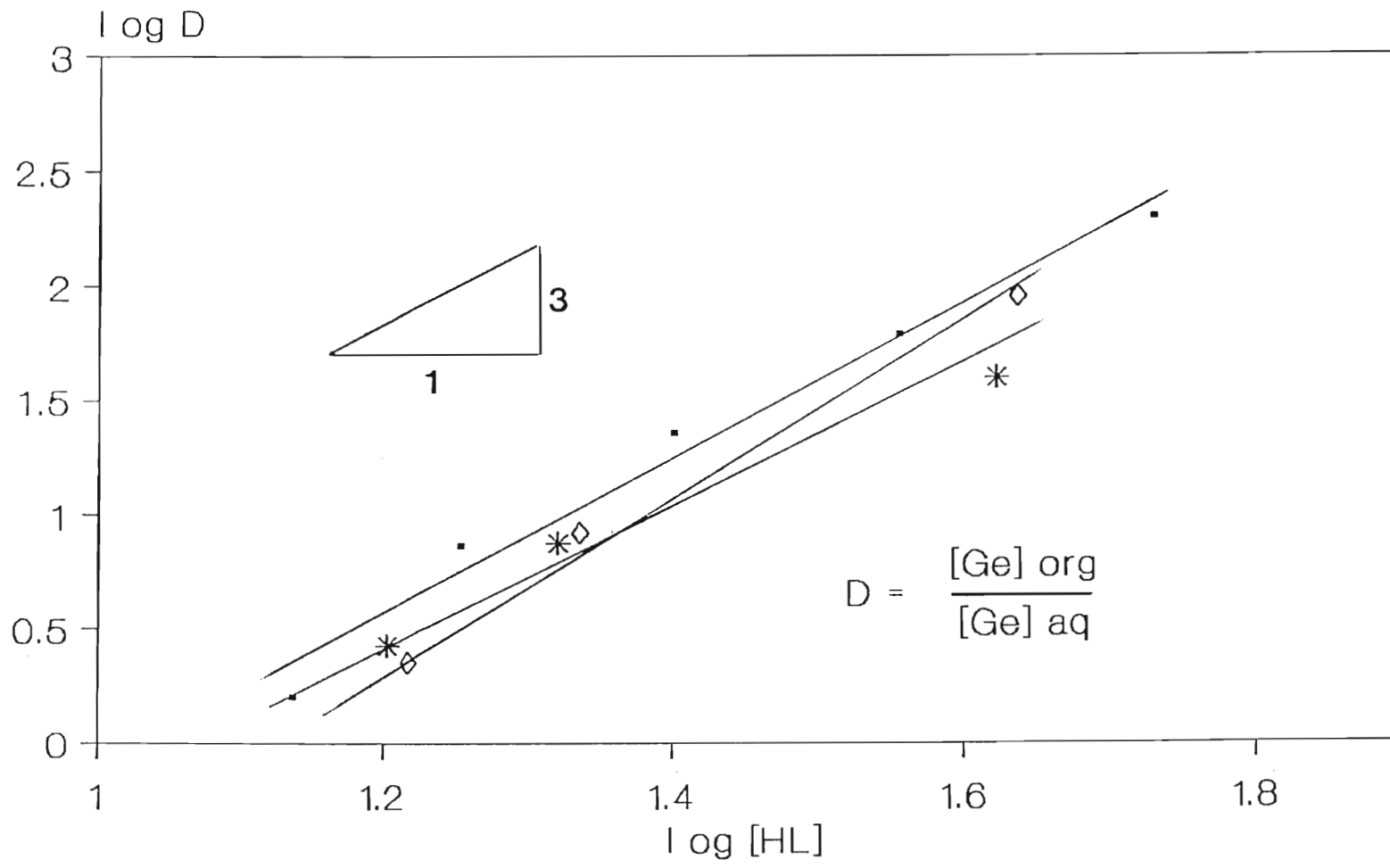
from which the following relation can be deduced:

$$\log D = \log K_o + n \log [HL]_{org} + \log f - \log f' \quad (70)$$

The relation shows that the slope of a plot of $\log D$ versus $[HL]_{org}$ is linear when the other experimental conditions i.e. f and f' remain constant. The importance of this statement will be made clearer in Section 3.4 since at high pH (i.e. $pH > 2$), two metal/ligand species (GeL_3^+ and GeL_2^{2+}) co-extract.

Examination of Equation (70) shows that the slope of the linear plot gives n , the number of ligand molecules complexed with germanium.

Figure (52) shows a family of $\log D$ vs $\log [HL]$ plots for the three extractants relevant to this work under the stated conditions. Least squares slopes of 2,98, 2,72 and 3,47 are indicated for Lix 26, TN 02181 and TN 01787 respectively. It follows therefore, that at this pH ($\sim -0,21$), the value of n



▪ Lix 26 ◇ TN 01787 * TN 02181

Figure (52). Log D versus log[HL] for Lix 26, TN 02181 and TN 01787 at low ligand concentration (< 50 g/l reagent). Aqueous phases : ~ 0,65 g/l Ge in 1,5 M H₂SO₄ ; Organic phases all made up in AR toluene. D is defined on the figure.

in Equation (70) is three and therefore germanium extracts as GeL_3^+ into the organic diluent and that since the diluent used in this work is toluene which is a non-dissociating solvent, the extractable complex must carry with it an appropriate counterion:- in this instance HSO_4^- is the most likely candidate. It must be noted that as $[\text{Ge}]_{\text{org}}$ tends towards $[\text{Ge}]_{\text{aq}}$ which occurs as 100% extraction at equilibrium is approached, then D in Equation (66) becomes very sensitive to small changes in the $[\text{Ge}]_{\text{org}}$ and therefore to the data set. This reasoning is offered as an explanation for the relatively high value of 3,47 calculated for TN 01787.

3.2.1.6. The Magnitude of the Observed Reverse Rate Constants for Germanium Extraction by Lix 26, TN 02181 and TN 01787.

The observed rate constant for the reverse reaction in the rate-determining step for germanium extraction, $k_b(\text{obs})$ (Equation (47)), which is reproduced below,

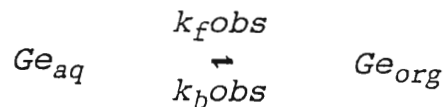
$$k_b t = \frac{a_e}{a_o} \ln \frac{a_o - a_e}{a_t - a_e}$$

can be calculated graphically via plots of the function on the right-hand-side against time. Inspection of this equation reveals that the observed reverse rate increases with time as the concentration of the products formed from the forward rate accumulate, but that this rate is negligible compared with the forward rate when $a_e \rightarrow 0$. Conversely, if extraction is slow,

as at low concentration, the reverse rate becomes increasingly significant. In order to determine the maximum concentration at which the reverse rate becomes significant, and thenceforth retards the observed extraction process, values of the reverse rate constant were calculated for the Lix 26 data for which the observed forward rate constants were summarised in Table (28). Values of $k_f(\text{obs})$ and $k_b(\text{obs})$ for $[\text{Lix 26}] \leq 35,0 \text{ g/l}$ (for $[\text{Lix 26}] > 35,0 \text{ g/l}$ values of $k_b(\text{obs})$ are $< 1 \times 10^{-7} \text{ s}^{-1}$ and therefore negligible compared with the forward observed rate constant), are compared in Table (29) below.

[Lix 26] /(g/l)	$k_f(\text{obs}) / \text{s}^{-1}$	$k_b(\text{obs}) / \text{s}^{-1}$	$\frac{k_f(\text{obs})}{k_b(\text{obs})}$
35,0	$2,51 \times 10^{-4}$	$5,33 \times 10^{-6}$	47,1
25,0	$1,62 \times 10^{-4}$	$2,26 \times 10^{-5}$	7,2
19,0	$4,66 \times 10^{-5}$	$1,88 \times 10^{-5}$	2,5
12,5	$3,29 \times 10^{-6}$	$1,67 \times 10^{-6}$	2,0

Table (29). Values of $k_b(\text{obs})$ and the ratio $k_f(\text{obs})/k_b(\text{obs})$ for the process:



Aqueous phase: $\sim 0,62 \text{ g/l Ge}$ in $1,5 \text{ M H}_2\text{SO}_4$; Organic phase :
Lix 26 in toluene (g/l).

Calculated values of $k_f(\text{obs})/k_b(\text{obs})$ for TN 02181 varied from 2,4-66,0 while those of TN 01787 ranged from 4,0-50,3 over the same set of conditions summarised in Table(29). It has been suggested (Section 3.2.1.3), that at low ligand concentration ($< 19,0$ g/l), deviations from kinetic linearity with respect to ligand are attributable to insufficient available ligand, however it is also apparent from the data presented here that at these low concentrations, the reverse rate may contribute significantly to the observed deviation. It is noteworthy that for TN 01787, which does not deviate from linearity (Figures (45) and (46)) at low ligand concentration, the ratio $k_f(\text{obs})/k_b(\text{obs})$ for a 12,5 g/l solution is significantly higher (4,0) than the values for Lix 26 (2,0) and TN 02181 (2,4) which do give an observed deviation.

3.2.1.7. The Lack of Correlation Between the Data Obtained from the Lewis Cell and the Shaking Apparatus

In Chapter 1 and in Section 3.1.3, the controversial aspects of the approaches by which investigators of solvent extraction processes have attempted to determine the site of the rate determining step was introduced. A key problem area for extraction mechanism investigations lies in the nature of the experimental configuration utilised by various workers. Although this work is not a criticism of either the static (Lewis Cell apparatus) or turbulent experimental techniques, it is apparent that some inconsistencies arise by using them alone. For instance, the shaking apparatus predicts that at low ligand concentration ($\leq 50,0$ g/l) the order of ligand efficiency is:

TN 01787 < Lix 26 < TN 02181

whilst the Lewis Cell data suggests the following order:

TN 01787 < TN 02181 < Lix 26

In discussing these apparently anomalous results it must be emphasized that Lewis Cell and shaking apparatus data are complementary rather than being directly comparable. In the former, the cell is designed with fixed interfacial area and therefore, inherent in the design, is the tacit assumption that the reaction is either diffusion or interfacially-controlled. Unfortunately however, the design does not reveal the features of extraction which become apparent during vigorous mixing. For instance, there is very little comparison between a static interface and a system which is designed to maximize mass transfer via maximum surface area contact between ligand-containing organic phase and metal-containing aqueous phase. Also, vigorously stirred systems are generally not amenable to interfacial studies but interfacial tension data reveal (Figure (53)) that the order of interfacial activity for the three reagents follows the order given above for the Lewis Cell. Figure (54) compares the percentage extraction data obtained by the shaking apparatus (upper curve) with that for the Lewis Cell for the conditions given. The plot illustrates the differences between the data obtained from these two assemblies. The static system is characterised by slow approach to equilibrium and an initial rate which cannot be directly compared with that observed for high speed mixing. The shaking apparatus establishes favourable conditions for maximum surface area contact between aqueous phase and organic phase. Additionally, mass transfer coefficients are forced to the limit diffusion will allow, whereas it has been suggested⁽¹⁸⁵⁾ that the conditions which apply to investigations with a Lewis Cell are such that it is

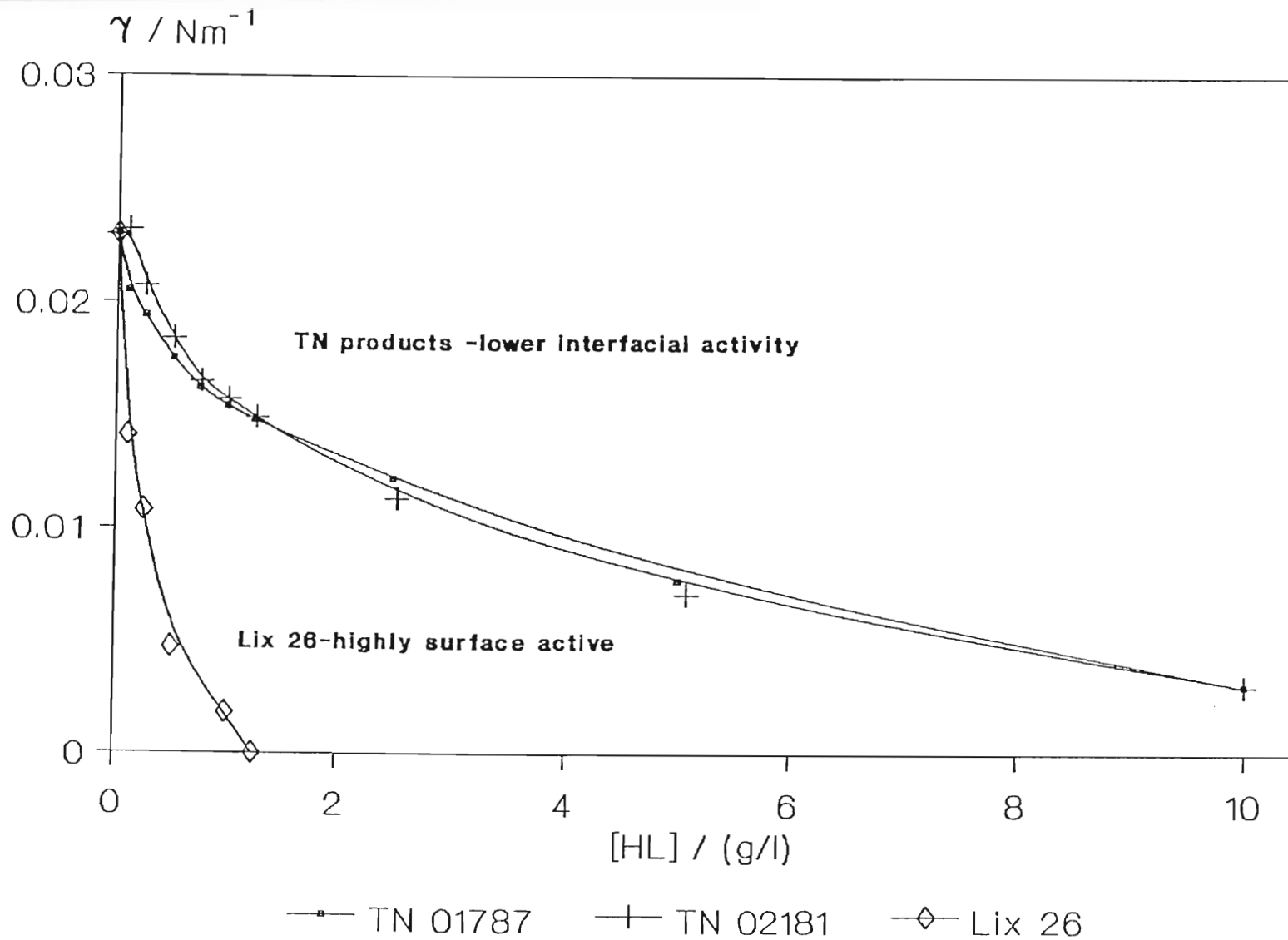


Figure (53). Interfacial tension, γ , as a function of $[\text{HL}]$ for Lix 26, TN 02181 and TN 01787. Data were obtained with a du Noüy ring tensiometer in a dish of diameter 5,5 cm (Area = 23,8 cm^2) and a 4 cm circumference platinum ring. Aqueous phases : 1,5 M H_2SO_4 ; Organic phases : extractant in AR toluene.

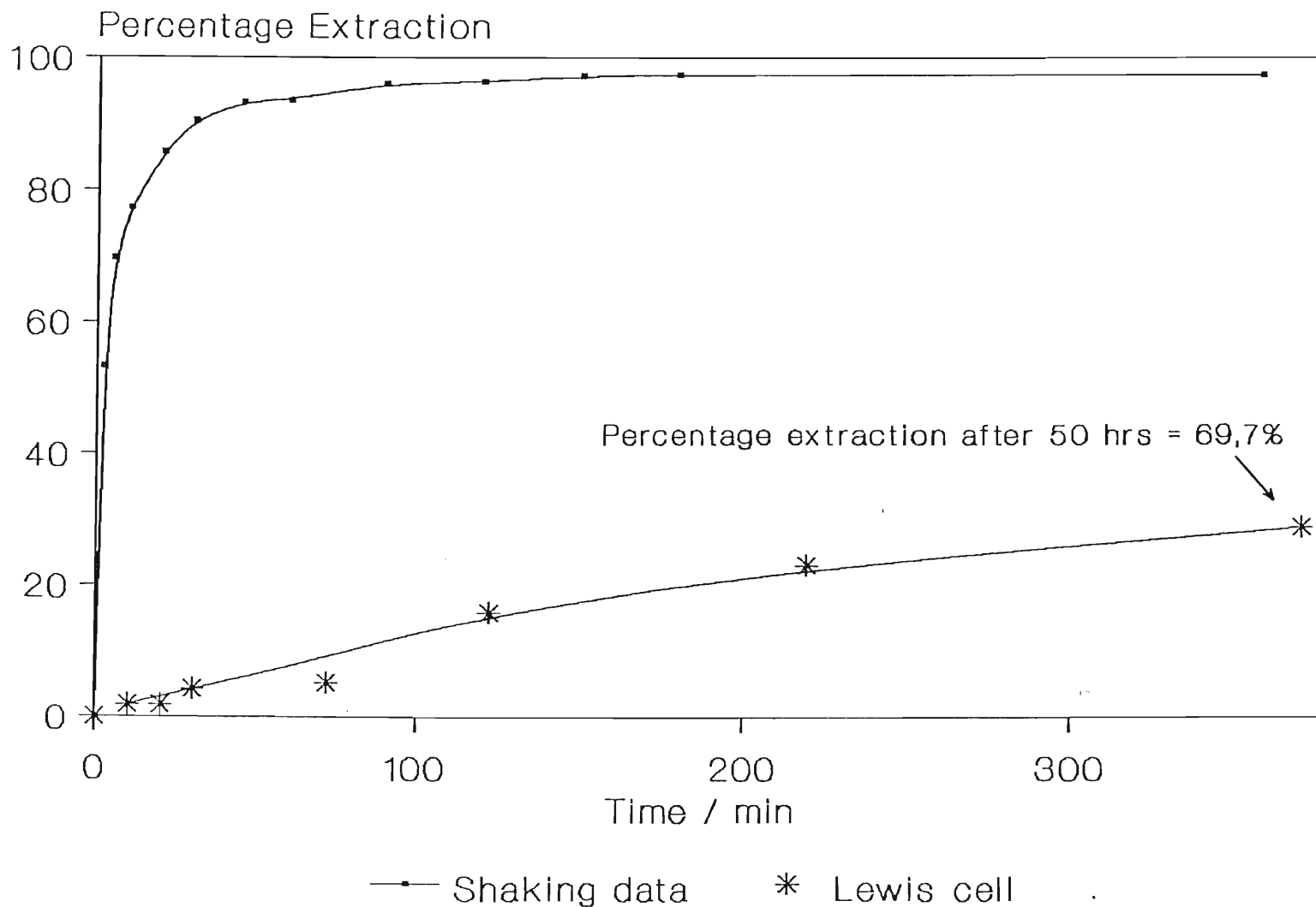


Figure (54). Comparison of the rates of extraction using the Lewis cell or vigorous shaking by Lix 26. Conditions : [Ge] : ~ 0,65 g/l in 1,5 M H₂SO₄, [Lix 26] : 75 g/l in AR toluene. Phase volumes 630:550 a:o for Lewis Cell, 100:100 a:o for shaking.

unlikely that diffusion effects can be totally disregarded.

Moreover, a number of recent investigations⁽¹⁸⁶⁻¹⁸⁹⁾ suggest that microemulsification occurs in vigorously stirred/mixed systems and under these circumstances the characteristics of static interfaces no longer apply. After prolonged agitation, it was noted that TN 01787 formed a stable emulsion indicating a tendency towards microheterogeneity: Kelex 100 has been observed to exhibit a similar proclivity⁽¹⁵⁵⁾ and it is therefore likely that Lix 26 and TN 02181 are analogous. It is well known that the rate of metal ion extraction is considerably improved in the presence of tensioactive agents^(53,190-193) (modifiers) although the mechanism of this improvement in efficiency still requires elucidation. Studies with a number of short and long chain aliphatic and aromatic alcohols in this work (Section 3.7), illustrate this effect and it is proposed that their ability to improve kinetics is associated with solubilizing the microheterogeneous amphiphilic extractant/toluene/water system into an isotropic dispersion in which the rate-determining-step is no longer strictly interfacial. The propensity with which these reagents exhibit this behaviour is related to their mutual solubility in the aqueous and organic phases. It is proposed therefore that a degree of microemulsification exists when the ligand-containing organic phases of interest in this work are agitated at fast enough rates to induce emulsion formation and that the extractive properties of the resulting microemulsion alter the observed extraction characteristics.

Although it is impossible to directly measure droplet sizes whilst the phases are intimately in contact with one another in a shaking apparatus such as the one used in this work (the Microporous Teflon Phase Separator^(77,78) mentioned in Chapter 1 is not limited in this respect), an estimation of the total interfacial area in the shaker and hence the average droplet size can be made from the Lewis Cell data presented in Section 3.1.2. It was shown that with all other experimental variables held constant ([Lix 26] = 75,0 g/l, aqueous phase = 0,65 g/l Ge in 1,5 M H₂SO₄, stirrer Speed = 80 rpm), the observed rate constant for germanium extraction was linearly related to the interfacial area according to Equation (71):

$$k_{obs} = (1,6 \times 10^{-7}A + 1,2 \times 10^{-6})s^{-1} \quad (71)$$

(A in cm²)

Equation (71) predicts, for example, that for the observed rate constant of $3,97 \times 10^{-5} \text{ s}^{-1}$ calculated for Lewis Cell data at a stirring speed of 120 rpm (Table (24)), where interfacial turbulence was experimentally observed, the interfacial area increases from 103,9 cm² for quasi-static conditions, to 240,0 cm². If it is assumed that Equation (71) applies to shaking data (obtained with the same ligand and metal ion concentrations, and similar phase ratio but different absolute phase volumes), then the observed rate constant of germanium extraction of $1,79 \times 10^{-3} \text{ s}^{-1}$ by 75,0 g/l Lix 26 in the shaking apparatus, suggests an interfacial area of 10618 cm²- a 102-fold increase in interfacial area compared with the Lewis Cell. Furthermore, if the 100 ml of ligand-containing organic phase comprises *n* spherical droplets with surface area $4\pi r^2$, then the total geometrical surface area available to ligand is

$n(4\pi r^2) = 10618 \text{ cm}^2$. Also $4/3n\pi r^3 = 100 \text{ cm}^3$ (the total organic volume), hence solving simultaneously, $r = 2,83 \times 10^{-2} \text{ cm}$ and $d = 5,65 \times 10^{-4} \text{ m}$:- the diameter of a single droplet in the shaker (assuming all droplets have the same diameter).

Droplets of this diameter are typical of 'fine dispersions',⁽¹⁹⁴⁾ and border on the diameter of droplets classified as emulsions ($0,1 \times 10^{-6} - 1 \times 10^{-5} \text{ m}$ ^(194,195)). The suggestions made above therefore regarding emulsion-forming tendencies are well founded.

The suppositions which have been made above do not negate previous discussion regarding the nature of the rate determining step: it is proposed, purely on stereochemical grounds that the formation of the triligand chelate GeL_3^+ at the interface is rate limiting, but that the ligand (and intermediate species) in a vigorously stirred system is not merely close to the interface but chemically adsorbed into it. A similar distinction between 'interfacial' and 'adsorbed' ligand has been made by Zhou⁽¹⁶⁴⁾ and coworkers from their studies of copper extraction by Lix 65N HS in which the rate-determining step is also interfacial.

The most significant result which is manifest by the Lewis Cell data in this work is the elucidation of the site of the rate determining step. In concurrence with the current body of opinion which supports interaction at the phase boundary for Kelex 100,^(57,62,127,196) this work proposes an interfacial-reaction rate-determining step for the structurally related ligands Lix 26, TN 02181 and TN 01787.

In Section 2.2.1, the identities of several impurities which are known to occur in 7-alkyl-8-hydroxyquinoline extractants were given. Present understanding relating to these impurities suggests that little is known of their effect upon extraction processes, however much has been published concerning the reactions of 8-hydroxyquinoline with metal ions. The section following details the results of a study undertaken to establish the effect, if any, of 8-hydroxyquinoline impurities upon germanium extraction.

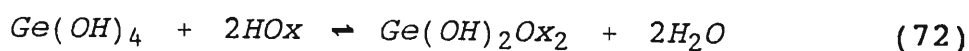
3.3. The Influence of 8-Hydroxyquinoline on the Extraction of Germanium by 7-Alkylated Derivatives.

Solvent extraction of metal ions in aqueous solution by 8-hydroxyquinoline (also referred to as 8-quinolinol and oxine and abbreviated as HOx in this discussion), has been used by analytical chemists for a number of years⁽¹⁹⁷⁾. A comprehensive study of the extraction of metal oxinates has been reported by Stary⁽¹⁹⁸⁾ who has summarised values of extraction constants, pH values for 50% extraction and stoichiometries of the extracted species for 32 metals.

Common to all of the studies which have been reported in the literature is the influence of pH upon the kinetics of complex formation and the stoichiometry of the species' formed. The pK values at 25°C and 0,1 M ionic strength for 8-hydroxyquinoline of 9,66 and 4,99⁽⁹⁰⁾, suggest that at pH > 9,66 the oxine exists predominantly as the deprotonated anion (Ox⁻), whereas at pH < 4,99 the tertiary amine group is protonated and the species H₂Ox⁺ predominates. For solutions of oxine in

chloroform, Stary⁽¹⁹⁰⁾ showed that between pH 4-11, the equilibrium concentration of oxine in the organic phase in contact with aqueous solution of varying pH, was practically equal to the initial concentration of oxine added, whereas outside these pH limits, solubility increased rapidly. Consequently, workers have been careful in selecting the pH conditions of the aqueous phase to favour first a particular form, i.e. H_2Ox^+ , HOx or Ox^- of the oxine and second a particular aqueous species of the metal ion:- complexation studies for example with Zn^{2+} could not be carried out at $pH > 7,5$ because $Zn(OH)_2$ begins to precipitate. Thus for example Turnqvist *et al.*⁽¹⁹⁹⁾ and Ki *et al.*⁽²⁰⁰⁾ determined values of formation constants between Fe^{3+} and oxine at $pH < 3,85$. Fleming and Nicol⁽¹²⁷⁾ determined the rate of extraction of Cu^{2+} into toluene and chloroform solutions of 8-hydroxyquinoline and showed that for $pH \leq 2$, extraction rates were negative second order in $[H^+]$ (demonstrating that Cu^{2+} complexes 2 ligand molecules). Ōki and Terada⁽²⁰¹⁾ determined the composition of nickel oxine complexes extracted into chloroform in the pH range 3,20-9,10.

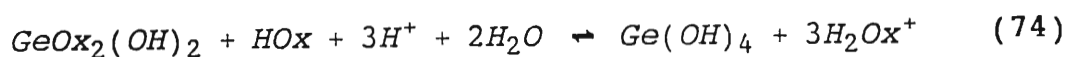
For germanium, the formation constant for the equilibrium:



HOx : 8-hydroxyquinoline

has been determined by Tsau *et al.*⁽²⁰²⁾ to be $10^{(6,89 \pm 0,05)}$. The value was obtained spectrophotometrically at a pH of 4,12 and indicates the high stability of the complex formed. Marchon *et al.*⁽⁶⁵⁾ have shown that the complexation reaction above (Equation 72) and further the formation of $GeOx_3^+$

(Equation (73) below :- this species, like the 7-alkylated-8-hydroxyquinoline reagents extracts with the acid counterion e.g. HSO_4^-), is in competition with the protonation reaction (Equation (74)) when $\text{pH} < 3-5$. Protonation destroys the germanium complex $\text{Ge}(\text{OH})_2\text{Ox}_2$ and hence hinders the formation of GeOx_3^+ which, by virtue of its greater hydrophobic character, would extract into non-dissociating solvents at a faster rate than $\text{Ge}(\text{OH})_2\text{Ox}_2$.



These considerations may be of relevance to the study of the kinetics of the commercial extractants of concern to this work since the manufacturer's specification for the Schering products Kelex 100, TN 02181 and TN 01787 is that [8-hydroxyquinoline] $\leq 1,5\%$ by mass. For Lix 26, which is of lesser purity (72%), this figure has been estimated to be significantly higher (Semi-quantitative GC/MS, Section 2.2.2.3, suggests an oxine content of $\sim 3\%$). When contacted with aqueous solutions of low pH, it would be anticipated that all oxine present in the extractants would distribute to the aqueous phase as H_2Ox^+ . According to Equation (74) above, this species excludes the formation of extractable germanium-oxine species and is therefore an unlikely disruptive influence upon the extraction processes of the active ligand? To substantiate this supposition, the experiments detailed in Section 2.4.2.2.3 were performed and the results of these are presented in the section following.

3.3.1. The Distribution Coefficient of 8-Hydroxyquinoline Between Toluene and 1,5 M H₂SO₄

Since, for the majority of experiments conducted in this work, an aqueous phase containing 1,5 M H₂SO₄ was used, it seemed pertinent to examine the behaviour of free oxine in contact with an aqueous phase of this composition. The distribution coefficient for 8-hydroxyquinoline between toluene and acid-containing aqueous phase is defined by Equation (75):

$$K_D = \frac{[HOx]_{aq}}{[HOx]_{org}} \quad (75)$$

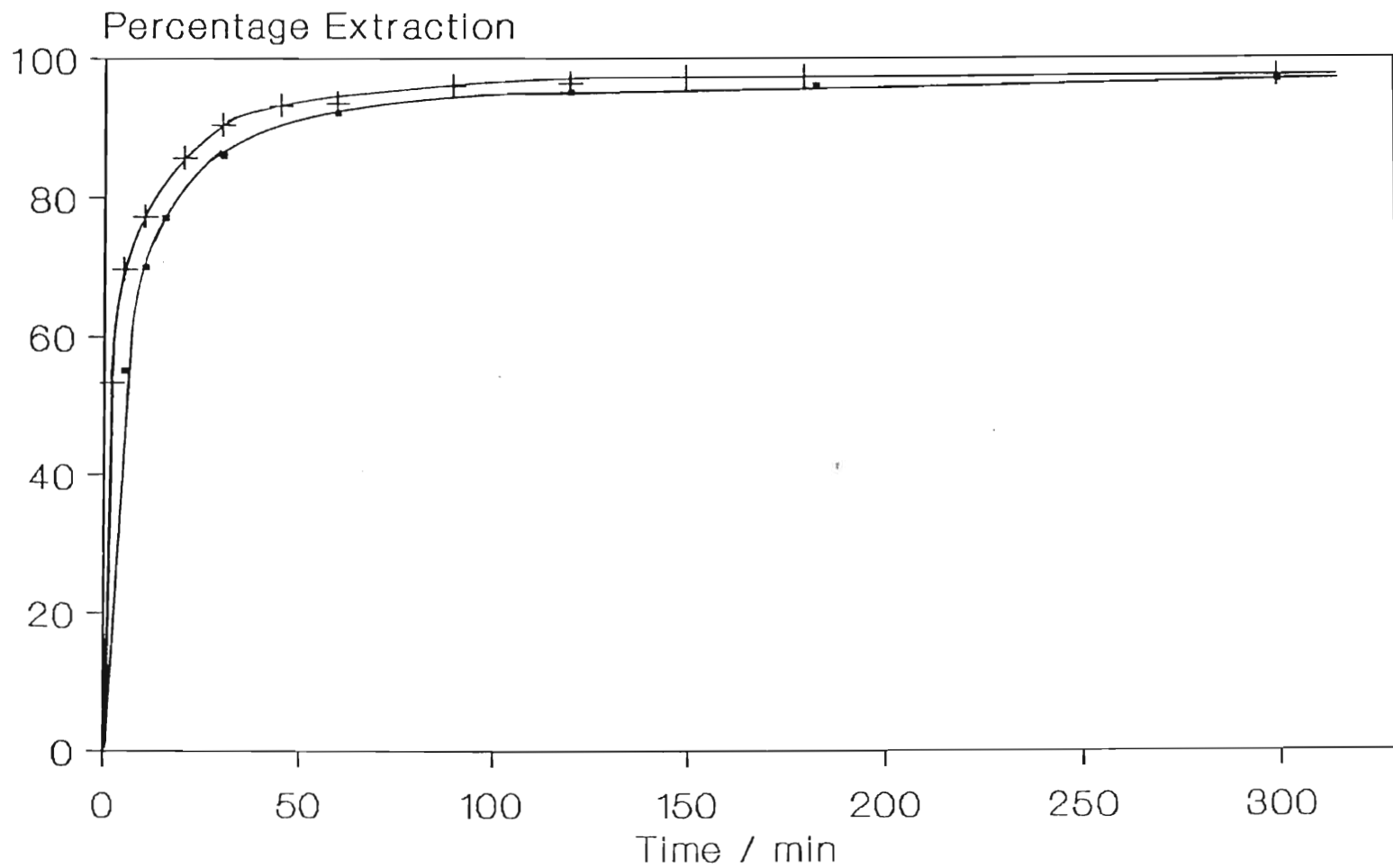
K_D was determined by dissolving a range of [oxine] in toluene ($6,9 \times 10^{-4}$ M - $2,07 \times 10^{-1}$ M, representing 0,1-30,0 g/l and therefore covering the maximum possible range in the unpurified extractants) and then determining the concentration in the aqueous phase by UV spectroscopy (ϵ_{360} (8-hydroxyquinoline) = $1,724 \times 10^3$ mol⁻¹ dm³ cm⁻¹ - determined in this work), following vigorous shaking for 12 hours. An average value of $K_D = 84,5 \pm 58,1$ over the range examined was obtained, implying that 98% or more of the oxine partitions to the aqueous phase at equilibrium.

3.3.2. The Effect of Free Oxine on the Rate of Germanium Extraction by Lix 26/toluene Solutions

The range of oxine concentration utilised for the determination of K_D in the previous section were also contacted with aqueous germanium-containing solutions and germanium concentration monitored with time. Within the limits

of detection of the phenylfluorone UV quantification technique (lower limit of detection approximately 0,001 g/l = 1 ppm Ge), no extraction of germanium from the acidic aqueous phase to the toluene was observed. Therefore it can be assumed that 8-hydroxyquinoline does not extract germanium from acidic solution into toluene. In addition, solutions of $\sim 0,20$ g/l Ge at pH 8,60 (at which pH 8-hydroxyquinoline would be neutral since $pK_a = 9,66^{(90)}$) and pH 11,10 (deprotonated 8-hydroxyquinoline) were contacted with a toluene solution of approximately 17,3 g/l 8-hydroxyquinoline. Similarly, within the limits of the quantification procedure no extraction was observed.

In order to ascertain whether free oxine has any effect upon the characteristics of germanium extraction by the alkylated reagents of interest, kinetic and equilibrium data were obtained for extraction experiments in which the organic phase contained a range of 1-30 g/l 8-hydroxyquinoline in addition to 50 g/l Lix 26. Although no effect was observed in the equilibrium percentage extraction (approximately 98%) for Lix 26, slight reductions in the rate of extraction in the initial reaction regime were discerned for $[\text{oxine}] \geq 20,0$ g/l (see Figure (55)). The retardation was of the same order for all three extractants of interest to this work. The cause of this effect is probably a combination of two effects: (i) the preferential occupation of the oxine at the aqueous/organic interface during protonation and partitioning, thereby reducing slightly the interfacial area available to the active extractants and (ii) the consumption of a proton in the protonation reaction which (Section 3.4.5) alters the aqueous phase speciation in a manner which is not favourable to



▪ Lix 26 and 30 g/l 8-hydroxyquinoline + Lix 26

Figure (55). The effect of 8-hydroxyquinoline on the kinetics and equilibrium percentage extraction of germanium. Aqueous phase : ~ 0,65 g/l Ge in 1,5 M H₂SO₄; Organic phase : 50 g/l Lix 26 in AR toluene. Phase volumes 100 ml. Vigorous shaking.

extraction. Albeit a small effect, this latter cannot be neglected as part of the overall reaction scheme.

In the section which follows, the effect of the aqueous phase pH on the rate of germanium extraction by the proprietary reagents of interest to this work is tackled.

3.4. The Influence of the Aqueous Phase pH on Germanium Extraction. Speciation Studies.

The experimental conditions chosen for the study of the influence of pH on germanium extraction kinetics were described in Section 2.4.2.2.2. In brief, buffer solutions as outlined in Table (19) were prepared for $\text{pH} \geq 0,25$ whereas sulphuric acid was utilised for values of pH below this value. For all experiments an organic phase containing 50 g/l reagent in toluene was employed. Phase volume ratios were 1:1 and sampling and quantitation of germanium were performed as previously described. The effect of pH upon the extraction kinetics of each of the ligands is first described separately, then comparisons and similarities in behaviour are described in Section 3.4.4.

3.4.1. Influence of Aqueous Phase pH on Germanium Extraction by Lix 26

Figure (56) summarises the effect of pH upon the kinetics and equilibrium percentage extraction of germanium by Lix 26 in the pH range -0,21 to 5,71. A number of important features are illustrated by this figure. First, the rate and percentage

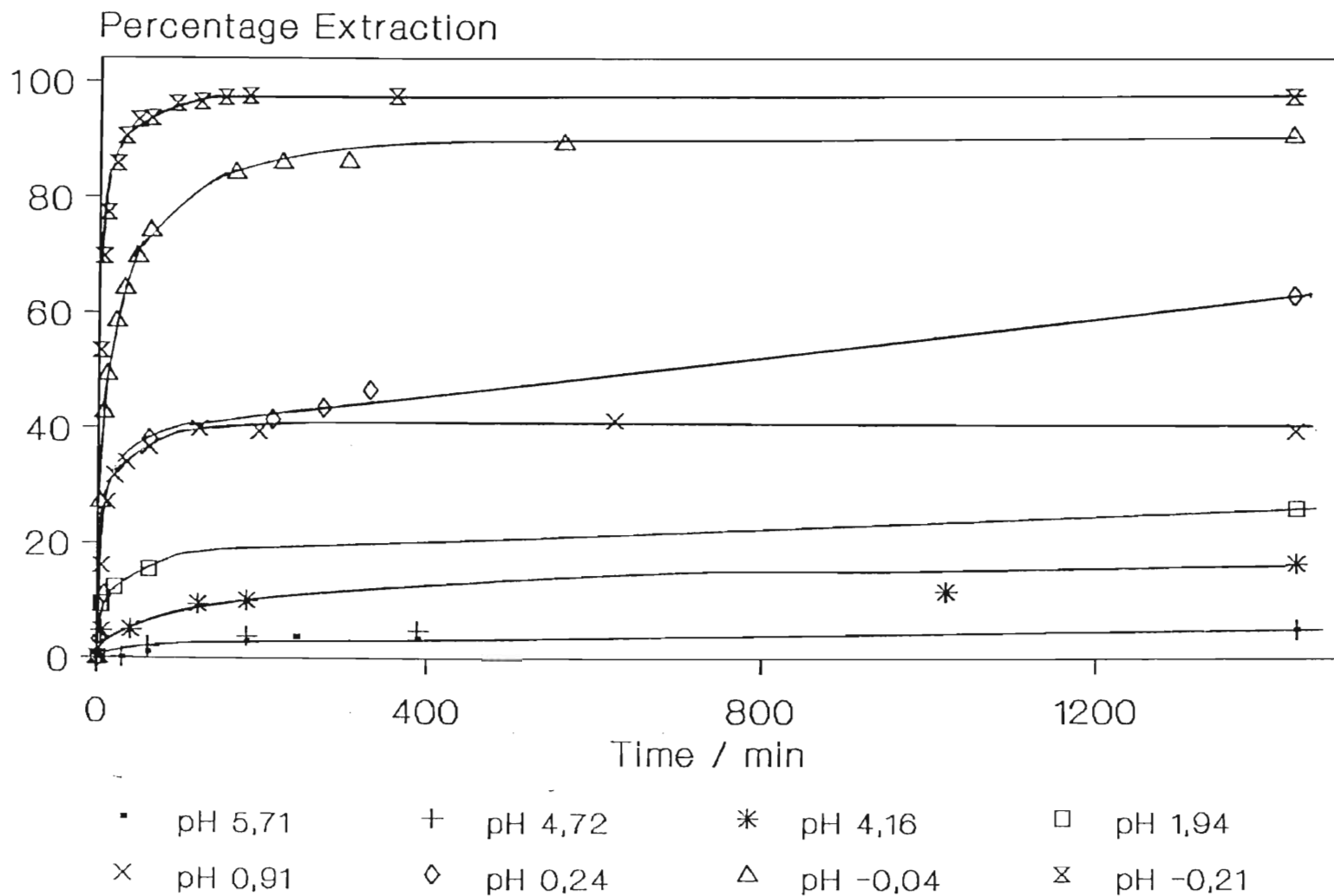


Figure (56). Percentage extraction as a function of pH for Lix 26. Aqueous phase : ~ 0,65 g/l Ge in solutions of varying pH (see Section 2.4.2.2.2 for the preparation of buffers for pH ≥ 1); Organic phase : 50 g/l Lix 26 in AR toluene.

extraction increase with decreasing pH and second, extraction is characterised by a fast initial regime (which becomes more prominent as the pH tends to zero), followed by a much slower kinetic regime. For $\text{pH} > 1$ the rate of extraction in both regions is significantly reduced, particularly in the initial region.

In order to examine these effects further, values of the observed forward rate constants, $k_f(\text{obs})$, were calculated from plots utilising Equation (46). Table (30) summarises the values of $k_f(\text{obs})$ and the initial rates, deduced from the gradients of $[\text{Ge}]_{\text{aq}}$ versus time plots in the initial linear region only, which were obtained. In all cases, best-fit straight lines to the data of the semi-logarithmic plots did not pass through the origin suggesting the existence of complex circumstances in the initial reaction region.

pH	Initial Rate /(g/l) s ⁻¹	log (Initial Rate)	$k_f(\text{obs})$ /s ⁻¹	log $k_f(\text{obs})$
-0,21	$2,70 \times 10^{-3}$	-2,57	$7,62 \times 10^{-4}$	-3,12
-0,043	$6,49 \times 10^{-4}$	-3,19	$4,34 \times 10^{-4}$	-3,36
0,24	$1,37 \times 10^{-4}$	-3,86	$2,08 \times 10^{-4}$	-3,68
0,91	$8,49 \times 10^{-5}$	-4,07	$1,90 \times 10^{-4}$	-3,72
1,94	$5,55 \times 10^{-5}$	-4,26	$5,67 \times 10^{-5}$	-4,25
4,16	$8,51 \times 10^{-6}$	-5,07	$1,15 \times 10^{-5}$	-4,94

pH	Initial Rate /(g/l) s ⁻¹	log (Initial Rate)	k _f (obs) /s ⁻¹	log k _f (obs)
4,72	3,33 x 10 ⁻⁶	-5,48	5,63 x 10 ⁻⁶	-5,25
5,71	2,78 x 10 ⁻⁶	-5,56	5,44 x 10 ⁻⁶	-5,26

Table (30). Initial extraction rates and observed forward rate constants for the slower first-order reaction regime for the extraction of ~ 0,65 g/l Ge at varying aqueous phase pH by a 50 g/l Lix 26/ toluene solution.

Figure (57) shows a plot of Initial rate versus pH, illustrating clearly the accelerated kinetics mentioned above for $\text{pH} \leq 0,24$ and the rapid decline thereafter. In Figure (58), the logarithms of these rates are plotted versus pH indicating two discrete regions, the first for $\text{pH} \leq 0,24$ in which the reaction possesses an inverse order of 2,83 with respect to H^+ and the second with an inverse order of 0,32 with respect to H^+ i.e. tending towards zeroth order behaviour in hydrogen-ion concentration. Figure (59) shows a plot of $\log k_{\text{obs}}$ versus pH in which the apparent reaction orders, calculated via least squares, are inverse 1,24 and 0,32 in these two regions. It is interesting to note that for $\text{pH} > 0,24$, the reaction order remains constant, indicating that the reaction(s) occurring initially and for the duration of germanium extraction possess the same dependence on $[\text{H}^+]$.

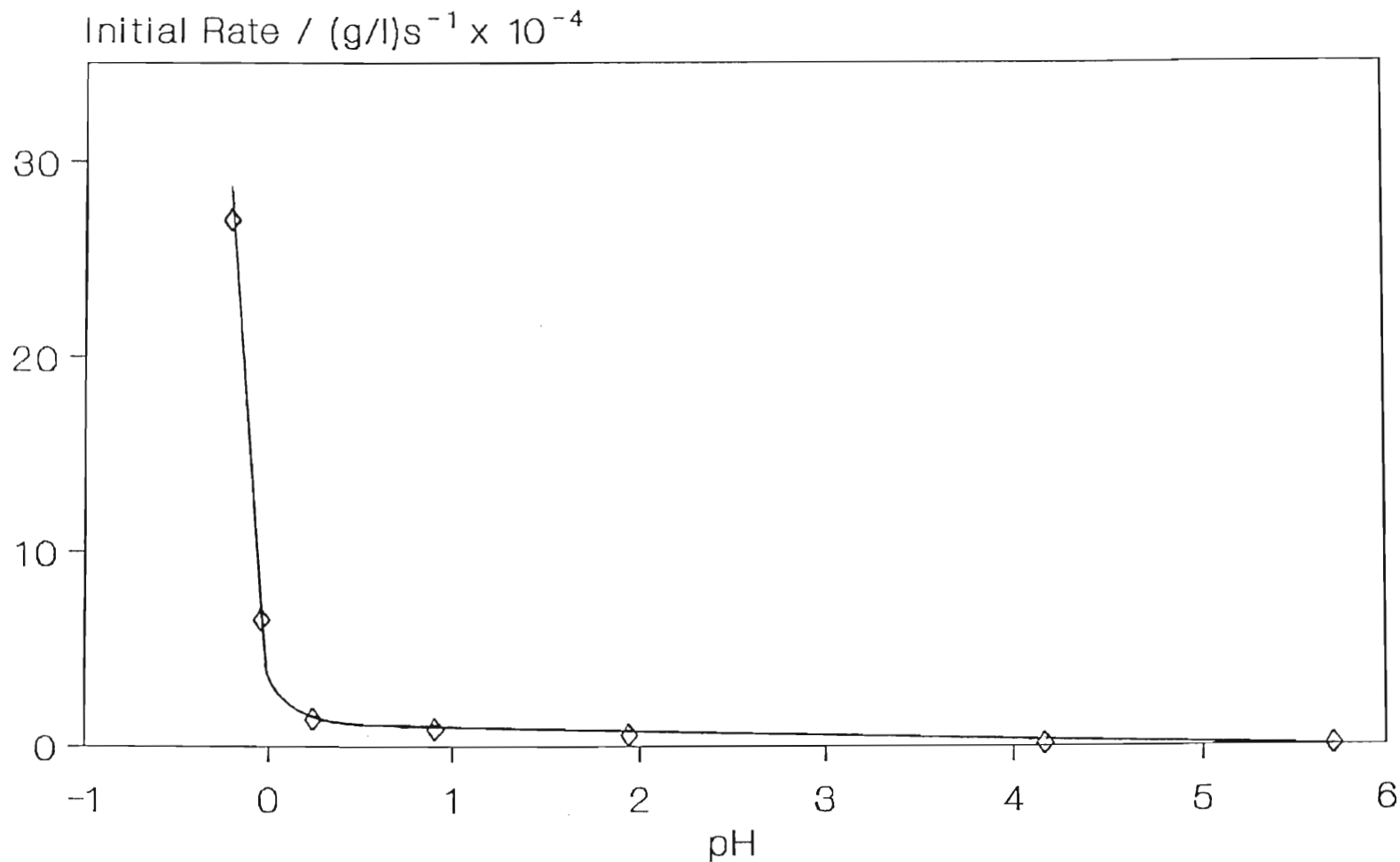


Figure (57). Initial rate of germanium extraction by Lix 26 as a function of aqueous phase pH in the mechanical shaker.

Organic phase : 50 g/l Lix 26 in AR toluene; Aqueous phase : ~ 0,65 g/l Ge at various pH's. Sulphuric acid was used for $\text{pH} \leq 0,24$ and buffers (Section 2.4.2.2.2) were used for $\text{pH}'\text{s} > 0,24$.

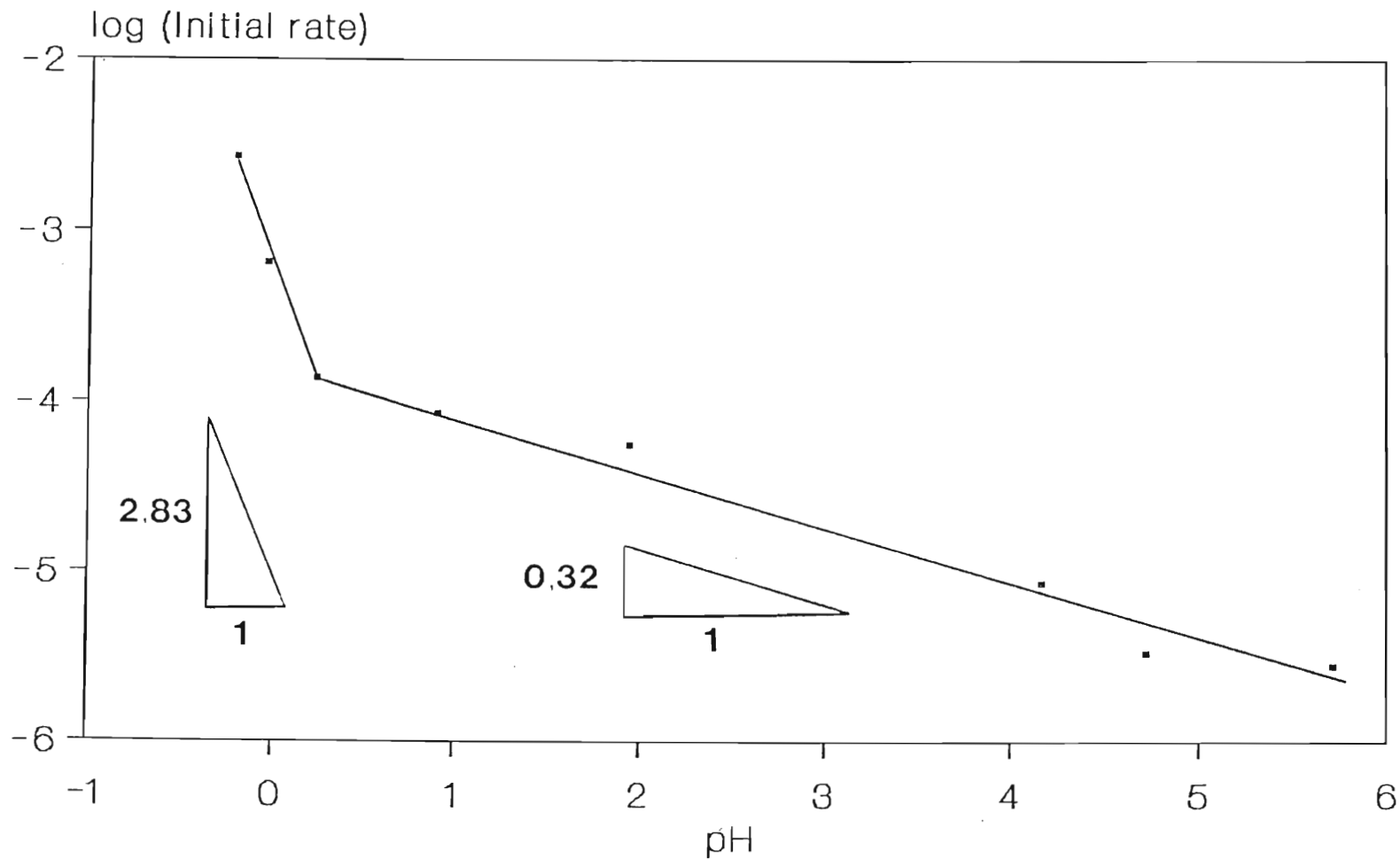


Figure (58). Log(Initial rate) of germanium extraction by Lix 26 as a function of pH under vigorous stirring conditions. Organic phase : 50 g/l Lix 26 in AR toluene; Aqueous phase : ~ 0,65 g/l Ge at various pH's (as for Figure (57)). The 'initial rate' applies over approximately the first 5 minutes of reaction at low pH (<1) and approximately 20 minutes for higher values of pH.

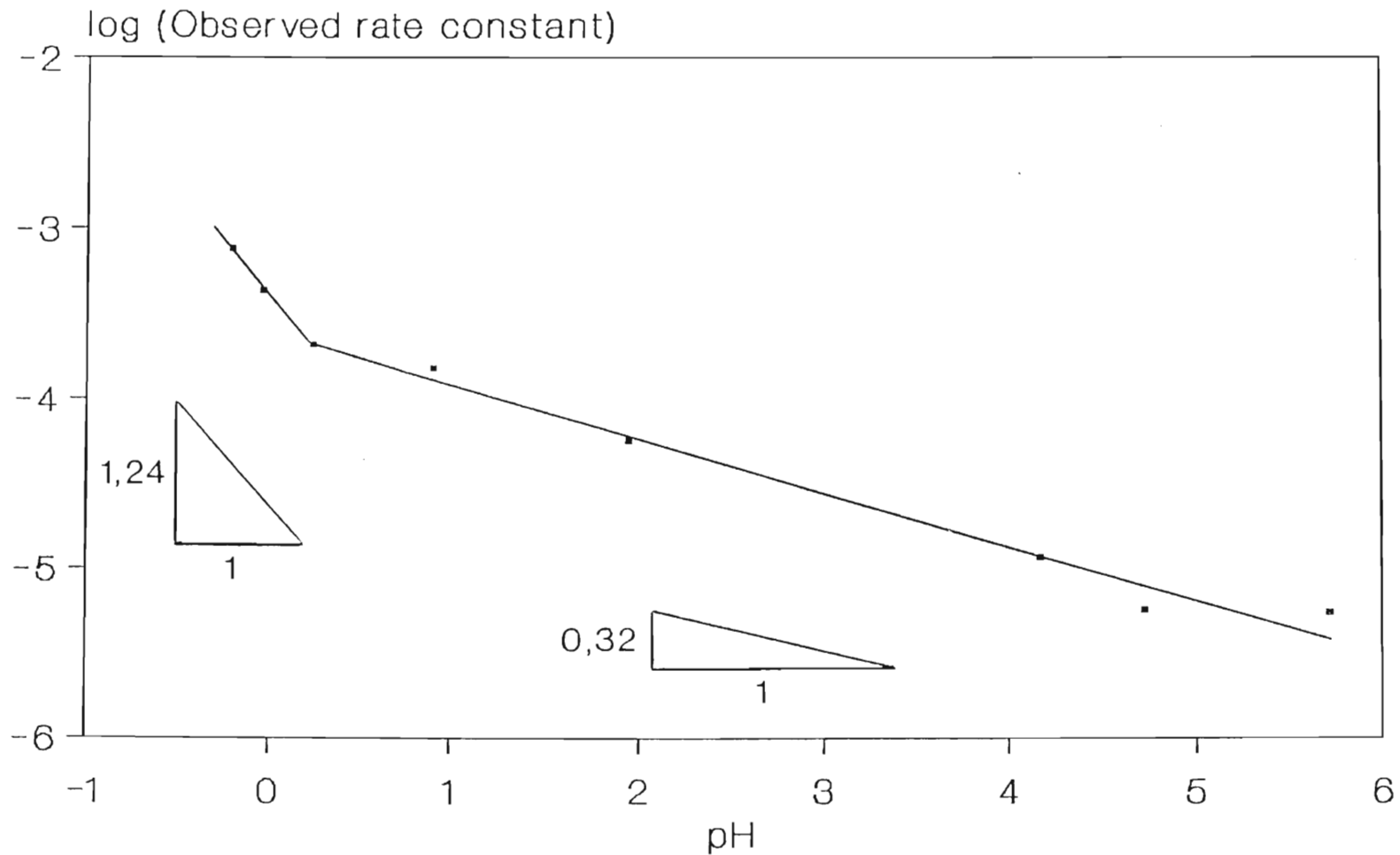
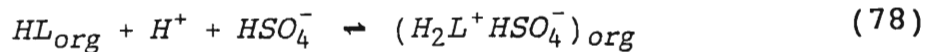
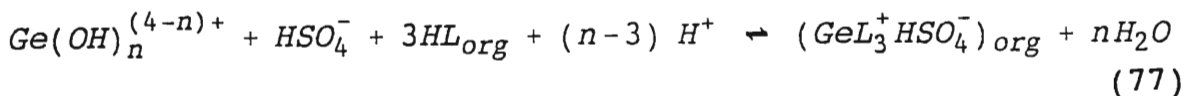
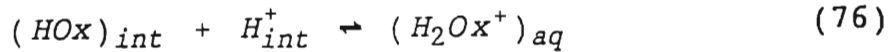


Figure (59). Log(Observed rate constant) for germanium extraction as a function of pH for Lix 26 under conditions of vigorous shaking. Organic phase : 50 g/l Lix 26 in AR toluene; Aqueous phase : ~ 0,65 g/l Ge at various pH's prepared according to the caption of Figure (57). The observed rate applies to the slower 'equilibrium' region which is referred to in the text.

There are three⁽⁶⁵⁾ possibilities for reactions occurring at the interface which consume hydrogen ions viz.



where : HOx = 8-hydroxyquinoline

L = Lix 26

Equation (76), represents the protonation of free oxine contained in the extractant to form a charged aqueous-soluble species (which has been shown to influence, to a marginal extent, the observed rate of germanium extraction if [oxine] > 2,0 g/l). Reaction of the species $Ge(OH)_4$ with ligand via Equation (77) where $n=4$, consumes one mole of H^+ per mole of $Ge(OH)_4$ (this equation is the overall representation of six equations which result in the formation of an extractable germanium species and is further discussed in Section 3.4.6). The reaction between the active ligand and H^+ represented by Equation (78), becomes important for $pH \sim 0$.

There are three equations which result in the net overall production of H^+ viz. Equation (77) where $n = 0, 1$ or 2 . These three equations represent the extraction of the germanium species Ge^{4+} , $Ge(OH)^{3+}$ and $Ge(OH)_2^{2+}$. In Section 3.4.6 it will

be shown that the observed rate at which Ge^{4+} is extracted from aqueous solution is proportional to $1/[\text{H}^+]^2$, whilst that for $\text{Ge}(\text{OH})^{3+}$ is proportional to $1/[\text{H}^+]$. $\text{Ge}(\text{OH})_2^{2+}$ and $\text{Ge}(\text{OH})_3^+$ do not have a term in $[\text{H}^+]$ in the rate equation. Since the total rate of germanium(IV) extraction is the sum of the rates at which each of the species in solution are extracted, then the total order with respect to $[\text{H}^+]$ has a maximum of inverse 2 - this cannot explain the observed order of 2,83 above.

Also in Section 3.4.6 a number of hypotheses are presented to explain the reason for the fast initial rate of germanium extraction which has been mentioned in previous sections. One of these hypotheses postulates that the rate of extraction of germanium is a function of the type of species present in aqueous solution, i.e. Ge^{4+} is proposed to extract faster than $\text{Ge}(\text{OH})^{3+}$ (which extracts faster than $\text{Ge}(\text{OH})_2^{2+}$ and so on). If this is the case, then it might be imagined that the order with respect to $[\text{H}^+]$ may vary with time from inverse 2 (if both Ge^{4+} and $\text{Ge}(\text{OH})^{3+}$ extract simultaneously) to 1 when only $\text{Ge}(\text{OH})^{3+}$ remains in solution. The non-integral values of 2,83 and 1,24 obtained above are an indication that some complex mixed-order kinetics occurs with respect to $[\text{H}^+]$ and this is an indication of the participation of all of the processes which are summarised by Equations (76) to (78) above. Of these three processes, Equation (77) is effective at all aqueous phase pH's $> -0,4$ (see Section 3.4.5), Equation (78) is effective for values of pH ~ 0 (and is therefore important over the range of pH for which the orders of reaction of 2,83 and 1,24 were determined) and Equation (76), which is probably the least important, has been shown (Section 3.3.2) to affect

the observed rate of germanium extraction only if the free oxine content of the reagent is $> 20,0$ g/l (i.e $> 2\%$ m/m).

It must be noted that on the plots of Figures (56)-(59), the data point at pH ~ 3 has been omitted. For this pH region, the most suitable aqueous buffers are either phthalate (see Table (19), buffer 4) or citrate systems. Both of these reagents are chelating ligands and thus actively complex metal ions. Hence pH 3 data was not obtained. The phthalate ion, for example, forms ML and ML₂ complexes with a number of metal ions e.g. Cu²⁺, Zn²⁺, Ga³⁺ and since the complex which would be formed with germanium would be hydrophobic i.e.

$C_6H_4(COO)_2 - Ge - (OOC)_2C_6H_4$, it is suggested that this buffer also extracts germanium. This was observed experimentally:- $\sim 72\%$ extraction was obtained at equilibrium from solutions buffered with phthalate, a result which deviates from the observed extraction trend apparent in this pH region. Similar results were obtained with the use of a citrate buffer. It is not suspected that the extraction behaviour in this pH region would deviate from the general decrease in extraction with increasing [OH⁻] which is discussed in this section.

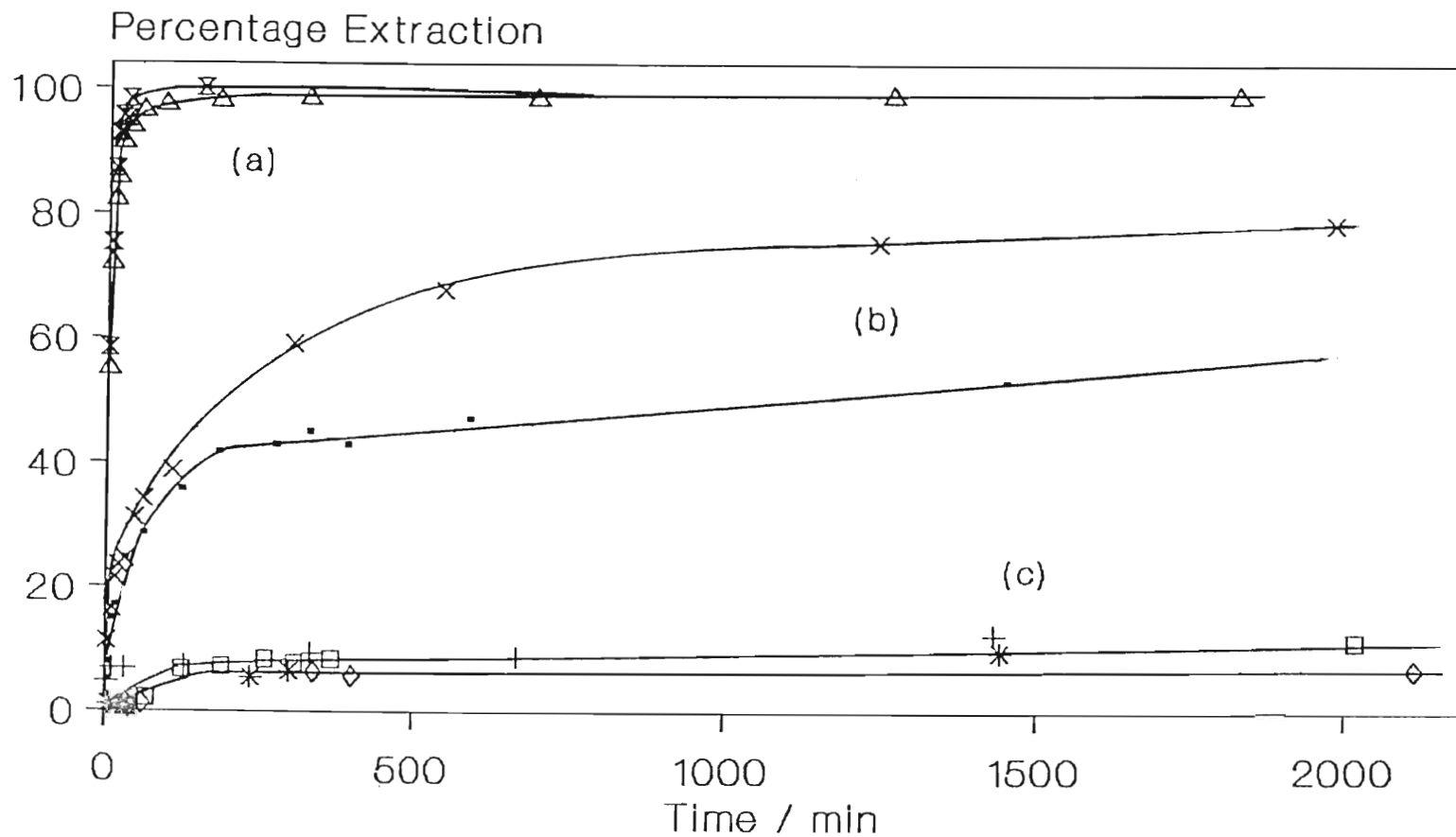
3.4.2. The Influence of Aqueous Phase pH on Germanium Extraction by TN 02181.

Initial rate and slower observed 'equilibrium' data are presented in Table (31) for germanium extraction by TN 02181 (50 g/l) versus 0,20 g/l germanium solutions.

pH	Initial Rate /(g/l)s ⁻¹	log (Initial Rate)	k _f (obs) /s ⁻¹	log k _f (obs)
-0,21	8,67 x 10 ⁻⁴	-3,06	2,04 x 10 ⁻³	-2,69
-0,043	4,47 x 10 ⁻⁴	-3,35	1,36 x 10 ⁻³	-2,87
0,24	1,20 x 10 ⁻⁴	-3,92	5,22 x 10 ⁻⁴	-3,28
0,92	4,52 x 10 ⁻⁵	-4,35	1,65 x 10 ⁻⁴	-3,78
1,90	7,50 x 10 ⁻⁵	-4,13	5,69 x 10 ⁻⁶	-5,25
4,15	5,56 x 10 ⁻⁶	-5,26	3,82 x 10 ⁻⁶	-5,42
4,88	1,78 x 10 ⁻⁶	-5,75	3,07 x 10 ⁻⁶	-5,51
5,67	9,38 x 10 ⁻⁶	-5,03	3,63 x 10 ⁻⁶	-5,44

Table (31). Initial rates and observed forward rate constants for the 'equilibrium' regime for germanium extraction by TN 02181 at varying aqueous phase pH. Organic phase: 100 ml 50 g/l TN 02181, aqueous phase: 100 ml ~ 0,20 g/l germanium.

Figure (60) gives an overall indication of the change in percentage extraction of germanium by TN 02181 with increasing pH. The plot shows three regions of behaviour: (a) pH < 0, initial rates are extremely fast ($t_{\frac{1}{2}}$ -time for 50% extraction is < 2 minutes) and 100% extraction is obtained, (b) an intermediate region where 0 < pH < 1 and initial rates are significantly slower than for (a) and the percentage extraction at equilibrium is 50-75% and (c) the region for which pH > 1 where neither the initial nor the slower kinetic regime rates are influenced by pH and extraction is inefficient.



▪	pH = 0,92	+	pH = 1,90	*	pH = 4,15	□	pH = 4,88
×	pH = 0,24	◇	pH = 6,75	△	pH = -0,04	⊗	pH = -0,21

Figure (60). Percentage extraction as a function of pH for TN 02181. Aqueous phase : ~ 0,20 g/l Ge in solutions of various pH (see Section 2.4.2.2.2. for the preparation of buffers for pH ≥ 1). Organic phase : 50 g/l ligand in AR toluene.

The $\log(\text{Initial rate})$ versus pH plot shown in Figure (61) possesses features analogous to those discussed for Lix 26 (Figure (58)), however there is one major difference in that an order of 1,92 for $[\text{H}^+]$ is suggested for the region $\text{pH} < 0,24$, contrasting with the value of 2,83 obtained for Lix 26. It must be emphasized that the calculation of these orders is an estimate since only three data points are utilised in the gradient calculation and thus this absolute difference in order is also a function of experimental reproducibility, however, it is likely that the active ligands of the two reagents have different rates of reaction with H^+ and this difference accounts for the variation in apparent order, i.e. Equation (78) is more relevant for TN 02181 (Section 3.4.5).

Examination of the plot of $k_f(\text{obs})$ versus pH of Figure (62) shows that for this ligand: (i) the rate of germanium extraction is proportional to $[\text{H}^+]^{-1,18}$ for $\text{pH} < 2$ and (ii) approximately zeroth order ($[\text{H}^+]^{-0,06}$) behaviour is observed for $\text{pH} > 2$. These orders are comparable with those of Lix 26 (orders of -1,24 and -0,32 in regions (i) and (ii) respectively). Again these apparent reaction orders are compared with the caveat mentioned above.

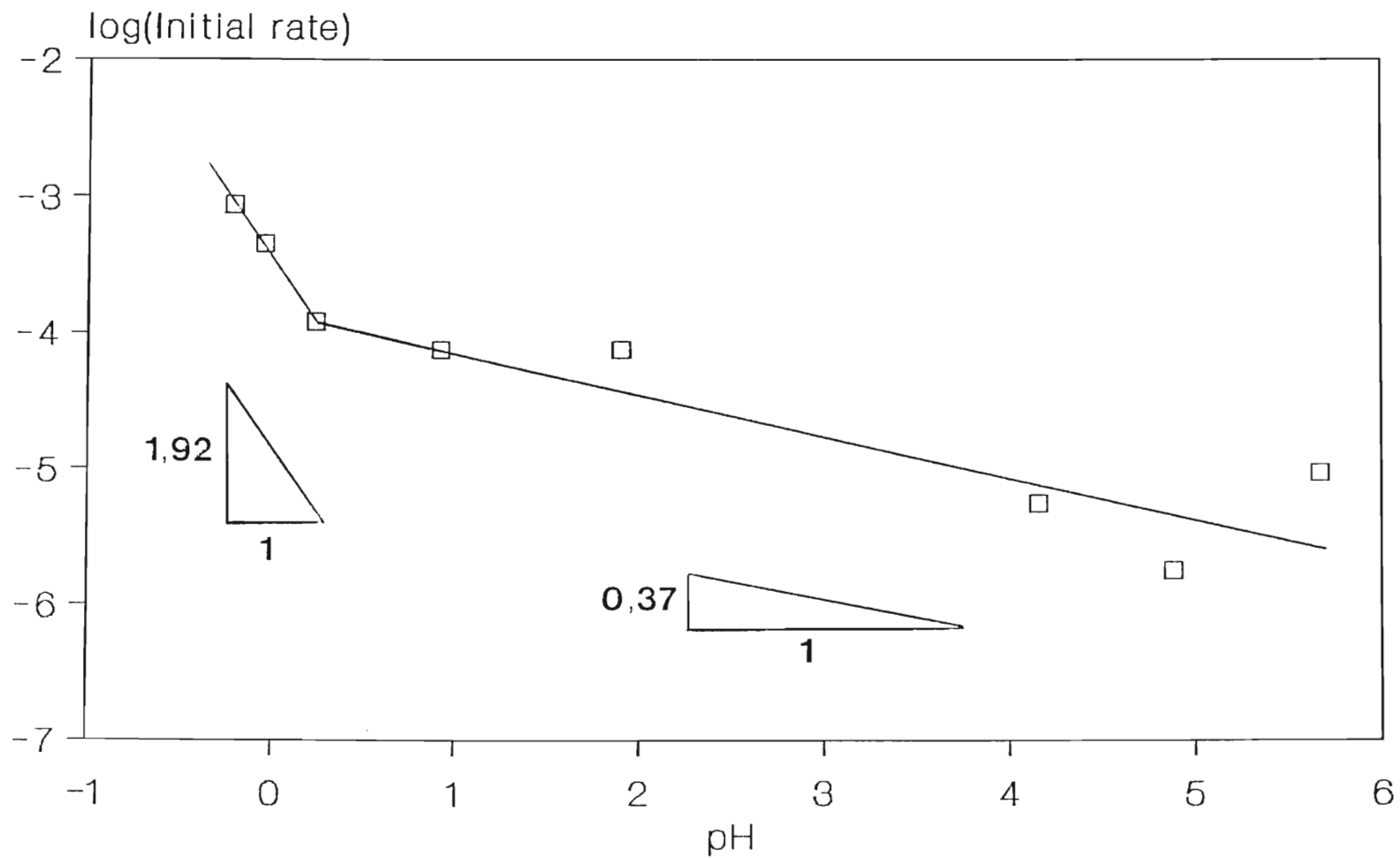


Figure (61). Log(Initial rate) of germanium extraction by TN 02181 as a function of aqueous phase pH in the mechanical shaker. Organic phase : 50 g/l TN 02181 in AR toluene. Aqueous phase : $\sim 0,20$ g/l Ge at various pH's.

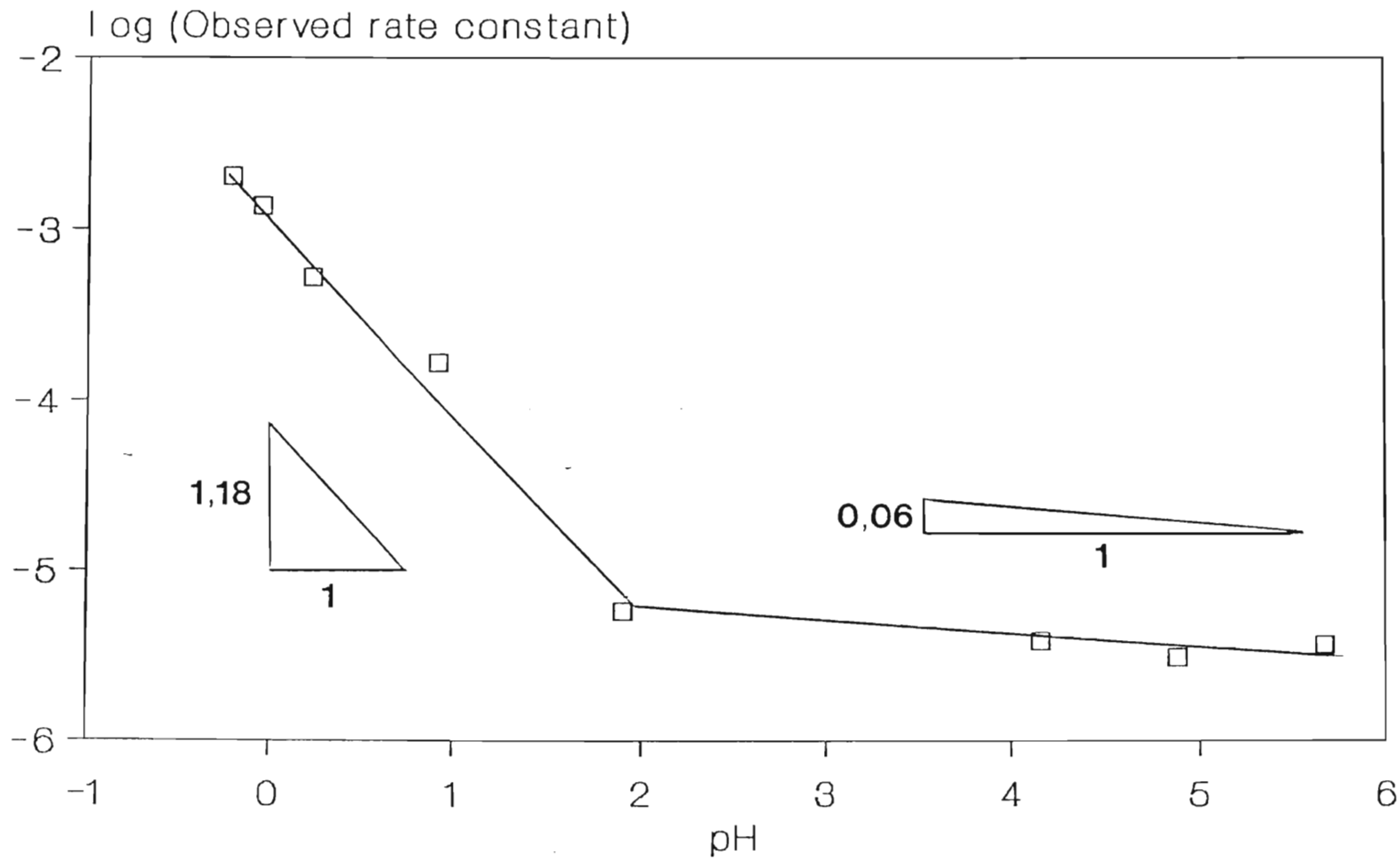


Figure (62). Log(Observed rate constant) for germanium extraction as a function of pH for TN 02181 under conditions of vigorous shaking. Organic phase : 50 g/l TN 02181 in AR toluene; Aqueous phase : $\sim 0,20$ g/l Ge at various pH's. The observed rate constant applies to the slow 'equilibrium' regime.

3.4.3. The Influence of Aqueous Phase pH on the Rate of Germanium Extraction by TN 01787.

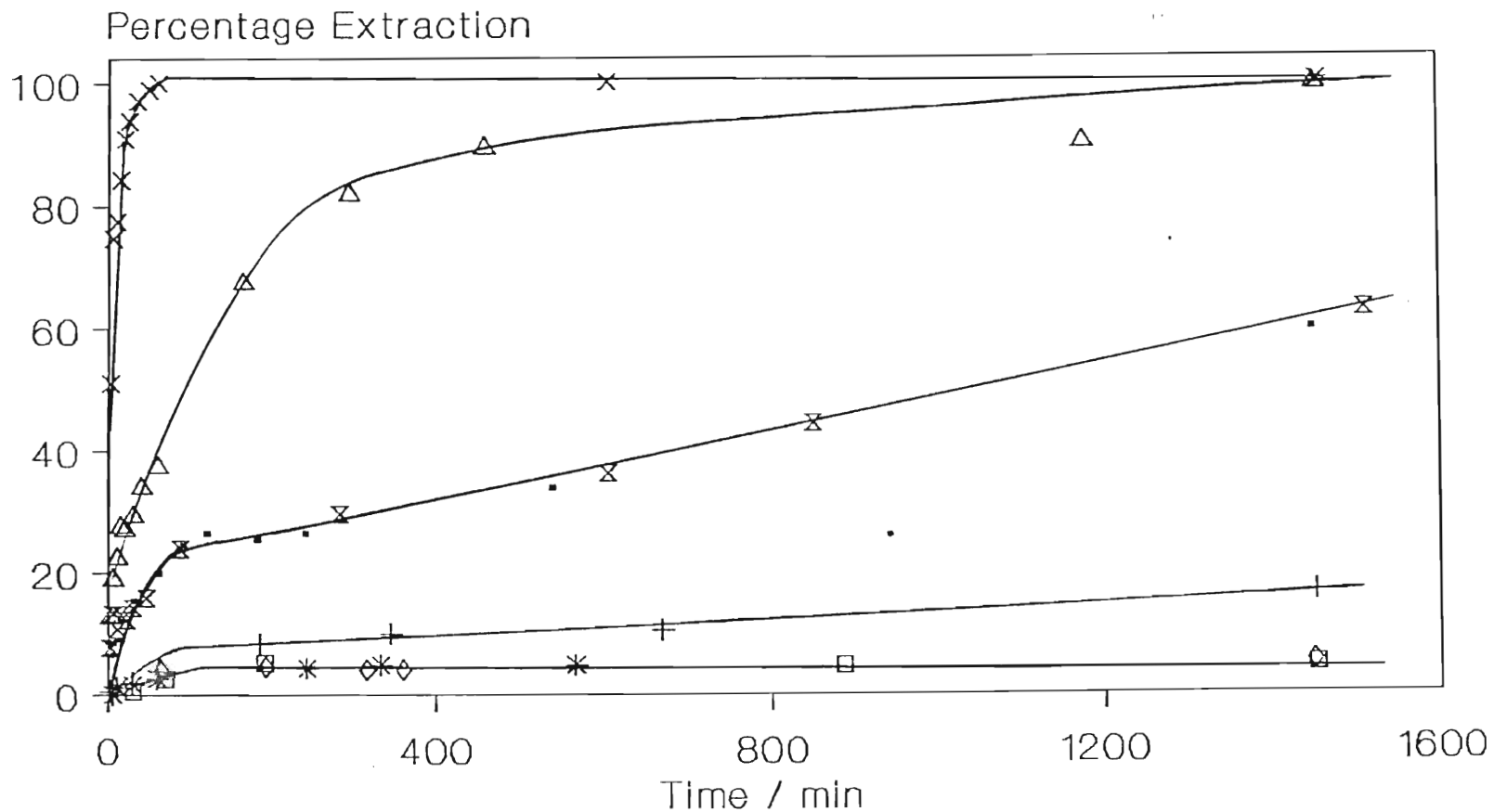
Values of Initial rate and $k_f(\text{obs})$ calculated in an analogous manner to those of Lix 26 and TN 02181 are shown in Table (32).

pH	Initial Rate /(g/l)s ⁻¹	log(Initial Rate)	$k_f(\text{obs})$ /s ⁻¹	log $k_f(\text{obs})$
-0,21	$7,58 \times 10^{-4}$	-3,12	$1,38 \times 10^{-3}$	-2,86
-0,043	$1,83 \times 10^{-4}$	-3,74	$2,34 \times 10^{-4}$	-3,63
0,24	$1,25 \times 10^{-4}$	-3,90	$7,29 \times 10^{-5}$	-4,14
0,97	$5,40 \times 10^{-5}$	-4,27	$4,87 \times 10^{-5}$	-4,31
1,90	$8,33 \times 10^{-6}$	-5,08	$1,00 \times 10^{-5}$	-5,00
4,15	$3,33 \times 10^{-6}$	-5,48	$7,33 \times 10^{-6}$	-5,14
4,88	$1,21 \times 10^{-6}$	-5,92	$3,06 \times 10^{-6}$	-5,51
5,67*	$1,33 \times 10^{-7}$	-6,88	$2,26 \times 10^{-7}$	-6,65

Table (32). Values of Initial Rates and $k_f(\text{obs})$ for the slow kinetic regime for germanium extraction by TN 01787.

(* Calculated kinetic constants are approximate only: the rate at this pH is very slow.)

Figure (63) assesses the overall sensitivity of germanium extraction by this ligand to pH. Compared with a similar plot



■ pH = 0.97 + pH = 1.90 * pH = 4.15 □ pH = 4.88
 × pH = -0.21 ◇ pH = 6.75 △ pH = -0.04 ⊠ pH = 0.24

Figure (63). Percentage extraction as a function of pH for TN 01787. Aqueous phase: ~ 0,20 g/l Ge in solutions of various pH. Buffers (Section 2.4.2.2.2.) were used to maintain aqueous pH for pH > 0,24 and H₂SO₄ was utilised for values of pH below this. Organic phase : 50 g/l TN 01787 in AR toluene.

for TN 02181 (Figure (60)), there are noticeable differences in the efficacy of this reagent in the region of pH which constitutes the optimum operating pH i.e. $\text{pH} < 0,24$. Thus, for example compare the following percentage extraction data (Table (33)):

Percentage Extraction after 10 minutes			
pH	Lix 26	TN 02181	TN 01787
-0,21	78,5	87,1	77,5
-0,043	* 49,2	82,1	22,5
0,24	* 13,5	16,3	10,7
% Purity	72	84	87

Table (33). Comparison of extraction efficiencies of Lix 26, TN 02181 and TN 01787: Conditions : organic = 50 g/l reagent in toluene, aqueous phase = $\sim 0,20$ g/l in Ge except * = 0,65 g/l.

It is apparent from Table (33) that for all values of pH, TN 01787 is the least effective reagent even though it is of the highest active-constituent purity. Referring to Section 3.2.1.4, it was also observed to exhibit the poorest extraction behaviour with varying concentration. These observations are correlated with structural differences in Section 3.13.

Figures (64) and (65) show the changes in $\log(\text{Initial rate})$ and $\text{Log}(k_f(\text{obs}))$ respectively for TN 01787. For the region of $\text{pH} > 1$, the kinetic behaviour parallels that which has been discussed for Lix 26 and TN 02181, however differences exist at low pH: first the apparent reaction order with respect to $[\text{H}^+]$ for the slow 'equilibrium' regime is much 'higher' at inverse 2,73 (cf. inverse 1,24 for Lix 26 and inverse 1,18 for TN 02181) and second the initial rate data do not permit the type of analysis which has been presented for Lix 26 and TN 02181 although, as stated above, the tendency to zeroth order in $[\text{H}^+]$ is evident at $\text{pH} > 2$. The 'higher' order during the initial reaction regime is proposed to be related to the low tendency of this ligand to extract hydrogen ions and this is dealt with in Section 3.4.5.

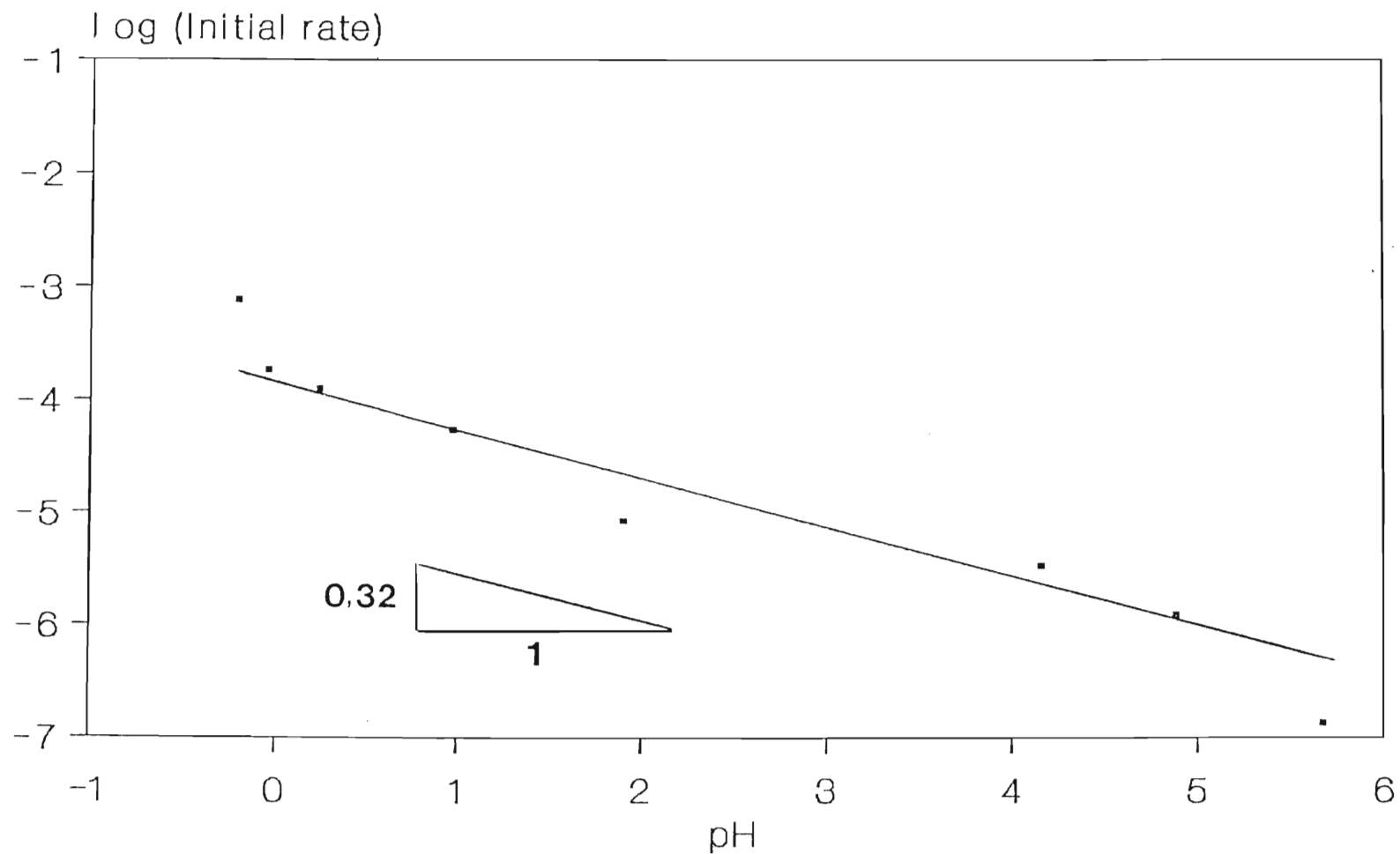


Figure (64). Log(Initial rate) of germanium extraction by TN 01787 as a function of aqueous phase pH. Organic phase: 50 g/l TN 01787 in AR toluene. Aqueous phase : ~ 0,2 g/l Ge in solutions of various pH. The criteria for calculation of initial rates are analogous to those given for Figure (58).

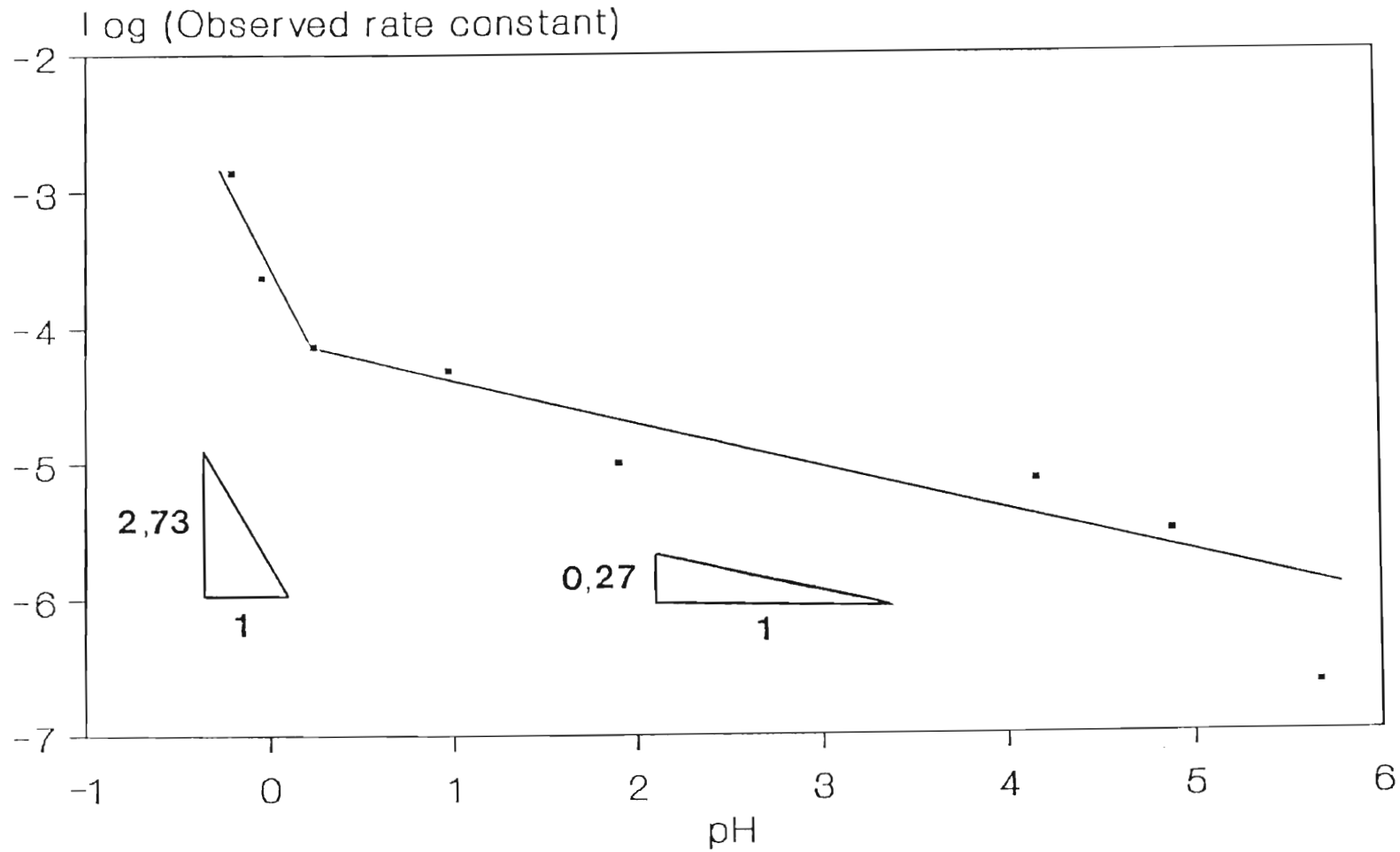


Figure (65). $\log(\text{Observed rate constant})$ for germanium extraction by TN 01787 as a function of pH under conditions of vigorous shaking. Organic phase : 50 g/l TN 01787 in AR toluene; Aqueous phase : $\sim 0,2$ g/l Ge in solutions of various pH. Least squares orders with respect to $[\text{H}^+]$ are indicated on the figure.

3.4.4. Comparison of the 'Equilibrium',¹ Percentage

Extraction of Germanium by the Various Extractants

It is customary to compare the 'equilibrium' percentage extraction of ligands in order to gain some insight into their overall performance, however the value of such data to a practical situation in which contact times on an industrial scale are of the order of minutes is limited. Table (34) and Figure (66) summarise percentage extraction data for a 24-hour shaking period. It must be noted that some of the values presented are not percentage extractions at reaction completion e.g. at pH > 5, actual equilibrium is only attained after 96 hours, however the duration selected is illustrative of the general trend.

Percentage Extraction after 24 hrs			
pH	Lix 26	TN 01787	TN 02181
-0,21	97,5	100,0	100,0
-0,043	90,7	99,5	98,9
0,24	63,0	62,8	81,6
0,91	39,5	59,7	53,3

¹In this context 'equilibrium' refers to the situation at reaction completion (i.e. no further observable change in germanium in either phase occurs). This use is discrete from the use of the word to describe the slow kinetic regime for germanium extraction.

Percentage Extraction after 24 hrs			
pH	Lix 26	TN 01787	TN 02181
1,90	26,0	16,7	12,5
4,15	16,5	7,5	9,7
4,88	5,0	4,7	9,8
5,71	4,9	2,1	6,9

Table (34). 'Equilibrium' percentage germanium extraction by Lix 26, TN 01787 and TN 02181, (50 g/l reagent in toluene) at various aqueous phase pH's. 24 hour shaking period.

The data in Table (34) and Figure (66) show that at equilibrium, (i) TN 01787 is comparable to the other two extractants for $\text{pH} < 2$ but (ii) is the worst extractant at $\text{pH} > 2$.

In the course of the discussion of the effect of pH on the kinetics and equilibrium percentage extraction of germanium by the proprietary reagents of interest to this work thus far, mention has been made of the importance of the aqueous phase speciation of germanium. In the section which follows (3.4.5), a description of the speciation phenomenon will be presented and will subsequently be used (Section 3.4.6) to rationalize the pH behaviour which has been noted in the previous sections.

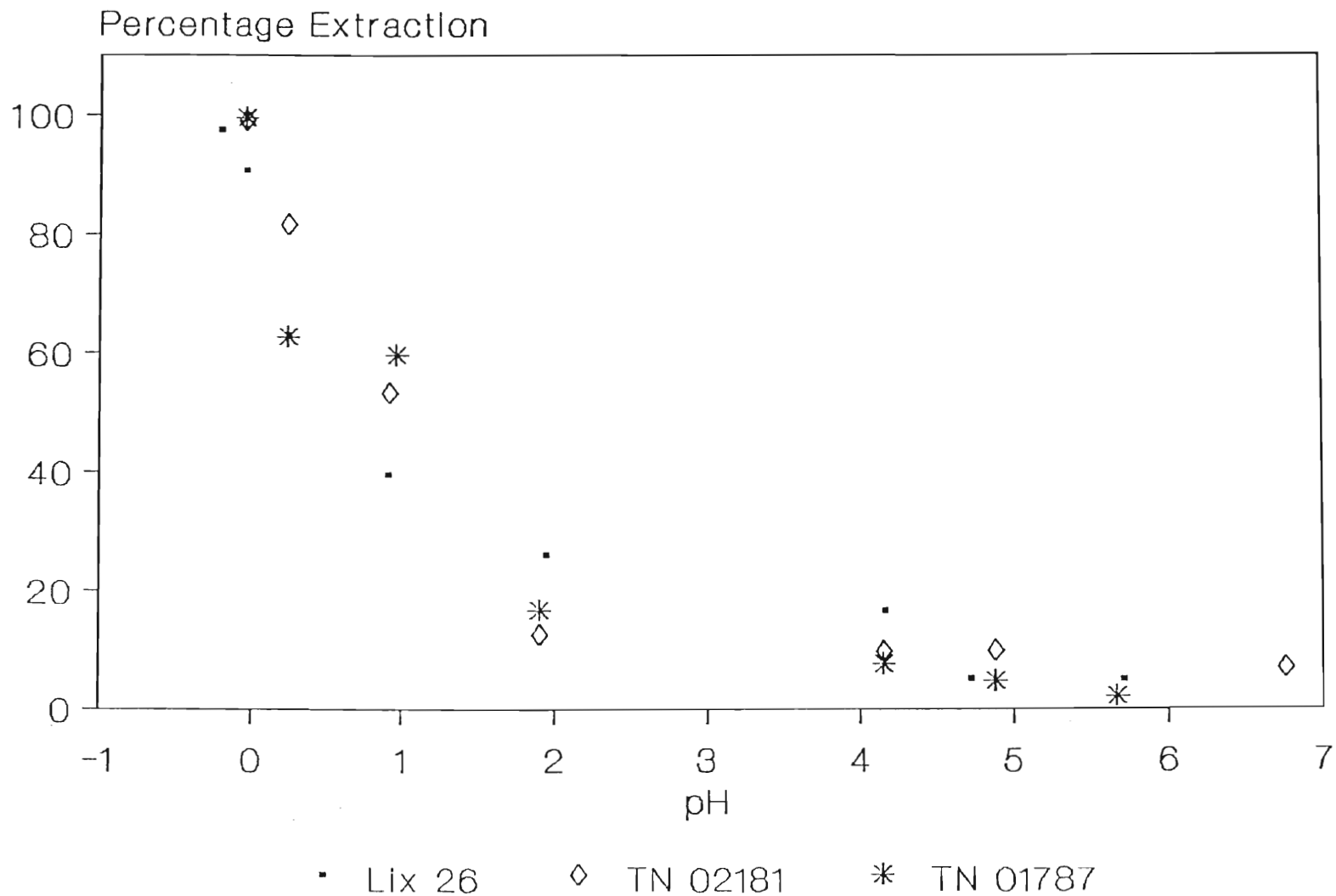
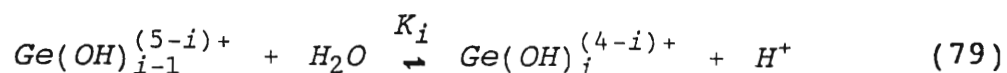


Figure (66). Comparison of the percentage extraction of germanium as a function of pH for TN 01787, TN 02181 and Lix 26 in the mechanical shaker. Shaking time : 24 hours. Organic phases : 50 g/l ligand in toluene; Aqueous phases : ~ 0,65 g/l (Lix 26) or ~ 0,20 g/l (TN 02181 and TN 01787) at various pH's.

3.4.5. Germanium Speciation and the Nature of the Reactions Competing for Active Ligand Sites

To help understand the influence of pH upon extraction (Sections 3.4.1-3.4.4), it is necessary to discuss the speciation of germanium in aqueous solution, that is the distribution of germanium species with changing bulk aqueous phase pH.

The apparent equilibrium constants K_i , of the reactions given by Equation (79):



are given by:

$$K_i = \frac{[\text{Ge}(\text{OH})_i^{(4-i)+}][\text{H}^+]}{[\text{Ge}(\text{OH})_{i-1}^{(5-i)+}]} \quad (i = 1, 2, 3, 4) \quad (80)$$

Values of K_i have been determined by Nazarenko⁽⁹⁴⁾ over a range of ionic strength. For $I = 0,5$ and $1,0 \text{ mol kg}^{-1}$, the following values of K_i (Table (35)) are quoted:

K_i	Ionic Strength = 0,5 mol kg ⁻¹	Ionic Strength = 1,0 mol kg ⁻¹
K_1	2,85	6,54
K_2	1,11	2,83

K_i	Ionic Strength = 0,5 mol kg ⁻¹	Ionic Strength = 1,0 mol kg ⁻¹
K_3	0,54	1,60
K_4	0,25	0,90

Table (35). Values of K_i for germanium-hydroxy complexes at 25°C⁽⁹⁴⁾. (Values shown apply to GeO₂ solutions ≤ 0,01 M:- thus avoiding the formation of polymeric complex species, see text.)

These particular values of ionic strength cover the range examined in this work viz. 0,5 - 0,72 (approx ionic strength of 1,5 M H₂SO₄) for the pH study. The concentration of germanium dioxide is also important since for [GeO₂] > 10⁻² M, condensed species such as Ge₅O₁₁²⁻, H₂Ge₇O₁₆²⁻ and HGe₈O₁₈³⁻ begin to form in solution⁽⁹⁴⁾. Since there are no adequate quantitative studies of the conditions under which these species form (pH, temperature etc.), it seemed prudent in this work to circumvent the problem by maintaining germanium concentrations at levels below the figure quoted above and thus avoid the problems associated with including them in the speciation model. Accordingly, in this study, the highest GeO₂ concentration utilised was 8,95 x 10⁻³ M (≡ 0,65 g/l Ge).

Using the values of K_i given in Table (35), it is possible to speciate germanium into seven discrete species. Figure (67) (taken from reference 94) shows an abbreviated form of the pH distribution from pH -0,8 to 3,2. Over this range, the metal ion exists simultaneously as a number of forms from Ge⁴⁺ to

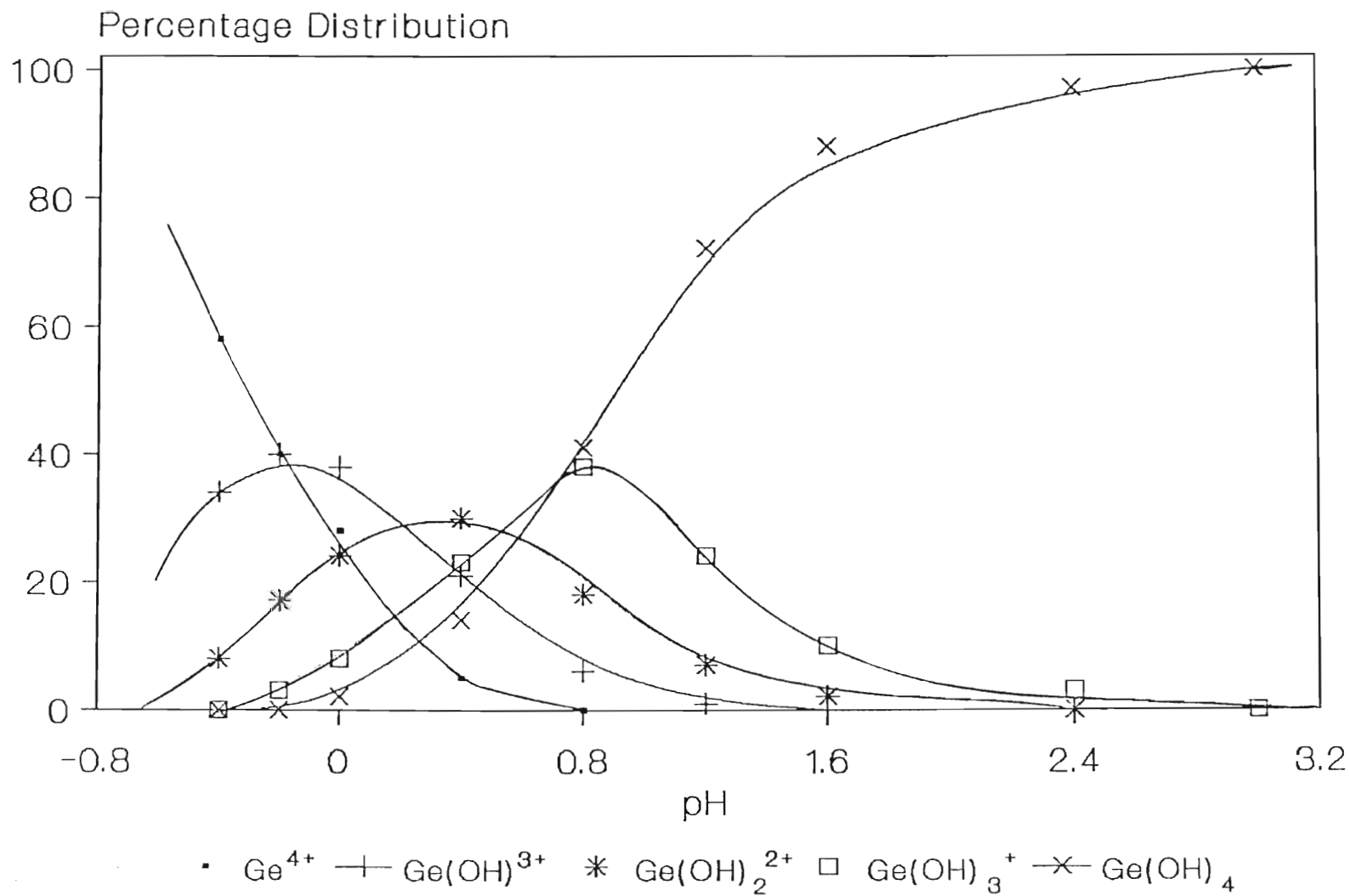


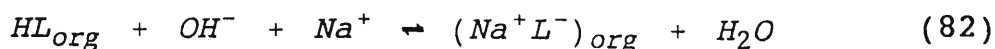
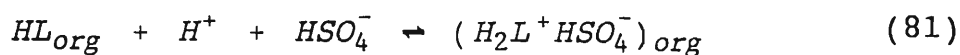
Figure (67). Distribution of germanium species as a function of $\text{pH}^{(94)}$, for $[\text{GeO}_2] \leq 1 \times 10^{-2}$ M.

$\text{Ge}(\text{OH})_4$ which is the only species present in solution for $2,9 \leq \text{pH} \leq 6,2$ after which H_3GeO_4^- and then $\text{H}_2\text{GeO}_4^{2-}$ are variously present either independently or simultaneously. For $\text{pH} > 13$, germanium exists in aqueous solution only as $\text{H}_2\text{GeO}_4^{2-}$. (The speciation for the pH region 3-14 is discussed in the context of the stripping kinetics in Section 3.10.)

It can be seen from Figure (67) that as the pH changes, the species present in aqueous solution change, however in interpreting the significance of altering the aqueous phase pH to the extraction characteristics, it must be borne in mind that the speciation model is an **equilibrium** model and therefore the removal of e.g. Ge^{4+} from aqueous solution will cause a shift in equilibrium. During extraction therefore, it is to be expected that the species composition of the aqueous phase changes with time from the initial distribution applicable to any particular pH.

The effect of altering the aqueous phase pH upon the species in the **organic** phase is not easy to understand. First, free oxine, as mentioned in Section 3.3, reacts with hydrogen ions when $\text{pH} \leq 4-5$ and with hydroxyl ions when $\text{pH} > 9-10$. Both reactions increase the aqueous phase solubility of 8-hydroxyquinoline ($K_D = 0,98$ for an aqueous phase 1,5 molar in H_2SO_4 , page 216). Because of the competition reaction in which oxine is protonated (Equation (74)) at low pH, free oxine does not complex germanium at $\text{pH} < 3-5$, however each mole of the impurity consumes a mole of H^+ , which must have implications upon the aqueous phase germanium speciation. Second, the

active ligand (7-alkylated-8-hydroxyquinoline), when dissolved in solvents such as toluene forms analogous ionic species to oxine viz. H_2L^+ and L^- , however they remain in the organic phase: the hydrophobicity of the 7-alkyl hydrocarbon chain ensures that only insignificant amounts enter the aqueous phase. Since toluene is a poorly dissociating solvent and hydrogen-bonding is not available to stabilize charged moieties, then if the species H_2L^+ and L^- exist in the organic phase they must do so as ion-pairs. Hence the following reactions can be proposed when solutions of 7-alkylated-8-hydroxyquinoline ligand are mixed with aqueous solutions containing for instance, sulphuric acid (Equation (81)) and sodium hydroxide (Equation (82)):



The uptake of hydrogen ions by Kelex 100 has been investigated by Marchon and coworkers⁽⁶⁵⁾, who contacted kerosene/Kelex 100 solutions of varying concentration with aqueous phases of varying sulphuric acid concentration. After mixing, aliquots of the organic phase were 'scrubbed' with water and the resulting acidic solution titrated with standard base. Figure (68) shows some of the results which were obtained by these workers. Examination of these data shows that in the absence of ligand (curve 1 of Figure (68)), no acid is extracted into the organic phase, whereas in the presence of ligand one H^+ is abstracted per ligand molecule, i.e. for curves 2 and 3 on Figure (68) the equilibrium concentration of

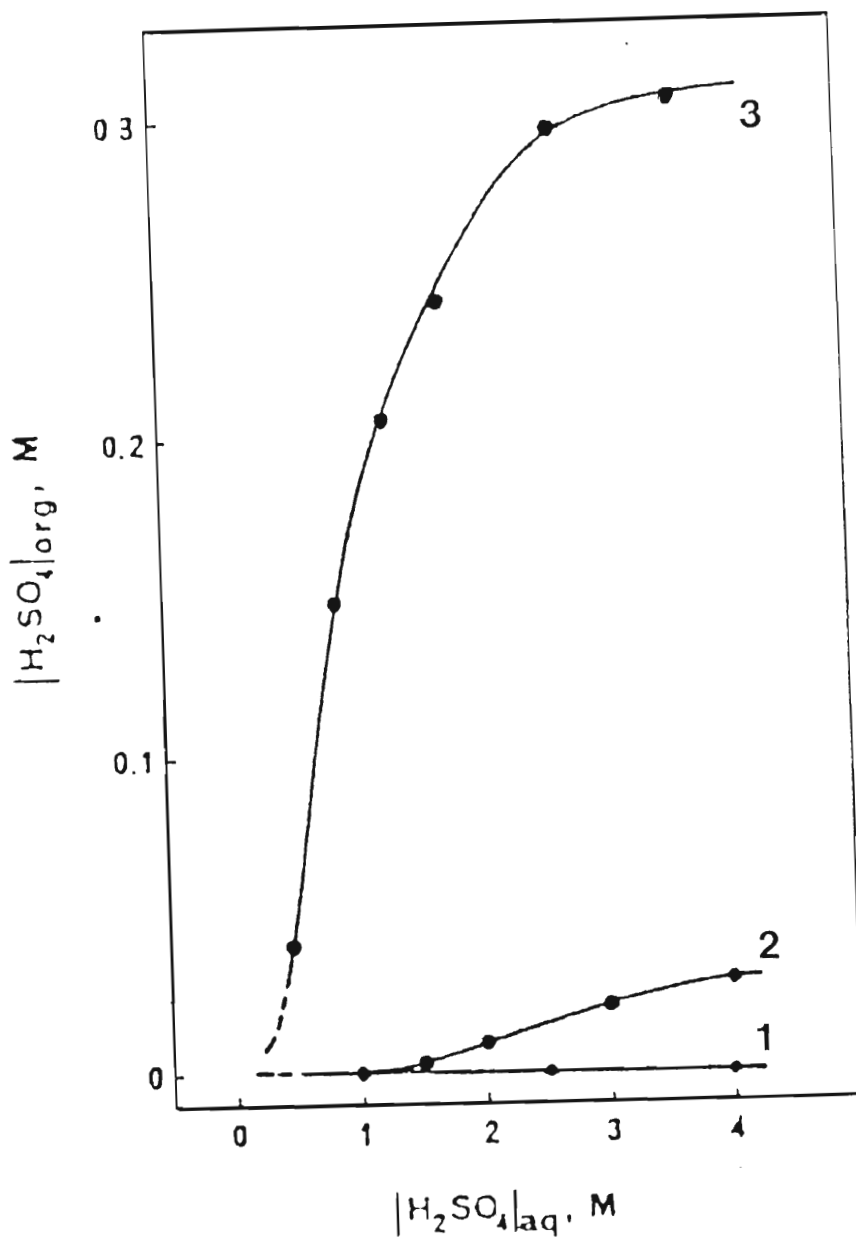


FIGURE (68). Distribution isotherms of sulphuric acid between an aqueous solution and kerosene containing various concentrations of Kelex 100. (1) : $[\text{Kelex 100}] = 0$; (2) : $[\text{Kelex 100}] = 3,0 \times 10^{-2} \text{ M}$; (3) : $[\text{Kelex 100}] = 0,32 \text{ M}$; after Marchon *et al.*⁽⁶⁵⁾

H_2SO_4 in the organic phase is equal to the ligand concentration. It would be reasonable to assume that, given the similarities in the structures of Kelex 100 and the ligand species of interest to this work, that similar behaviour exists. One point which is evident from Figure (68) is that for $[\text{H}_2\text{SO}_4]_{\text{aq}} < 0,2 \text{ M}$ (which is an approximate pH of 0,60), acid uptake via Equation (81) will not be an issue.

The acid-uptake characteristics of the reagents of concern to this work are summarised in Tables (36) to (38) below. Details of the determination of the concentration of acid in the aqueous phase after vigorous mixing of the ligand-containing phases and aqueous solutions containing approximately 1,5 M H_2SO_4 , were given in Section 2.4.2.2.11.

[Lix 26] / (g/l) purity-corrected	[Lix 26] /M	$[\text{H}_2\text{SO}_4]_{\text{org}}$ /M	$[\text{H}_2\text{SO}_4]_{\text{aq}}$ /M
18,0	$5,78 \times 10^{-2}$	0,007	1,476
25,2	$8,09 \times 10^{-2}$	0,021	1,462
36,0	$1,16 \times 10^{-1}$	0,038	1,445
54,7	$1,76 \times 10^{-1}$	0,055	1,428
72,0	$2,13 \times 10^{-1}$	0,091	1,392

[Lix 26] / (g/l) purity-corrected	[Lix 26] /M	[H ₂ SO ₄] _{org} /M	[H ₂ SO ₄] _{aq} /M
90,0	$2,89 \times 10^{-1}$	0,125	1,358
112,3	$3,61 \times 10^{-1}$	0,167	1,316

Table (36). Concentrations of H₂SO₄ extracted by Lix 26 into the organic phase after 24 hours shaking with an aqueous phase initially containing 1,485 M H₂SO₄ (determined by titration). Phase volume ratio 1:1 (100 ml).

[TN 01787] / (g/l) purity-corrected	[TN 01787] /M	[H ₂ SO ₄] _{org} /M	[H ₂ SO ₄] _{aq} /M
22,0	$7,04 \times 10^{-2}$	0,004	1,493
44,0	$1,48 \times 10^{-1}$	0,014	1,486
66,0	$2,22 \times 10^{-1}$	0,032	1,465
88,0	$2,96 \times 10^{-1}$	0,065	1,432
136,4	$4,56 \times 10^{-1}$	0,157	1,340

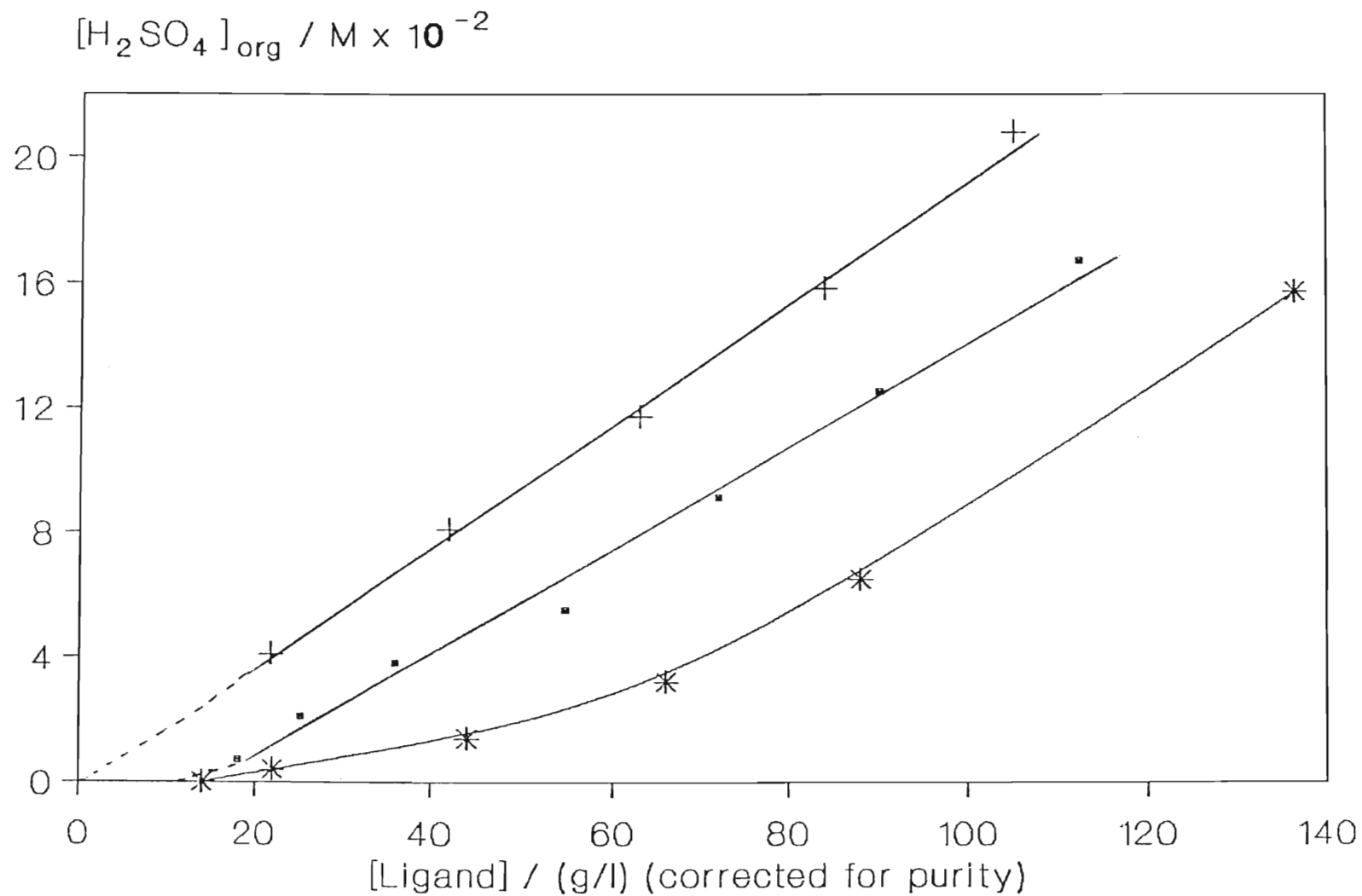
Table (37). Concentration of [H₂SO₄]_{org} at equilibrium after 24 hours shaking of solutions of TN 01787 of varying concentration with 1,497 M H₂SO₄. Phase volumes 100 ml.

[TN 02181] / (g/l) purity-corrected	[TN 01787] /M	[H ₂ SO ₄] _{org} /M	[H ₂ SO ₄] _{aq} /M
21,8	$7,01 \times 10^{-2}$	0,041	1,456
42,0	$1,35 \times 10^{-1}$	0,081	1,416
63,0	$2,02 \times 10^{-1}$	0,117	1,380
84,0	$2,70 \times 10^{-1}$	0,158	1,339
105,0	$3,37 \times 10^{-1}$	0,208	1,289

Table (38). The uptake of sulphuric acid into the organic phase by TN 02181 in toluene via Equation (81) after vigorous shaking for 24 hours with a 1,497 M solution of H₂SO₄. Phase volumes 100 ml.

Examination of the third columns of Tables (36) - (38) illustrate the difference in tendency of the reagents to extract hydrogen ions via Equation (81). It is clear that TN 02181 extracts much greater quantities of acid than either Lix 26 or TN 01787 at any particular ligand concentration. TN 01787 is the least effective reagent in this regard.

Figure (69) shows plots of the concentration of acid extracted into the organic phase by the reagents versus the concentration of purity-corrected ligand. Both TN 02181 and Lix 26 are characterised by a linear relationship between [HL] and [H₂SO₄]_{org}, whilst TN 01787 shows low hydrogen ion extraction at low ligand, which increases in a non-linear fashion with increasing [HL].



▪ Lix 26 + TN 02181 * TN 01787

Figure (69). Concentration of sulphuric acid in the organic phase $[H_2SO_4]_{org}$ after 24 hours shaking of solutions of Lix 26, TN 01787 and TN 02181 in toluene with aqueous phases of 1,5 M H_2SO_4 . Volumes 100 ml. Ligand concentrations are corrected for the purity of the active constituent.

It is not clear to what extent the impurities present in the ligand reagents supplied would also extract hydrogen ions. It is possible that structures (4), (5) and (8) of Table (6), accounting for an additional 4-5% by mass of the commercial reagents, possess the same protonation characteristics as the predominant active constituents at $\text{pH} \leq 0$ and would therefore extract a quantity of additional acid.

By absorbing acid, the characteristics of the ligand-containing organic phase and the aqueous phase are altered. Consider first the organic phase. When $\text{pH} \leq 0$, some of the HL is transformed into H_2L^+ (and extracted as an ion pair $\text{H}_2\text{L}^+\text{A}^-$ where $\text{A} = \text{HSO}_4^-$ for sulphuric acid aqueous phases). H_2L^+ possesses sites which are more hydrophilic than those of HL i.e. $=\text{NH}^+$ in place of $=\text{NH}$ and its formation can greatly modify interfacial properties. For the aqueous phase, there is evidence to suggest^(65,203) that the rates at which the various species of germanium in aqueous solution, $\text{Ge}(\text{OH})_n^{(4-n)+}$ ($n = 0 - 4$), are extracted by 7-alkylated-8-hydroxyquinoline ligands differ (Ge^{4+} faster than $\text{Ge}(\text{OH})^{3+}$ and so on) and thus the extraction of hydrogen ions from aqueous medium by the active ligand competes directly with the removal of germanium i.e. the withdrawal of hydrogen ions from the aqueous phase affects the speciation of germanium in this medium. Consider, for example, the contact of an organic phase containing 100 g/l Lix 26 (\equiv 72 g/l purity-corrected active ligand), with an aqueous phase containing approximately 1,5 M H_2SO_4 (see Table (36)). Following vigorous shaking (for approximately 10

minutes - see later for rate of acid uptake), the aqueous phase sulphuric acid concentration is reduced from 1,485 M to 1,392 M. If, in the worst possible case, no germanium were removed from the aqueous phase during this initial period of phase contact, then the following percentages of germanium species (Table (39)), would prevail in the aqueous medium prior and subsequent to phase contact (data taken from Figure (67)).

Species	% Species in 1,485 M H ₂ SO ₄	% Species in 1,392 M H ₂ SO ₄
Ge ⁴⁺	41	34
Ge(OH) ³⁺	38	39
Ge(OH) ₂ ²⁺	17	31
Ge(OH) ₃ ⁺	3	4
Ge(OH) ₄	1	2

Table (39). Comparison of the distribution of germanium species in the aqueous phase before and after contact of a 1,485 M H₂SO₄ solution with a 50 g/l Lix 26/toluene organic solution.

While the changes in germanium speciation indicated in Table (39) are low, this is merely a result of the small overall change in pH which occurs at this high initial sulphuric acid concentration, however the events occurring in the organic phase may have significant repercussions in the distribution of species in the aqueous phase if the initial concentration

of sulphuric acid in the aqueous phase is somewhat lower, e.g. 0,5 M H₂SO₄.

The section which follows is a summary of the observed effects of the aqueous phase pH on the rate of germanium extraction by 7-alkylated-8-hydroxyquinoline ligands, which were discussed in Sections 3.4.1 - 3.4.4 and the speciation data and the concepts which have been presented in this section (particularly with regard to the metal-ligand stoichiometry) and gives an overall understanding to the effect of changing the aqueous phase pH upon the rate and equilibrium percentage extraction.

3.4.6. The Nature of Extracted Germanium Species. Towards a Kinetic Model.

At this point it is appropriate to summarise the observations and results which have been presented in preceding sections:

(i) As the pH decreases the rate of germanium extraction increases and the equilibrium percentage extraction increases.

(ii) The phenomenon in (i) above is most pronounced in the initial 'fast' kinetic regime where typically $t_{\frac{1}{2}}$ is of the order of minutes for $\text{pH} \leq 0,24$ and the order with respect to the hydrogen ion concentration varies from inverse 1,92 (TN 02181) to inverse 2,83 (Lix 26) and is indicative of a complex mechanism involving uptake of H⁺ by ligand and reaction with germanium - hydroxy species. At 'high' pH ($> 0,24$), zeroth order dependence on [H⁺] is suggested for the entire course of reaction and extraction efficiencies are poor.

(iii) Semi-logarithmic plots (Equation (46)) of the rate of disappearance of germanium from the aqueous phase are first order in germanium but do not pass through the origin as a result of the complex nature of the initial reactions.

(iv) Rates are augmented by a high $[\text{HL}]_{\text{org}}$, but in general fast reaction rates are observed if a large excess of ligand is present in solution i.e. the interface is fully saturated.

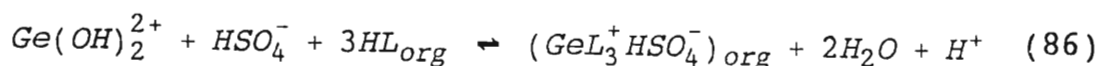
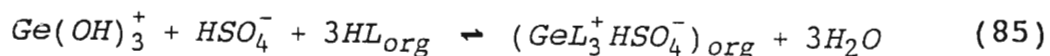
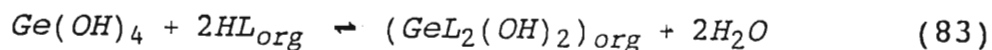
(v) At low pH ($\text{pH} \leq 0,24$), Lix 26 and TN 02181 are characterised by similar dependence on $[\text{H}^+]$ in the slow 'equilibrium' reaction regime (orders of inverse 1,24 and inverse 1,18 with respect to hydrogen ion concentration respectively, suggesting an inverse first order dependence), but a different dependence on H^+ for the fast initial reaction regime (orders of -2,83 and -1,92 respectively). Data for TN 02181 suggests a order of inverse 2,73 with respect to H^+ in the slower region. Data obtained in the fast kinetic regime for this reagent could not be interpreted in the same manner as for Lix 26 and TN 02181. At $\text{pH} > 0,24$, all three extractants showed an approximately -0,3th order dependence on $[\text{H}^+]$.

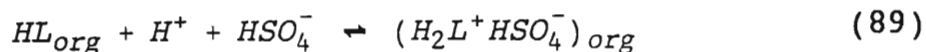
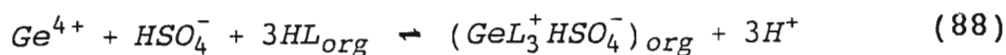
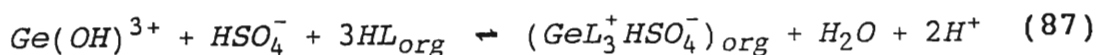
It is also evident that the nature of the reaction(s) which occur at the aqueous/organic phase boundary are dependent upon the pH since this is the sole factor which determines which species of germanium will be present in aqueous solution.

Results presented in this work (Section 3.2.1.5) for Lix 26, TN 02181 and TN 01787 and those of Marchon *et al.*⁽⁶⁵⁾ for Kelex 100 show, via distribution isotherms, that for $\text{pH} < 1$, the

extracted species has a metal:ligand ratio of 1:3 which is indicative of extraction of $\text{GeL}_3^+\text{HSO}_4^-$. For pH 3-8, this ratio changes⁽⁶⁵⁾ to 1:2, indicating the extraction of a GeL_2^{2+} species. For the latter pH range, the above authors showed that neither HSO_4^- nor SO_4^{2-} were extracted into the organic phase and this result suggests the formation of $\text{GeL}_2(\text{OH})_2$ as the extractable germanium/ligand species:- the species which has been shown to form when 8-hydroxyquinoline complexes germanium⁽⁹⁴⁾. At very high pH i.e. ≥ 12 , no extraction is observed since $\text{Ge}(\text{OH})_4$ is transformed into H_3GeO_4^- and $\text{H}_2\text{GeO}_4^{2-}$ and these anions do not react with ligand⁽⁵³⁾:- although of little importance to the extraction data reported in this work where $\text{pH} < 7$, this comment is relevant to the germanium stripping process which is discussed in Section 3.10.

On the basis of the formation of $\text{GeL}_2(\text{OH})_2$ and $\text{GeL}_3^+\text{HSO}_4^-$, the overall reactions between the various aqueous germanium species for $\text{pH} < 7$ and the 7-alkylated-8-hydroxyquinoline reagents of interest to this work can be summarised as follows:





where : HL_{org} is TN 02181, TN 01787 or Lix 26

Equations (83) to (89) represent a comprehensive scheme of the reactions occurring according to Equations (55) to (57), hence for each of the equations (84) to (88), the formation of the extractable species is a three-step process in which the rate-determining step is the formation of the tri-ligand chelate, GeL_3^+ . Equation (83) constitutes the **only** route to germanium extraction for pH 3-8, while, depending upon the exact pH (hence the speciation of germanium), some or all of the Equations (84) to (88) summarise the reactions occurring for $pH < 2$.

It is evident from Figures (59), (62) and (65) that for all three ligand reagents, the rate of extraction of $GeL_2(OH)_2$ is much slower than that of $GeL_3^+HSO_4^-$ and reasons for this are presented in the discussion following. Between pH 2-3, both species are extracted, although the biligand route (Equation (83)) contributes less to the overall extraction than Equations (84) to (88). Equation (89) becomes important for $pH \sim 0$ and competes with Equations (84)-(88) for active ligand.

It was mentioned above that the rate of extraction observed for $pH > 2$ for all the ligand reagents was an indication of

the lower extractability of $\text{GeL}_2(\text{OH})_2$ compared with $\text{GeL}_3^+\text{HSO}_4^-$. Marchon *et al.*⁽⁶⁵⁾ determined values of formation constants for these two species with L = Kelex 100 dissolved in a kerosene diluent viz.:

$$\text{GeL}_2(\text{OH})_2 \quad \log K = 2,24 \pm 0,09$$

$$\text{GeL}_3^+\text{HSO}_4^- \quad \log K = 6,44 \pm 0,35$$

These formation constant values can be correlated with the nature of the species formed and their compatibility with the diluent. Consider first the structure of the GeL_3^+ chelate (Figure (70)). This molecular complex is highly hydrophobic with no exposed electronegative atoms i.e. O and N. The positive charge on the germanium atom, which is not visible in the diagram is delocalised over the entire molecule. Conversely, $\text{GeL}_2(\text{OH})_2$ (Figure (71)) is more hydrophilic by virtue of the exposed OH groups and is therefore likely to be much less tolerated by the organic phase than GeL_3^+ .

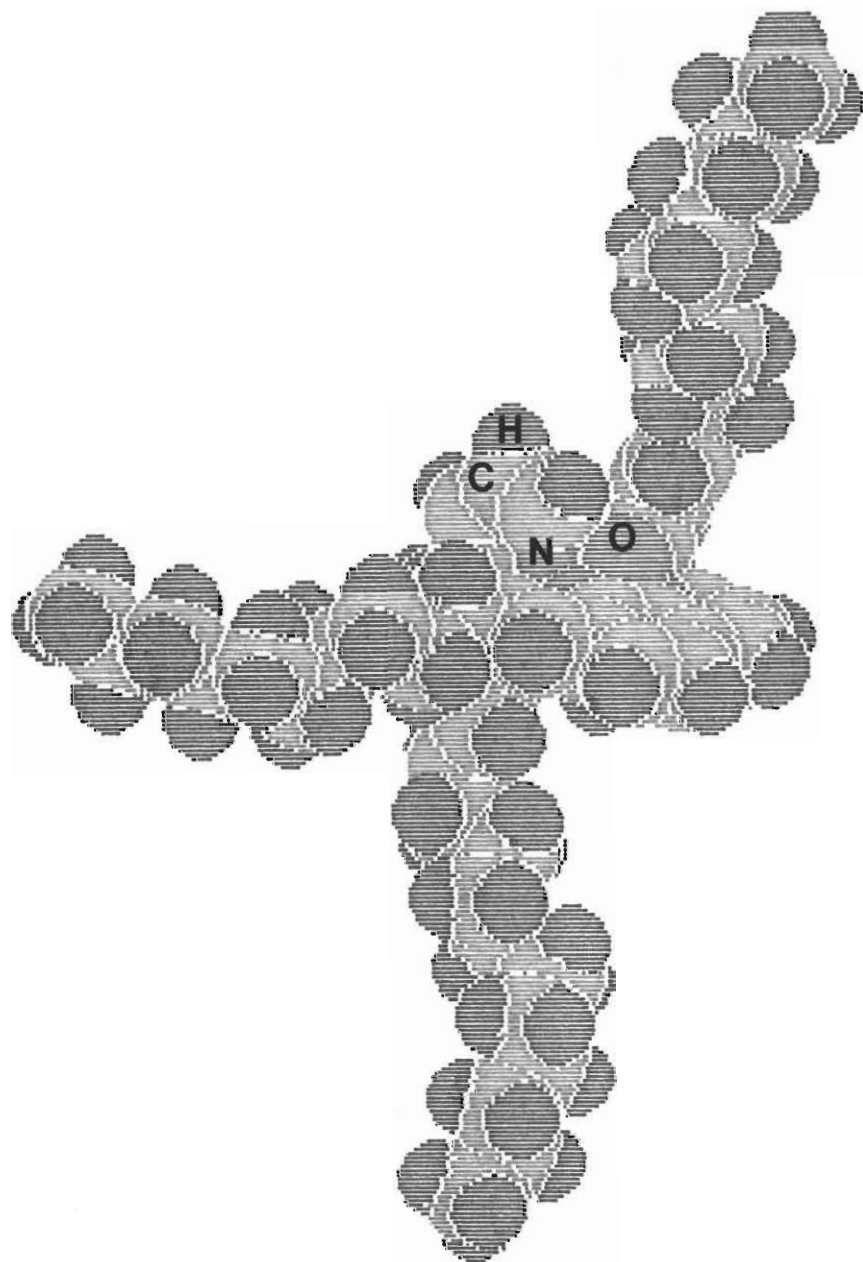


Figure (70). The Alchemy-minimized structure of the triligand chelate of germanium with Lix 26, $\text{GeL}_3^+\text{HSO}_4^-$.

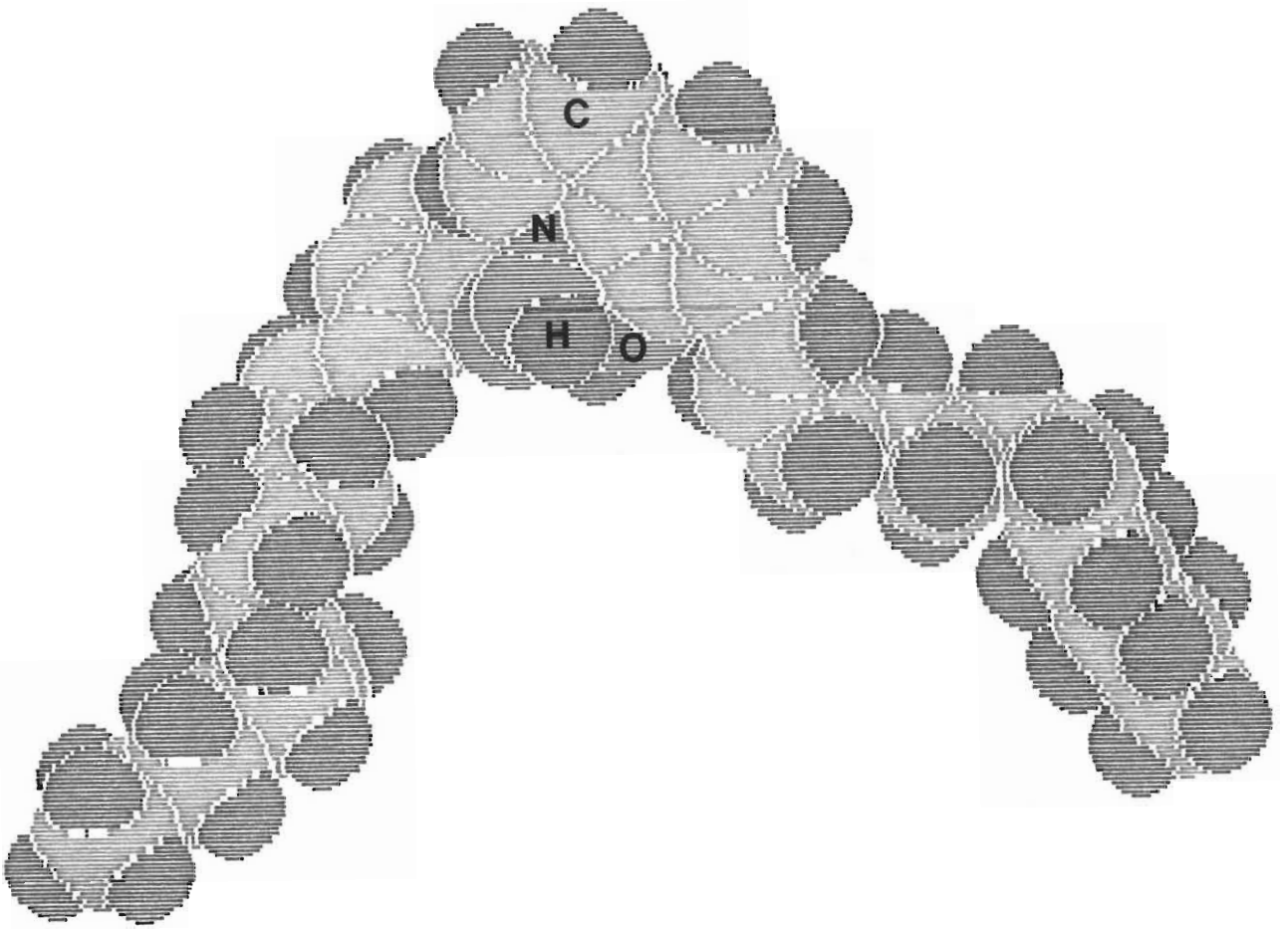


Figure (71). The Alchemy-minimized structure of the biligand hydroxylated chelate molecule between Lix 26 and germanium, $\text{GeL}_2(\text{OH})_2$.

The previous sections of this work rationalised the pH trends of Figures (57) - (66) by considering the germanium extraction behaviour of the ligands as comprising two discrete regions : (i) the region for $\text{pH} > 3$ where extraction is slow because the extractable species possesses hydrophilic centres and in which the kinetics tend to zeroth order in $[\text{H}^+]$. The mechanism for extraction, like that of low pH shows a first order dependence on $[\text{Ge}]$ but the fast and slower kinetic equilibrium regimes characteristic of low pH extraction data are not observed, and (ii) the region of $\text{pH} < 1$ in which the germanium is extracted by the ligand at a fast rate initially and then at a slower 'equilibrium' rate. Each of these regimes shows a different dependence on hydrogen ion concentration. In addition, an intermediate region of pH behaviour (approx 2-3) has been identified in which the characteristics of extraction are a function of both (i) and (ii) above.

A number of hypotheses which would explain the change in extraction kinetics noted in (ii) above were considered. Since all parameters (ligand concentration, phase volumes etc.) except $[\text{H}^+]$ were held constant throughout this investigation of the effect of pH on the rate of germanium extraction, there is reasonable justification to assume that it is the hydrogen-ion concentration which dominates the operation of the fast initial rate. The rationale of three hypotheses which were envisaged in order to explain the change in kinetics at low pH were considered and are discussed below.

(A) **Hypothesis 1:** A possible model which was considered involves competition for the active ligand by the germanium species and by hydrogen ions. Thus during the initial stages of extraction it was imagined that both germanium in various extractable forms (Ge^{4+} , $\text{Ge}(\text{OH})^{3+}$ etc.) and H^+ would compete for HL during the first few minutes of reaction. At some stage during the reaction therefore, all active ligand molecules would be complexed with germanium (which depletes 3 ligand molecules) or with H^+ forming H_2L^+ and this point in the reaction would become the slower since germanium species would be required to react with the quantity of HL which is formed via the equilibrium $\text{H}_2\text{L}^+ \rightleftharpoons \text{HL} + \text{H}^+$. It was postulated that the charged ligand species would not be amenable to cationic germanium hydroxy species because the nitrogen lone pair is involved in the $\text{N}-\text{H}^+$ bond. Naturally, the removal of HL by the germanium in a chelation reaction would eventually deplete the system of all protonated ligand and thus the extraction would eventually attain equilibrium. The operation of this model becomes even more attractive when it is realised that if the initial concentration of H^+ in the aqueous phase is not so high as to render a small change irrelevant to the aqueous germanium speciation, then the germanium speciates toward the higher hydroxy species (e.g. $\text{Ge}(\text{OH})_4$) which are postulated below (hypothesis 2) to be of a lower reactivity than lower hydroxylated species (e.g. Ge^{4+}). This scenario would explain a fast initial or competitive rate process, followed by a much slower one. In order to examine this theory, kinetic runs were performed in which ligand solution (50 g/l) was pre-equilibrated with sufficient stoichiometric quantity of acid solution (1,5 M H_2SO_4) to protonate all ligand sites, by

shaking 100 ml of each phase together for 90 minutes. (Note that if a competition reaction is a legitimate postulate then as short a time as 10 minutes would suffice.) An aliquot of germanium-containing solution at the same pH as the residual aqueous phase was then added to the acid pre-equilibrated ligand solution. The final phase ratio was 1:1 and sampling and germanium quantification were as previously described. If the above theory is correct then the result of such experiments should show reduced initial extraction rates. Figure (72) shows the difference in percentage germanium extraction for acid pre-conditioned Lix 26 (lower curve) and untreated Lix 26 (upper curve). It is evident that, to some extent the availability of active reagent is decreased via acid pretreatment and this indicates that some competition for active ligand must occur throughout the course of the germanium complexation reaction, however the plot for the acid-preconditioned ligand shows the same general trend of fast initial extraction followed by a slower 'equilibrium' regime and therefore this postulate cannot fully account for the rate differences which are observed.

(B) **Hypothesis 2:** A second hypothesis which was considered in order to explain the changing kinetic behaviour at low pH involved the consideration of the germanium speciation in the aqueous phase. It was thought possible that to some extent, the reactivity of the germanium species in solution, decreases in the order $\text{Ge}^{4+} > \text{Ge}(\text{OH})^{3+} > \text{Ge}(\text{OH})_2^{2+}$ and so on.

Attempts were therefore made to correlate the extent of the initial fast reaction (at a chosen pH) with the removal of only Ge^{4+} from aqueous solution i.e. the kinetics were visualised as comprising two consecutive rate processes, the

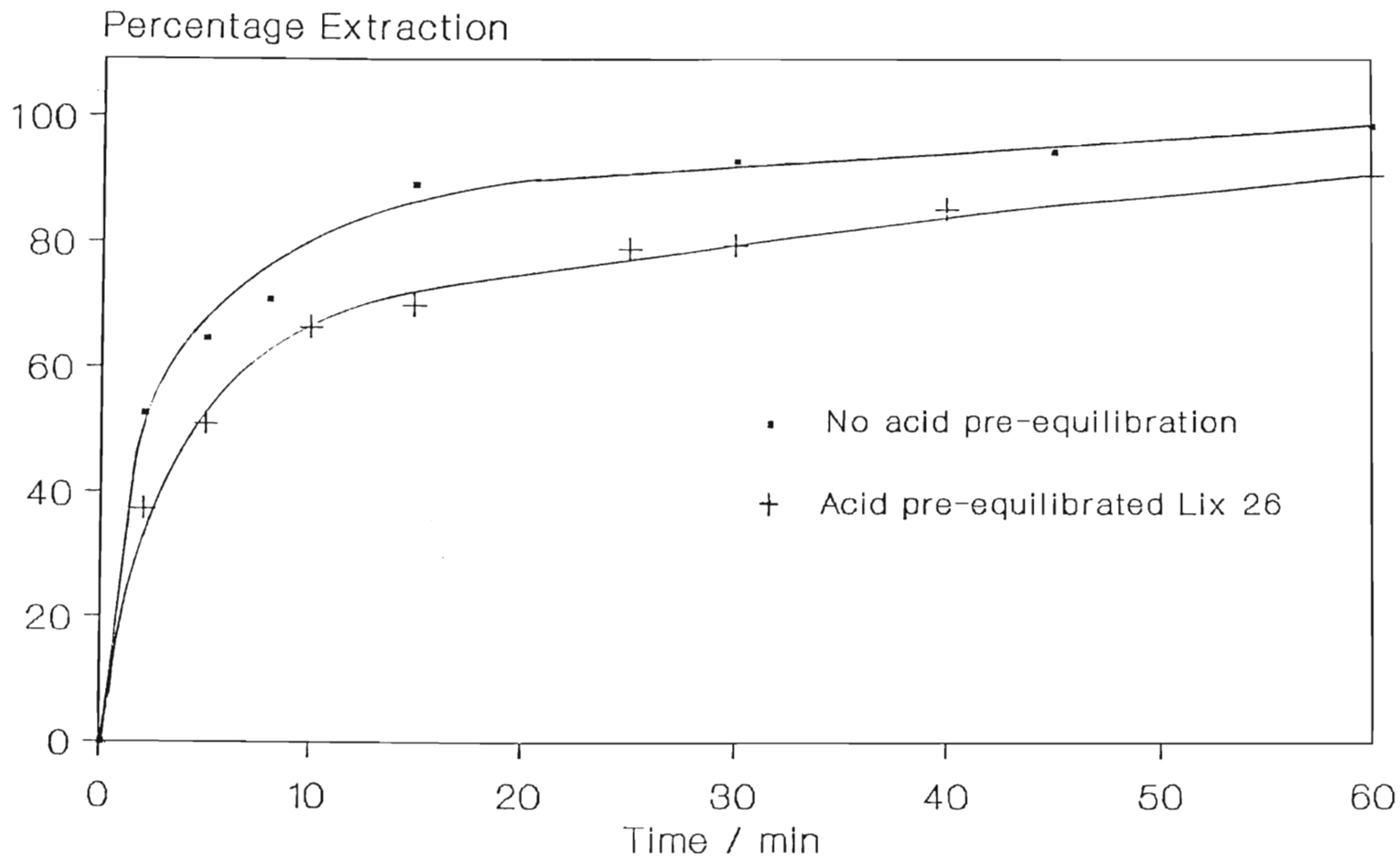


Figure (72). Comparison of the percentage of germanium extracted as a function of time for acid pre-equilibrated and non-equilibrated Lix 26. Organic phase : 50 g/l Lix 26 in toluene; Aqueous phase : ~ 0,65 g/l Ge in 1,5 M H₂SO₄. For the upper curve, germanium extraction was monitored from the time the two phases were in contact and for the lower curve, germanium was introduced into the aqueous phase after the ligand solution had equilibrated with acid for 90 minutes.

first being the fast first-order removal of Ge^{4+} and the second being the slower removal of the remaining germanium-hydroxy species. To test this hypothesis it was necessary to estimate the point in time at which the observed kinetics indicated a deviation to the slower rate of extraction. For the most part the divergence would be indicated by the inflexion in the semi-logarithmic plots of $(a_0 - a_e)/a_0 \ln (a_0 - a_e)/(a_t - a_e)$ versus time, indicated usually by the first (and sometimes second) data points and as a first approximation the percentage extraction at this point would indicate the quantity, as a percentage, of Ge^{4+} initially present in the aqueous phase. If the first few data points were obtained after the same times of shaking contact, the results obtained would be useful in that they would at least be relative, however for the extraction data obtained in this work, aqueous phases were not sampled at set times, thus in order to evaluate the percentage germanium extracted in the fast initial step, the following procedure was adopted: the straight lines attributable to the slower rate were extrapolated to $t=0$ and the germanium concentration a_t calculated by insertion of this value into the logarithmic function given in Equation (46). The percentage germanium extraction was thence calculated by subtracting the value of a_t obtained from the initial (total) germanium concentration. A typical graphical construction performed in this way is shown in Figure (42a). Two sets of data were manipulated in this way to investigate the relevance of this hypothesis: (i) the percentage germanium extracted by Lix 26 from aqueous solutions containing 0,5, 1,0 and 1,5 M H_2SO_4 and (ii) the percentage germanium extracted in the fast initial step by Lix 26 solutions of varying concentration for

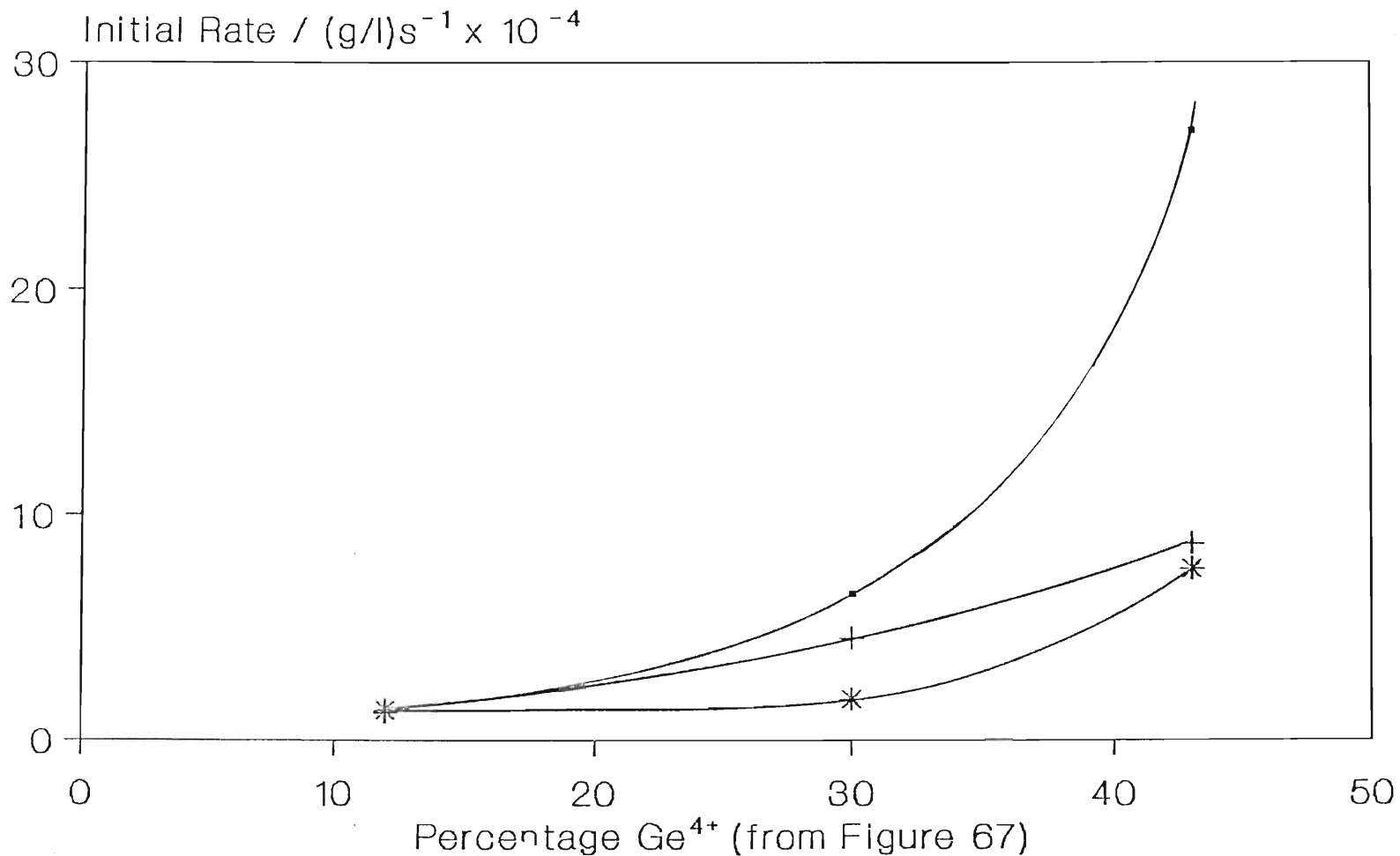
which $[H_2SO_4]$ in the aqueous phase was 1,5 M.

Consider first the percentage extraction data of Table (40):

$[H_2SO_4]$ /M	% Initial Extraction	% Ge^{4+} in Solution *	Initial Rate / $(g/l)s^{-1}$
1,5	59,7	43,0	$2,7 \times 10^{-3}$
1,0	38,0	30,0	$6,5 \times 10^{-4}$
0,5	16,0	12,0	$1,4 \times 10^{-4}$

Table (40). Percentage germanium extracted during the initial 'fast' extraction regime and initial rates versus sulphuric acid concentration. * Determined by interpolation of Figure (67). $[Lix\ 26] = 50,0\ g/l$.

If the hypothesis which has been proposed is correct, then it might be expected that the percentage extraction in the initial fast step would, within experimental error, show some correlation with the percentage of Ge^{4+} initially present in aqueous solution. The data in columns 2 and 3 of Table (40) reflect a reasonable correlation in this respect, however, if the kinetics in this region of extraction can be summarised by the relation $Rate = k_f(obs)[Ge^{4+}][Lix\ 26]^{2,1}$ (the order with respect to ligand was discussed in Section 3.4.1), then since $[Ge^{4+}]$ is the only variable parameter, it might be expected that the initial rate would decrease in a proportional manner with decreasing initial Ge^{4+} concentration. Figure (73) shows a plot of Initial Rate versus percentage Ge^{4+} determined by



▪ Lix 26 + TN 02181 * TN 01787

Figure (73). Initial rate of germanium extraction by Lix 26 (50 g/l in toluene) as a function of the percentage Ge⁴⁺ in aqueous solution calculated from Figure 67 for the pH region < 0,24. Also shown on the figure are the data for TN 02181 and TN 01787, for which the relationship between initial rate and Ge⁴⁺, like that of Lix 26, is not linear.

interpolation of Figure (67) and it is evident that the above relation does not apply since the initial rate is apparently also a function of $[H^+]$, i.e.

Rate = $k_f(\text{obs})[Ge^{4+}][Lix\ 26]^{2,1}[H^+]^x$ where x is the order with respect to $[H^+]$ for the extraction of Ge^{4+} .

Table (41) summarises the percentage of germanium extracted in the initial fast reaction with varying Lix 26 concentration.

[Lix 26] g/l	Percentage Germanium Extracted in the 'Fast' Initial Step
12,5	5,3
19,0	10,8
25,0	22,1
35,0	43,8
50,0	59,7
75,0	76,3
100,0	79,8
150,0	91,7

Table (41). Percentage germanium extracted during the initial 'fast' step versus [Lix 26], $[H_2SO_4] = 1,5\ M$. $[Ge^{4+}]_{aq}(\text{initial}) \approx 59,7\%$ (from interpolation of Figure (67)).

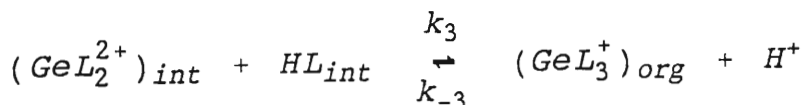
The data presented in Table (41) further supports the view that the initial fast reaction is not a function only of $[\text{Ge}^{4+}]$ removal for if it were then, in the presence of excess ligand ($> 50 \text{ g/l}$ shows a tendency towards zeroth order behaviour in [Lix 26] - see Figure (44), and it is suggested that this concentration can be considered to be an 'excess'), where initial rates are constant, the percentage of germanium extracted in the initial step should be constant and correspond to the percentage of Ge^{4+} present in the aqueous phase at the pH of 1,5 M H_2SO_4 i.e. 59,7 % : these data do not reflect such constancy.

Clearly, during the initial period, both Ge^{4+} and $\text{Ge}(\text{OH})^{3+}$ (at the pH of 1,5 M H_2SO_4 , germanium exists mainly as these two species with $< 20\%$ as higher hydroxy species) are extracted by the ligand.

(C) Hypothesis 3: As opposed to hypothesis 1 above, which postulated a competitive process between germanium species and H^+ for ligand, this postulate proposes that the uptake of sulphuric acid by the ligand and the resulting formation of the species $\text{H}_2\text{L}^+\text{HSO}_4^-$ is also responsible for the fast initial rate of germanium extraction. It is proposed that acid uptake is responsible for the difference in order with respect to $[\text{HL}]$ in the initial fast reaction regime compared with the slow 'equilibrium' regime and for the difference in observed ligand efficacy.

In Section 3.1.3, it was proposed, on stereochemical grounds, that the rate determining step during extraction is the

attachment of the third ligand molecule to the intermediate GeL_2^{2+} at the interface viz.

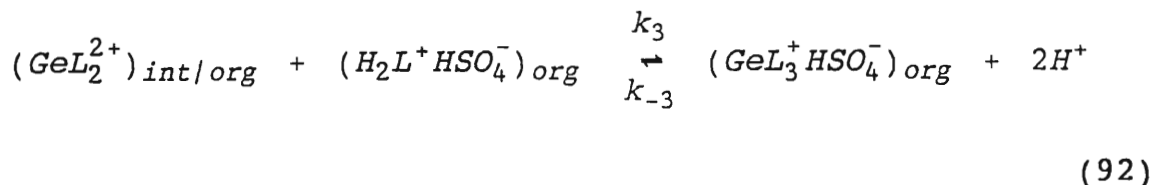
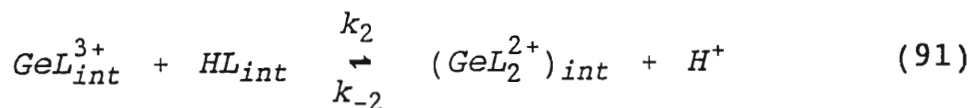
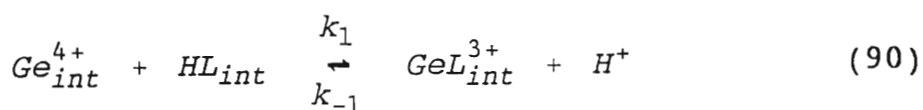


By invoking the Steady State Approximation for this process and assuming that k_{-3} was negligible, it was shown that the rate of extraction of germanium via this process was related to $[\text{HL}]$, $[\text{Ge(IV)}]$ and $[\text{H}^+]$ by the relation:

$$\text{Rate} = \frac{k_3 k_2 k_1 [\text{Ge}] [\text{HL}]^3}{(k_{-2} [\text{H}^+] + k_3 [\text{HL}]) (k_{-1} [\text{H}^+] + k_2 [\text{HL}])}$$

and this rate equation predicts closely the apparent orders of 3,08 and 2,7 with respect to $[\text{HL}]$ for TN 01787 and Lix 26 respectively in the slow 'equilibrium' regime. The rate equation also predicts a first order dependence in $[\text{HL}]$ at high ligand concentration. This form of rate equation cannot however explain ligand orders of two which are indicated for Lix 26 (order of 2,1) and TN 01787 (order of 1,77) in the initial reaction regime and nor can it explain the observed change in rate from a fast initial step to a slower equilibrium step. It is clear that another rate-determining process must operate during the initial reaction regime and that this process is related to the uptake of acid by the ligand reagents in the initial stages of phase contact.

It is proposed in this hypothesis that during the initial fast period, the following general mechanism applies:



where $\text{H}_2\text{L}^+\text{HSO}_4^-$ is formed via Equation (89). In the scheme shown, Ge^{4+} is used to illustrate the kinetic processes occurring, however any of the species $\text{Ge}(\text{OH})_n^{(4-n)+}$ could be treated in analogous manner (although the products of the reactions may be H_2O instead of H^+). In this scheme, the first two equations are analogous to those proposed previously i.e. successive attachments of ligand to the germanium(IV) species at the interface, however the third step in the scheme proposes that $\text{H}_2\text{L}^+\text{HSO}_4^-$, reacts with GeL_2^{2+} at the interface. It is hypothesized that this species is as capable of reacting with GeL_2^{2+} as is neutral HL, except that if GeL_2^{2+} can exist in the organic phase (which is possible if the germanium species reacting is any of Ge^{4+} , $\text{Ge}(\text{OH})^{3+}$ or $\text{Ge}(\text{OH})_2^{2+}$ because the OH groups would be lost during the first two reactions above- Equations (90) and (91)), then the reaction $(\text{GeL}_2^{2+})_{org} + \text{H}_2\text{L}^+\text{HSO}_4^- \rightarrow \text{Products}$ occurs, which is likely to be more stereochemically favourable than attachment of HL to the GeL_2^{2+} species at the interface which has greater stereochemical demands. This rationale accounts for the use of int/org for the locale of the GeL_2^{2+} intermediate in Equation (92). From

Equation (92), the observed rate of formation of $\text{GeL}_3^+\text{HSO}_4^-$ (assuming elementary kinetics) is:

$$\text{Rate} = k_3[\text{H}_2\text{L}^+\text{HSO}_4^-]_{\text{org}}[\text{GeL}_2^{2+}]_{\text{int/org}} - k_{-3}[\text{GeL}_3^+\text{HSO}_4^-][\text{H}^+]^2 \quad (93)$$

Invoking the Steady State Approximation for the species GeL^{3+} and GeL_2^{2+} (see Section 3.1.3), gives on substitution:

$$\text{Rate} = \frac{k_3 k_2 k_1 [\text{Ge}][\text{HL}]^2 [\text{H}_2\text{L}^+\text{HSO}_4^-]}{(k_{-2}[\text{H}^+] + k_3[\text{H}_2\text{L}^+\text{HSO}_4^-])(k_{-1}[\text{H}^+] + k_2[\text{HL}])} - k_{-3}[\text{GeL}_3^+\text{HSO}_4^-][\text{H}^+]^2 \quad (94)$$

The second term of Equation (94) is probably negligible on account of the hydrophobicity of the product formed which would tend towards existing in the organic bulk rather than at the phase boundary.

There are a number of implications associated with this form (Equation (94)) of rate equation:

(i) The rate law predicts that during the initial fast reaction, the observed rate of germanium extraction is proportional to $[\text{HL}]^2$. During this reaction regime, the following rate laws have been found experimentally for Lix 26, TN 02181 and TN 01787:

$$\text{Rate} = k_f(\text{obs})[\text{Ge}][\text{Lix 26}]^{2,10}[\text{H}^+]^{-2,83} \quad (95)$$

$$\text{Rate} = k_f(\text{obs})[\text{Ge}][\text{TN 02181}]^{1,06}[\text{H}^+]^{-1,92} \quad (96)$$

$$\text{Rate} = k_f(\text{obs}) [\text{Ge}] [\text{TN 01787}]^{1,77} [\text{H}^+]^x \quad (97)$$

(It is recalled that the data relevant to the initial fast step (Figure (64)) for TN 01787 did not allow for the calculation of x , see Section 3.4.3.) The rate law thus predicts the apparent second order behaviour characteristic of Lix 26 and TN 01787 in the initial reaction regime for TN 01787 and Lix 26. For TN 02181 however, for which the apparent order with respect to [HL] is 1,06 in the fast reaction regime, this rationale would appear to be inadequate. This reagent is also anomalous in considering the slow 'equilibrium' regime since the predicted third order behaviour (Equation (64)) is not observed experimentally (order with respect to [HL] = 1,12). It is clear that this reagent, which is the most efficient at low concentration, is available at the interface to a greater extent than either of TN 01787 or Lix 26 at any particular concentration of ligand and this behaviour must be related to its structure. The propensity to which this ligand reagent undergoes the protonation reaction (Equation (89)) has been shown experimentally to be far greater (Figure (69)) than either of TN 01787 or Lix 26, particularly at low ligand concentration. In the fast reaction regime therefore, it is suggested that $k_{-2}[\text{H}^+] < k_3[\text{H}_2\text{L}^+\text{HSO}_4^-]$ and $k_{-1}[\text{H}^+] < k_2[\text{HL}]$ in Equation (94) and this gives, on cancellation where possible $\text{Rate} = k_1[\text{Ge}][\text{HL}]$ which thus indicates a tendency towards first order behaviour in [HL]. In the slower 'equilibrium' kinetic regime, TN 02181 is observed

to tend towards first order behaviour in [HL] at approximately 25 g/l of the reagent (Figure (45)). It was proposed in Section 3.1.3 that an expected first order dependence on [HL] occurs when $k_{-2}[H^+] \ll k_3[HL]$ and $k_{-1}[H^+] \ll k_2[HL]$ in Equation (64). It is therefore suggested that the relative difference in the sizes of the ligand reagents (Table (63)) and of the triligand chelates (Table (66)) are such that this approximation becomes relevant for TN 02181 at a lower ligand concentration (25 g/l as opposed to > 50 g/l for the other two reagents) than for Lix 26 and TN 01787.

(ii) At high ligand concentration, it can be assumed that $k_{-1}[H^+] \ll k_2[HL]$ and thus cancelling in Equation (94):

$$\text{Rate} = \frac{k_3 k_1 [Ge] [HL] [H_2L^+ HSO_4^-]}{k_{-2}[H^+] + k_3 [H_2L^+ HSO_4^-]} \quad (98)$$

In accordance with the slower 'equilibrium' kinetics, this rate law correctly predicts the tendency towards first order behaviour in [HL] at high ligand concentration for all three reagents. This phenomenon has been attributed to the saturation of the interface by ligand (Section 3.2.1.2.).

(iii) Equation (94) predicts that the rate of germanium extraction increases as $[H_2L^+ HSO_4^-]_{org}$ increases. This of course assumes that sufficient of this species is available in the organic phase shortly after phase contact. Figure (74) shows a plot of the sulphuric acid concentration taken into an organic phase containing 100 g/l TN 02181 versus time, where it is evident that the equilibrium organic concentration of acid is attained in

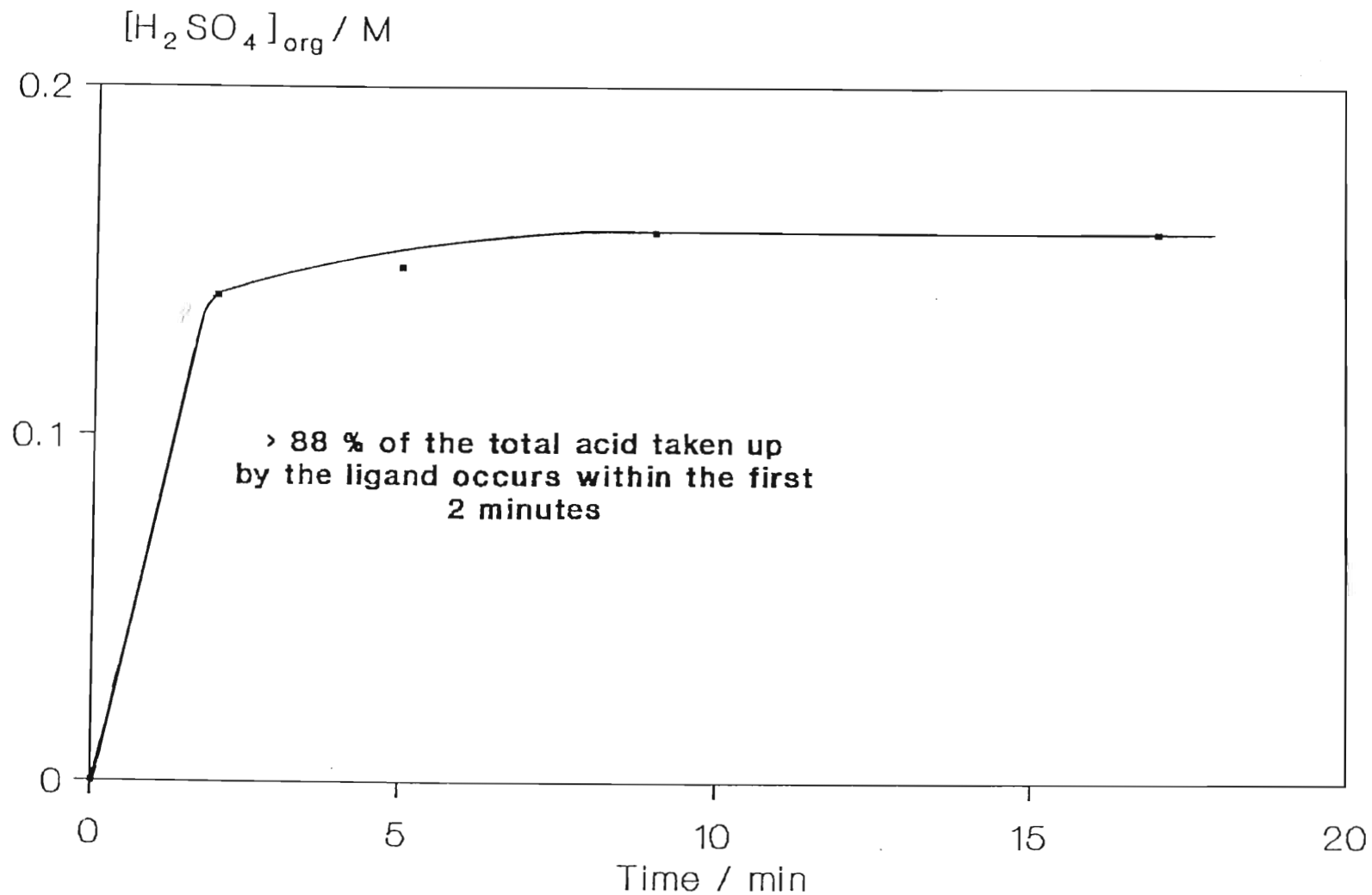


Figure (74). The rate of acid uptake plotted as $[H_2SO_4]$ in the organic phase as a function of time by a 100 g/l (0,270 M) solution of TN 02181 in AR toluene. Aqueous phase : 1,5 M H_2SO_4 .

< 5 minutes, with approximately 88% taken up within the first 2 minutes of phase contact. The acidified ligand species is therefore available in the organic phase throughout the course of the fast reaction kinetic regime. Examination of Figure (69) and Tables (36) to (38), which summarised the quantities of acid extracted into the organic phases by each of the ligands of concern to this work, shows that at low ligand concentration (< 50 g/l), the quantity of acid taken up by the reagents are not equivalent. Whilst TN 02181 and Lix 26 show an almost linear increase in $[H_2SO_4]_{org}$ with increasing $[HL]$, TN 01787 shows much lower acid absorption. at low ligand concentration. For example, at a concentration of 40,0 g/l of the three reagents (which are corrected for purity in Figure (69)), the following concentrations of H_2SO_4 are extracted into the organic phase at equilibrium (approximated by extrapolation of the curves of Figure (69)):

Ligand Reagent	$[H_2SO_4]_{org}$ at equilibrium / M
TN 02181	0,079
Lix 26	0,040
TN 01787	0,015

As suggested above, since the rate of extraction of germanium in the initial fast regime is proportional to $[H_2L^+HSO_4^-]$, these data suggest that the order of extraction efficiency of these three ligands is:

TN 01787 < Lix 26 < TN 02181

This order of efficiency (at low ligand concentration) was noted in Section 3.2.1.4 and thus the rationale which is presented here is offered as an explanation for this

order. Furthermore, it would be expected that if the rate of germanium extraction is proportional to $[H_2L^+HSO_4^-]$, then the percentage of germanium extracted during the initial fast rate process would be linearly related to the quantity of acid extracted into the organic phase by each of the ligand reagents. Figure (75) shows such plots for all three ligand reagents, in which the initial percentage extraction was calculated according to the method given in hypothesis 2. For TN 02181 and Lix 26, the expected linearity is observed, however for TN 01787, a non-linear plot is obtained and this is an indication of the change in acid uptake with increasing $[HL]$ which is characteristic of this reagent and which is apparent in Figure (69). In this regard, a comparison of the equilibrium percentage extraction plots of TN 01787 (Figure (50)), with those of TN 02181 (Figure (48)) and Lix 26 (Figure (49)) shows that for the last two, the increase in percentage extraction with increasing ligand concentration for the first \pm 5 minutes is reasonably linear for ligand concentrations \leq 75 g/l, whereas for TN 01787 such increases are non-linear and parallel the behaviour noted above and depicted in Figure (75).

Since this hypothesis gives a form of rate equation which adequately predicts orders of reaction with respect to ligand in the fast kinetic regime for two of the reagents of concern to this work and since it predicts the correct order of ligand efficacy at low concentration, it is proposed that this model is the most satisfactory of the three which have been proposed as explanations for the fast initial rate. In summary, this hypothesis asserts that for the period of the initial fast

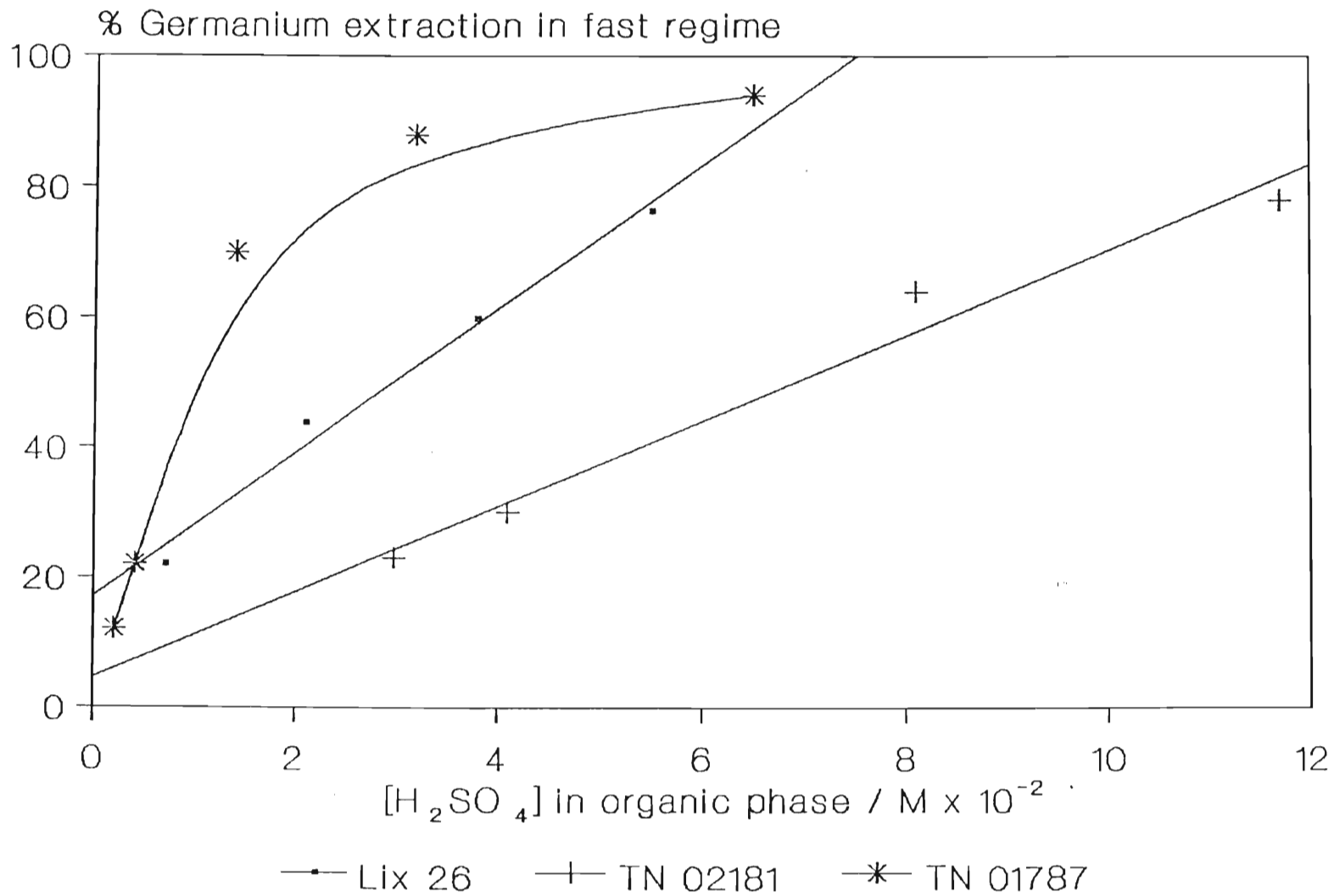


Figure (75). Percentage extraction of germanium in the fast initial regime as a function of $[H_2SO_4]$ in the organic phase. Percentage germanium extraction was calculated by extrapolation of semi-logarithmic plots to $t=0$ to give a_t . This value was subtracted from the initial germanium concentration to obtain the quantity extracted in the fast reaction region.

rate, Equation (94) is rate-determining, and the rate is proportional to the quantity of the acid extracted by the ligand as the species $\text{H}_2\text{L}^+\text{HSO}_4^-$ and to $[\text{HL}]^2$. However once the quantity of the protonated ligand species is depleted (and it is clear from Tables (36) to (38) that it is only a proportion of the ligand which uptakes acid), then Equation (64) is the rate-determining step which is proportional to $[\text{HL}]^3$ at low ligand concentration. It is envisaged that this latter rate is a slower process because it is strictly an interfacial mechanism which operates.